Universidade de Aveiro Departamento de Geociências
2009

Henrique Canto e Castro Guerreiro Duarte

Estudo da acumulação e escape de gás nos canais de maré da Ria de Aveiro com sísmica de reflexão de alta resolução

High-resolution seismic reflection investigation of gas accumulation and seepage in the tidal channels of the Ria of Aveiro barrier lagoon (Portugal)

Universidade de Aveiro Departamento de Geociências
2009

Henrique Canto e Castro Guerreiro Duarte

Estudo da acumulação e escape de gás nos canais de maré da Ria de Aveiro com sísmica de reflexão de alta resolução

High-resolution seismic reflection investigation of gas accumulation and seepage in the tidal channels of the Ria of Aveiro barrier lagoon (Portugal)

tese apresentada à Universidade de Aveiro para cumprimento dos requisitos necessários à obtenção do grau de Doutor em Geociências, realizada sob a orientação científica do Professor Doutor Luís Menezes Pinheiro, Professor Associado do Departamento de Geociências da Universidade de Aveiro, com co-orientação científica da Professora Cristina Bernardes, Professora Associada do Departamento de Geociências da Universidade de Aveiro.

O trabalho desenvolvido no decorrer desta tese foi financiado por uma bolsa de da Universidade de Aveiro e uma bolsa (FSRH/BD/2017/2004) da Fundação para a Ciência e Tecnologia (FCT).

This work was supported by one scholarship from the University of Aveiro and one scholarship (FSRH/BD/2017/2004) from the Fundação para a Ciência e Tecnologia (FCT).

Dedico este trabalho à minha esposa Sara

o júri

presidente

Professor Doutor Aníbal Manuel de Oliveira Duarte
Professor Catedrático do Departamento de Electrónica, Telecomunicações e Informática da Universidade de Aveiro

Professor Doutor António Augusto Ramos Ribeiro
Professor Catedrático Aposentado da Faculdade de Ciências da Universidade de Lisboa

Professor Doutor Pedro António Gancedo Terrinha
Professor Convidado da Faculdade de Ciências da Universidade de Lisboa
Investigador Auxiliar do Laboratório Nacional de Energia e Geologia

Professor Doutor Luís Filipe Fuentefria de Menezes Pinheiro
Professor Associado do Departamento de Geociências da Universidade de Aveiro

Professora Doutora Cristina Maria de Almeida Bernardes
Professora Associada do Departamento de Geociências da Universidade de Aveiro

agradecimentos

Esta tese demorou a ver a luz do dia mas, ainda assim, dificilmente teria sido concluída sem o apoio de muitos que quero aqui reconhecer.

Gostaria de começar por agradecer aos meus orientadores Luís Pinheiro e Cristina Bernardes por apoiarem o meu projecto de doutoramento. A curiosidade, espírito de trabalho e amizade do Luís foram uma enorme força para levar este trabalho a bom porto. Faltam-me palavras para reconhecer com justiça os inúmeros contributos da criatividade e esforço do Luís para a realização desta tese.

Ao Pedro Terrinha e à Fátima Abrantes, do Departamento de Geologia Marinha (DGM) do LNEG, ex-INETI, ex-IGM (e isto apenas durante a minha estadia), agradeço os muitos anos de amizade e apoio que me permitiram beneficiar da experiência de um grupo de trabalho único, onde o trabalho de equipa funciona e o bom ambiente fazem passar rapidamente os dias mais difíceis. Agradeço em particular aos que me acompanharam no grupo de Geologia e Recursos, Pedro Terrinha, Hipólito Monteiro, Vasco Valadares, Cristina Roque, Rui Quartau, Gabriela Carrara, João Duarte, Tiago Alves, Tiago Cunha, José Vicente, João Noiva, Luís Batista e Carlos Pinto.

A visão sobre o Método Científico perfilhado neste trabalho foi fortemente influenciada pelas discussões com o António Ribeiro e o Hipólito Monteiro. Estou-lhes grato pela amizade constante e por me terem mostrado porque é que a Ciência também tem o nome de Filosofia Natural.

Durante este trabalho houve uma voz de crítica racional inquebrantável que muito melhorou esta tese. É escusado procurar uma saída fácil quando se discute interpretação sísmica (ou qualquer outra coisa!) com o Pedro Brito. Agradeço-lhe a paciência, perseverança e amizade durante as nossas muitas, longas e por vezes acesas discussões.

Ao Vitor Magalhães, Serguei Bouriak, Cristina Roque, Rui Quartau e José Vicente agradeço toda a ajuda na preparação e execução dos cruzeiros.
Agradeço ao Francisco Teixeira, à Zuzia Stroynowski e ao Tiago Cunha a revisão de partes do manuscrito.

Um agradecimento especial é devido à Margarida Henriques, cuja inteligência e esforço para ultrapassar a plasticidade da “burocracia moderna” na ciência muito me facilitaram a vida.

agradecimentos

À Joan Gardner, Peter Vogt, Clyde Nishimura e Brian Parsons agradeço o caloroso acolhimento e experiência enriquecedora no Naval Research Laboratory, Washington D.C. De entre muitas coisas, aprendi a importância de ser capas de lidar com os dados sem depender de ferramentas de terceiros. Assim que cheguei a Lisboa comecei a aprender a programar o software que viria a ser fundamental para processar os dados de navegação desta tese.
Agradeço também ao Alan Judd, à Soledad Garcia-Gil e ao Martin Hovland pelos conselhos na interpretação de muitos dos perfis sísmicos.

São devidos agradecimentos também à Administração do Porto de Aveiro (APA) que providenciou o tempo de navio, ao Comandante Francisco Pontes, ao Mestre da "Ria Azul" Licínio Rama e à tripulação dos cruzeiros científicos RIAV99, RIAV02, RIAV02A e RIAV03. Ao Senhor Rama e ao Senhor Caçoilo agradeço terem partilhado a vasta experiência e conhecimento da Ria, bem como o apoio que deram durante os cruzeiros, muito para além das suas obrigações profissionais, sem o qual muitos dos perfis sísmicos adquiridos nunca veriam a luz do dia.

Este doutoramento foi apoiado por uma bolsa da Universidade de Aveiro e por uma bolsa (FSRH/BD/2017/2004) da Fundação para a Ciência e Tecnologia (FCT). Os dados sísmicos foram adquiridos na Ria de Aveiro graças ao projecto EICOS (PRAXIS/2/2.1/MAR/1750/95), ao projecto INGMAR (FCT-PLE/4/98) e a três Acções Ciência Viva da FCT.

O processamento e interpretação de muitos dos dados sísmicos foi possível graças ao apoio dado ao Instituto Nacional de Engenharia, Tecnologia e Inovação pela Landmark Graphics Corporation, via a Landmark University Grant Program, e também, ao apoio à Universidade de Aveiro pela Seismic Micro-Technology, via um Kingdom Suite Educational User-License Grant.

À minha família e amigos agradeço a paciência e os momentos perdidos, passados longe ou atrás de um teclado.

Não há páginas suficientes para agradecer à Sara, e mesmo que houvesse, creio que as minhas palavras não lhe fariam justiça.

palavras-chave Metano, gas, laguna, canal de maré, reflecção sísmica, Ria de Aveiro

resumo

O metano é um gás de estufa potente e uma importante fonte de energia. A importância global e impacto em zonas costeiras de acumulações e escape de gás metano são ainda pouco conhecidas. Esta tese investiga acumulações e escape de gás em canais de maré da Ria de Aveiro com dados de cinco campanhas de reflexão sísmica de alta resolução realizadas em 1986, 1999, 2002 e 2003. Estas incluem três campanhas de Chirp (RIAV99, RIAV02 e RIAV02A) e duas campanhas de Boomer (VOUGA86 e RIAV03). O processamento dos dados de navegação incluíram filtros de erros, correcções de sincronização de relógios de sistemas de aquisição de dados, ajuste de "layback" e estimativa da posição de "midpoint". O processamento do sinal sísmico consistiu na correcção das amplitudes, remoção de ruído do tipo "burst", correcções estáticas, correcção do "normal move-out", filtragem passa-banda, desconvolução da assinatura e migração Stolt F-K. A análise da regularidade do trajecto de navegação, dos desfasamentos entre horizontes e dos modelos de superfícies foi utilizada para controlo de qualidade, e permitiu a revisão e melhoria dos parâmetros de processamento. A heterogeneidade da cobertura sísmica, da qualidade do sinal, da penetração e da resolução, no seu conjunto constrangeram o uso dos dados a interpretações detalhadas, mas locais, de objectos geológicos da Ria. É apresentado um procedimento para determinar a escolha de escalas adequadas para modelar os objectos geológicos, baseado na resolução sísmica, erros de posicionamento conhecidos e desfasamentos médios entre horizontes. As evidências de acumulação e escape de gás na Ria de Aveiro incluem turbidez acústica, reflexões reforçadas, cortinas acústicas, domas, "pockmarks" e alinhamentos de "pockmarks" enterradas, horizontes perturbados e plumas acústicas na coluna de água (flares). A estratigrafia e a estrutura geológica controlam a distribuição e extensão das acumulações e escape de gás. Ainda assim, nestes sistemas de baixa profundidade de água, as variações da altura de maré têm um impacto significativo na detecção de gás com métodos acústicos, através de alterações nas amplitudes originais de reflexões reforçadas, turbidez acústica e branqueamento acústico em zonas com gás. Os padrões encontrados confirmam que o escape de bolhas de gás é desencadeado pela descida da maré. Há acumulações de gás em sedimentos Holocénicos e no substrato de argilas e calcários do Mesozóico. Evidências directas de escape de gás em sondagens em zonas vizinhas, mostraram gás essencialmente biogénico. A maioria do gás na área deve ter sido gerado em sedimentos lagunares Holocénicos. No entanto, a localização e geometria de estruturas de escape de fluidos em alguns canais de maré, seguem o padrão de fracturas do substrato Mesozóico, indicando uma possível fonte mais profunda de gás e que estas fracturas funcionam como condutas preferenciais de migração dos fluidos e exercem um controlo estrutural na ocorrência de gás na Ria.

Acknowledgements

This thesis took a long time coming, and still, it would hardly have been done if not for the support of many that will try to acknowledge here. I hope I do not forget anyone but, in case I do, my sincere apologies.

I would like to start by thanking my supervisors Luis Menezes Pinheiro and Cristina Bernardes for sponsoring this Ph.D.. Luis' curiosity, work ethics and friendship were a driving force to push this work to completion. I do not have the ability to justly acknowledge the multitude of ways in which Luis' creativity and hard work contributed to this thesis.
To Pedro Terrinha and Fátima Abrantes, from the Marine Geology Department (DGM) of LNEG…former INETI…former IGM (and this just during my stay!), I thank for the years of support that allowed me to benefit from the expertise and friendship of a quite unique research group, a group where team work works and good spirits make the harder days go by easier.

The views on Scientific Method that are espoused in this thesis were strongly influenced by most enlightening discussions with António Ribeiro and Hipólito Monteiro. I thank them for a constant friendship and for making clearer to me the reason for that Ph. in Ph.D.

Through much of this work there was a voice of unforgiving rational criticism that significantly improved this thesis. One cannot cut corners when discussing seismic interpretation (or anything else for that matter) with Pedro Brito, and I thank him for is patience, perseverance and friendship during many lively discussions.

To Vitor Magalhães, Serguei Bouriak, Cristina Roque, Rui Quartau and José Vicente I thank, for all their help in the preparation and execution of the seismic surveys.

I thank Francisco Teixeira, Zuzia Stroynowski and Tiago Cunha for reviewing and discussing parts of the manuscript.

A special acknowledgment is due to Margarida Henriques, whose intelligence and hard work in cutting through endless red tape of modern bureaucracy in science made my work life so much easier.
.

Acknowledgements

Thanks also to the Administration of the Harbour of Aveiro (APA) who provided the surveys ship time, to Cmd. Francisco Pontes, the Master of “Ria Azul” Mr. Licínio Rama, and to the crew and scientific parties of cruises RIAV99, RIAV02, RIAV02A and RIAV03. An heartfelt thanks to Lícinio and

Joan Gardner, Peter Vogt, Clyde Nishimura and Brian Parsons I thank for their welcome and for the enriching experience in the Naval Research Laboratory, Washington D.C. These were the scientists that showed me the importance of being able to fully handle data without resorting to third party resources. As soon as I arrived in Lisbon I set out to learn how to write my own software code, with which much of the navigation data processing was done.

Thanks also to Alan Judd, Soledad Garcia-Gil and Martin Hovland for their helpful comments on the interpretation of several seismic sections.

This Ph.D. work was supported by one scholarship from the University of Aveiro and one scholarship (FSRH/BD/2017/2004) from the Fundação para a Ciência e Tecnologia (FCT). The seismic data collected in the Ria de Aveiro was possible thanks to the EICOS Project (PRAXIS/2/2.1/MAR/1750/95), the INGMAR Project (FCT-PLE/4/98) and three FCT Ciência Viva Actions.

Processing and interpretation of much of the seismic data was possible thanks to the support to the Instituto Nacional de Engenharia, Tecnologia e Inovação (INETI) by Landmark Graphics Corporation via the Landmark University Grant Program, and also to the support to the University of Aveiro from Seismic Micro-Technology Inc. via a Kingdom Suite Educational User-License Grant.

To my family and friends I thank for the patience and for the lost moments spent far away or behind a keyboard.

There are not enough pages to thank Sara, and even if there were, I am afraid my words would be lacking.

keywords Methane; gas; barrier lagoon; tidal channels; seismic reflection; Ria de Aveiro

abstract

Methane is a powerful greenhouse gas and an important energy source. The global importance and impact in coastal zones of methane gas accumulation and seepage in sediments from coastal lagoon environments is still largely unknown. This Ph.D. investigates gas accumulation and seepage in tidal channels of the Ria of Aveiro with data from five high resolution seismic surveys carried out in 1986, 1999, 2002 and 2003. These include three Chirp surveys (RIAV99, RIAV02, RIAV02A) and two Boomer surveys (VOUGA86 and RIAV03). The navigation data processing included instrumental error filters, system clock synchronization corrections, layback adjustment and trace midpoint position estimate. The seismic signal processing consisted in amplitude corrections, burst noise removal, static corrections, normal move-out corrections, band-pass filtering, spike deconvolution and Stolt F-K migration. The analysis of the track line regularity, the horizon misties and the first-break surface models were applied as quality control procedures, and allowed the revision and improvement of the processing parameters. The heterogeneity of the seismic coverage, signal quality, penetration and resolution all constrain the use of the data to mostly local but detailed interpretations and modeling of the geological objects of the Ria of Aveiro. A procedure is presented to determine adequate choice of scales of these geological models based on the seismic resolution, known positioning errors and mean mistie values. Evidence of extensive gas accumulation and seepage in tidal channel sediments from the “Ria de Aveiro” barrier-lagoon includes acoustic turbidity, enhanced reflections, acoustic blanking, domes, pockmarks and buried aligned pockmarks, disrupted horizons and acoustic plumes in the water layer (flares). The stratigraphy and the structural framework control the distribution and extent of the gas accumulations and seepage in the study area. However, in these shallow systems, tidal altitude variations have a significant impact on gas detection with acoustic methods, by changing the raw amplitude of the enhanced seismic reflections, acoustic turbidity and acoustic blanking in gas-prone areas. Amplitudes are clearly stronger during low tide with maxima during ebb, decreasing with flood with minima during high tide; this pattern confirms that bubbling and gas escape is triggered mainly by the falling tide. There are accumulations of gas both in the Holocene sediments and in the Mesozoic bedrock of marls and clays. Direct evidence of gas escape from drill-holes in the surrounding area has shown that the gas recovered in the “Ria de Aveiro” consists of biogenic methane. Most of the gas in the study area was probably mainly generated in Holocene lagoon sediments. Nevertheless, the location and geometry of fluid escape features in some channels follows the fracture pattern affecting the Mesozoic bedrock, indicating a possible deeper source of gas and that these fractures function as preferential pathways for fluid migration and exert a structural control on gas occurrences in the Ria of Aveiro.

Table of contents

List of tables

List of figures

Chapter 1. Introduction

1.1 Nature and scope of this work

Estuaries and coastal lagoons are prime locations from both a human and environmental perspectives. These systems encompass some of the most productive and diverse regions of the globe, and are the breeding grounds for multiple species. This wealth also attracted and still attracts human settlement, making these the areas with the highest population density of the globe. The economic importance of estuaries and coastal lagoons is also obvious, with oceanic and river trade lanes meeting at the harbor facilities that seem to grow relentlessly along its shores. Also, for all these reasons, anthropogenic impact is usually significant because of the widespread construction and polluting activities changing the landscape and ecosystems. The knowledge about the geological processes governing the evolution of estuaries and coastal lagoons is essential for the adequate assessment and management of its natural resources, for the evaluation of the risk of geological hazards and to provide fundamental knowledge for environmental impact studies.

The Associated Laboratory, Center for Environmental and Marine Studies (Centro de Estudos do Ambiente e do Mar, CESAM) of the University of Aveiro Research Institute has a research group on Geological and Geophysical Processes which focuses on the dynamics of coastal and marine sediments. The work presented here was done within the framework of CESAMs' Geological and Geophysical Processes research line, and its initial aim was to study the geological evolution of the Ria of Aveiro, a barrier lagoon located in on the west Portuguese coast, and its adjacent continental shelf using high resolution seismic reflection methods and borehole log data from water wells (see location of the Ria of Aveiro in figure 1). The initial exploration of the available data and of the first results from the seismic reflection surveys showed previously unknown seismic

evidence of gas in the profiles of the Ria of Aveiro (Pinheiro, L., pers. communication), and was intensively investigated by several cruises (Monteiro and Pinheiro, 1986; Pinheiro and Monteiro, 1999; Pinheiro and Duarte, 2003a; Pinheiro and Duarte, 2003b; Pinheiro *et al.*, 2003). The investigation of these occurrences became the topic of this thesis (Duarte et al., 2007).

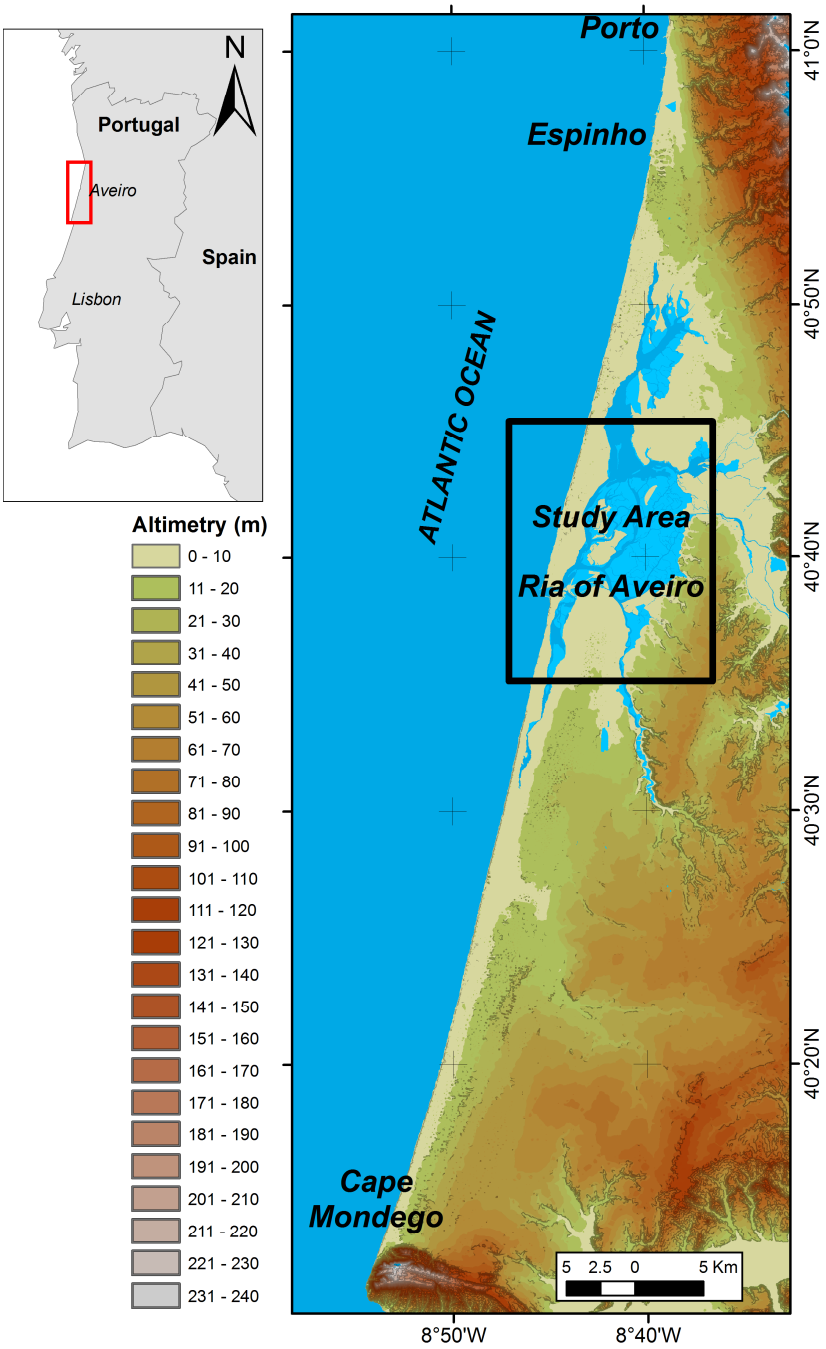

Figure I-1 – Physiography and location of the study area, the Ria of Aveiro barrier lagoon (Northwest Portugal).

Estuaries and coastal lagoons are depocenters of organic-rich sediments which are sources of methane (Kelley et al., 1995; Van der Nat and Middelburg, 2000). These systems are excellent and easily accessible natural laboratories to investigate the mechanisms of methane generation, accumulation, migration and escape (e.g. Garcia-Gil, 2003). Nevertheless, the geological investigation of estuaries and, in particular, barrier lagoon environments is particularly difficult, because these are complex, very dynamic, fast changing and evolving systems that require extensive and detailed data for their study. In addition, the acquisition of large data sets is hindered by the methodological limitations imposed by the difficulty in accessing the geological objects, usually partially or permanently submerged, which also involves access to ship time. Furthermore, the spatial and temporal variability and the complexity of these shallow gas systems require dense grids of geophysical data in order to get representative sampling. As a result, the importance of the escape of methane gas from sediments of estuarine and lagoon environments to the atmosphere is still poorly known or underestimated, and has not been taken into account in the International Panel for Climate Change assessment reports of the geological emissions of methane (Hovland *et al.*, 1993; I.P.C.C., 2001; Etiope, 2004; Judd, 2004). Estuaries and coastal lagoons where the loci in the geological past for the generation of large accumulations of oil and gas now being exploited. Accumulations of shallow gas in such present-day systems where the volume and concentration are adequate, may also be exploited for biogas, for local use in the near future, similarly to what is already happening in African lakes and in artificial dairy lagoons (e.g. Williams and Frederick, 2001; Hirsch *et al.*, 2005). Thus, understanding the importance, the controlling factors and the mechanisms of methane generation, accumulation and escape in coastal shallow water systems may yield useful indicators for oil and gas exploration and contribute to the evaluation of the potential of present day biogenic methane gas in estuaries and coastal lagoons as a possible alternative energy source.

This work was planned in order to implement methods to overcome the difficulties with processing sub-surface data from the Ria of Aveiro, acquired at

different times. Furthermore, it aimed to investigate the seismic evidence of gas in the sediments of coastal lagoons and the importance of understanding the controlling factors and the mechanisms of methane gas generation, its accumulation and escape. The work was structured around three major questions:

- What are the best procedures to acquire and process the seismic reflection data in a shallow barrier-lagoon environment?
- What are the types of seismic evidence of gas in the tidal channels of the Ria of Aveiro and what is the appropriate way to map them?
- What are the geological controls on gas accumulation and seepage in the tidal channels of the Ria of Aveiro?

This thesis was structured to present in separate chapters a self-sufficient answer to each of these questions. The chosen organization of the chapters allows for an efficient preparation of the work for publication in scientific journals, whilst, at the same time, maintaining an evolving character, addressing more technical issues first and addressing the more theoretical issues towards the end.

The introduction, Chapter I, consists on the presentation of the nature and scope of the thesis, as well as, of the objectives and methods of the research. A more detailed and adequate account of the state of the art and methods specific is provided in later chapters. A general description of the study area, the Ria of Aveiro, is provided in Chapter II. The next three chapters are structured as research papers, each one of them addressing a specific topic this thesis. The methodological issues related to the acquisition and processing of high resolution seismic reflection data in shallow lagoons such as the Ria of Aveiro are dealt in Chapter III. Chapter IV, already published as a paper in Geo-Marine Letters, presents the main types of seismic evidence of gas in the Ria of Aveiro using the Espinheiro tidal channel sector as a case study (Duarte et al., 2007). The structural and tidal controls of gas in the Ria are discussed in Chapter V, using the data from the Cidade Channel and the Terminal Sul. The final chapter of this work, Chapter VI, presents a review of the answers to the questions that guided research, discusses the new issues that arose from this investigation and

proposes guidelines for future work in the study of gas generation and flow in the Ria of Aveiro, and in similar coastal environments. The thesis includes one Appendix with seismic evidence of gas, mainly to complement the figures of Chapter IV, which were of limited number due to constraints established by the rules of its publication in Geo-Marine Letters. The appendix also serves to document evidence of gas in other surveyed sectors of the lagoon that were not investigated in detail due to the sparse seismic coverage.

1.2 Objectives

This Ph.D. thesis studies gas accumulation and seepage in the Ria of Aveiro barrier-lagoon with seismic reflection data. The distribution and extent of seismic evidence of gas were mapped out in major tidal channels of the lagoon and the structural and tidal controls of gas were investigated. The specific objectives were the following:

1. To describe the data acquisition systems and to document the operational procedures used for future reference.
2. To propose processing flows of the seismic signal and navigation data and discuss the results of the application of these flows.
3. To assess the constraints imposed by the processed seismic dataset on the interpretation and mapping of geological features.
4. to map the high-resolution seismic evidence of gas accumulation and seepage in the sediments of the surveyed tidal channels in the “Ria de Aveiro” barrier-lagoon
5. to characterize the 3D geometry of the Holocene lagoon sediments architecture and of the structure of the Mesozoic bedrock, allowing the identification of structural controls on the fluid migration pathways and gas accumulation zones.
6. to perform a statistical analysis of the amplitudes of the bottom reflection of the Chirp data in order to determine if there is a significant change in amplitude strength as the tidal cycle evolves

1.3 Methods

The study of gas in the Ria of Aveiro presented here was based on very high-resolution 2D seismic reflection surveys (Boomer and Chirp), complemented by log data from water wells and geotechnical soundings. The seismic reflection data acquired in the Ria of Aveiro is of multiple vintages, and the acquisition systems used were an EG&G Uniboom system with a boomer source and a Datasonics Chirp system with a modulated chirp source. High resolution seismic reflection surveying of the Ria of Aveiro started in 1986 (Monteiro and Pinheiro, 1986) and a total of five surveys with Chirp and Boomer systems were carried out until late 2003 (Monteiro and Pinheiro, 1986; Pinheiro and Monteiro, 1999; Pinheiro and Duarte, 2003a; Pinheiro and Duarte, 2003b; Pinheiro *et al.*, 2003). Three of these surveys were done during the timeframe of this work: the Chirp surveys RIAV02 (Pinheiro and Duarte, 2003a), RIAV02A (Pinheiro and Duarte, 2003b) and the Boomer RIAV03 survey (Pinheiro *et al.*, 2003), and the author participated in the latest two (RIAV02A and RIAV03); the two earliest ones, the VOUGA86 Boomer survey (Monteiro and Pinheiro, 1986) and the RIAV99 Chirp survey (Pinheiro and Monteiro, 1999), were revisited and also used here. The boomer data consists of approximately 65km of analog profiles and 47km of digital profiles. The digital chirp profiles total over 200 km. Positioning of the seismic profiles was done with GPS, DGPS and RTK-GPS systems.

Seismic processing was carried out with SPW software package (Seismic Processing Workshop, from Parallel Geoscience Corporation), and with Radex Pro (from Deco Geophysical). SEG-Y seismic data management and interpretation was carried out using the Kingdom Suite (Seismic Micro-technology Inc) and the Openworks and Seisworks-2D (Landmark Graphics Corporation) seismic interpretation software packages.

The available hydrological and geotechnical sounding log data of Ria of Aveiro is relatively extensive due to the significant human occupation of the area. Unfortunately, only a couple of hydrological core logs are available close to the seismic profiles. Still, these logs are close enough to the seismic profiles to allow a calibration of the main geological units. The geotechnical logs are mainly near

harbor infrastructures in parts of the lagoon, and several are located in the neighborhood of the surveyed areas. These logs were used for the calibration of the vertical datum of the seismic profiles and for the geological interpretation.

All available borehole, seismic and geographical data were collated into a GIS database (ArcGis, ESRI) which was used throughout this work for spatial computations.

Chapter 2. Setting of the Ria of Aveiro

The Ria de Aveiro is a barrier-lagoon system, located along the northwest Portuguese coast, composed of a complex network of tidal channels, tidal flats, salt marshes and supra-tidal sand isles, separated from the sea by a sand-barrier and inlet, encompassing an area of approx. 530 km^2, making it the largest coastal lagoon system in Portugal. It is located at the mouth of a drainage basin of 3,635 km^2, fed mainly by the Vouga River and its tributaries. The lagoon is a sedimentary basin overlying a Mesozoic bedrock whose topmost sediments consist mainly of Upper Cretaceous age (Maestrichtian). These Cretaceous sediments are mainly mad up of clays also deposited in a barrier-lagoon environment. At depth, the Cretaceous sequence consists of more diverse lithologies (sands, marls, and limestones) and hosts a multilayer coastal aquifer, the Aveiro Cretaceous aquifer, which extends over 1,800 km^2 in the Aveiro region (Condesso de Melo, 2002).

The main morphological, hydrographic, climatic, and geological features that characterize the Ria of Aveiro are presented in the following paragraphs, in order to introduce the basic background necessary to understand the object of this study. Some of this information is partly revisited and further detailed in chapters III, IV and V, tailored to the specific problems addressed in these chapters.

2.1 The barrier-lagoon

Sand-barrier

The natural protection to the Ria de Aveiro lagoon is its shoreface sand barrier system that extends for 100 km, from Espinho, to the north, to Cape Mondego to the south (Fig. I-1). The sand beaches are of an intermediate dynamic domain (between reflective and dissipative) with a prevailing unique submarine bar at water depths of less than 10 m (Teixeira, 1994). The sub-aereal segment of the

beaches extends for 50 to 100 m, and is commonly characterized by a frontal dune, occasionally replaced by sand dykes, that reaches 9 m above the ZH (Hidrographic Zero). Littoral drift transports sediments from the northern river basins (e.g. Douro river basin) and feeds the beaches at the coast of the Ria de Aveiro. This fluvial sediment output as been steadily decreasing for the last 200 years (Teixeira, 1994), and, nowadays, the Ria of Aveiro shoreline suffers from sedimentary deficit, particularly to the south of the lagoon inlet where significant shoreline retreat is occurring (Baptista et al., 2002).

Inlet

The lagoon communicates with the Atlantic Ocean via a dynamic inlet that suffered significant migration in the last 1000. By the late XVIII century the inlet was mostly closed and communication with the Atlantic interrupted (see the evolution of the Ria of Aveiro in Fig. II-1). Only after extensive engineering work at the inlet from the early XIX century until 1950s did the inlet acquire self-regulating capacity; with episodes of shoaling reducing the channel section causing increased current velocities and consequent greater erosion and, conversely, episodes of greater erosion increasing the channel section causing a decrease in current velocities, sediment deposition and shoaling (Abecasis, 1954; Teixeira, 1994; da Silva and Duck, 2001).

Tidal channels

The inner lagoon is composed by a network of tidal channels that crisscross extensive tidal flats and salt marshes. The tidal channels are the deepest morphological elements of the lagoon, and distribute the tidal prism to the interior of the lagoon (see the main tidal channels location in Fig. II-2). A local terminology describes the hierarchy of the hydrographic network: first order channels, also called “Cales”, are always immerse and, generally, become deeper closer to the inlet; second order channels, called ”Esteiros”, promote the connection between ”Cales”, isolate inner isles and almost dry up during more extreme low tides (e.g. neap tides); third order channels or ”Regueiros”, make up the incipient network over the tidal flats and salt marshes; they undergo considerable emersion and are

usually only totally flooded during the second half of the flooding (Teixeira, 1994).

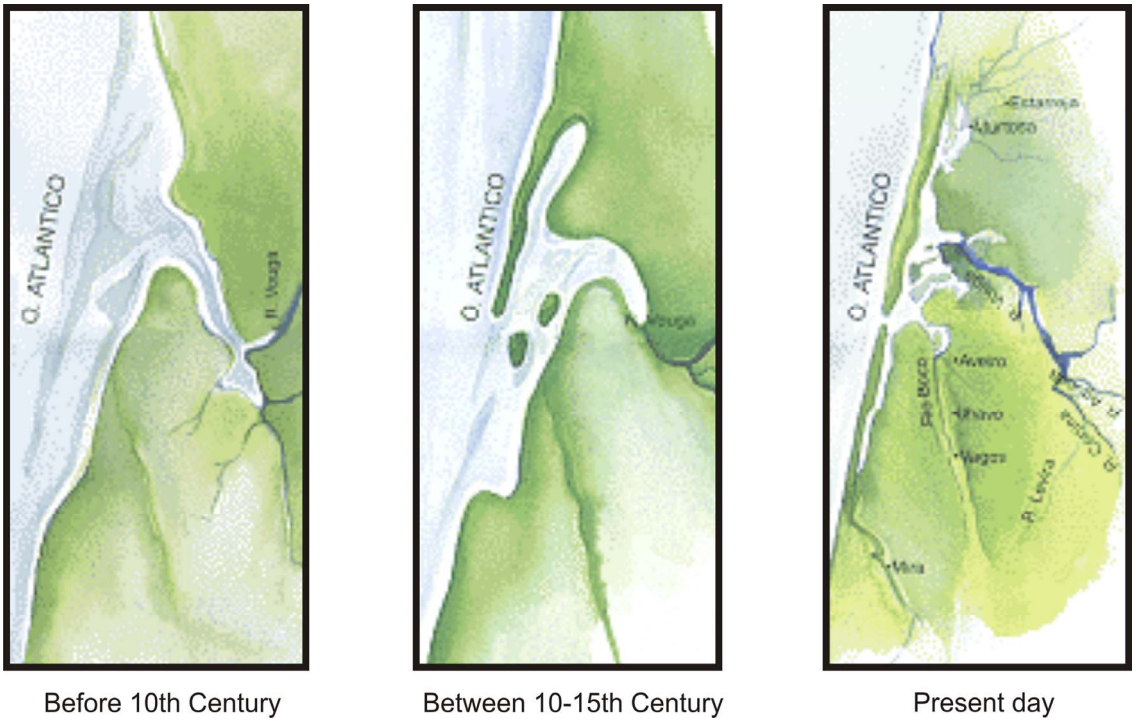

Figure II-1: Evolution of the Ria of Aveiro since Xth century to present day (a colored version by an unknown author of the black and white original from Abecasis, 1954).

Tidal flats

The tidal flats correspond to sandy to muddy deposits neighboring the tidal channels that emerge during low tide and submerge during the highest tides (Klein, 1967; Woodroffe, 2003). Teixeira (1994) described the three main evolution mechanisms for the tidal flats of the Ria de Aveiro.

1. Natural differentiation of tidal flats from the marginal deposits of tidal channels is the primary mechanism for the generation of tidal flats. Margin sediments are reworked by changing tides forming flat surfaces which are drained by an incipient runoff channel network, and dip slightly towards the tidal channels.

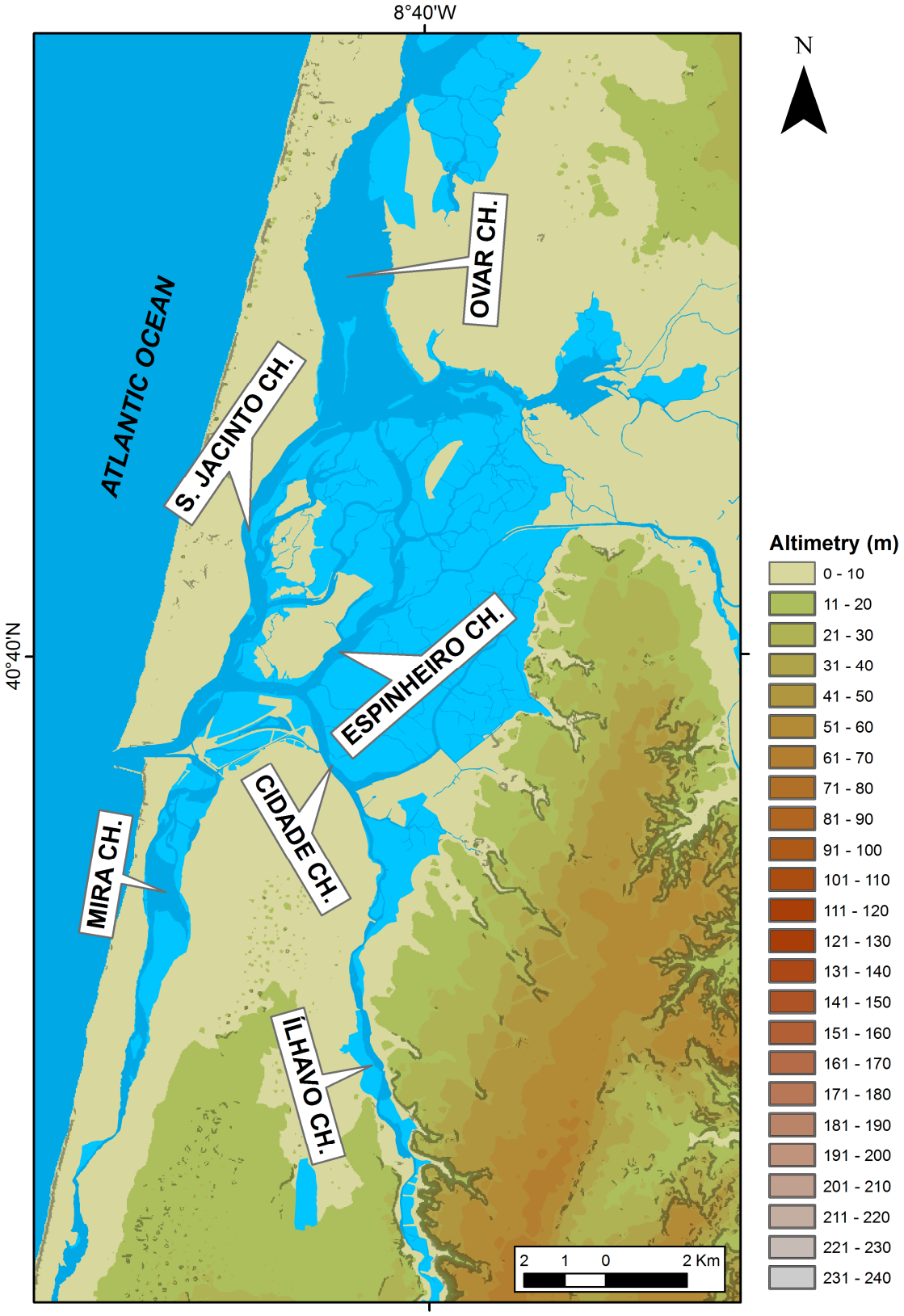

Figure II-2: Location of the main tidal channels of the Ria of Aveiro.

2. Increasing tidal amplitudes during the second half of the 20th century are responsible for the majority of the tidal flats in the Ria de Aveiro (Teixeira 94). This process increases channel bottom erosion, steepens channel margins and favors marsh levee construction, frequently colonized by Spartina. In this case tidal flats are formed from levee reworking.
3. The increase in tidal amplitudes sometimes causes the formation confined basins dominated by tidal flats. This confinement is accomplished within an area delimited by connected tidal channels through marsh levee buildup, as described in point 2. The levees only allow inundation to occur near high tide, when most sediment transport occurs through suspension, causing the shoaling of these basins with flattened fine sediment deposits.

Salt marshes

The salt marshes are upper intertidal environments of mostly muddy sediments covered by a variety of halophyte vegetation (salt tolerant). They can be sub-divided in upper and lower salt marshes according to their degree of emersion which, in turn, determines flora distribution. The lower salt marshes are characterized by relatively higher salinity and longer periods of emersion, whereas the upper salt marshes are characterized by lower salinity and better oxygenation. Teixeira (1994) presents a case study illustrating the speed of the evolution of salt marshes in the Ria de Aveiro, where a tidal flat evolved to a salt marsh in approximately one century, indicating sedimentation rates of approximately 1.0 cm/year. The upper marshes comprise 90% of all marshes of the Ria de Aveiro, cover approximately 35% of the intra-lagoon space, and most of the marsh deposits were already in place by late XVIth century (Teixeira, 1994).

2.2 Climate and river discharge

The climate of the Aveiro region is characterized by a prevalence of westerly winds during the winter which induce instability and precipitation. Arid conditions prevail during the summer due to the northwards movement of the North Atlantic anti-cyclone, which carries with it the precipitation front. Thus, winter

precipitation tends to be three times larger than the precipitation during the summer.

Average temperature fluctuates between 6ºC during the winter and 20ºC during the summer (Faria and Machado, 1979; Rebelo, 1992). Average annual precipitation in the lagoon is about 1000mm, and, usually, the October-March period receives ca. 75% of the annual precipitation and the summer trimester only receives 5%. The total drainage network that feeds the Ria of Aveiro is of 3109 Km^2 and includes nine hydrographic basins: 1 - Ovar creek; 2 - Antuã river; 3 - Vouga river; 4 - Angeja creeks; 5 - Aveiro creeks; 6 – Águeda river; 7 - Boco river; 8 - Cértima river; 9 – Mira river (see Fig. II-3). According to Loureiro *et al.* (1986) potential evapotranspiration of the Ria de Aveiro basin is of 730 mm, i.e. smaller than the average precipitation in the same area.

The annual surface runoff to the Ria de Aveiro lagoon is approximately 2.0 km^3, corresponding to an average output of $1.37x10^6$ m^3 for each half tidal cycle (6h) (Teixeira, 1994). It should be noted that there are strong asymmetries in the runoff during the year, with the average annual runoff being approximately one tenth of the maximum annual runoff.

Wind regime in the Ria de Aveiro is dependent on the dynamics of the Azores anticyclonic cell (Fiúza et al., 1982). The regime of steady northerly winds during the summer changes to more volatile conditions during the winter with frequent changes in wind direction. The thermal gradient between the ocean and continent, that changes with the day and night cycle, causes a local breeze climate that overprints the annual wind regime. Typically, daytime is marked by a westerly to northwesterly wind, which becomes increasingly stronger towards the afternoon. During the night, the winds rotate, blowing from the east to southeast, usually with lower velocity than during the day. The local wind regime is more obvious during the summer, when the regional wind regime is weaker.

2.3 Hidrography

The tide is the main forcing factor inside the lagoon. The tidal currents mobilize and distribute the sediments, producing the tidal flats and feeding the

sediments to the marsh. The tidal flooding carves an internal channel network and carries marine salt into the lagoon. Tides are predominantly semi-diurnal, with an average amplitude at the inlet of 1.90 m, ranging between 1.22 m and 2.57 m, during neap and spring tides respectively (Teixeira, 1994). The tidal amplitude decreases with the distance from the inlet, but it is present in the entire lagoon. The phase lag, variable in high and low water, increases upstream up to 5 hours, with low and high tides sometimes occurring simultaneously in different parts of the lagoon (Dias et al., 2000a). Water volume at low spring tides is 65 hm^3 and the tidal prism at spring tides is about 80 hm^3, with an estimated time of residence of the water of three days (Teixeira, 1994). The tidal prism has gradually increased since the beginning of the century due to the engineering work done on the inlet. According to Teixeira (1994, and work referred therein), from 1900 to 1930 the spring tide tidal prism should not have been larger than $25x10^6$ m^3, and the neap tide tidal prism half of this value. As the inlet and tidal channels stabilized with the engineering works post 1930, gradually the tidal prism increased by $1x10^6$ m^3 per year to the actual values and marine invasion spread into the lagoon (see Fig. II-4). Also, the tidal prism is significantly larger than the fluvial input to the lagoon, with the fluvial input being only equal to the volume of the prism of neap tides for one tide every 5 years.

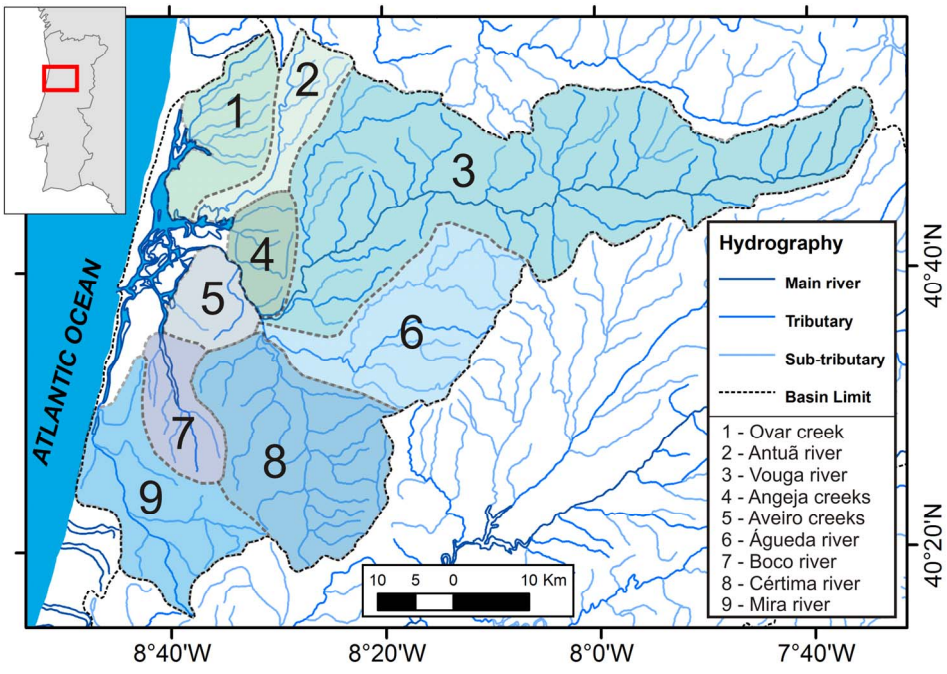

Figure II-3: Hydrographic basins of the Ria of Aveiro (adapted from Teixeira, 1994).

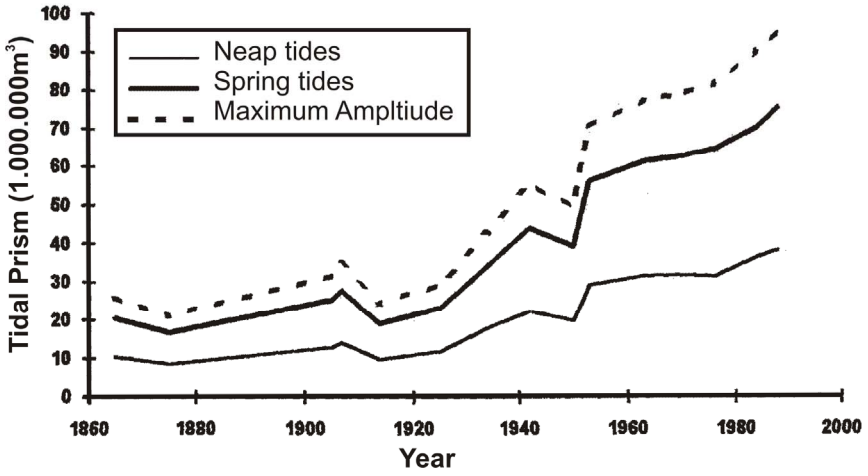

Figure II-4: Tidal prism evolution of the Ria of Aveiro in the last 125 years (Teixeira, 1994).

The tidal prism is distributed asymmetrically into the lagoon; the Mira channel to the south of the inlet receives 10% of tidal prism volume, whereas the three subsidiary channels of the main navigation channel, S.Jacinto, Espinheiro and Cidade, receive respectively 34, 34 and 12% of the prism and the remaining 10% occupy the surface of the common channel (Teixeira, 1994).

The offshore wave agitation is related to the North Atlantic wind regime, with predominant directions from the North during the summer, and with increasingly varying directions as the winter progresses. The modal and average wave origin direction is from WNW and maximum wave heights decrease as the wave origin direction rotates to the NW. The observed wave period ranges from 6s to 18 s, with a modal value around 9-11 s, for every wave direction. The average wave height is 2 m and approximately 35% of waves recorded during a year have greater heights. According to Teixeira (1994), three quarters of the sediment transport is carried by waves lower than 6 m, whereas storm conditions are only responsible for 20% of the sediment transport. Wave conditions at the shoreface of the Ria de Aveiro are relatively stable due to the fact that the relatively smooth water bottom and linear coastline preclude the occurrence of preferential locations for wave energy concentration (Abecasis et al., 1968).

The Ria of Aveiro functions as a well mixed estuary close to the inlet, and progressively behaves as a more stratified estuary upstream. During high tide, the salinity is maximum, and falls during ebb until it reaches minimum value at low tide, with a resultant residual salt transport into the lagoon (Matos, 1990). Salinity values are typically high, around 3.5%, comparable to marine salinity, under the more common conditions of low fluvial runoff (Teixeira, 1994). As with the tidal prism, and for the same reasons (i.e. changes in the inlet), the salinity regime in the lagoon was significantly different in the beginning of the century, with high salinity limited to the proximity of the inlet and to the lower water layer up to S.Jacinto channel (Nobre, 1915 in Teixeira, 1994).

The analysis of previous work on the tidal and salinity regimes of the lagoon allowed Teixeira (1994) to conclude that the work on the Aveiro inlet during the 1950s significantly altered the hydraulic regime of the lagoon: “The tidal amplitude and the daily water outflow nearly doubled at the inlet. As a consequence, the relative importance of the fluvial debit contracted, allowing the appearance and expansion of the sedimentary environments of lagoon zones. The Ria de Aveiro, that, during the last centuries, had the common attributes of an estuarine environment, literally grow, and, from 1950 onwards, became a genuine coastal lagoon (translated from the original).”

2.4 Geological framework

The Ria of Aveiro is a Holocene sedimentary basin located in the northernmost part of the Lusitanian basin, a rift-basin formed during the Mesozoic opening of the North Atlantic Ocean. The basement underlying the Lusitanian basin is the Variscan orogen, mainly made up of igneous and sedimentary rocks metamorphosed during the Paleozoic (see geological map of the region in Fig. II-5). The geodynamic evolution of the Ria of Aveiro region reflects the major extensional and compressional events caused by the relative movements of the Eurasia, Africa and Iberia from Triassic till the Present (for an overview of the geodynamic evolution of the Iberian Peninsula see Andeweg, 2002) .

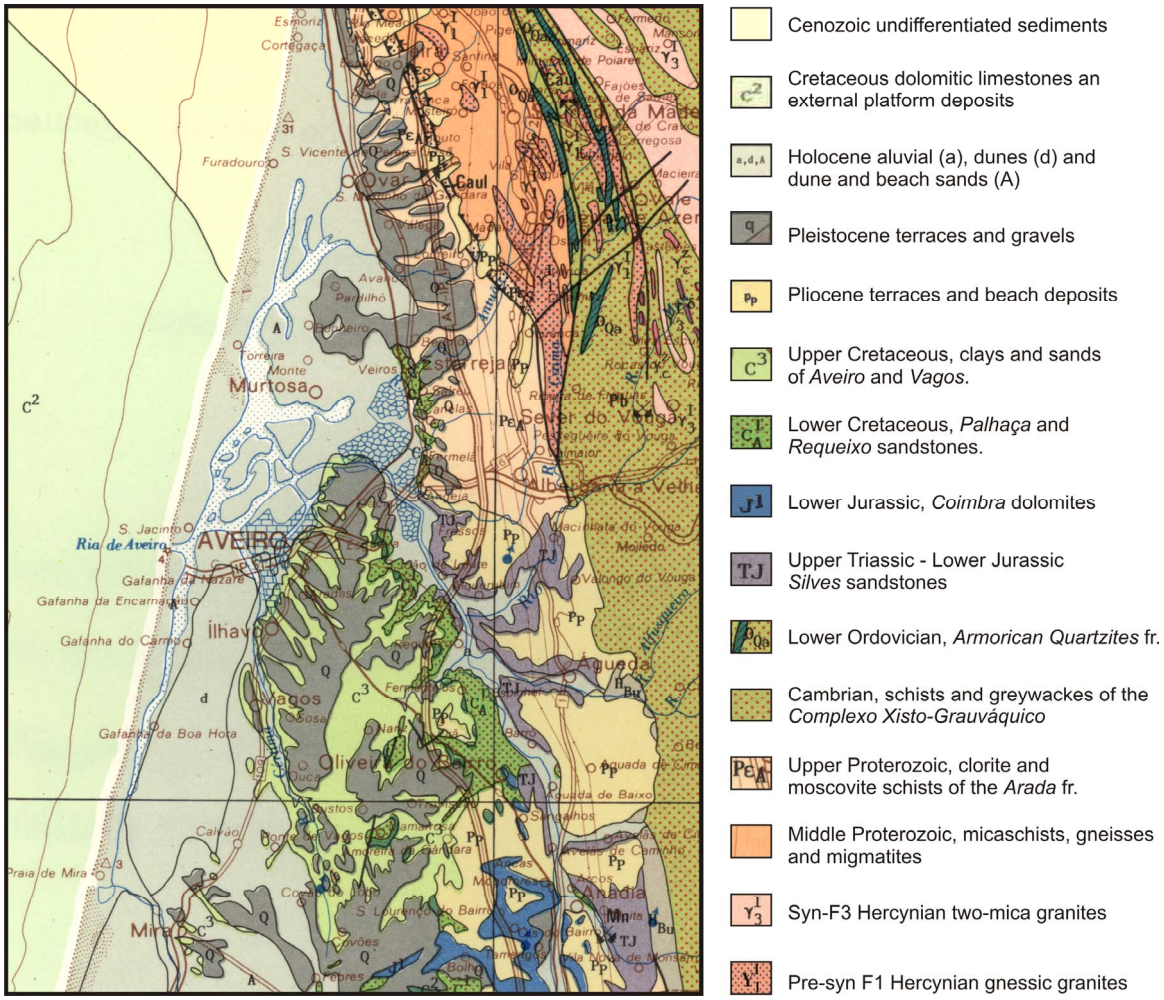

Figure II-5: Geological map of the Aveiro region (from the Geological Map of Portugal 1:500.000; Oliveira *et al.*, 1992).

The Western Iberian margin experienced two major stages of rifting separated by periods of quiescence, from the Triassic to the Cretaceous, which strongly controlled the stratigraphy and tectonic evolution of the Meso-Cenozoic sedimentary basins of the Portuguese continental margin (Boillot *et al.*, 1979; Ribeiro *et al.*, 1979; Vanney and Mougenot, 1981; Uchupi, 1988; Wilson *et al.*, 1989; Pinheiro *et al.*, 1996; Rasmussen *et al.*, 1998; Andeweg, 2002; Alves *et al.*, 2003b). Folds and thrusts within the Hercynian basement trend NW-SE, at an angle to the NNE-SSW trend of the main Lusitanian rift faults. Various NNE-SSW left-lateral strike-slip faults, formed during the late Variscan fracturing event of Permian age faults, functioned as rift half-graben faults, defining syn-rift fluvial

clastic depocenters. These faults were also later reactivated with strike-slip movement, during the Tertiary Alpine orogenesis (Uphoff et al., 2002).

The first rifting stage occurred during Late Triassic to Early Jurassic. The important regional hiatus that follows the Early Jurassic rifting is probably related to the opening of the Central Atlantic Ocean, for it coincides with the beginning of oceanic spreading at the Iberian Abyssal plain at 126 Ma (Whitmarsh and Miles, 1995).

Two other extensional phases are described, one during the Late Jurassic and another during the Late Jurassic and Early Cretaceous (Wilson *et al.*, 1989; Rasmussen *et al.*, 1998). These phases of deformation were more pronounced in outer basins of the Western Iberian Margin and the Lusitanian basin became part of an aborted rift with relatively limited subsidence since then. Regional uplift occurred during the Callovian to Early Oxfordian and, in the Lusitanian basin, this was followed by fault-block rotation and rapid subsidence along NNE-SSW trending faults during Late-Oxfordian-Earliest Kimeridgian.

During the Early Cretaceous the Lusitanian basin sedimentation was characteristic of a post-rift regime (Dinis et al., 2008). Fault controlled subsidence and halokinesis determined the deposition of a mixed carbonate-siliciclastic system. The sedimentation changed laterally from shallow carbonates in topographic highs to fluvial-deltaic siliciclastic deposits close to the water lines, which gradually passed to marine shale and limestones towards the deeper parts of the basin (Bernardes, 1992).

In sharp contrast with the Mesozoic, the Cenozoic in the Western Iberia is characterized by periods of compressional deformation related to the Pyrenean and Alpine orogenies. The closure of the Bay of Biscay-Piyrenean zone migrated to the west and caused the inversion of the Mesozoic extensional basins (Garcia Mondejar, 1988). The short-lived southward subduction of the oceanic crust in the Biscay region during the latest Cretaceous to Early Eocene (Boillot and Mallod, 1988) formed the Cantabrian Cordillera in the north of the Iberia. Sedimentation in the Lusitanian basin during the Pyrenean compression was controlled by pre-existing late Variscan basement faults, often amplified by halokinesis, sometimes leading to the formation of diapirs that pierced the entire sedimentary cover (Alves

et al., 2003a).

Sedimentation during the Paleogene consisted mostly of sands and conglomerates, while in the Neogene, sedimentation evolved to shallow marine clastic and carbonate deposits due to subsidence and marine transgression. The NNW-SSE compression was mostly accommodated by ENE-WSW thrusts and by pre-existing NNE-SSW and NW-SE faults.

The main NNW convergence between Africa and Eurasia changed to NW in Tortonian, and triggered the build up of the Betic range. The end of the frontal convergence of Iberia and Eurasia around 30 Ma also marked the activation of the right lateral Azores-Gibraltar plate boundary (Srivastava et al., 1990).

According to a review by Andeweg (2002), the whole of Iberia exhibits high level of internal deformation during the Plio-Pleistocene, evidenced by crustal scale folding (Cloetingh et al., 2002), large scale Pliocene uplift of several hundreds of meters in coastal areas (Janssen et al., 1993), present day seismicity (Buforn et al., 1988) and the development of new crustal shear zones in the Alboran basin (Andeweg, 2001) as well as south of Portugal in the Gulf of Cadiz (Rosas *et al.*, 2008; Zitellini *et al.*, 2009). All this evidence records the ongoing convergence between Africa and Iberia (Argus *et al.*, 1989). In the North Lusitanian basin, Pliocene sedimentation recorded multiple transgression and regression cycles. Several erosional surfaces developed during the Quaternary, and deposition consisted mainly of coarse sand and gravel, often affected by mild neotectonic movements (Rocha, 1993; Granja *et al.*, 1999; Dinis, 2004).

Recently compiled evidence in Western Iberia of regional progressive rotation of the compression direction (S-Hmax), from NNW-SSE to WNW-ESE, since the upper Pliocene the led Ribeiro *et al.* (1996; 2002) to propose the hypothesis that a North Atlantic westwards subduction is initiating in the western Iberian margin, marking a major shift of plate dynamics in the region.

Lithostratigraphy

The lithostratigraphy of the Aveiro region comprehends, from bottom to top, Proterozoic-Paleozoic Variscan metasediments and plutonic rocks, followed by Mesozoic Atlantic-rift deposits, culminating in Pleisto-Holocene estuarine and

lagoon sediments (see synopsis of the lithostratigrapy in Table II-1). Rocha (1993) points out the occurrence of Tertiary “relics” in the geological logs of boreholes drilled along the Aveiro littoral, between the villages of Gafanha and Muranzel. This section provides a short lithostratigraphic account of these rocks with emphasis on the Upper Cretaceous and Quaternary sedimentary units, which, as will be explained in future chapters, are of particular relevance for this work.

The Variscan bedrock consists of mica schists and schists of Proterozoic age, with occasional Proterozoic gneisses, migmatites and Paleozoic granitoids in the northern part of the Aveiro region. It is exposed close to the Porto-Tomar fault, along a NNW-SSE trend, east of the Ria of Aveiro. The basement dips westward and is faulted by N-S and NNE-SSW faults, forming a system of horsts and grabens.

The onshore and offshore stratigraphy of the Lusitanian basin has been investigated by multiple authors (e.g. Berthou, 1973; Teixeira and Zbyszewski, 1976; Berthou and Lauverjat, 1979; Boillot *et al.*, 1979; Ribeiro *et al.*, 1979; Barbosa, 1981; Vanney and Mougenot, 1981; Wilson *et al.*, 1989; Bernardes, 1992; Rocha, 1993; Alves *et al.*, 2003a; Dinis *et al.*, 2008). The Ria of Aveiro region corresponds to the northernmost part of the “Beira Litoral” sub-basin of the Lusitanian basin. It is characterized by two significant hiatus in the stratigraphic sequence during the Carixian-Aptian and Late Cretaceous-Pliocene.

The Mesozoic lithostratigraphy ranges from the Upper Triassic, Rhaetian stage, red marly-clayey sandstones of the “Grés de Eirol” formation, to the clays, marly clays and carbonates of the Upper Cretaceous, Campanian-Maastrichtian stage, “Argilas de Aveiro” formation (see synopsis in Table II-1).

The “Argilas de Aveiro” formation is of particular interest for this work because the Pleisto-Holocene sediments of the Ria of Aveiro frequently occur directly on top of it. The “Argilas de Aveiro” formation consists of the grayish marly clays, with occasional important sand content and with marly limestone layers deposited during a long regression in temperate climate. Towards the base, sediments become gradually coarser marly-sands, with bottom deposits mostly of sandstones. Clay mineralogy is very homogenous, dominated by illite followed by calcium smectite (Rocha and Gomes, 1989).

Table II-1: Synopsys of the lithostratigraphy in the north part of Aveiro region (from Condesso Melo, 2002)

Era	Period	Stage	Lithostratigraphic Units		Lithology
CENOZOIC	QUATERNARY	Holocene	Sand dunes, eolian and beach sands, alluvials		Fine to medium sands
		Plio-Pleistocene	Old beaches and alluvial terraces		Medium to coarse sands with some clayey levels
MESOZOIC	CRETACEOUS	Campanian-Maastrichtian	'Aveiro clay formation', C_3		Clay and marly clay, with some carbonate levels
		Coniacian-Santonian	Upper sandstone formation, C_3	'Verba sandstone'	Marly sandstones and sandy marls
		Upper Turonian-Lower Coniacian		'Oiã sandstone'	Clayey sandstones and sandy clays
		Upper Cenomanian-Turonian	'Furadouro sandstone', C_2		Coarse to medium micaceous sandstone, with some marly-clayey levels
		Cenomanian	Carbonate formation, C_2	'Mamarrosa limestone'	Marly limestone, marls and fine marly sandstone
		Aptian/Albian-Lower Cenomanian	Lower sandstone formation, C_{1A}	'Palhaça sandstone'	Medium to coarse sub-arkosic sandstone
	JURASSIC	Carixian-Domerian	'Eiras marls'		Sandy marls and marly sands
		Upper Lotharingian-Lower Carixian	'Camadas de S. Miguel'		Marly limestone
		Sinemurian-Lower Lotharingian	'Camadas de Coimbra s.s.'		Marly dolomitic limestone
		Hettangian	'Dagorda marls'		Sandy marls
	TRIASSIC	Rhaetian	'Eirol/ Silves sandstone'		Red marly-clayey sandstone
PALEOZOIC	CAMBRIAN				Granitoids
PRE-CAMBRIAN	PROTEROZOIC		Schist-grauwaque Complex		Mica schists, schists migmatites and gneisses

The unit is roughly uniform in the Aveiro region, with thicknesses over 150 m near the coast. Bernardes (1987) defined four facies associations of a coastal plain system for the Argilas de Aveiro formation. *Association I* corresponds to subtidal conditions of a barrier-lagoon complex, with central and marginal lagoon deposits as well as washover deposits. *Association II* deposited in intertidal conditions, consists of mud flat deposits with recurrent exposure and inundation periods. *Association III* includes sandy deposits of high sinuosity tidal channels, small tidal creeks with simple architecture and larger and more complex tidal inlets. *Association IV* deposited in supratidal conditions, with sedimentation governed by vegetation colonization.

The Pliocene, Pleistocene and Holocene deposits are mainly recent alluvial and sand dunes of Holocene age, old beach deposits and fluvial terraces of

Pleistocene age (mainly clays and clayey sands in the upper part and coarse sands and pebbles at the bottom). Lagoon sedimentation occurs over a marine ravinement surface related to the Holocene marine transgression (see Dias et al., 2000b for a synthesis on coastal evolution and marine transgression in Portugal). Investigation of the sediment record in the sand barrier has provided some insights on the onset and development of estuarine and lagoonal sedimentation in the Ria of Aveiro. Galera *et al* (1997) described three minor sedimentation cycles in the Mira channel related to the last 1000 years: 1) “Ancient Cycle” of estuarine sedimentation of muddy facies, prior to the 16th century; 2) “Recent cycle” of subtidal channel deposits of sands and intertidal mudstones and tidal sand bars; 3) “Present cycle” sedimentation of subtidal channel sands and mudstones related to the opening of the artificial inlet. A more recent study of the sand spit evolution between Torreira and Furadouro, the northern branch of the sand-barrier (Bernardes and Rocha, 2007), also describes three sedimentary units which may in part correlate with the sedimentation cycles described by Galera (1997): a lower unit of estuarine lagoonal deposits developed in retrograding conditions of stationary sea level which indicates the lagoon was formed prior to 1997-1992 years BP; a middle unit related to landwards prograding sand ridges, possibly associated with minor sea level rise; and an upper dune unit related to a period of shoreline stability.

2.5 Gas in the Lagoon

Early descriptions of possibly methane gas related phenomena in the lagoon area date back to the 1755 great Lisbon earthquake. The answers from local parishes to the Marquês de Pombal enquiries on the 1755 earthquake report that the Vouga river waters “boiled as if they were on fire” and that the waters from the Mira lagoon (at the south end of the Ria) “appeared to boil so hard that they would break at the lagoon shore as if they were sea waves” (Coelho, 2005; Oliveira, 2005); these tales may be explained by gas releases from seismically destabilized sediments. The first unequivocal direct observations of escape of

biogenic methane from several drill holes in Quaternary sediments from the area surrounding the Ria of Aveiro were reported by the Portuguese Geological Survey in 1967 (Faria et al., 1967). Since then, similar evidence has been observed in other land wells for water exploration. During previous work, Duarte et al. (2003) identified several high-backscatter patches on sidescan sonar images acquired in the Ria de Aveiro by the Portuguese Hydrographic Institute in 1998, which they interpreted as related to gas escape. Recently, in September of 2006, gas samples were collected from extensive bubble trains observed during falling tide in a docking pier ("Doca Pesca") in the Ria of Aveiro (Pinheiro and Duarte, 2006, unpublished data). The analysis of the samples revealed that the gas composition was mostly methane (Luis Pinheiro and João Coutinho, personal communication).

Chapter 3.

Acquisition and processing of high-resolution seismic reflection profiles in shallow coastal lagoons: Case study of the Ria of Aveiro (Portugal)

Duarte H. & Pinheiro, L. M. (to be submitted)

This chapter is presented in a paper format to be submitted to a peer reviewed SCI journal.

Abstract

This paper addresses the methodological problems and limitations associated with the acquisition and processing of high-resolution seismic reflection data (Boomer and Chirp systems) in very shallow water systems such as estuaries and lagoons. Examples from the Ria of Aveiro, a shallow barrier lagoon located in NW Portugal, are shown. The main limitations are: ship traffic, tides and channel morphology and bathymetry, which often affect the deployment and operation of the seismic systems, and the extent of the profile coverage. The processing of the navigation data included data errors detection, system clock synchronization corrections, layback adjustment and trace midpoint position estimation. The seismic signal processing consisted in amplitude corrections, burst noise removal, static corrections, normal move-out corrections, frequency band pass filtering, signature deconvolution and migration. The analysis of the track line regularity, the horizon misties and the first-break surface models were applied as quality control procedures, and allowed the revision and improvement of the processing parameters. The heterogeneity of the seismic coverage, signal quality, penetration and resolution all constrain the use of the data to mostly local but detailed interpretations of the geological objects of the Ria of Aveiro. A new procedure is proposed to determine adequate scales for the geological interpretation based on the seismic resolution, known positioning errors and mean mistie values.

3.1. Introduction

3.1.1. Objectives

The present work addresses the methodological problems faced in the study of the bedrock structure and sediment architecture in shallow water estuarine and lagoon systems using very high-resolution 2-D seismic reflection systems (Boomer and Chirp). A case study of the Ria of Aveiro barrier lagoon (Portugal) is presented. The study of the bedrock structure and sediment architecture with seismic reflection methods requires adequate and reliable seismic imaging of the geological features. For this purpose, a precise control of the seismic data acquisition conditions and of the accuracy in the positioning is essential. Data processing is frequently necessary to improve positioning quality, as well as to enhance the interpretability of the seismic signal.

The persecution of such broad methodological goals in this study met with an uncommon conjunction of obstacles for the case of the Ria of Aveiro. The seismic reflection data acquired in the Ria of Aveiro is of multiple vintages, with various acquisition systems, navigation systems and operational procedures and conditions. Various characteristics of the Ria of Aveiro further constrained the seismic acquisition, affecting signal quality, the systems deployment geometry and the characteristics of the seismic coverage. Variable and frequently high current speeds caused by tides and winds affected signal quality due to turbulence caused by drag effects on the towed equipment; the system geometry was affected by frequent changes of ship direction due to the abundant navigation hazards (e.g. fishing nets, ship traffic, etc) that are common in the lagoon; also, the 2 meter tidal range and several hours tidal lag inside the lagoon caused a constant and difficult to control change in the vertical datum of the seismic data. The very shallow waters in most of the lagoon meant that seismic acquisition was limited to the deeper, navigable, tidal channels, and that the seismic coverage was very irregular within the lagoon.

In order to address these problems the following specific objectives of this paper are:

1. To describe the data acquisition systems and to document the operational procedures used.
2. To propose specially tailored data processing flows of the seismic signal and navigation data and to discuss the results of the application of these flows to the available data.
3. To assess the constraints imposed by the processed seismic dataset on the interpretation and mapping of geological features.

3.1.2. State of the art

High resolution seismic reflection surveying of the Ria of Aveiro started in 1986 (Monteiro and Pinheiro, 1986; Moreira, 1988; Teixeira and Pinheiro, 1998) and a total of five surveys with Chirp and Boomer systems were carried out until late 2003. Three of these surveys were done in the scope of this project and data from earlier surveys were revisited and also discussed here. Most of the publications from other high resolution seismic reflection surveys conducted in somewhat similar systems, conditions and environments such as the Venice lagoon (McClennen et al., 1997; Zechhin et al., 2008) and the Rias Bajas of Galicia (Ferrin et al., 2003; Garcia-Gil, 2003), do not address in detail the data acquisition and processing challenges of acquiring high resolution data in very shallow coastal environments.

A seismic survey of a sub-tidal to intra-tidal area in the Bay of Fundy, Canada, bypassed a significant part of the navigation and geometry control problems addressed in this work through technical innovations of the seismic acquisition systems (Dashtgard et al., 2007). The authors of that study used a boomer system that had its signal source mounted together with the receiver array in a single catamaran, which simplified the deployment geometry, and also resorted to RTK-GPS to infer tidal heights with centimeter precision.

Research in very high-resolution 3-D seismic reflection systems is the current field of study where the issue of the relationships between shallow water seismic acquisition and processing and the characteristics of the study object has had more attention. Marsset *et al.* (1998) have emphasized the importance of tidal

correction in shallow coastal environments in order to improve the correlation between profiles. Missiaen (2005) provides insights on how the work in shallow water environments and at high frequencies implies constraints on sampling, array directivity and positioning accuracy, constraints that are in good part also found in the work in the Ria of Aveiro. An example of how to tackle the challenges in positioning of 3-D seismics that deals with issues such as data quality control and navigation and seismic systems integration, which are also present in this work, can be found in the technical report of a 3-D seismic survey in the Gulf of Cadiz (Duarte, 2006).

General signal processing workflows for single and multi channel seismics can be found in multiple books (e.g. Yilmaz, 1987; Sheriff and Geldart, 1995). Proposed processing flows for chirp systems generally consist of match filtering, Hilbert transform and instantaneous amplitude computation (for reviews on chirp processing see Quinn *et al.*, 1998; Henkart, 2006). Published boomer signal processing flows typically include static corrections to compensate for swell and/or tides, spherical divergence correction, frequency bandpass filtering, spike deconvolution and, occasionally, a constant velocity time migration (Dashtgard et al., 2007).

3.1.3. Seismic surveying and the hydrography of the Ria of Aveiro

The seismic reflection acquisition in the Ria of Aveiro was significantly controlled by morphological characteristics of the navigable waterways, as well as by its tidal and current patterns. The Ria of Aveiro is composed by an intricate network of tidal channels that crisscross extensive mud flats and salt marshes (see Fig. III-1). The tidal channels correspond to the deeper lagoon segments through which the tidal prism is distributed to the interior of the lagoon. A local nomenclature describes the hierarchy of the hydrographic network: first order channels, also called “Cales”, are always immersed and, generally, become deeper closer to the only inlet of the lagoon barrier; the second order channels, called “Esteiros”, promote the connection between different “Cales”, isolate inner isles and almost dry up during more extreme low tides (e.g. neap tides); third order

channels, or “Regueiros”, make up the inicipient network over the tidal flats and salt marshes, undergo considerable emersion and are usually only totally flooded during the second half of the flooding (Teixeira, 1994).

The tidal flats correspond to flattened deposits neighboring the tidal channels that occur at depths between spring low tide altitude and the average tidal altitude. The upper limit corresponds to the surface marking predominant emersion and coincides with the minimal altitude for the halofite colonizations, typically *Spartina* (Teixeira, 1994). The salt marshes are upper intertidal environments of mostly muddy sediments covered by a variety of halofite vegetation (salt tolerant).

As the surface area of the Ria of Aveiro consists predominantly of tidal flats and salt marshes (over three quarters of the lagoon area), seismic coverage of the lagoon was spatially constrained, for it was limited to the deeper tidal channels. The first order, navigable tidal channels, where most of the Aveiro harbor facilities are located, suffer from heavy cargo ship traffic. This heavy traffic coupled with the abundant fishing nets deployed haphazardly, sometimes with poor signalization, constituted serious navigation hazards during acquisition and were the cause of multiple trackline irregularities. Also, hydrographic surveys were not available outside the main harbor area and navigation channels, and all the surveying into those areas required careful monitoring of the water depth. Still, even with great care, the towed equipment was accidently grounded a couple of times. Success in navigating the uncharted waters was due to the vast experience and personal knowledge of the lagoon of the harbor pilots that commanded the survey vessels.

Tides in the Ria of Aveiro are predominantly semi-diurnal, with an average amplitude at the inlet of 1.90 m, ranging between 1.22 m and 2.57 m, during neap and spring tides respectively (Teixeira, 1994). The tidal amplitude decreases with the distance from the inlet, but it is present in the entire lagoon. The phase lag, variable in high and low water, increases upstream up to 5 hours, with low and high tides sometimes occurring simultaneously in different parts of the lagoon (Dias et al., 2000). Available tide prediction data had to be used to control this complex tidal behavior, because no altitude data was recorded during acquisition (see tide prediction locations in Fig. III-1).

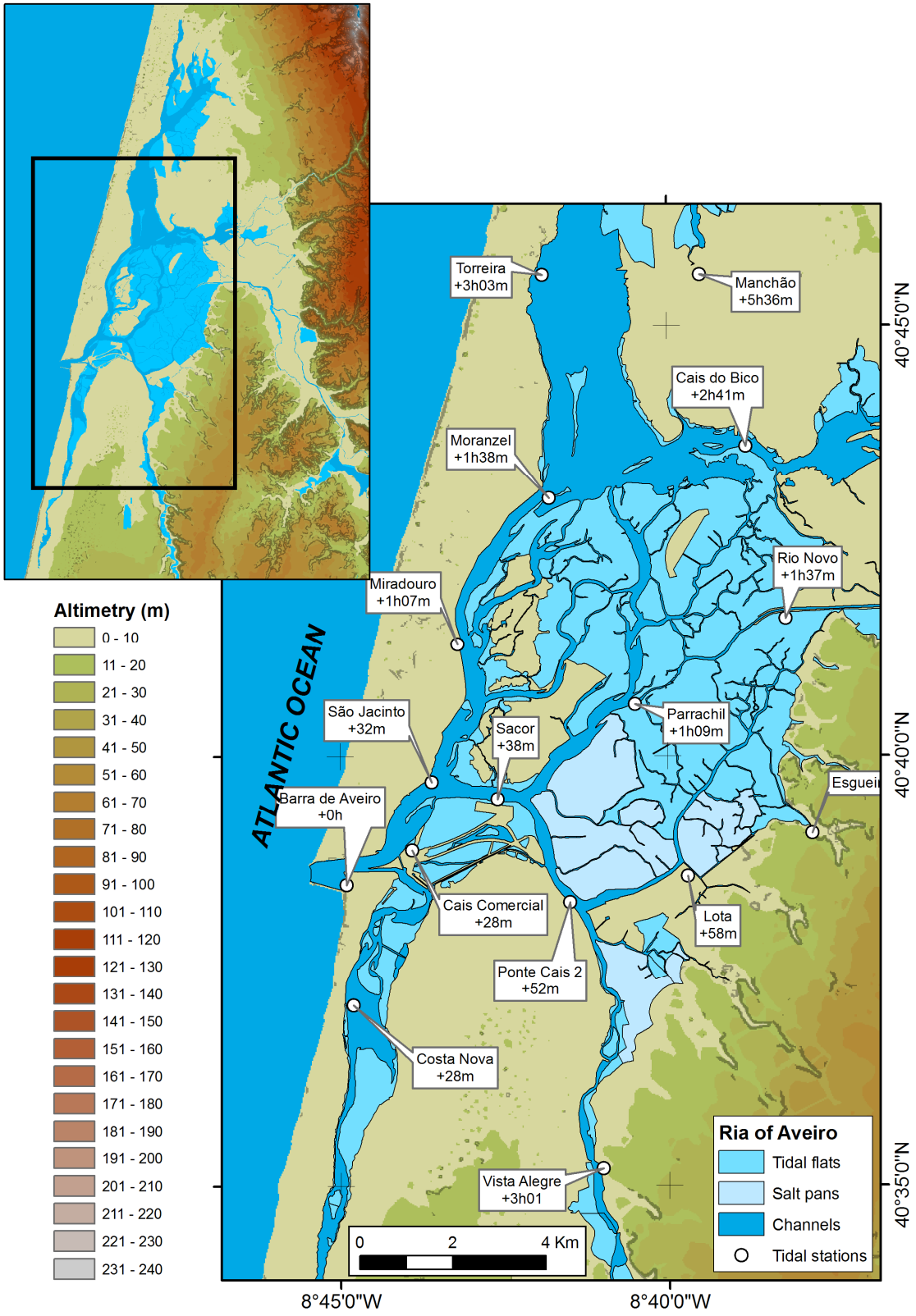

Figure III-1: Hidrography of the Ria of Aveiro. Labeled locations indicate the name of the tide prediction stations, followed by the estimated delay of the low tide during spring tides, according to the tide table of the Aveiro harbor Authorities (APA).

The strong influence of tides in the lagoon was particularly felt during ebb when current speeds could reach up to 5 knots closer to the inlet. Such strong currents caused significant difficulties in handling the ship at the low survey speeds (normally 4-5 knots). Navigation against the tide caused increased drag on the towed equipment, and the turbulence produced noise was recorded by the seismic systems. On the other hand, navigation with the tide direction sometimes caused the equipment to lose its planned deployment geometry because current speeds closely matched surveying speeds.

Currents in the Ria of Aveiro are also sometimes significantly influenced by winds. The Ria of Aveiro has a regime of steady northerly winds during the summer that changes to more volatile conditions during the winter, with frequent changes in wind direction. Typically, daytime is marked by a westerly to northwesterly wind, which becomes increasingly stronger towards the afternoon (Teixeira, 1994). The stronger afternoon wind promoted stronger currents and turbulence in the upper water layer, which introduced noise to the seismic records. The worst surveying conditions occur when a strong afternoon wind coincides with an ebbing tide close to the lagoon inlet.

3.2. Methods and data

The seismic data used in this work was acquired between 1986 and 2003 (Monteiro and Pinheiro, 1986; Pinheiro and Monteiro, 1999; Pinheiro and Duarte, 2003a; Pinheiro and Duarte, 2003b; Pinheiro *et al.*, 2003). Naturally, the seismic and navigation systems deployed and modes of operation were specific to each survey and evolved through time. This chapter presents the data acquisition systems and the geometry parameters that describe their deployment which are relevant for data processing. This is followed by the technical summary specific to each survey, including objectives, equipment and operational details. Finally, the data quality control protocol is described, and the navigation and seismic signal processing flows explained.

3.2.1. Data acquisition systems

The seismic data acquisition systems in this work were an EG&G Uniboom system with a boomer source and a Datasonics Chirp Sonar system with a modulated chirp source. In broad terms, these systems comprise an energy source that powers a signal source, a hydrophone receiver array and a recording unit (for an overview on high resolution seismic reflection systems see Mosher and Simpkin, 1999).

The EG&G Uniboom system (Boomer)

The EG&G 230-1 UNIBOOM (Unit Pulse Boomer) is a high resolution seismic reflection system with a boomer source which has a signal frequency bandwidth ranging from 400 to 14000 Hz. This boomer unit has three modes of operation: 700-14000 Hz and a maximum of 6 pings per second (pps) for 100 watt-second energy level; 500-10000 Hz and 5 pps for 200 watt-second and 400-8000 Hz and 3.3 pps for 300 watt-second. The signal source is mounted on a catamaran that can be towed at 2 to 8 knots with a 30.5m long cable. This signal source is powered by a EG&G Model 232-A power supply with an EG&G Model 231 triggered capacitor bank.

Twenty four Aquadyne AQ-1 hydrophones with an Aquadyne AQ-200 amplifier are arrayed in a streamer with 2 sections, and a total 15 m active length. This streamer can be towed at speeds of up to 15 knots and records a frequency bandwidth of 0.5 Hz to 3 KHz.

A Technical Survey Services, Ltd. (TSS) analog filtering unit was used to process the analog signal. This unit included a TVG amplifier, model 307B; a Tape Replay Unit, model 306 and a Stacking Unit, model 303.

During the earliest survey (VOUGA-86, described below) an EPC 4603 printer was available to control the signal trigger and plot the analog signal. The later Boomer survey (RIAV03) was carried out with an Analog-to-Digital signal Converter (ADC) installed on a workstation powered by an INTEL P4 processor unit. The software BoomDiRec (INGMARDEP 19/FCT/2003) was used in this workstation to control the triggering mechanism and record the digital signal in a SEG-Y format file. A simplified schematics of the deployment of the boomer

system is presented in figure III-2. The nominal signal penetration depth of this Boomer unit is of up to 75 m with a resolution of 75 cm to 1 m, depending on the type of sub-bottom materials and on the energy level used.

The Datasonics Chirp system

The Datasonics CAP-6000W Chirp sonar has a signal bandwidth of 1.5 to 10 KHz, with 1 KW power. The chirp length can be of 5, 10, 20, 50 or 60 ms, with possible ping rates of 0.25 s, 0.5 s, 1.0 s, 2.0 s, 4.0 s, 8.0 s. The nominal resolution of the system is between 8 and 15 cm and the depth measurement precision is approximately 0.1% of the depth, with a known sound velocity. The sub-bottom penetration may reach, in ideal conditions, 30 to 40 m, depending on the sediment type.

The sonar fish has a towing speed of 1 to 10 knots, has four AT-472 transducers and a hydrophone array of 8 elements with +12 dB of pre-amplification. This fish can be operated down to 300m depth.

Processing of the uncorrelated chirp data is automated and done prior to recording, inside the fish. The processing flow includes a match filter and the determination of the amplitude envelope (for a detailed discussion on chirp signal processing see Quinn *et al.*, 1998; Henkart, 2006).

The GPS

The Global Positioning System (GPS) is a space-based radio navigation system managed and operated by the United States (U.S.) Government. It comprises three segments, known as the Space Segment, the Control segment and the User Segment. The Space Segment and the Control Segment are maintained and operated by the U.S. Government (detailed description can be found in Stenbit, 2001). In general terms, the Space Segment consists of 24 satellites that emit their spatial position and time information to the surface of the earth, and the Control Segment consists of a main control station and 5 monitoring stations that command and keep track of the satellites, as well as process and correct the information that these satellites emit.

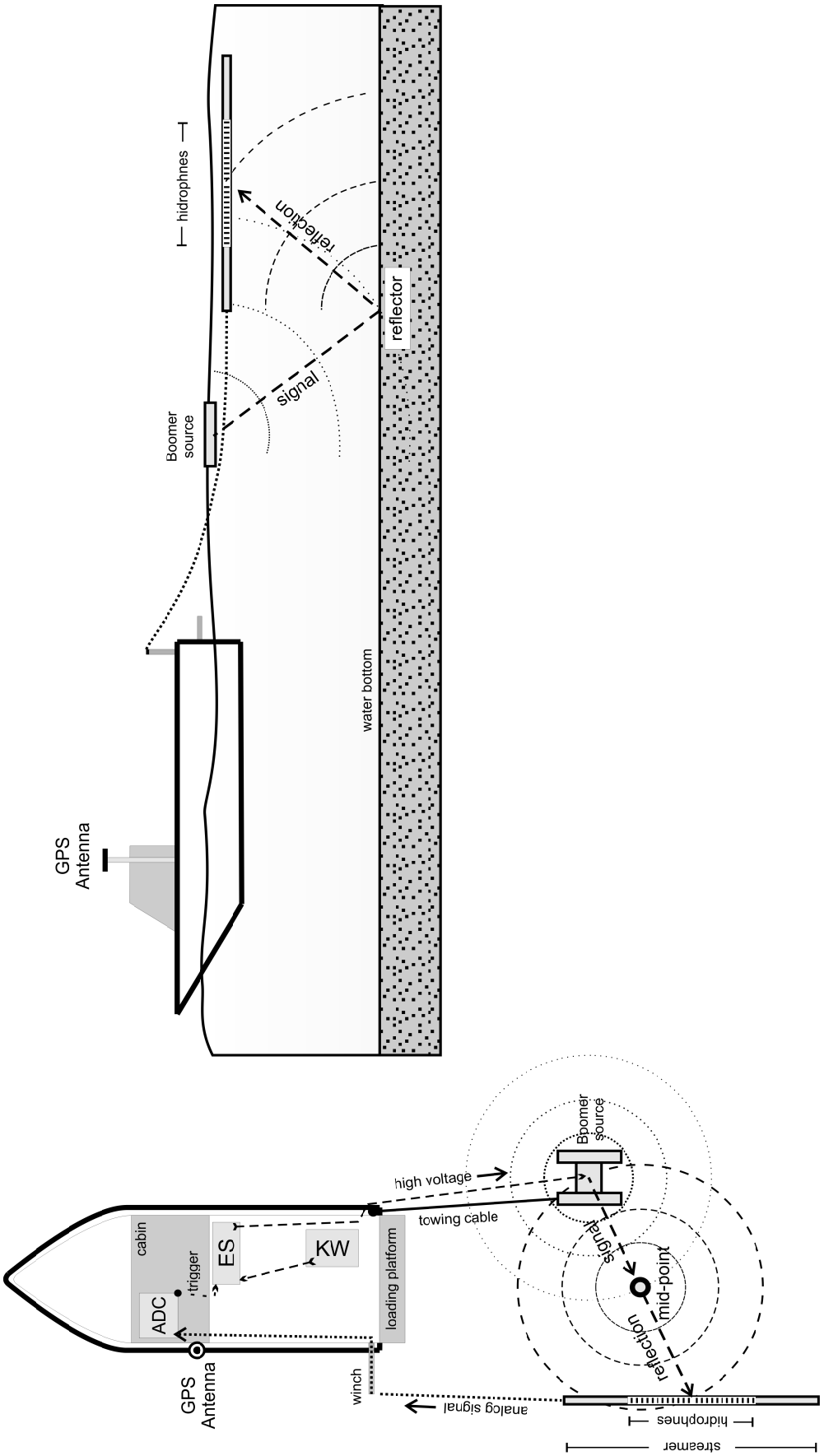

Figure III-2: Schematic representation of a Boomer system deployed from a small vessel.

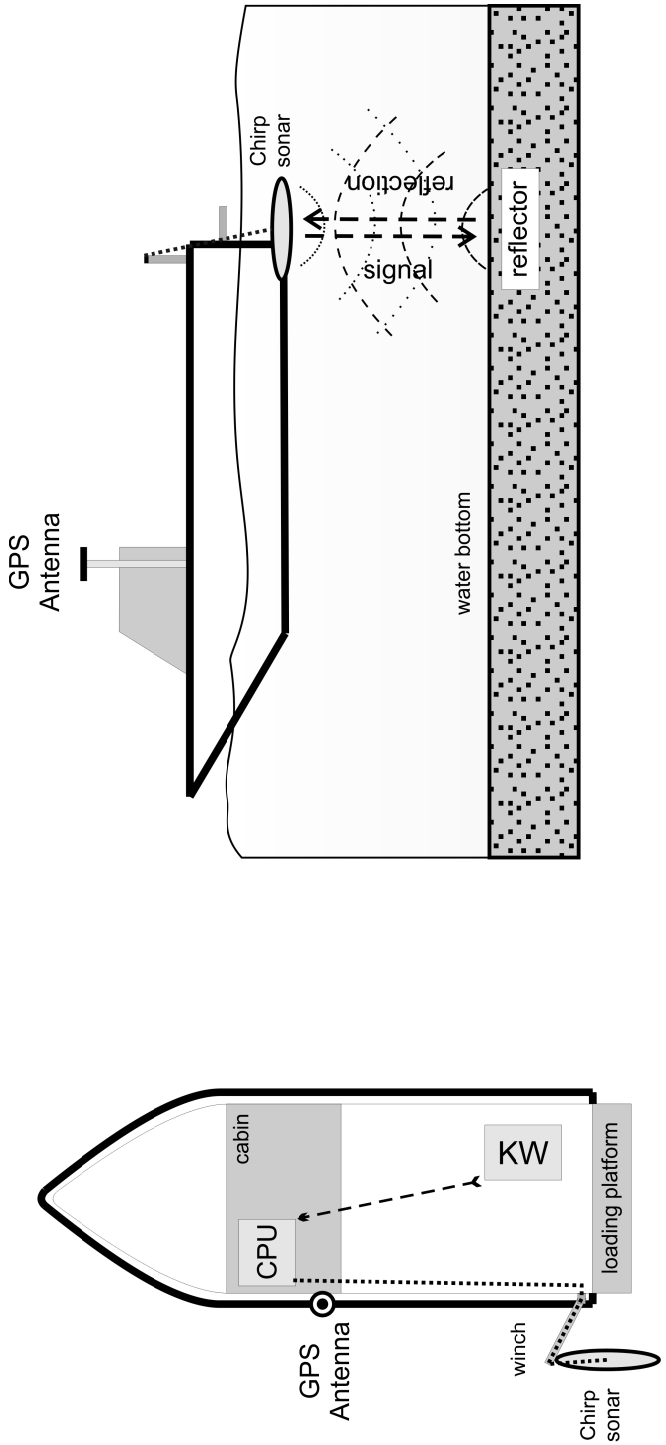

Figure III-3: Schematic representation of a Chirp system installed on a small vessel.

The User Segment is specific to each of the data acquisition surveys. It pertains to the user receivers, GPS antennas and software that allow the reception, decoding and processing of GPS signals emitted by the satellites. It is the User Segment that calculates the position, velocity and timestamp of the antenna. The GPS data acquisition methods for the user segment can divided into three types according to the way the GPS signal carrier waves (called L1 and L2) are handled:

1) The “Absolute Mode” or “Single Point” is the simplest method of operation that involves a single frequency receiver of the GPS signal information modulated by L1. The received data is processed to obtain the navigation information of the receiver Antenna. This method of operation has an approximate error in the range of 1 to 10 m in static mode, for continental Portugal;
2) The “Differential GPS” method (also known as DGPS) and the “Real-Time Kinematic GPS” (RTK) method both imply the use of two receivers, one placed on a location with known coordinates and another one mobile. The static station receives the L1 and L2 carrier waves and determines the differences between the known and received coordinate information. When these differences are applied in real time (more precisely near real time) to the pseudo distances to the mobile receiver, the method is called DGPS. When the differences are applied in real time to the wave phase, the method is called RTK. The DGPS has an accuracy of approximately 1 m and the RTK has an accuracy in the order of 1 to 2 cm.

An important aspect of the GPS is that, until the 1st of May, 2000, the United States Government imposed intentional civilian GPS signal degradation called “Selective Availability” that reduced the accuracy of data acquired in “Single Point” mode to values in the order of 30m.

The GPS navigation data for the seismic profiles presented in this work was acquired with either handheld single frequency receivers, working in “Single Point” mode, or with dual frequency receivers from the Aveiro Harbor Authority (APA)

operating in RTK-GPS mode and a single frequency receiver, operating in “Single Point” mode for backup.

The synchronization of the GPS clocks with the clock of the seismic acquisition systems was done manually, due to the lack of an integrated hardware solution, and the maximum bias, estimated by periodic comparison of the clock displays, was approximately 1 s.

3.2.2. Acquisition geometry parameters of the deployed systems

The spatial configuration of the various components of the seismic reflection and navigation systems (i.e. signal source, receiver array, GPS antenna) constitute part of the basic framework that must be adequately described in order to determine and parameterize both the navigation and the seismic data processing flows. The system geometry is fundamental in this work to estimate the seismic trace horizontal positions; to establish a common vertical *datum* for all the seismic traces; and to obtain a constant vertical sample interval, normal to the horizontal *datum* (see Fig. III-4 and Fig. III-5 for a representation of the relevant geometry parameters respectively of the boomer system and the chirp system).

Horizontal geometry parameters

The *horizontal geometry parameters,* described hereafter, refer to the parameters used in this work to estimate the horizontal coordinates of the seismic traces (see figures III-4 and III-5).

Layback – distance measured along the GPS antenna track-lines, between the GPS antenna position and the across-track line (i.e. line perpendicular to the track-line) that contains a certain reference point (e.g. the center of the receiver array, the center of the signal source, etc). Under normal conditions the layback corresponds to a distance towards the stern, for seismic equipments are normally towed behind the vessel. For this reason, in this work, layback distances are always measured as positive values. The types of layback are receiver layback,

source layback and mid-point layback, and are explained below (see figures III-4 and III-5).

Offset (definition only used for the horizontal geometry parameters) – distance measured along the lines that are perpendicular to the GPS antenna track-line, and that contain a certain reference point (e.g. the center of the receiver array, the center of the signal source, etc). As a convention for this work, offset distances measured towards starboard are positive, whereas distances measured towards port are negative. The types of offset are receiver offset, source offset, source-receiver offset and mid-point offset, and are explained below (see figures III-4 and III-5).

Receiver offset (RecO) – The offset between the GPS antenna track-line and the center of the receiver array. The **RecO** is relevant to the acquisition with a separate source and receiver such as the boomer system (see figure III-4).

Receiver layback (RecL) – The layback between the GPS antenna position and the across-track line containing the center of the receiver array. The **RecL** is relevant to the acquisition with a separate source and receiver such as the boomer system (see figure III-4).

Source offset (SrcO) – The offset between the GPS antenna track-line and the center of the signal-source. The **SrcO** is relevant to the acquisition with a separate source and receiver such as the boomer system (see figure III-4).

Source layback (SrcL) – The layback between the GPS antenna position and the across-track line containing the center of the signal-source. The **SrcL** is relevant to the acquisition with a separate source and receiver such as the boomer system (see figure III-4).

Mid-point offset (MptO) – The offset between the GPS antenna track-line and the mid-point (trace position). The mid-point offset depends on both the source and

receiver offsets according to the Equation III-1. The **MptO** is relevant to the acquisition with both boomer and chirp systems (see figures III-4 and III-5).

$$MptO = SrcO - \frac{SrcO + \mathrm{Re}cO}{2} \qquad \text{(Equation III-1)}$$

Mid-point layback (MptL) – The layback between the GPS antenna and the across-track line containing the mid-point. The mid-point layback depends on both the source and receiver laybacks according to the Equation III-2. The **MptL** is relevant to the acquisition with both boomer and chirp systems (see figures III-4 and III-5).

$$MptL = SrcL + \frac{\mathrm{Re}cL - SrcL}{2} \qquad \text{(Equation III-2)}$$

Vertical geometry parameters

The vertical geometry parameters described hereafter refer to the parameters used to establish a common vertical datum for the seismic traces, and to obtain a constant vertical seismic sample interval, normal to the horizontal *datum*.

Source-receiver offset (SrcRec) – The distance between the center of the signal source and the center of the receiver array, according to the Equation III-3. In this work, the **SrcRec** is derived from horizontal geometry parameters, despite being considered a *vertical geometry parameter*. The **SrcRec** is relevant to the acquisition with a separate source and receiver such as the boomer system (see figures III-4).

$$Src\,\mathrm{Re}c = \sqrt{(\mathrm{Re}cL - SrcL)^2 + (\mathrm{Re}cO + SrcO)^2} \qquad \text{(Equation III-3)}$$

Source to reflector (S2Ref) – Signal travel time from the source to a reflector. The *source to reflector* time is half the two way travel time (TWT) of unprocessed seismic record, when the signal source and receiver array are at towed the same

depth. The **S2Ref** is relevant to the acquisition with both boomer and chirp systems (see figures III-4 and III-5).

Reflector to receiver (Ref2R) – Signal travel time from a reflector to the receiver array. As with the previous parameter, the *reflector to receiver* time is half the two way travel time (TWT) of unprocessed seismic record, when the signal source and receiver array are at towed the same depth. The **Ref2R** is relevant to the acquisition with both boomer and chirp systems (see figures III-4 and III-5).

Towing depth (TowDp) – Mean depth of the towed equipment i.e. signal source and receiver array. The **TowDp** is relevant to the acquisition with both boomer and chirp systems (see figures III-4 and III-5).

Tidal altitude – Water height relative to the local mean sea level datum at the time of the data acquisition. For the Ria of Aveiro the so called “Zero Hidrográfico” (ZH) is used as the vertical *datum* relative to which tidal altitudes are measured. According to Barahona Fernandes (1971), the ZH is slightly bellow the maximum low tide, and is the reference surface for the depths of the Maritime Charts and for the predicted tidal altitudes published in the Tide Tables of the Instituto Hidrográfico. The tidal altitude is relevant to the acquisition with both boomer and chirp systems (see figures III-4 and III-5).

3.2.3. Seismic reflection surveys

The seismic reflection data used in this work was acquired during 5 scientific cruises in the Ria de Aveiro: the VOUGA86 Boomer survey (Monteiro and Pinheiro, 1986), the RIAV99 Chirp survey (Pinheiro and Monteiro, 1999), the RIAV02 Chirp survey (Pinheiro and Duarte, 2003a), the RIAV02A Chirp survey (Pinheiro and Duarte, 2003b) and the RIAV03 Boomer survey (Pinheiro *et al.*, 2003).

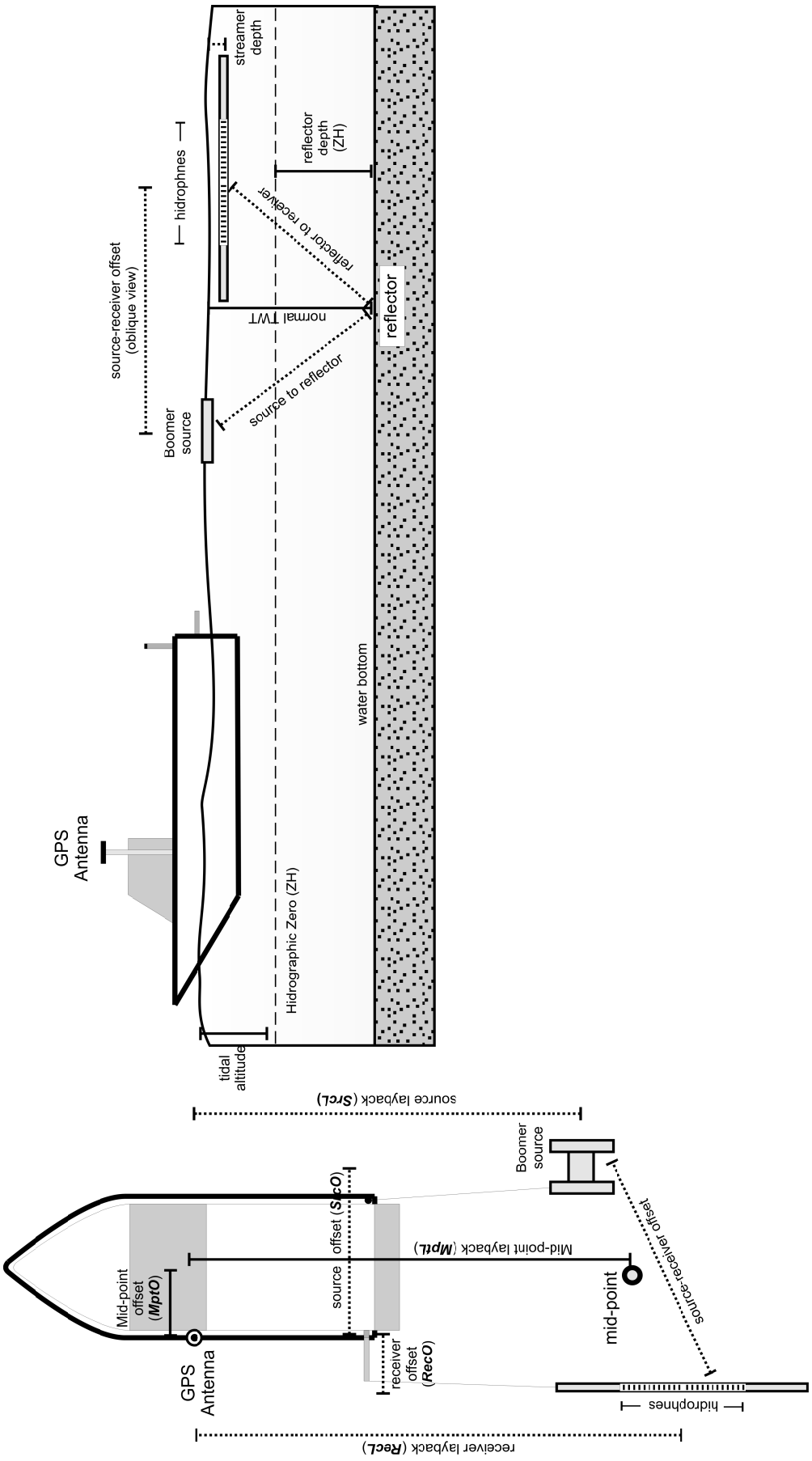

Figure III-4: Boomer acquisition geometry parameters

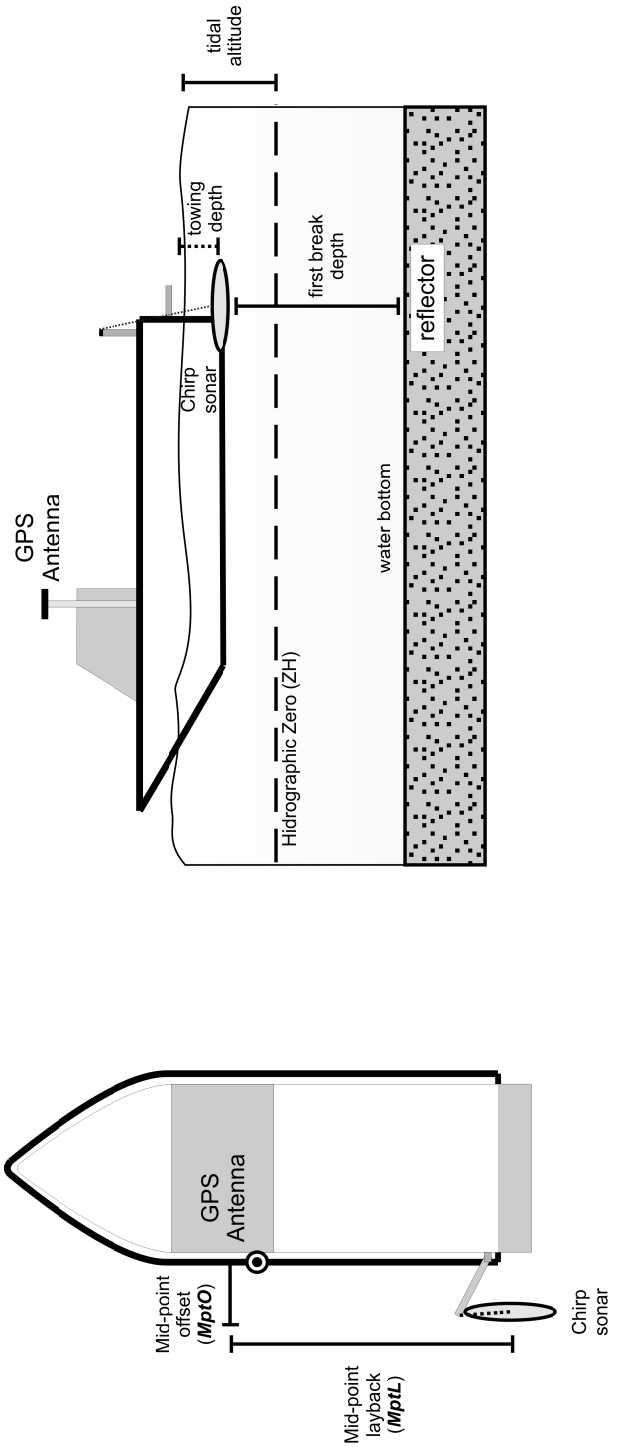

Figure III-5: Chirp acquisition geometry parameters.

The seismic profiles are 313 km long (112 km of Boomer profiles and 201 km of Chirp profiles) and cover the navigable channels of the lagoon (see simplified representation of the available seismic coverage of the Ria de Aveiro in figure III-6)

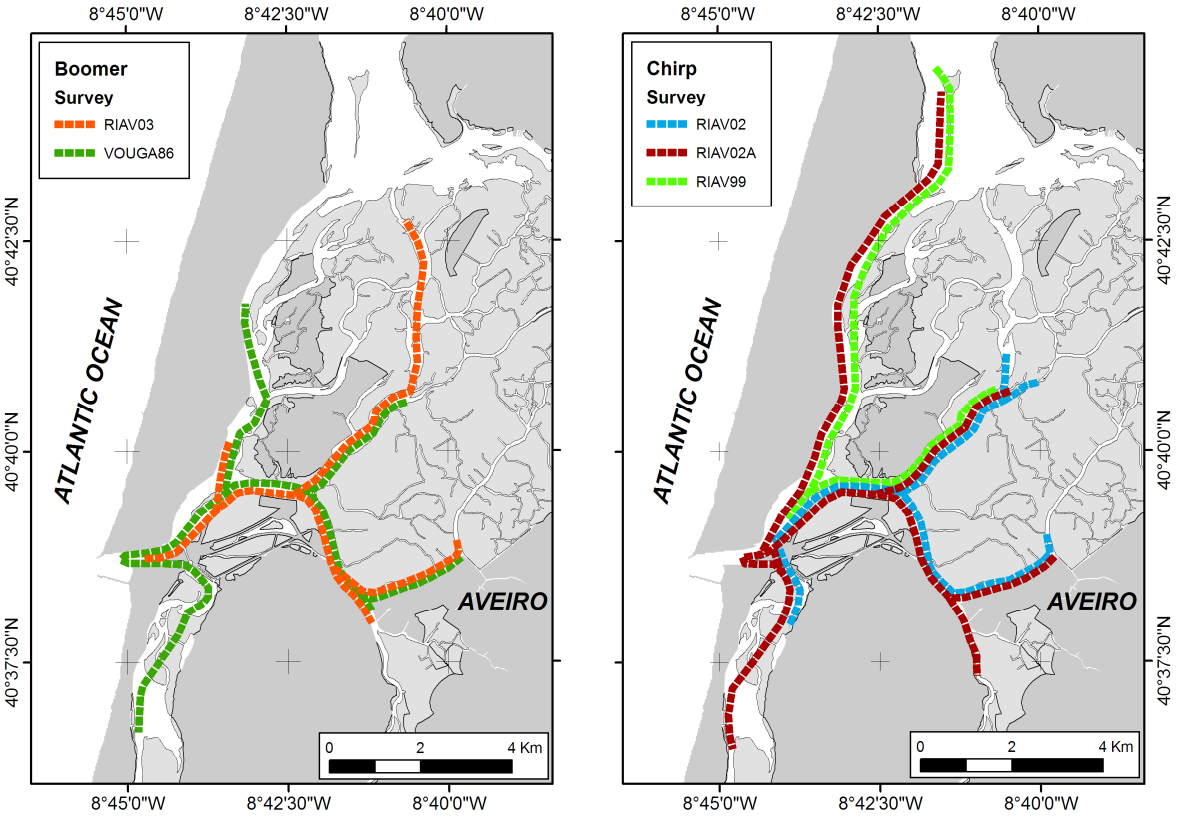

Figure III-6: Simplified representation of the seismic data coverage of the Ria de Aveiro used in this work, acquired during the cruises VOUGA86, RIAV99, RIAV02, RIAV02A and RIAV03 (references in text).

The Vouga 86 boomer survey

The Vouga 86 survey (Monteiro and Pinheiro, 1986) was carried out the Ria de Aveiro between the 19th and the 21st of September of 1986, and was undertaken by the Instituto Geológico e Mineiro (IGM) in cooperation with the University of Aveiro (UA).

The objective of this survey was to explore the subsurface geology of the Ria of Aveiro and to characterize the lagoon sediment architecture and bedrock structure, as well as test the recently acquired Uniboom seismic reflection system.

The Uniboom was deployed on the tugboat "Porto de Portimão" (courtesy of Somague Ltd.) and 65 km of seismic profiles were acquired along the main channels of the Lagoon. In this work, the navigation fixes were obtained with a sextant every 10 minutes and were marked on a navigation chart and on the profile paper plots. The sextant navigation fixes have an estimated accuracy of 150 meters (J. H. Monteiro, personal communication). The navigation chart was digitized, geo-referenced and the resulting coordinates of the navigation fixes and estimated trace positions (figure III-6) were extracted to ASCII files.

The inferred systems deployment geometry parameters for the Vouga 86 survey are 15 meters for the mid-point layback and 10 meters for the source-receiver offset. Both the boomer catamaran and the streamer were towed near the surface, at most 10-20 cm below the water surface. The remaining geometry parameters were considered irrelevant, because their variations were an order of dimension smaller than the 150 meter accuracy of the navigation method.

The Vouga 86 profiles used in this work were acquired with a firing rate of two shots per second and an energy source level of 100 Joules. The vertical resolution varied with the EPC printer plotting parameters but these values were not documented (J.H. Monteiro, personal communication).

The RIAV99 Chirp survey

The RIAV99 survey (Pinheiro and Monteiro, 1999) occurred on the 27th and 28th May of 1999, onboard the "Pangim" launch of the Aveiro Harbor Authorities (Administração do Porto de Aveiro – APA), equipped with the Chirp sonar; Drs. Hipólito Monteiro (IGM) and Luis Pinheiro (UA) were the co-chief scientists.

Twelve profiles, 23.9 km long in total, were acquired during this survey (Figure III-6), three of which have no navigation data. The chirp impulse used was 10 ms long and the seismic data was acquired at a rate of 2 shots per second.

The navigation tracks were obtained with a GPS from the University of Aveiro and the position fixes were affected by signal quality deterioration due to the *Selective Availability* (SA) still imposed by the government of the United States of America at the time of the RIAV99 survey. Values for the geometry parameters

were not estimated because the GPS error of 30 m was significantly greater than the combined effect of the geometry parameters (less than 5 m).

The RIAV02 Chirp survey

The RIAV02 survey (Pinheiro and Duarte, 2003a) was integrated in a science promotion action called "Acção Ciência Viva da Geologia no Verão" (which translates approximately as "Live Science Activity of Summer Geology"), coordinated by the Geosciences Department of the Unviersity of Aveiro (DG-UA), in collaboration with the Marine Geology Department of the Instituto Geológico e Mineiro (DGM-IGM) and by the Aveiro Harbor Authority (APA). The scientific aims of this survey were twofold:

1) To image the sediment architecture and bedrock structure of the Ria of Aveiro sedimentary basin;

2) To do a detailed survey near the Northern Terminal ("Terminal Norte") of the Aveiro harbor, for the Underwater Archeology Group of Aveiro, to search for evidence of shipwrecks.

The campaign was carried out between the 17th and the 19th of September of 2002, on board the "Ria Azul" launch of the Aveiro Harbor Authority, under the supervision of Prof. Luis Menezes Pinheiro (DG-UA). Ninety kilometers of Chirp profiles were acquired along the channels Espinheiro, São Jacinto, Vila, Mira, Aveiro and Boco (see seismic coverage in figure III-6). The chirp impulse used was 10ms long and the seismic data was acquired at a rate of 2 shots per second.

Navigation data was acquired with a RTK GPS system of the Aveiro Harbor Authorities, with the antenna placed aft, on the port side, less than half a meter away from the Chirp fish, using a single frequency GPS receiver from the University of Aveiro (for redundancy), placed inside the pilot's cabin, 2-3 meters away from the Chirp fish.

The seismic profiles were digitally recorded in a Datasonics native format, later converted to SEG-Y. The GPS geographic coordinates referred to the *datum*

WGS84 were recorded in ASCII files, together with their respective UTC (Coordinated Universal Time) timestamps.

For more technical information on the RIAV02 survey please consult the survey report by Pinheiro and Duarte (2003a).

The RIAV02A Chirp survey

Similar to the survey RIAV02, the survey RIAV02A (Pinheiro and Duarte, 2003b) was coordinated by the DG-UA, in collaboration with the DGM-IGM and the APA. The purpose of this survey was to improve the Chirp profile coverage of the Ria of Aveiro that was started with surveys RIAV99 and RIAV02, and continue the geophysical study of the sub-surface geology of the Ria of Aveiro. Also, a detailed survey was carried out for APA on the Aveiro Channel, near the "Terminal Sul" (the Southern terminal of the Aveiro Harbor, see Fig. III-6), to determine the unconsolidated sediment thickness in order to investigate the causes of recent, unexplained problems of harbor maintenance dredging operations.

The RIAV02A cruise was carried out onboard the "Ria Azul" launch of the APA, between the 21st and the 23rd of October, 2002. The Chirp profiles were acquired in the channels Espinheiro, São Jacinto, Mira, Aveiro, Ovar and Boco, totaling 87 km in length (see schematic coverage in figure III-6). The chirp impulse used was 10 ms long and the seismic data was acquired at a rate of 4 shots per second.

Navigation data was acquired in same conditions of the RIAV02 survey, with a RTK GPS system of the Aveiro Harbor Authorities, with the antenna placed aft, on the port side, less than half a meter away from the Chirp fish, and, with a single frequency GPS receiver of the University of Aveiro (for redundancy), placed inside the pilot's cabin, 2-3 meters away from the Chirp fish.

The seismic profiles were digitally recorded in a Datasonics native SEG format, later converted to SEG-Y. The GPS geographic coordinates referred to the *datum* WGS84 were recorded in ASCII files together with their respective with UTC (Coordinated Universal Time) timestamps.

For more technical information on the RIAV02A survey please consult the survey report by Pinheiro and Duarte (2003b).

The RIAV03 Boomer survey

The RIAV03 boomer survey (Pinheiro *et al.*, 2003) integrated the science promotion activity called "Acção Ciência Viva da Geologia no Verão", as did survey RIAV02, but this time integrated in a 2003 activity, and was coordinated by the DG-UA, in collaboration with the DGM-IGM and APA,.

The scientific purpose of this campaign was to continue the exploratory geophysical surveying of the sub-surface geology of the Ria of Aveiro, with improved navigation and digital recording methods (when compared with previous boomer data of the Vouga 86 survey).

This survey lasted for 4 days, from the 2nd to the 5th of September, 2003, and was carried out onboard the "Ria Azul" launch of the APA. A total of 47,1 km of boomer profiles were acquired along the channels Vila, S. Jacinto, Espinheiro, Sama and Bulhões (see seismic coverage in figure III-6). The source energy level used was 100 watt-second, with a ping rate of 2 shots per second.

The navigation fixes were obtained with the Aveiro Harbor Authorities RTK-GPS and with the DG-UA single frequency GPS receiver (again, for the sake of redundancy), both placed close to the pilot's cabin. The following geometry parameters of the acquisition systems and the DGPS were estimated onboard during the operations:

- **Receiver offset (RecO)** = 3 m
- **Receiver layback (RecL)** = 20 m
- **Source offset (SrcO)** = 7 m
- **Source layback (SrcL)** = 14 m
- **Mid-point offset (MptO)** = +2 m (see Equation III-1)
- **Mid-point layback (MptL)** = 17 m (see Equation III-2)
- **Source-receiver offset (SrcRec)** = 10.5 m (see Equation III-3)

The seismic profiles were digitally recorded in SEGY format (little endian byte order) and the geographic coordinates of the navigation fixes, referred to the *Datum* WGS84, were stored in ASCII files together with their respective timestamps.

For more technical information on the RIAV03 survey please consult the survey report by Pinheiro *et al.* (2003).

3.2.4. Data processing flow

The data processing flow tested with the seismic data acquired in the Ria of Aveiro can be divided into three stages, as depicted in figure III-7. The first stage consisted of navigation data processing to obtain trace position estimates. The second stage consisted of processing procedures applied to the seismic files to obtain a common vertical datum and to improve the signal quality. Finally, the third step consisted of quality control procedures to evaluate the consistency of the processed data. The errors diagnosed through the quality control procedures provided better constrained parameters for the processing flow, in a feedback loop. The necessary processing steps were repeated until either the quality control results were acceptable or no further improvements were obtained. The recorded Chirp profiles did not preserve phase information and, for that reason, the processing flow for the Chirp profiles was limited to gain corrections and static corrections.

The navigation processing procedures were applied using C++ or Visual Basic code specifically developed to accommodate the data file formats. The seismic signal processing procedures were applied using the seismic processing software tools SPW (developed by Parallel Geosciences Corporation) and ProMax and PostStack Data Loader (developed by Landmark Graphics Corporation).

The processing flow diagram used in this work is illustrated in Fig. III-7. The description of each processing step is illustrated with real data examples in the next chapter, together with the processing results.

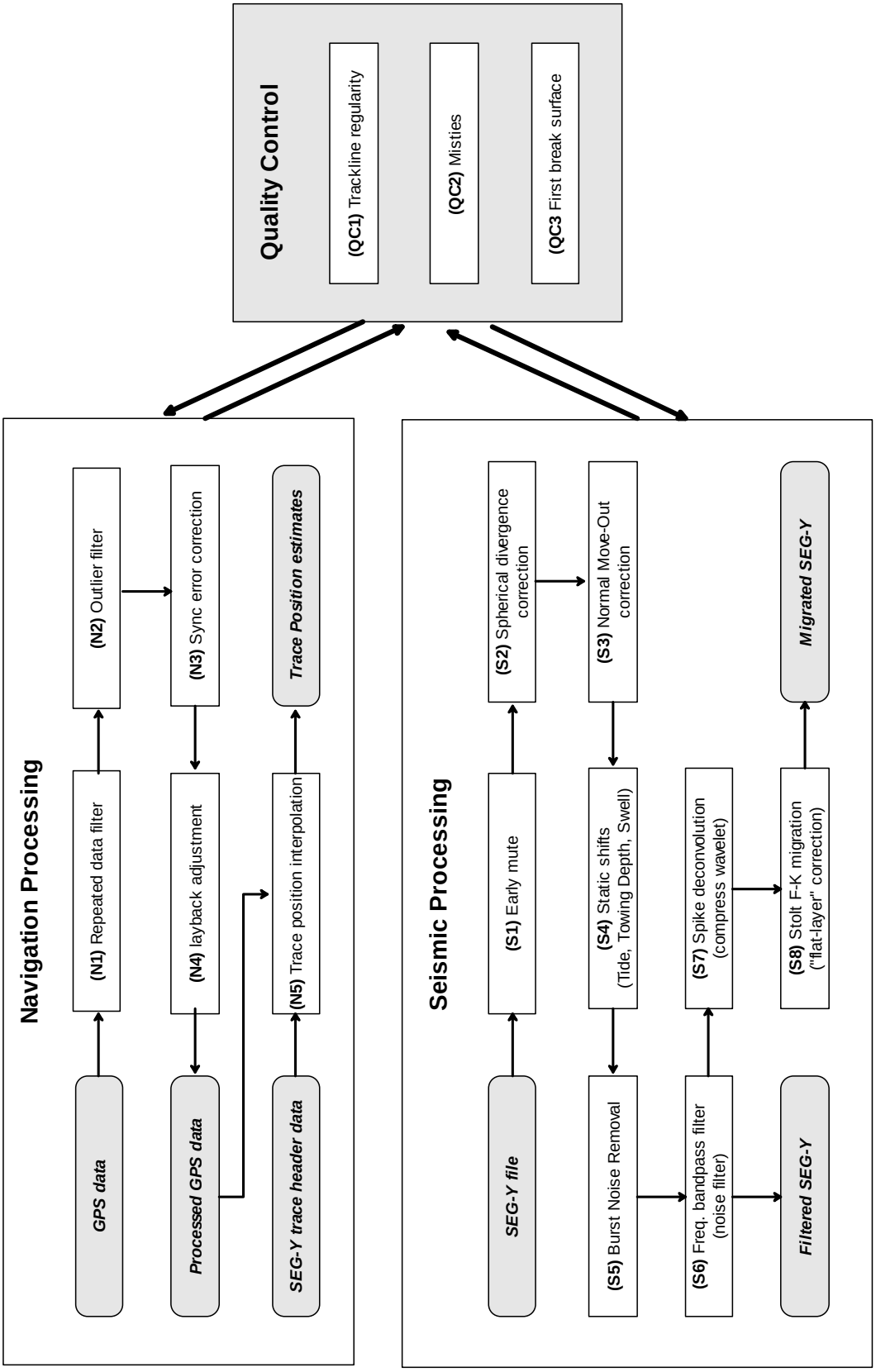

Figure III-7: Seismic data processing flow diagram.

3.3. Data processing results

This section presents the results of the processing flow as applied to the Boomer and Chirp datasets. First, each processing step is briefly described and illustrated with data examples. Then, the most common problems detected through the quality control procedures and the strategies to address them are described. Finally, representative examples are presented of the seismic coverage after navigation processing, and of the processed boomer and chirp profiles used for seismic interpretation.

3.3.1. Estimation of seismic trace positions

The aim of the navigation data processing was to integrate the GPS navigation data with the seismic trace headers in order to estimate trace positions. The processing flow applied to the navigation data involved the removal of corrupt navigation data entries and outlier position fixes, as well as correcting the clock bias between the seismic system and the GPS. After these data corrections, the midpoint layback was factored into the GPS timestamps and, finally, the trace positions were estimated based on the relationship between the navigation timestamps and the trace timestamps. A more detailed description of the navigation processing procedures is presented and illustrated below (process numbering indicates the order of execution and follows the flowchart in Figure III-7).

N1. Repeated GPS sentences filter

GPS navigation data frequently includes sentences with either repeated position fixes or repeated timestamps that were removed, always preserving the first sentence.

N2. Outlier position fixes filter

The GPS navigation track frequently has outlier fixes that are identified as artifacts because their time and spatial distances relative to their neighbors are

excessive, given the vessels speed. A specific code was developed in this work to filter outlier position fixes; position fixes were filtered out if the distance to their neighbors exceeded a user input threshold value. The maximum valid distance parameter was chosen according to the relationship between the GPS sentence output frequency and the ship average speed, e.g. for an output frequency of 1 Hz and a speed of 4 knots a ballpark value of 4 m was used for the outlier filter (at 4 knots a vessel covers approximately 2 m in 1 second).

N3. Synchronism error correction

All detected systematic biases between the acquisition system clock and the GPS clock were corrected on the timestamps of the navigation files.

N4. Midpoint layback adjustment

The midpoint layback correction was applied to the position fixes through an adjustment to the positioning timestamps: the time for the vessel to cover the layback distance was added to the position timestamp. This procedure assumes that the midpoint follows closely the track line of the GPS antenna, which usually only approaches reality when the vessel's travel direction is constant and the towed equipment is not affected by cross currents. Figure III-8 shows a comparison of a fault mapped pre- and post-layback adjustment.

N5. Trace position interpolation

The trace numbers and respective timestamps were extracted from the SEG-Y headers. Repeated or corrupted timestamp values were removed and new timestamps interpolated using valid neighboring timestamps. Trace X,Y coordinates were interpolated based on the X,Y timestamp processed navigation data (geographic coordinates were converted to Universal Transverse Mercator Zone 29N coordinates in the World Geodetic System *datum* for 1984 – WGS84). For each trace number, the Interpolation algorithm used the coordinates of the two closest time neighbors found in the navigation data, and computed a linear position interpolation weighted by the relative time difference of the trace to each coordinate pair. The algorithm used is expressed in Equation III-4.

$$TR_{(x,y)} = N1_{(x,y)} + (TR_t - N2_t) / (N2_t\text{-}N1_t) \times (N2_{(x,y)} - N1_{(x,y)}) \quad \text{(Equation III-4)}$$

Were TR_t and TR(x,y) are respectively the timestamp and the x,y coordinates of the trace and $N1_t$, N1(x,y) and $N2_t$, N2(x,y) are, respectively, the timestamp and coordinates of the two time neighbors of the trace. The figure III-9 shows the relationship between the processed navigation fixes and the trace position estimates obtained with the algorithm developed in this work.

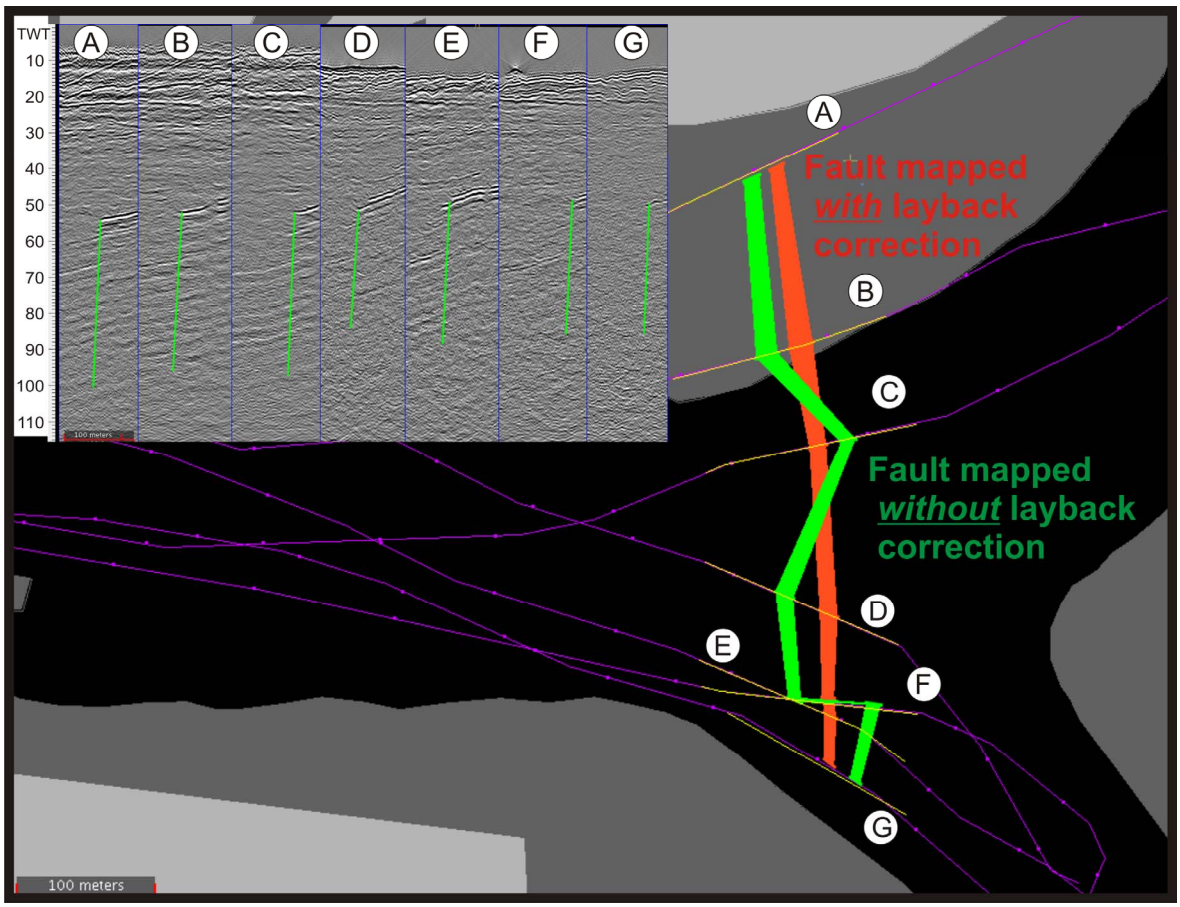

Figure III-8: Comparison of a fault mapped in boomer profiles acquired during the RIAV03 survey (Pinheiro *et al.*, 2003) pre- and post-layback adjustment.

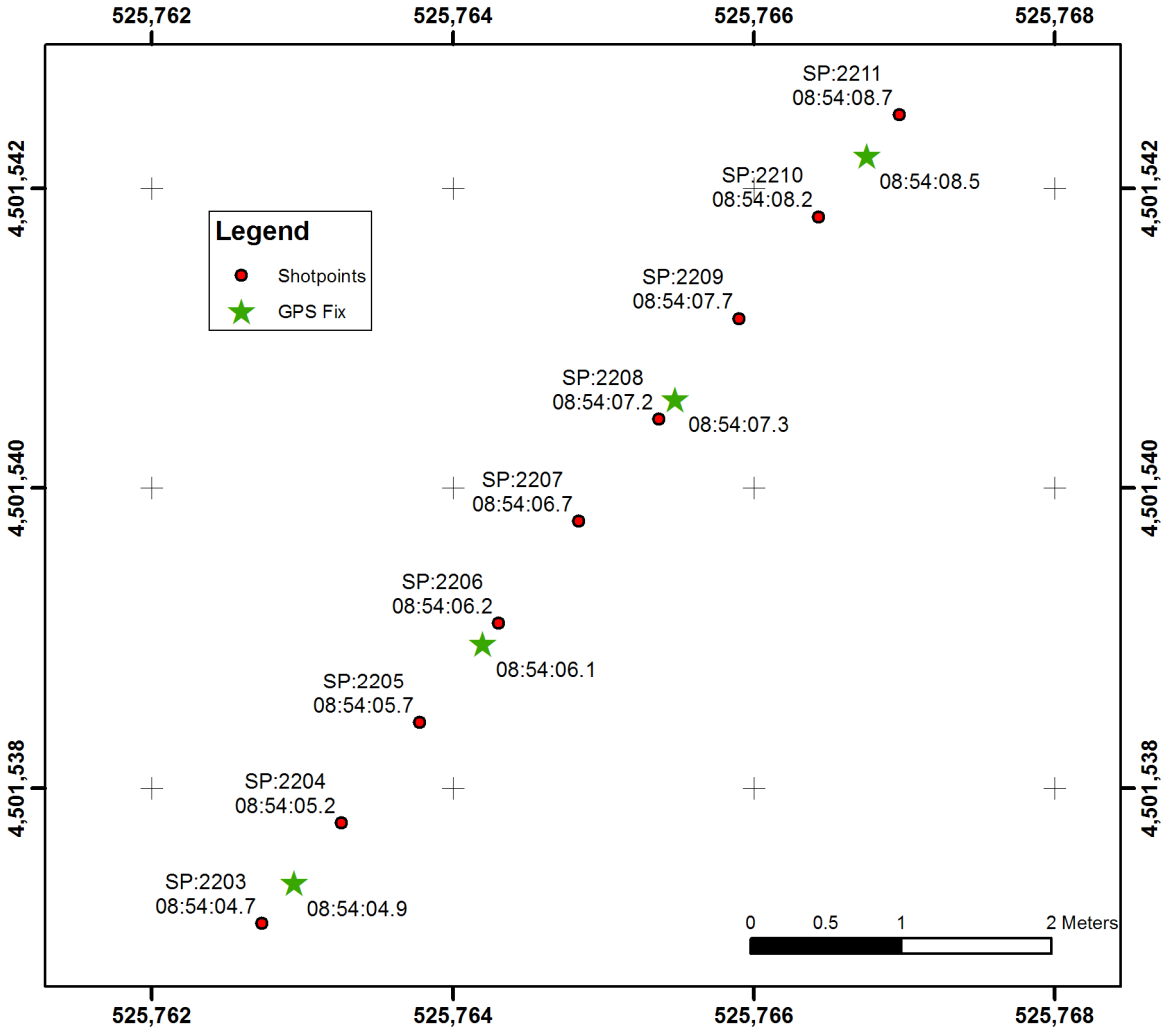

Figure III-9: Plot of the processed navigation fixes and of the derived interpolated trace positions**.**

3.3.2. Processed seismic signal

The aim of processing the seismic signal was twofold: (1) to improve the geometrical consistency of the seismic data, and, (2) to enhance the seismic imaging of the sub-surface geology. The improvement of the geometrical consistency of the seismic data was attempted with static corrections for tidal altitude variations. The boomer data also required normal move-out corrections to minimize the differences between normal move-out time and the recorded two way time (TWT) affected by the system acquisition geometry. The main processing steps to enhance the geological imaging of the boomer records included: (1) a bandpass frequency filter to reduce noise; (2) a predictive deconvolution filter to

attenuate the water multiples; (3) an amplitude correction to compensate for the spherical divergence of sound propagation; (4) a spike deconvolution to compress the wavelet energy; and (5) a Stolt F-K migration procedure to correct for the “flat layer” assumption.

As mentioned previously, the Chirp data was processed by automated hardware algorithms of the Chirp system that include match filtering, Hilbert transform and instantaneous amplitude computation (for a review of the chirp processing flow see Quinn *et al.*, 1998; Henkart, 2006). For this reason the recorded Chirp data did not preserve phase information which prevented wavelet processing, such as data migration.

The processing flow described below was fully applied to the boomer profiles, whereas the Chirp profiles were only corrected for static shifts and, later processed with an automated gain control to improve the identification of reflection continuity patterns. Both Chirp datasets, with and without AGC were used for interpretation, so that AGC-related artifacts could be easily detected.

The applied seismic processing steps, in order of execution, are as follows:

S1. Early mute

The water column portion of the seismic records was muted in all processed boomer profiles. When required, an unprocessed profile was used to interpret the water column portion of the profile. The early mute was applied to prevent the introduction of unnecessary noise to the signal frequency spectrum analysis and to the spike deconvolution and migration processes.

S2. Spherical divergence correction

The amplitude values were corrected with a linear time variant gain, common to all boomer profiles, to compensate for the energy loss due to the spherical divergence of the propagating signal.

S3. Normal move-out correction

The normal move-out corresponds to the sound travel time for a hypothetical geophone placed at the source point. The source-receiver offset of

the Uniboom system can result in significant differences between the recorded two-way travel times and the normal move-out time. For very shallow water acquisition (less than 5 m), these time differences can be of a magnitude equivalent to tidal altitude variations (see effect of source-receiver offset in recorded travel times in Fig III-10).

S4. Static shifts

The static shifts were applied to the seismic profiles in order to refer their time axis to a common vertical time *datum*, and thus minimize the vertical misties between profiles. The static shifts accounted for the correction of towing depths of the Chirp fish and for the tidal altitude variations inside the lagoon. The equipment towing depths were estimated onboard, during the data acquisition. The tidal altitude variations were estimated according to the tidal altitude tables and tidal delays table for the Ria of Aveiro, provided by the Hidrographic Institute of the Portuguese Navy (Instituto Hidrográfico). For each profile, a single mean tidal altitude value was used to compute the static shift. A test was done at a later date to correct tidal altitude variations on a trace to trace basis, using software specifically developed for the effect, but due to time constraints, the method was not applied to the full data set. An example of the importance of the tidal correction can be seen in figure III-11.

S5. Burst noise removal

The burst noise removal algorithm aims to remove high amplitude noise bursts from the seismic traces. This algorithm compares the amplitude of a sample with an amplitude average of samples from neighboring traces. It interpolates new amplitude values for samples that are N times greater than neighboring average (where *N* is a processing parameter). The boomer profiles had abundant burst noise and relatively low *N* values (*N*=2) had to be used to sensibly reduce the noise bursts. This meant that local and sudden changes in amplitude of geological significance were filtered out and had to be interpreted on unprocessed profiles.

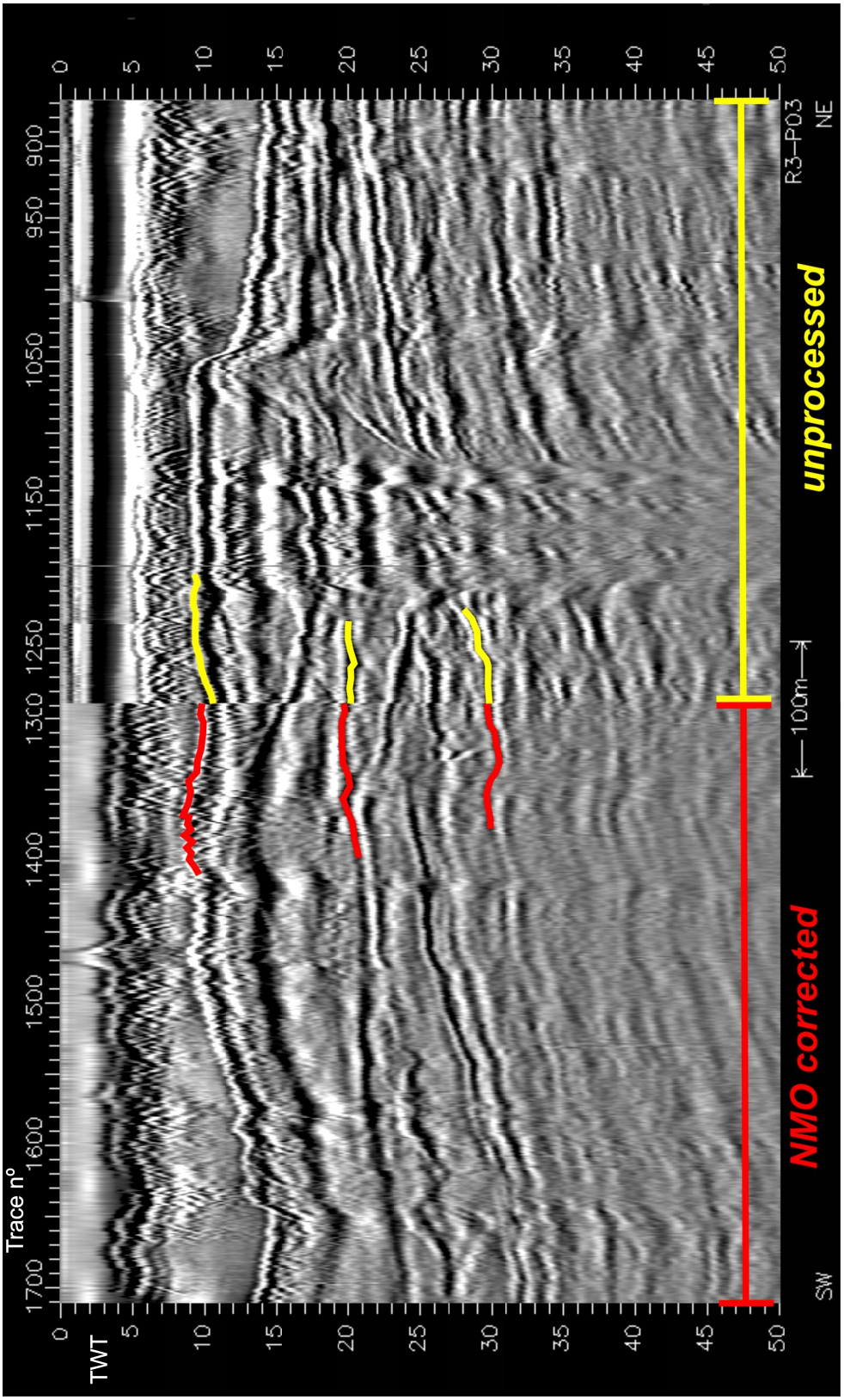

Figure III-10: Comparison of boomer profiles pre- and post-normal move-out correction showing the effect of source-receiver offset in recorded travel times. The red and yellow lines indicate the position of reflections respectively with and without NMO correction.

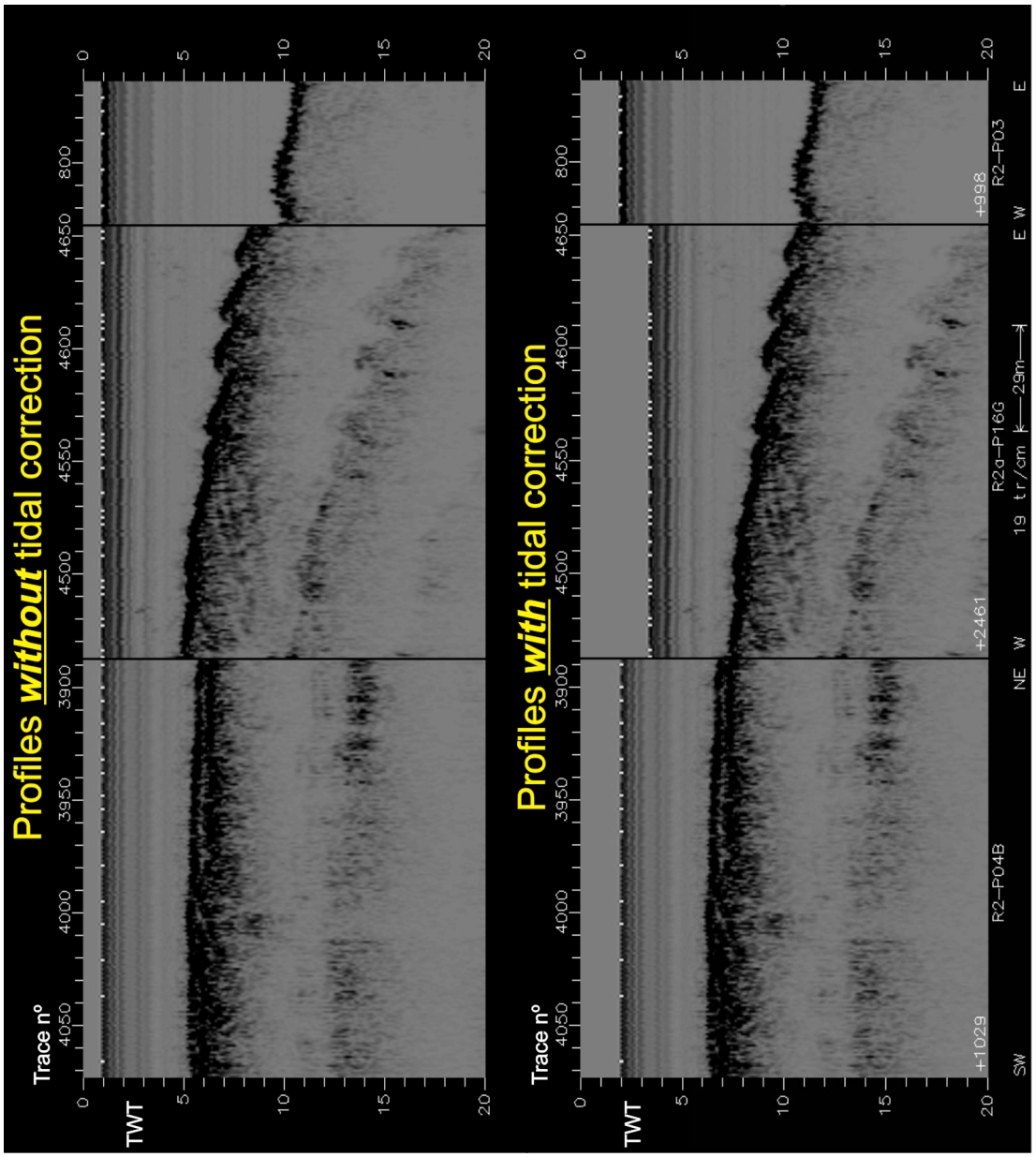

Figure III-11: Intersection between two boomer profiles before and after tidal correction.

S6. Bandpass frequency filter

An Ormsby bandpass frequency filter was applied to the boomer data to attenuate noisy frequencies and to obtain a minimum phase dataset, necessary for the spike deconvolution filter. The frequency spectrum of typical profile segments was calculated in order to determine approximate low and high pass frequencies (see figure III-12 for a typical frequency spectrum of boomer profiles). The low-cut and low-pass frequencies used were 50 and 100 Hz, respectively, and the high-pass and high-cut frequencies were 1500 and 2500 Hz, respectively.

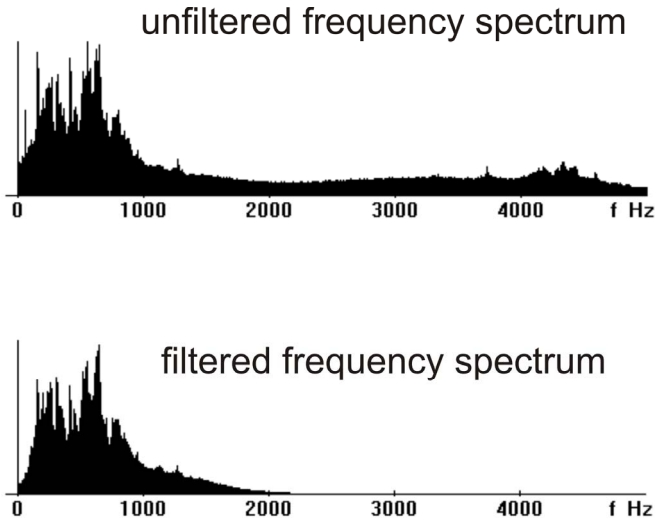

Figure III-12: Typical frequency spectra of the boomer profiles before and after applying a bandpass frequency filter.

S7. Spike deconvolution

The spiking deconvolution desired output is ideally the earth's impulse response, which is obtained by compressing the wavelet energy as close as possible to a single spike, thus improving resolution and clarity of the seismic record (Sheriff and Geldart, 1995). The deconvolution operator length used here was 9 ms, based on the analysis of the autocorrelation function, with 0.5% white noise applied before the inverse filter calculation. The high frequency noise

generated by the spike deconvolution was then filtered with a bandpass frequency filter (the parameters used were the same as in step S6).

S8. Stolt F-K migration

According to Sheriff and Goldart (1995) "…migration involves repositioning data elements to make their locations appropriate to the locations of the associated reflectors or diffracting points". In other words, unmigrated data presents an image which is only correct for flat-layers, since reflector dip is not taken into account. As the imaged geological objects frequently are not flat, the seismic image is distorted and migration aims to correct that distortion. Stolt F-K migration is a simple migration method in the frequency-wavenumber domain, that assumes a constant medium velocity (Stolt, 1978). Trace spacing for the boomer profiles varied between ~0.5 m and 1 m due to frequent changes in traveling speeds (a consequence of navigating the tidal channels of the Ria of Aveiro). This fact, together with the natural medium velocity variations, affected the migration results, with evidence for both under migration (hyperbolae) and over migration (crossovers), which frequently coexist in the same profile.

A comparison of the various processing stages of the boomer data is presented in figure III-13.

3.3.3. Quality control results

Quality control procedures aim to detect processing errors, caused either during the execution of the non-automated procedures or due to inadequate choices of the processing parameters. As discussed earlier, quality control results feedback into the processing flow, which is partially or totally repeated until the necessary non-random errors are corrected. Next, the results of the last iteration of the quality control procedures, prior to the geological interpretation of the seismic data, are presented and discussed.

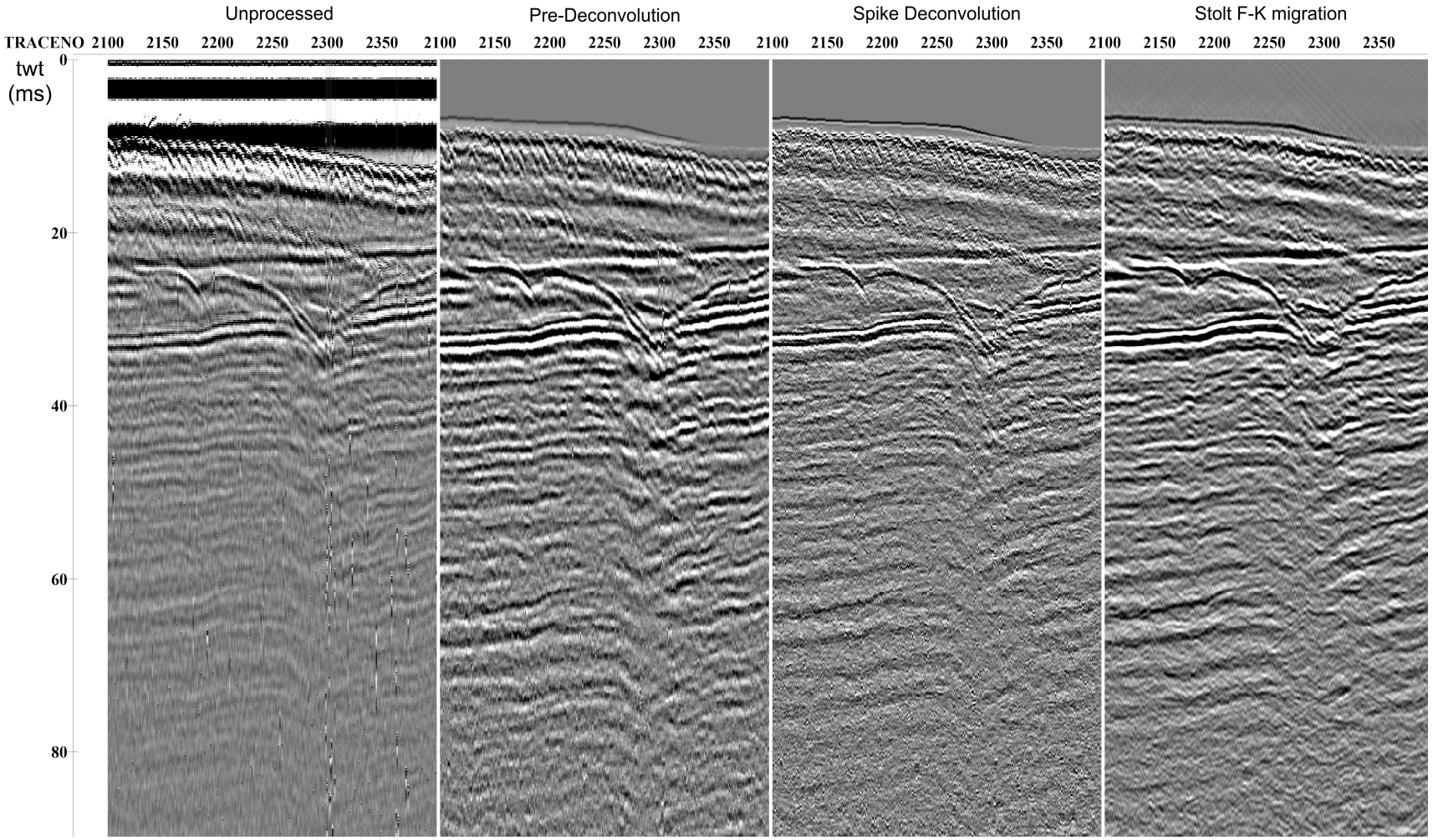

Figure III-13: Comparison between various processing stages of one boomer profile (see text for detailed description of the processing steps): ***Unprocessed*** – raw trace amplitude display; ***Pre-Deconvolution*** – amplitude display after applying (S1) the early mute, (S2) the spherical divergence correction, (S3) the normal move-out correction, (S4) the static shifts, (S5) the burst noise removal and (S6) the bandpass frequency filter; ***Spike Deconvolution*** - amplitude display after applying (S7) the spike deconvolution followed by a bandpass frequency filter; ***Stolt F-K migration*** – amplitude display after applying (S8) the Stolt F-K migration with a constant sound velocity model of 1500 m/s

Trackline analysis

A visual analysis of the track lines was first carried out to identify gross trace position estimate errors, such as position estimates over land and sharp navigation turns not documented on the survey logbook. Most non-automated procedural errors tend to be detected during this step of quality control. If trace positioning data repeatedly fails this quality check, then it should not be used for 3-D modeling (e.g. seismic unit mapping). The RIAV02 Chirp profiles acquired in the Terminal Norte for the underwater archeology survey had significant track line anomalies with multiple mismatches between documented ship turns and the plotted tracks. These errors, caused by triggering and recording problems of the chirp system, were not quantified, and could not be corrected, which meant that these profiles were not used for 3-D interpretation. Apart from these Chirp profiles no significant track line anomalies were observed in the interpreted datasets.

Residual misties

The first break reflection was picked in every seismic profile and the intersection misties were computed. These misties are referred here as residual, for they are determined after the NMO, towing depth and tidal altitude corrections were applied. Non-random residual misties may result from errors in estimates of the mentioned static corrections and/or from errors in trace position estimates. The final residual misties have a mean value of 0.75 ms with a maximum of 2 ms and a minimum below the sampling interval (<0.1 ms).

First break surface analysis

The analysis of systematic irregularities of the first break time surface allows the estimate of non documented variations of the geometric parameters (both horizontal and vertical). Figure III-14 illustrates one case of poor static

correction that was found and corrected through of this procedure. A particular type of position error related artifacts were frequently observed on the first break surface of the processed dataset: V-shaped patterns that can be significantly pronounced near profile intersections when the lines cross steep morphologies. In the cases where residual misties are minimal, these artifacts can be explained either by GPS errors (e.g. non differential receiver data) or by the un-corrected midpoint offset value: this last situation may be aggravated by lateral currents affecting the towed equipment.

3.4. Discussion

The processing flows described aim at improving the interpretation conditions, to allow for a better identification, seismic characterization and mapping of the geological features of interest. Still, an assessment of several characteristics of the processed data set is required before the start of the interpretation work. The focus of the present discussion on the processed data is threefold:

1. to inspect the signal quality and penetration on typical profiles and assess how noise and artifacts interfere with the geological signal;

2. to determine the theoretical vertical and horizontal resolutions and compare them with data examples in order to determine practical resolution values;

3. to assess what are the appropriate 3-D imaging scales according to the shape and size of the studied geological features and the relevant properties of the multiple seismic datasets (i.e. resolution, positioning quality and profile separation).

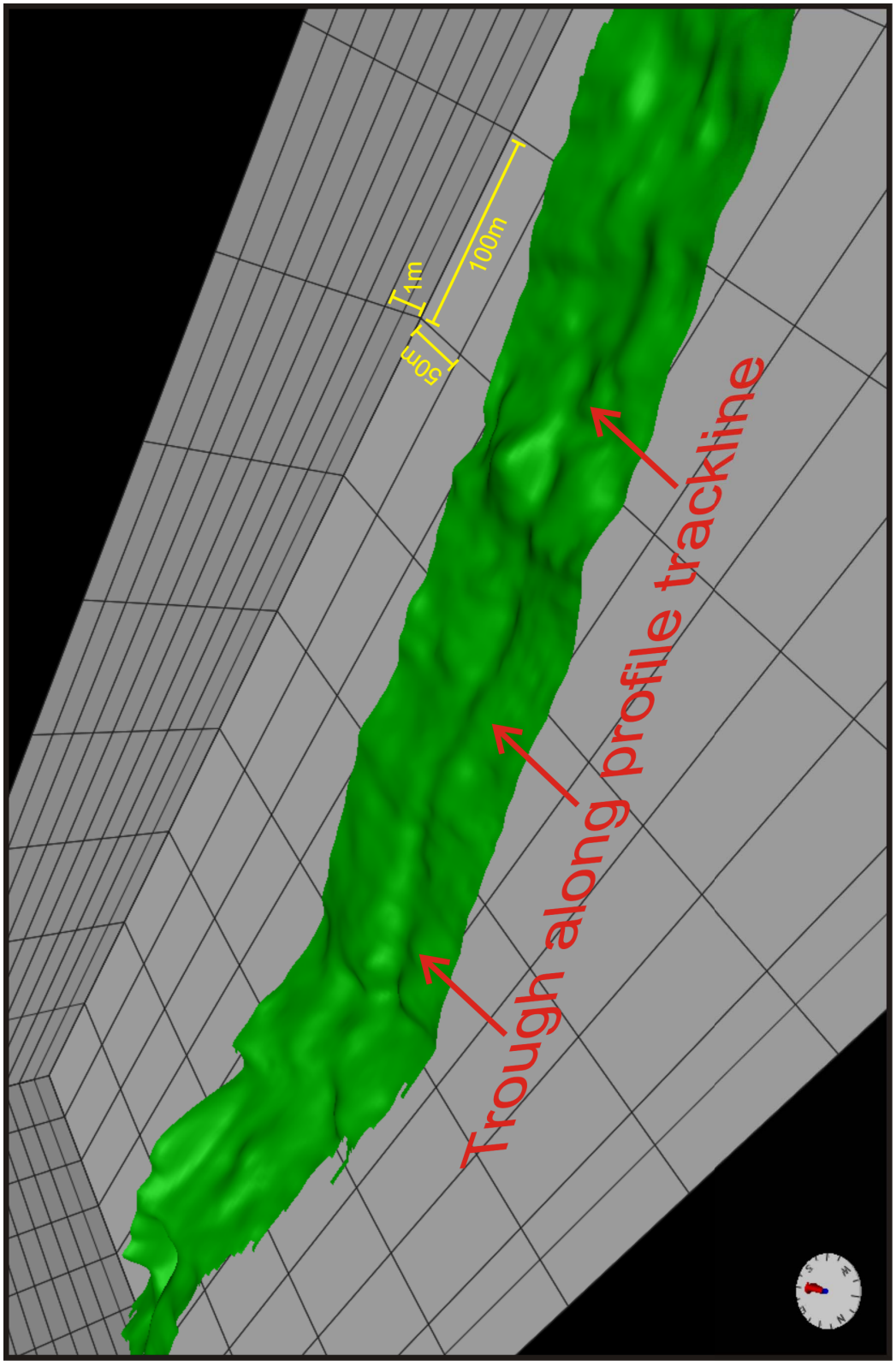

Figure III-14: 3-D display of a first break surface affected by an undocumented static correction error. The trough indicated by the red arrows occurs along the track line of a profile with a systematic vertical mistie of 0.35 ms. This static error was likely due to an undocumented and non-corrected change in towing depth of the chirp sonar.

3.4.1. Signal quality and penetration

The unprocessed boomer data shows frequent burst noise and a very long direct arrival that frequently interferes with first break and deeper reflections. The long direct arrival also provides evidence for a long ringing wavelet that significantly affects interpretation below strong reflections. The occurrence of deep reflections below transparent zones in processed profiles indicates that the spike deconvolution appears to effectively reduce some of these ringing effects and that most of the deeper coherent events are primary reflections (see Fig. III-15). The boomer signal had an observed penetration that varied between 50 and 90 ms, i.e. approximately 68 m, assuming a constant sediment velocity of about 1500 m/s.

When present, sub-bottom coherent reflections in Chirp profiles usually have high continuity and amplitude. Signal penetration rarely exceeds the 15 to 20 ms. Some weaker coherent reflections were recognized through comparison of data sets with and without automatic gain control (AGC) amplitude treatment (see Fig. III-16). This lack of variety of the seismic facies and poor penetration determines that distinguishing seismic units can be done mostly either locally or through correlation with the interpretation of boomer profiles from the same area, where available.

Navigation conditions, tidal and wind currents in particular also seriously affected data quality. The characteristic mid to late afternoon northerly winds that cross the Ria of Aveiro tended to generate turbulence on the upper water layer which degraded the signal quality. When navigating against strong tidal currents, in particular closer to the lagoon inlet, the towed equipment suffered significant drag, which caused turbulence and added noise to the data. The changes in the surface current speeds caused by both wind and tides affected the navigation speed (varying between 2,5 and 7 knots). These speed variations resulted in the variable trace separation already described and, occasionally, in sudden changes in the pitch of the Chirp fish that are recognizable on the profiles by series of blank traces. Profiles Riav03-P02B and RIAV03-P02C illustrate some of these issues (see Fig. III-17).

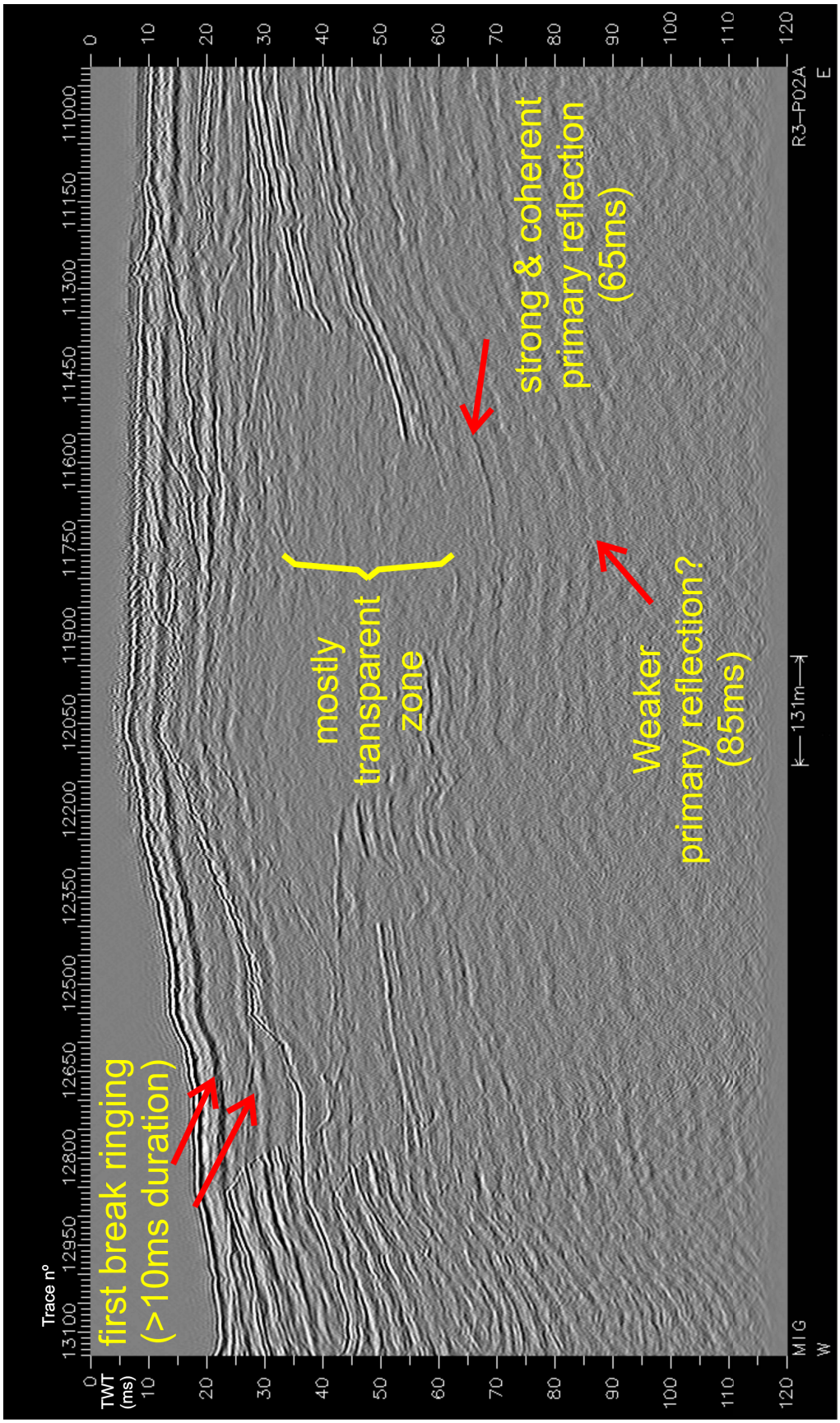

FiFigure III-15: Evidence for deep primary reflections in a processed boomer profile. The strong ringing effect can be over 10ms long, as shown below the first break, and may mask primary reflections. The reflections indicated in the figure ocurr below a mostly transparent zone, at 65 and, possibly, at 85ms.

Strong coherent reflections corresponding to side echoes were identified both in boomer and chirp data when tracklines run near harbor infrastructures or docked vessels (see Fig. III-18). As expected given the shallow water conditions of acquisition, the water multiple is the most generalized and strongest seismic artifact observed on both boomer and chirp profiles.

An ubiquitous amplitude pattern in the Chirp data not discussed in this chapter should be mentioned here: the mean amplitude values of each profile appear to vary significantly with tidal altitude, independently of the source to reflector distance. This particular characteristic of the data set and its impact on the resolution and geological interpretation is analyzed and discussed in a later chapter of this work.

3.4.2. Resolution of seismic data

In seismic data, resolution commonly refers to "…the minimum separation between two features such that we can tell that there are two features rather than one" (Sheriff, 1985; Sheriff and Geldart, 1995). The horizontal and vertical resolutions, and related interpretation scales of the Boomer and Chirp profiles will now be discussed here and illustrated using some features surveyed with both systems.

Horizontal resolution

In theory, the horizontal resolution of un-migrated seismic data corresponds roughly to the diameter of the "footprint" of the seismic wave on a reflector. This footprint can be described as the area of constructive signal reflection off a reflective surface. This area is called the First Fresnel Zone and is a function of the signal frequency and of the distance of the reflector to the signal source (see Equation III-5). Note that when reflector dimensions are smaller than the Fresnel zone, their response is that of a diffraction point (Sheriff and Geldart, 1995).

$$\text{Radius of the first Fresnel Zone} = \frac{V}{2}\sqrt{\frac{t}{f}} \qquad \text{(Equation III-5)}$$

where V is the average sound velocity, t the depth in time and f the signal frequency.

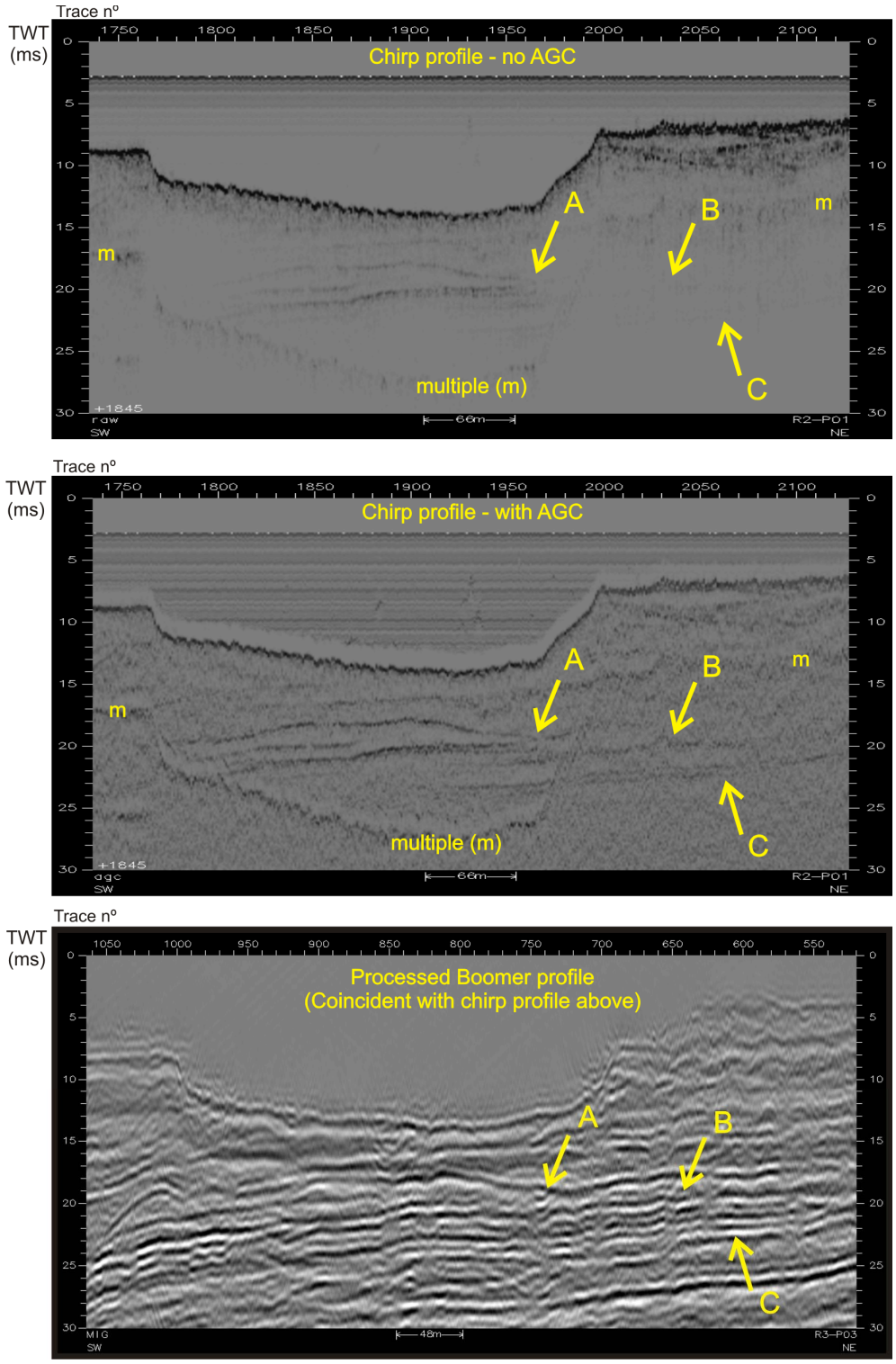

Figure III-16: Lateral reflection continuity inferred through the comparison of a profile with and without Automatic Gain Control (AGC). A coincident boomer section is also shown, where comparable reflections are observed, providing further evidence for the lateral continuity of the reflections. Arrows indicate comon locations to the three sections. Arrow ***A*** indicates a reflection visible in all profiles; Arrows ***B*** and ***C*** indicate reflections below the water bottom multiple observed in the chirp profile with AGC and in the Boomer profile.

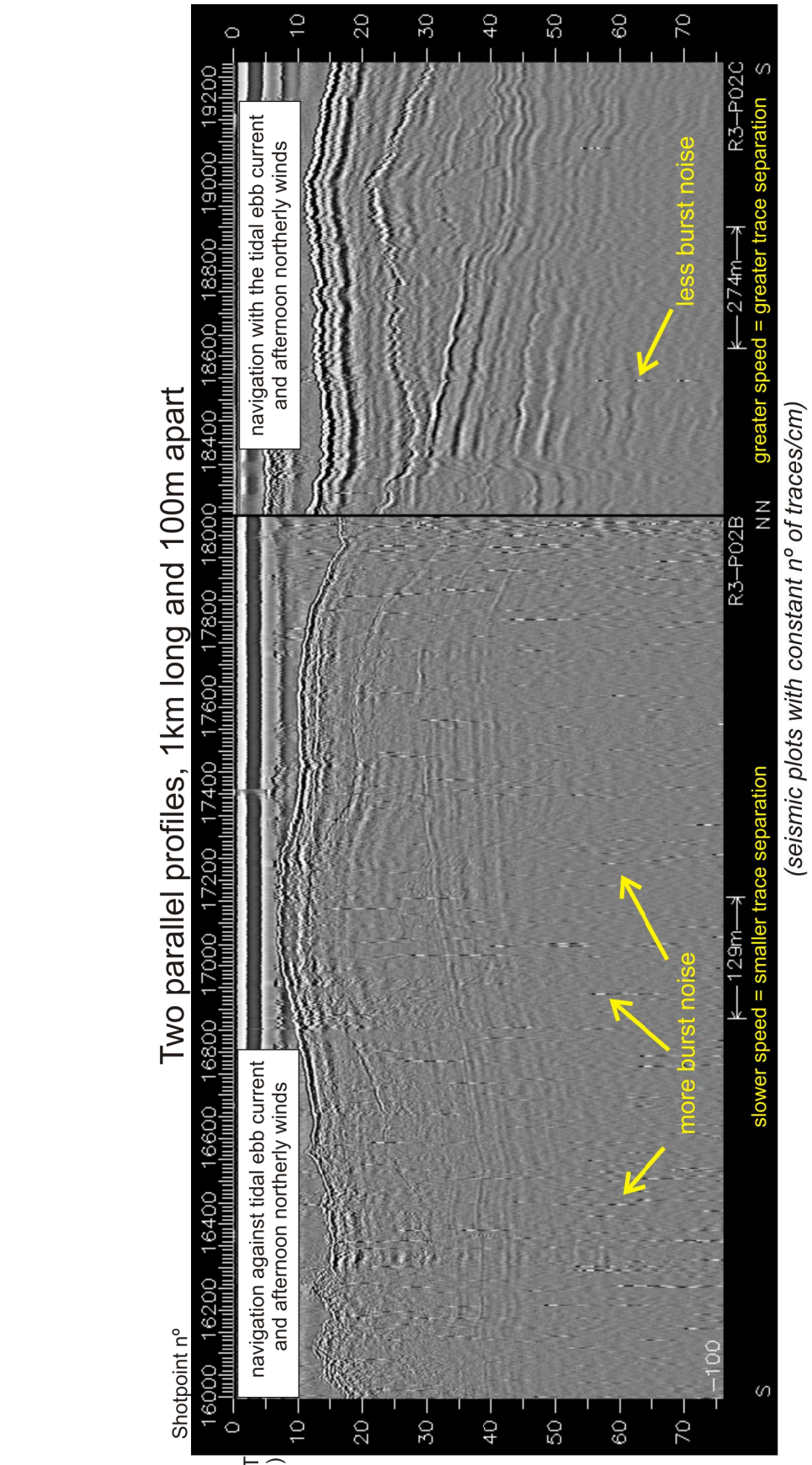

Figure III-17: Example of signal degradation and variable trace separation on boomer profiles caused by poor navigation conditions due tidal and wind related surface currents. Profile Riav03-P02B was acquired against the tidal current and the strong afternoon northerly wind, whereas profile Riav03-P02C was acquired 100 m apart in the opposite direction. Compared with profile P02C, profile P02B has a poorer signal to noise ratio and more burst noise. The change in acquisition speed imposed by the strong currents is clearly illustrated by the difference in the graphical scales, considering that the profiles are plotted with a constant trace/cm ratio.

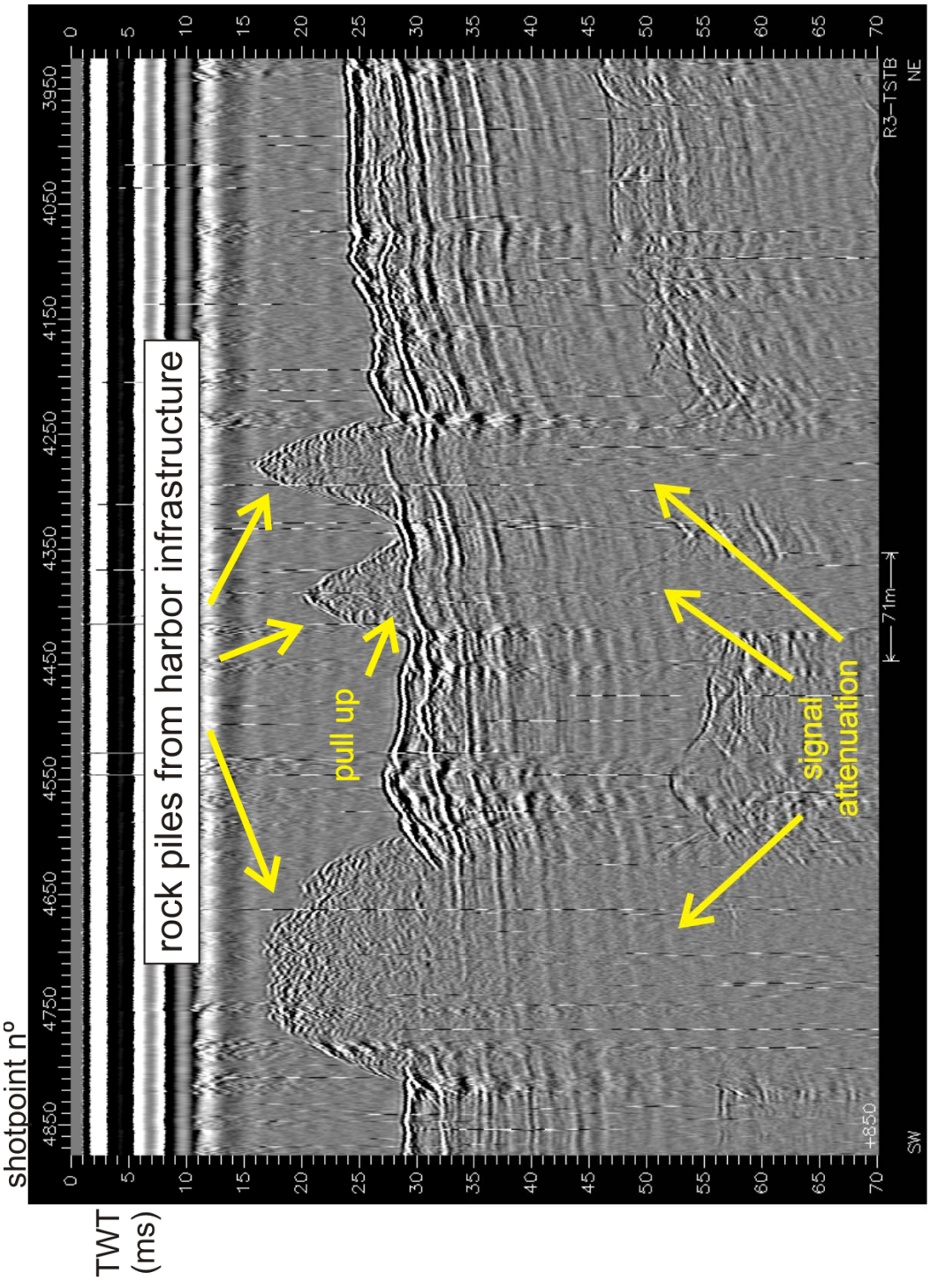

Figure III-18: Rock piles from harbor infrastructure observed on a boomer profile as side reflections. The higher sound velocity in the rocks causes reflections pull-ups. The physical properties of the rock medium also cause a signal attenuation that results in weaker reflection amplitudes bellow the rock piles.

Horizontal resolution of the Boomer profiles

The boomer data has a predominant signal frequency of approximately 1 KHz at shallower depths, which decreases to 350 Hz at depth. For these frequencies and an average sound velocity of 1500 m/s, the horizontal resolution of the boomer profiles ranges from 4 m at shallow depths, up to 25 m at greater depth. Considering that the trace separation of the boomer profiles ranges from 0.5 to 1 m, the Fresnel zone of each boomer shot overlaps those of 2 to 4 neighbor shots at shallow depths and 25 to 50 shots at depth.

Migration of seismic data aims to collapse the Fresnel zone energy (thus "repositioning" energy to its point of origin). The horizontal resolution of migrated data is harder to assess and is affected by issues such as errors in migration velocities and noise rearrangements. Still, assuming the sampling theorem that at least two samples must be obtained per feature wavelength, then the horizontal resolution of the migrated data should be greater than two migration bin widths. For the migrated boomer profiles the bin size corresponds to the trace separation, which means that the horizontal resolution of the migrated boomer data probably varies between 1.5 to 3 m (for three bin widths).

The resolution values presented above for the migrated boomer profiles are optimistic for two reasons: (1) side echoes remain un-migrated and, where these occur, horizontal resolution is reduced; (2) trace separation varies along the same profile due to ship velocity variations and, as the Stolt F-K migration algorithm used requires constant trace separation and a constant sound velocity, the migrated profiles have under-migrated and over-migrated reflections which also contribute to reduce horizontal resolution.

Horizontal resolution of the Chirp profiles

The chirp data has a dominant frequency circa 2.5 KHz and a corresponding Fresnel zone of approximately 2.5 m at 5m depth and of 10 m at 30 m depth (assuming a sound velocity of 1500 m/s). Trace separation of the chirp data also varies between 0.5 and 1 m, as with the boomer profiles, which means that each trace Fresnel zone roughly overlaps three Fresnel zones of neighboring shots, at the shallowest depths. According to the documentation provided by the

chirp manufacturer (Datasonics Corp.), the automated processing flow of the chirp data also has a "collapsing" effect of the Fresnel zone and the characteristic horizontal resolution of the processed chirp data is 1 to 2 m.

Vertical resolution

The vertical resolvable limit between two reflections was proposed by Lord Rayleigh as a half-cycle in order to minimize interference effects. In practice, the ballpark value used to estimate vertical resolution of most seismic reflection systems is ¼ of the dominant wavelength. In the case of the boomer data, the vertical resolution is estimated according to depth, to account for the perceptible changes in the dominant frequencies and seismic velocities with depth. At shallow depths, for a frequency of 1 KHz and a seismic velocity of 1500 m/s, the boomer vertical resolution is roughly 35 cm, whereas at greater depths, for a frequency of 350 Hz and a seismic velocity of 2000 m/s, the boomer vertical resolution is approximately 1.5 m.

The vertical resolution for the Chirp data corresponds approximately to the inverse of the source bandwidth (Gutowski et al., 2002). For the 8.5 KHz bandwidth of the Chirp data and an average sound velocity of 1500 m/s, the estimated vertical resolution is of approximately 17 cm.

A visual comparison of a Boomer and chirp profiles crossing the same features is shown in figure III-19, which illustrates the differences in the resolution of both systems discussed above, providing a practical assessment of the theoretical estimates.

Seismic resolution and interpretation scale

The horizontal resolution for migrated boomer data is 1.5 to 3 m (varying with trace separation), and the vertical resolution is between 35 cm near the surface and 1.5 m at depth. Thus, the maximum interpretation scales for migrated boomer data are between 1:3000 and 1:6000, in the horizontal plane, and 1:700 near the surface to 1:3000 at depth, in the vertical plane. Chirp data has theoretical horizontal resolutions of 1 to 2 m, and vertical resolution of 17 cm,

which correspond to maximum horizontal interpretation scales between 1:2000 and 1:4000, and maximum vertical scale of 1:340.

3.4.3. Coverage constraints on seismic imaging

The positioning errors, profile separation and signal penetration are, together, the properties of a 2-D seismic coverage that will constrain the imaging of geological features. This section discusses the impact of positioning errors and misties on 3-D imaging of a geological feature with 2-D seismic data from two different perspectives: 1) the production of accurate images, versus 2) the production of consistent images. A simple method to determine maximum 3-D imaging scales is proposed. This is followed by the discussion on how profile separation and signal penetration determines if a geological feature can beadequately imaged in 3-D.

Positioning errors and misties

The problem of dealing with the impact of positioning errors and misties on 3-D imaging of a geological feature with 2-D seismic data can be stated according to two different approaches:

1) Accurate 3-D imaging: the 3-D image has to be an accurately positioned representation of the seismic observations;
2) Consistent 3-D imaging: the 3-D image has to be a consistent representation of the seismic observations; i.e. the horizon misties at profile intersections are below the scale of the representation of the image.

From the accurate 3-D imaging point of view, positioning errors and the seismic resolution values will determine the maximum 3-D imaging scales. Given the variability in the positioning errors of multiple surveys, the data with the poorest positioning will control maximum scale of an accurate 3-D image. A slightly different problem is presented when the main objective is to obtain a consistent 3-D image. In these cases, it is the residual interpretation misties, determined on a feature by feature basis, taken together with seismic resolution values that determine the maximum 3-D imaging scales.

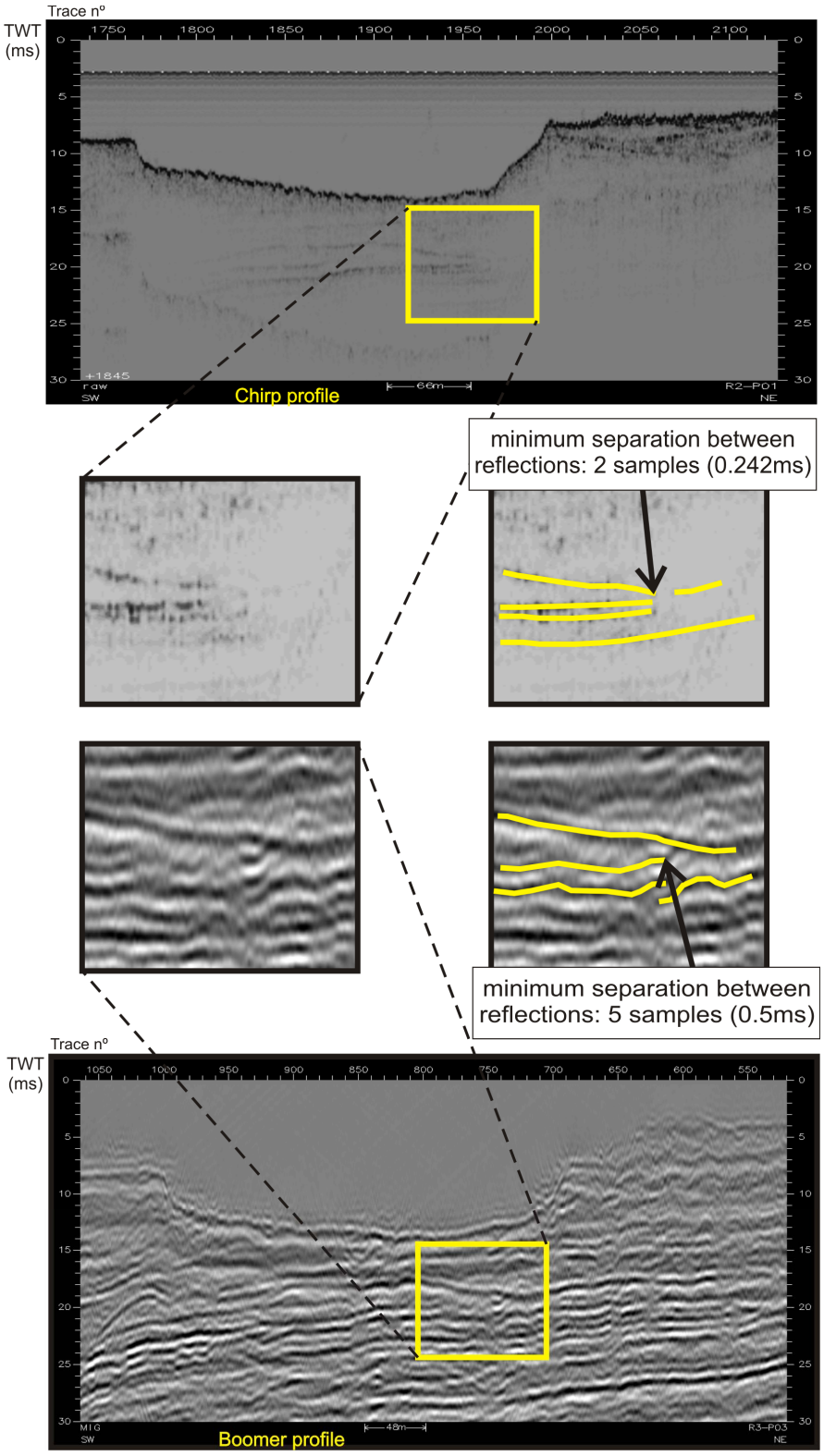

Figure III-19: Reflections of the same structure imaged both by Boomer and Chirp profiles. Analysis of these profiles illustrates the practical seismic resolution of the two datasets. The minimum separation of the reflections observed in the chirp profile is of 2 samples (0.242 ms, corresponding to 18 cm for a sound velocity of 1500 m/s). The minimum separation of the reflections observed in the boomer profile is of 5 samples (0.5 ms, corresponding to 38 cm for a sound velocity of 1500 m/s).

It should be noted that the misties are a result of both horizontal and vertical positioning errors (as described in a previous sub-chapter), as well as a result of interpretation problems. Also, the misties of an interpreted feature are differently affected by the positioning errors depending on the relationship between the real positioning errors and the shape of the feature (e.g. the misties of a flat horizontal feature will only be the result of the vertical positioning errors and of the interpretation errors).

A 3-D image that is both accurate and consistent will respect the seismic resolution, the positioning error and the horizon misties. It is possible to obtain a ballpark value for the scale of such 3-D image by adding the seismic resolution, the known positioning errors and the misties. Still, the resulting image may not be fully accurate for some positioning errors may remain unaccounted due to the complex relationship between positioning errors and misties.

The Table III-1 presents examples of the 3-D imaging scale estimates for the seismic data of the Ria of Aveiro, determined following the guidelines presented above.

Table III-1 - Horizontal (***hor.***) and vertical (***ver.***) estimates of 3-D imaging scales for the boomer and chirp data. ver.shallow and ver.deep refer to shallow and deep vertical scale computations; ***seis.res.*** – seismic resolution; ***gps*** – gps positioning error; ***clock sync*** – error of synchronism between the seismic acquisition system and the positioning system; ***offsets*** – errors resulting from the gps antenna layback and offset to the seismic trace; ***towing depth*** – error in estimating the mean depth of the towed equipment; ***tidal height*** – error in the tidal height altitude estimate; ***mistie*** – seismic profile intersection mistie of interpreted horizons; ***Consistent*** 3-D image resolution = seismic resolution + misties; ***Accurate*** 3-D image resolution = seismic resolution + know positioning errors + misties; ***res.m*** – Image resolution in meters; ***scale*** = 1:(***res.m*** x 2000).

	Data Properties							Models			
		known positioning error						Consistent		Accurate (est.)	
System	seis. res.	gps	clock sync	offsets	towing depth	tidal height	mistie	res. (m)	scale	res. (m)	scale
Boomer (hor.)	1.5	1	1	2			1.5	3	1:6000	7	1:14000
Boomer (ver.shallow)	0.35					0.5	1.5	1.85	1:3700	2.35	1:4700
Boomer (ver.deep)	1.5					0.5	2	3.5	1:7000	4	1:8000
Chirp (hor.)	1	0.01	1	0.5			0.75	1.75	1:3500	3.26	1:6520
Chirp (ver.)	0.17				0.25	0.5	0.75	0.92	1:1840	1.67	1:3340

Profile separation and seismic penetration

An estimate of the expected wavelength and directionality of the geological features to be imaged should be done a priori to assess if the available or planned seismic coverage (i.e. profile separation and signal penetration) can adequately image those features. The preliminary estimate of the shape and size of the geological objects can be based on multiple seismic profiles (if available) that image the same feature. According to Hengl (2006), the signal frequency that describes an object can be determined by the *density of inflection points*. Therefore a simple assessment can be done by determining by minimum distance (Δ_x, Δ_y, Δ_z) between ***inflection points*** observed along the feature's major axis, as well as the ***strike*** and ***dip*** *of these axes*. These can be determined by resorting to stereographic projection methods. Large scale, reasonably flat surfaces like a marine transgression erosion surface may be described as having long wavelengths (i.e. Δ_x, Δ_y of several kilometers and a comparatively small Δ_z) dipping towards the offshore. Such a surface can be adequately modeled with widely spaced profiles perpendicular to the surface dip sense. In contrast to these simpler features, channel features like the modern small irregular tidal channels of the Ria of Aveiro are characterized by comparatively smaller wavelengths. A simple model of these tidal channels can be described by Δ_x (1/2 length) < 250 m; Δ_y (1/2 width) < 50 m; Δ_z (1/2 depth) < 5 m), with various dominant trends and very gentle dips. Such features would require more densely packed, orthogonal and equally spaced profile coverage (less than 250 m apart).

According to the sampling theorem, for a wave to be properly represented it has to be sampled at least twice per cycle (Nyquist sampling frequency). From a 3-D imaging point of view, this means that the maximum profile separation directly determines the minimum width between inflection points for a feature to be properly imaged. In other words, if we consider that a geological feature can be characterized by certain wavelength, e.g. the extent of a symmetrical sedimentary basin, then this basin has to be crossed at least by two parallel profiles separated by a maximum of half the basins diameter. A greater separation between profiles will result in spatial aliasing of the features to be imaged. Nevertheless, the way

profile separation limits the choice of model scale is also dependent on the preferred orientation of the modeled object.

The penetration of the seismic signal adds another dimension to this problem. A geological feature may have a shape and size that could, theoretically, be adequately imaged by a profile grid, and yet, modeling this feature may not be possible if the changes in dip (a function of the ratios of Δ_x/Δ_z and Δ_y/Δ_z) put the feature "beyond reach" of the seismic system penetration. A simple method to assess if a certain seismic coverage allows the correct imaging of a feature is to compare the ratio of profile separation (Δ**prof**) to system penetration (Δ**pen**) with the ratios of Δ_x/Δ_z and Δ_y/Δ_z that describe the shape and size of the feature. If Δ**prof /**Δ**pen** is greater than Δ_x/Δ_z **or** Δ_y/Δ_z, then the object cannot be reliably imaged with the available seismic coverage. This means that either more closely spaced profiles or a system with better penetration are required to properly image this feature.

The adequate 3-D imaging and consequent geometrical characterization of a geological feature with 2-D seismic reflection profiles is further complicated by the frequently fractal nature of the geological features (for an introductory overview of fractals in nature see Mandelbrot, 1983). Although fractal objects are self-similar or scale-invariant, i.e., are made of parts that resemble the whole object, Euclidian measures of fractal objects are not scale independent as they are for Euclidian shapes (Barton *et al.*, 1992). In other words, Euclidian measures of fractal objects are only comparable when made at the same scale. This means that problems arise when attempting to characterize the geometry of a geological object with a variable 2-D seismic coverage. Measures such as length or strike determined on profiles with various resolutions, signal penetration and profile separations can vary significantly for the same geological object, simply because the scale of observation changes from place to place, and not because of a significant difference in the objects geometry. Figure III-20 illustrates this problem applied to the mapping of a morphological feature and of a fault surface with variably spaced profiles.

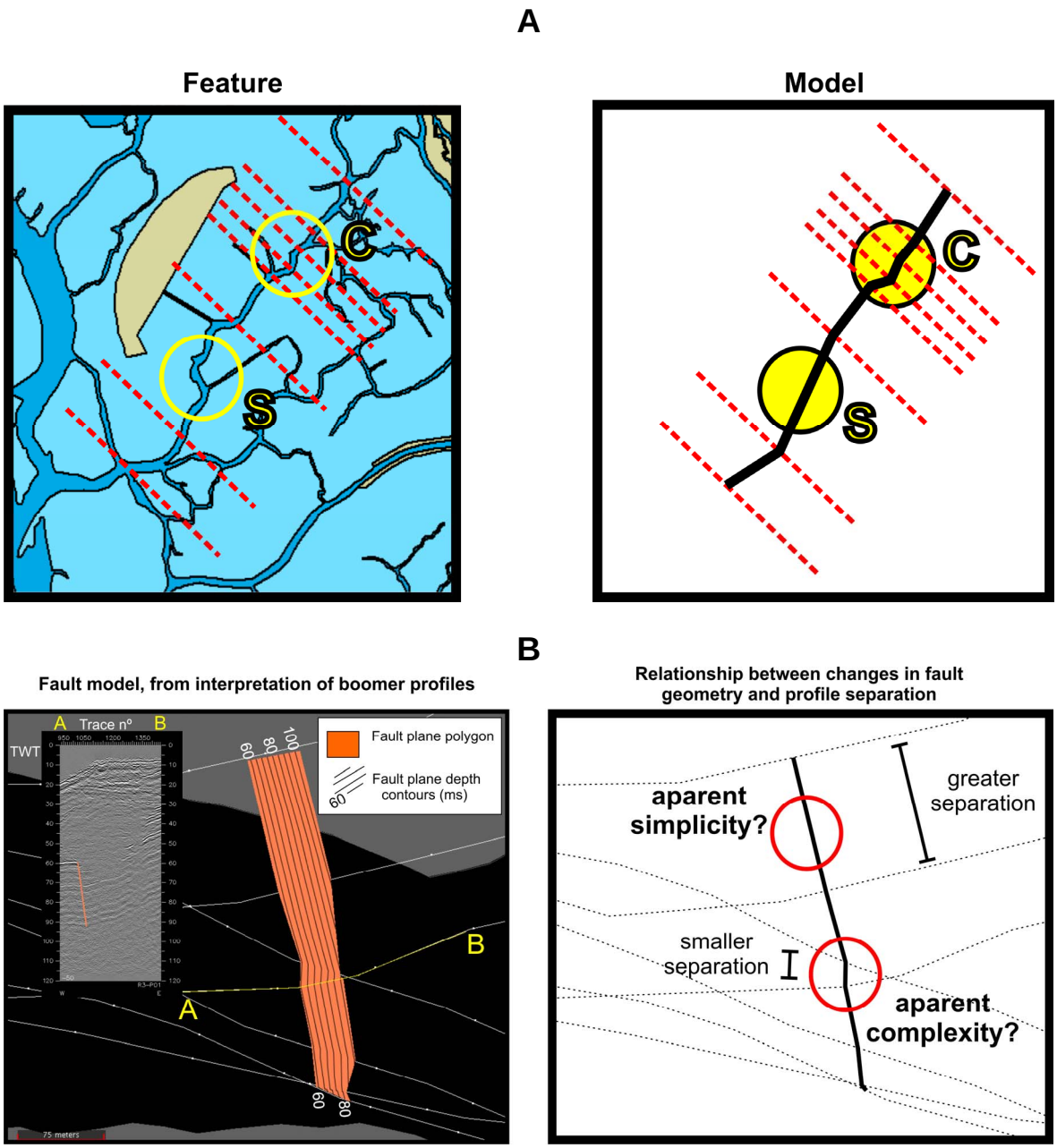

Figure III-20: Effects of variable profile spacing when mapping a fractal object. **A** –hipothetical model of a channel morphology from the Ria of Aveiro; red lines represent sampling profiles. Zones of closely spaced lines will show a more complex model geometry (red circle with label ***C***) than zones of sparsely spaced lines, that will show a simpler model geometry (red circle with label ***S***). **B** – fault model from interpreted boomer profiles in the Ria of Aveiro. In areas of closely spaced profiles, the fault model will show greater aparent complexity when compared to areas of more widely spaced profiles.

Finally, when trying to determine the orientation of linear features, the relationship between sample proximity and positioning errors has to be inspected in order to determine if the interpreted orientation is sufficiently accurate to suit

research needs. For certain threshold relationships between profile separation and trace positioning errors, interpreted rectilinear features will present significant angular deviations that tend to produce “kink” like patterns. This is a common artifact observed near profile intersections, related to positioning errors. Therefore, there is a minimum effective profile separation for reliable interpretation of this type of features, which depends on trace positioning errors. The relationship between profile separation, positioning errors and error of the modeled direction is presented in figure III-21. This figure can be used as a guide to assess whether irregularities in an imaged linear feature are positioning error related artifacts or a reliable representation of the interpreted feature.

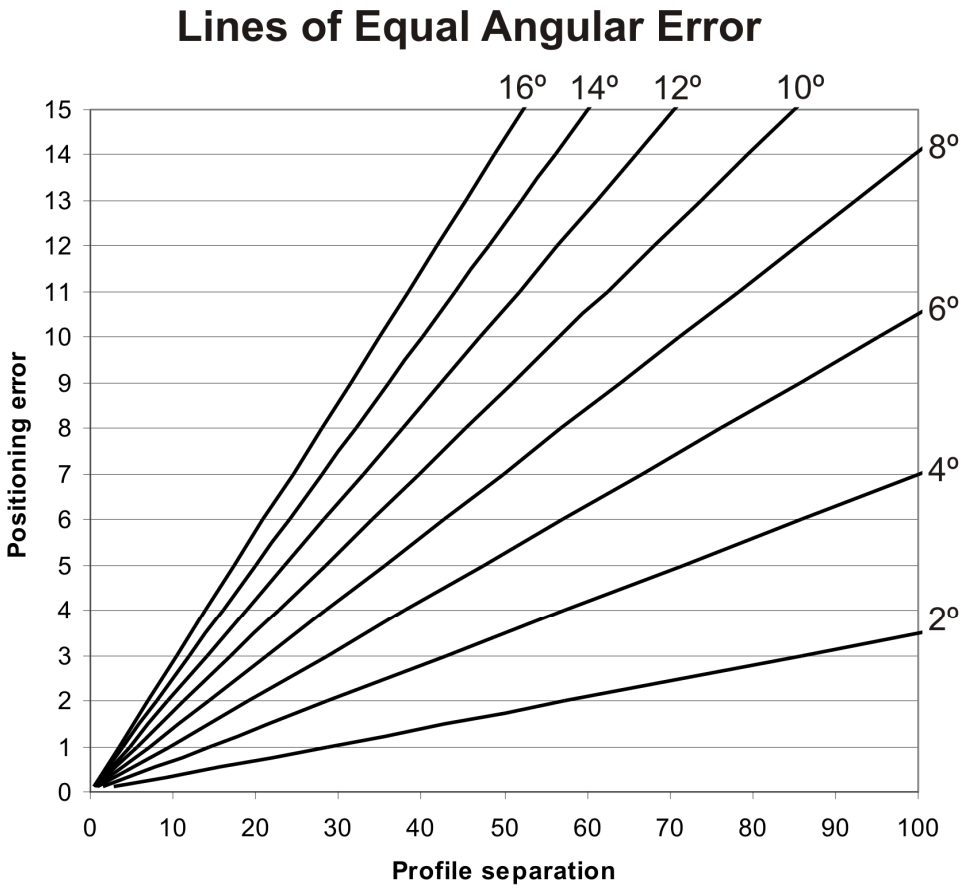

Figure III-21: Relationship between profile separation, positioning errors and angular error of the modeled direction of a linear feature. This abacus plots lines of equal angular error for a given relationship of positioning error and profile separation. Increases in positioning error and/or decreases in profile separation result in a greater error of the modeled direction of a linear feature. The positioning error related irregularity of a modeled linear feature can be minimized by limiting data input from profiles with adequate separation. Axes are labeled in arbitrary but consistent distance units.

In the case of the Ria of Aveiro, the separation between the profiles varies significantly, mainly because the navigation was strongly constrained by the lagoon's hydrography. Profile separation ranges from near coincidental (tens of centimeters apart along several tens of meters), up to hundreds of meters apart, in a same tidal channel, and kilometers apart when considering profiles acquired in different channels. A generalized value for the profile separation in different areas/channels of the lagoon is difficult to determine because local track line variations are very common and often significant. Consequently, the choice of the appropriate interpretation scale as a function of the seismic coverage will have to be done on a case by case situation. The final decision will be one of whether to use a single interpretation scale or to make multiple interpretations at different scales for different locations.

3.5. Summary and conclusions

The seismic data set used for this study has multiple vintages and the profile coverage was significantly constrained by the lagoon's hydrography. This work shows that appropriate documentation of the acquisition procedures and adequate processing of the navigation data are necessary for a reliable estimate of the trace positions. Corrections such as static corrections to compensate for tides and normal move-out corrections allow for a better constrained common vertical datum and time scale of the seismic profiles. These data positioning improvements result in a better spatial consistency for different data vintages.

The study of the relatively small geological objects on a coastal system like the Ria of Aveiro requires closely spaced profiles. For profile separations smaller than 100 meters, errors in the seismic trace position estimates are significantly influenced by the systems acquisition geometry and tidal altitude variations. Errors in the order of several meters due to the use of single mode GPS, lack of control of mid-point layback/offset values, tidal altitudes of up to 2.5 meters all add up. These errors can be comparable or even greater than 2-D seismic resolution of boomer and chirp systems. This will significantly degrade the quality of the seismic

interpretation and 3-D imaging, with effects being more relevant the smaller the object of study.

Ideally, trace and sample positioning errors should be less than half the seismic resolution, so that no sample is placed within the sampling area of a neighbor sample (for a discussion on this issue see Hengl, 2006). This could be achieved with full horizontal and vertical RTK GPS positioning of both source and receiver; synchronization of the GPS and the seismic acquisition system should be within 10 ms, so that, when surveying at 5 knots, errors are at most equal to the RTK-GPS. RTK GPS altitude data is essential to properly correct the tidal and or the eventual swell effects on the towed equipments.

The seismic signal processing proposed in this work, particularly of boomer data, provides significant improvements in signal quality and interpretability. Of particular importance when surveying shallow environments is the normal moveout correction, which allows shallower samples to be adjusted to a common vertical datum and improve significantly the ability to correlate interpretations between different seismic data vintages.

The heterogeneity of the seismic coverage, signal quality, penetration and resolution all constrain the use of the data to mostly local but detailed interpretations of the geological objects of the Ria of Aveiro. Particular care must be taken in assessing the impact of the variable horizontal coverage implied by the variable profile separation, and the probable fractal nature of the imaged geological features. The greatest profile separation used in a 3-D image should constrain the maximum imaging scale because imaging a fractal object at different scales may lead to unreliable results (see Fig III-20). To a certain extent, a parallel can be drawn between the approach that has to be adopted in this type of studies and onshore geological mapping. As with onshore geological mapping, the coastal geological map will have to be constructed from local meso-scale observations, where densely packed seismic data has to be locally interpreted in a similar way to the interpretation onshore of available rock outcrops. Correlation between these windows of observation (clusters of profiles or outcrops), if possible, has to be inferred from other indirect evidence (nature of soil, morphology etc). A good example of what can be accomplished in 3D imaging with 2D seismic data, by

following the workflow presented here, is the 1:5000 map of horizon isobaths shown in figure V-21 of the Chapter V of this thesis. Producing a map at such a detailed scale was only possible after a strict control and correction of the numerous processing issues discussed in the work.

The relative scarcity of published works that deal with the problems of acquisition and processing of very resolution seismic reflection data in shallow waters probably reflects the fact that the typical study sites and objectives of other shallow water studies allowed for the use of more straightforward surveying strategies. Typical study targets extend for several kilometers and regular survey grids appropriate for such targets are reasonably followed. Positioning requirements it these cases can be met by the available navigation methods such as GPS, and the uncertainties in the geometry of the deployed system are irrelevant given the typical scale of the studies. Navigation constraints inside a lagoon like the Ria of Aveiro require different exploration strategies, which involve locally detailed studies of relatively small targets (less than 100 meters wide). This requires greater integration and control of navigation and of the deployed seismic system in order to describe the study targets with sufficient detail. The priorities in future work should include improving the operational conditions and positioning control, in order to acquire data over the shallower areas of the lagoon (water depth less than 2 meters) and better constrain such factors as tidal altitude and synchronization between the seismic system and the navigation system. Developments in these areas can contribute to the development of a functional very high resolution 3-D seismic reflection system capable of operating in these environments and with sub-meter resolutions and signal penetration of up to 100 meters. Such a system would be well suited towards the study of costal environments characterized by geological features with highly variable shapes and sizes.

Chapter 4.

"High-resolution seismic imaging of gas accumulation and seepage in the sediments of the "Ria de Aveiro" barrier-lagoon (Portugal)"

This chapter is presented in a paper format, as published in Geo-Marine Letters (Duarte et al., 2007). The number of figures illustrating the seismic evidence of gas was limited due to the publication constrains. Further seismic evidence of gas is presented in this thesis only Apendix.

Abstract

Methane is a powerful greenhouse gas and an important energy source. The global importance and impact in coastal zones of methane gas accumulation and seepage in sediments from coastal lagoon environments is still largely unknown. This paper presents results from four high resolution seismic surveys carried out in the "Ria de Aveiro" barrier-lagoon (Portugal) in 1999, 2002 and 2003. These include three Chirp surveys (RIAV99, RIAV02, RIAV02A) and one Boomer survey (RIAV03). Evidence of extensive gas accumulation and seepage in tidal channel sediments from the "Ria de Aveiro" barrier-lagoon is presented here for the first time. This evidence includes: acoustic turbidity, enhanced reflections, acoustic blanking, domes and acoustic plumes in the water layer (flares). The stratigraphy and the structural framework control the distribution and extent of the gas accumulations and seepage in the study area. However, in these shallow systems, tidal altitude variations have a significant impact on gas detection with acoustic methods, by changing the raw amplitude of the enhanced seismic reflections, acoustic turbidity and acoustic blanking in gas-prone areas. Direct

evidence of gas escape from drill-holes in the surrounding area has shown that the gas present in the “Ria de Aveiro” consists of biogenic methane. Most of the gas in the study area was probably mainly generated in Holocene lagoon sediments. Evidence of faults affecting the Mesozoic limestones and clays underlying some of the shallow gas evidence, and the presence of high amplitude reflections in these deeper units, raise the possibility that some of this gas could have been generated in deepersedimentary layers, and then migrated upwards through the fractured Mesozoic strata.

4.1. Introduction

Estuaries and coastal lagoons are depocenters of organic rich sediments which are sources of methane (Kelley et al., 1995; Van der Nat and Middelburg, 2000). These systems are excellent and easily accessible natural laboratories to investigate the mechanisms of methane generation, accumulation, migration and escape (e.g. Garcia-Gil, 2003). However, the spatial and temporal variability and the complexity of these shallow gas systems require dense grids of geophysical data in order to get representative sampling. As a result, the importance of the escape of methane gas from sediments of estuarine and lagoon environments to the atmosphere is still poorly known or underestimated, and has not been taken into account in the International Panel for Climate Change assessment reports of the geological emissions of methane (Hovland *et al.*, 1993; I.P.C.C., 2001; Etiope, 2004; Judd, 2004). Estuaries and coastal lagoons where responsible for the generation of large accumulations of oil and gas now being exploited. Accumulations of shallow gas in such present-day systems were the volume and concentration are adequate, may also be exploited for biogas, for local use in the near future, similarly to what is already happening in African lakes and in artificial dairy lagoons (e.g.Williams and Frederick, 2001; Hirsch *et al.*, 2005). Thus, understanding the importance, the controlling factors and the mechanisms of methane generation, accumulation and escape in coastal shallow water systems may yield useful indicators for oil and gas exploration and contribute to the

evaluation of the potential of present day biogenic methane gas in estuaries and coastal lagoons as a possible alternative energy source.

Seismic evidence of gas accumulation and seepage in sediments has been reported in all marine and coastal environments, both in deep and shallow water (e.g. Hovland and Judd, 1988). Seismic reflection methods have proven to be particularly useful for the identification, characterization and mapping of the distribution of gas accumulations and seepage. Nevertheless, comprehensive seismic investigations of barrier-lagoon environments are still sparse (e.g. the Venice lagoon in McClennen *et al.*, 1997).

The aim of this paper is to present, for the first time, high-resolution seismic evidence of gas accumulation and seepage in the sediments of a tidal channel in the "Ria de Aveiro" barrier-lagoon, and to characterize the stratigraphic and structural control of these occurrences. Data from 4 different cruises carried out in 1999, 2002 and 2003, all with a very dense seismic coverage, was used. The purpose was three-fold: (1) to have enough detail and resolution to adequately map small gas accumulations (of the order of 30 m long); (2) to verify the consistency of these gas accumulations in a period of several years; (3) to analyze profiles acquired in the same area at different tidal altitudes, in order to investigate the likely influence of tidal effects on the detection of gas accumulations and escape.

4.2. Setting: The "Ria de Aveiro"

The Ria de Aveiro is a very recent barrier-lagoon system, located in the Northwest Portuguese coast (Fig. IV-1). It is a remarkable example of a fast coastal evolution, from an open bay to the sea, formed ca. the X^{th} century, to the present barrier-lagoon system (Abecasis, 1954). The Ria de Aveiro is composed of a complex network of tidal channels, tidal flats, salt marshes and supra-tidal sand isles and it encompasses an area of approximately 530 km^2, making it the largest coastal lagoon system in Portugal. It is located at the mouth of a drainage basin of 3,635 km^2, covered mostly by the Vouga River and its tributaries. Water

depths are usually quite shallow, of 1 to 2 meters, reaching locally more than 20m on the navigable channels. Water breaks and harbor installations are common along several of the navigable channels of the lagoon, and the communication with the sea, originally through a natural migrating inlet, is now made via an artificial inlet created in 1808. Tides are predominantly semi-diurnal, with an average amplitude at the inlet of 1.90m, ranging between 1.22m and 2.57m, during neap and spring tides respectively (Teixeira, 1994). The tidal amplitude decreases with the distance from the inlet, but it is present in the entire lagoon. The phase lag, variable in high and low water, increases upstream up to 5 hours, with low and high tides sometimes occurring simultaneously in different parts of the lagoon (Dias *et al.*, 2000). Water volume at low spring tides is 65hm^3 and the tidal prism at spring tides is about 80 hm^3, with an estimated time of residence of the water of three days (Teixeira, 1994).

Onshore geology reveals dune, beach and lagoonal sediments of Quaternary age, composed essentially of unconsolidated sands and clays, overlying a sedimentary succession of Mesozoic clays and limestones of the Lusitanian Basin gently dipping to the west. Borehole data ranging from a few meters to over 200 meters and seismic reflection profiles (Chirp and Boomer) show that the Quaternary sediments are less than 10 meters thick to the East of the study area, and over 100 meters thick to the West (the deeper sediments are probably Neogene), with an erosive lower boundary, locally channelized, mostly flat and gently dipping less than 1º to the west (Marques da Silva, 1992; Teixeira and Pinheiro, 1998). Direct observations of escape of biogenic methane from several drill holes in Quaternary sediments from the area surrounding the Ria of Aveiro were reported for the first time by the Portuguese Geological Survey in 1967 (Faria *et al.*, 1967). Since then, similar evidence has been observed on other land wells for water exploration. More recently, Duarte *et al.* (2003) identified several high backscatter patches on the sidescan sonar imagery acquired in other parts of the Ria de Aveiro by the Portuguese Hydrographic Institute in 1998, which they interpreted as related to gas escape; some of these features may correspond to pockmarks.

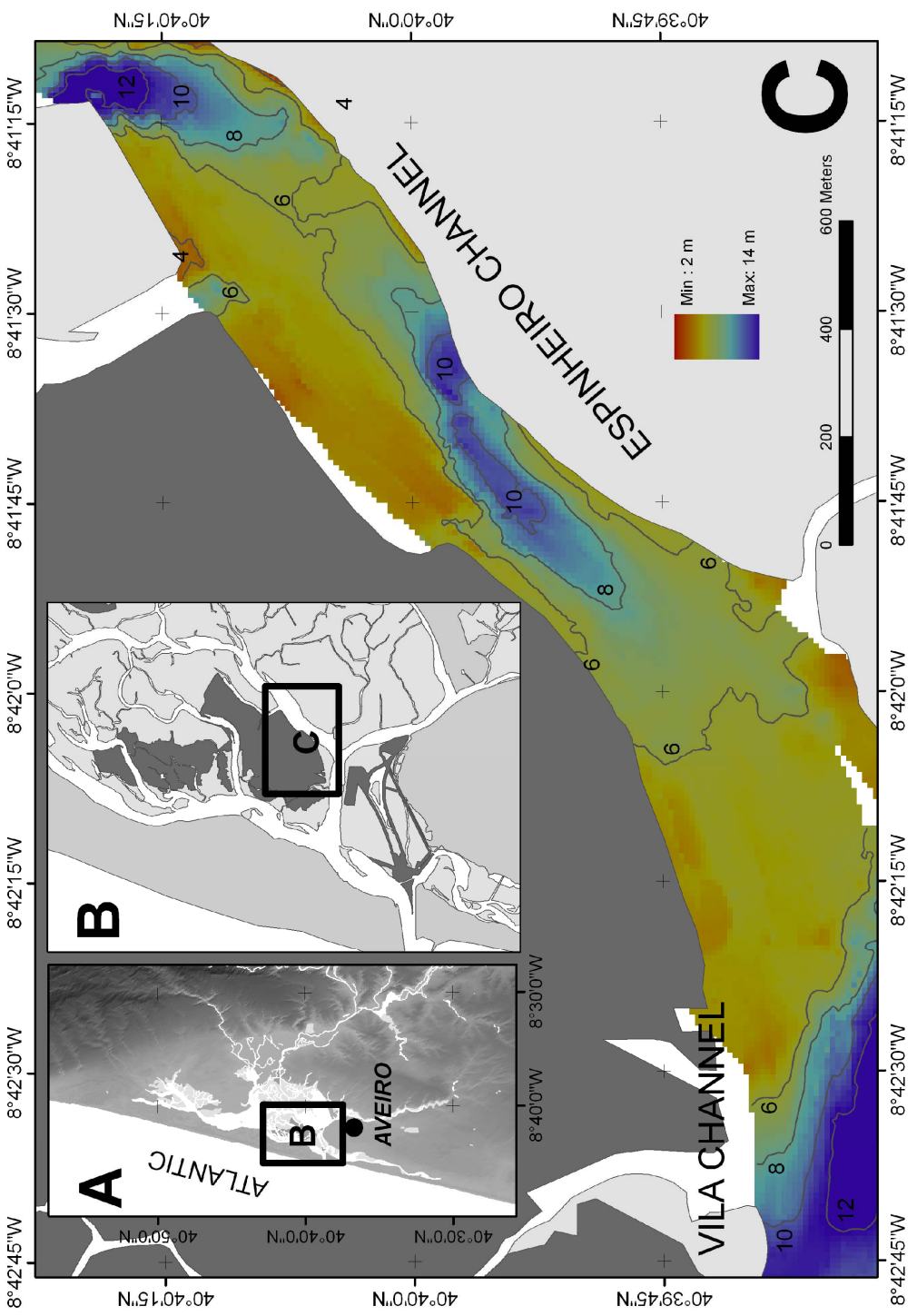

Figure IV-1: The study area: a tidal channel domain of the Ria de Aveiro barrier lagoon, Northwestern Portugal, that includes part of the Espinheiro and the Vila channels. The bathymetry of the study area shown here was derived from first break picks of the Chirp data acquired during the RIAV02 and RIAV02A cruises. This figure also shows the supra-tidal zones (dark grey) and the intertidal zones (light grey) surrounding the study area.

The study area discussed in this paper (Fig. IV-1) consists of a tidal channel domain of the Ria de Aveiro (roughly 1 km^2) that includes part of the Espinheiro and the Vila channels, where a dense seismic coverage was acquired to investigate the seismic stratigraphy, the structural control and the existence of gas accumulations. The Espinheiro channel is the main outflow conduit of the Vouga River. It feeds the Vila channel that communicates with the lagoon inlet. The Espinheiro channel has an inner meandering channel and a prograding sand body where it meets the Vila channel. The Vila channel is regularly dredged to maintain ship navigation conditions.

4.3. Database and Methods

Four high resolution seismic reflection surveys, RIAV99, RIAV02, RIAV02A and RIAV03, were carried out in the "Ria de Aveiro", on board the “Ria Azul”, from the Aveiro Harbor Authority, to investigate the seismic stratigraphy, the structural control and the existence of gas accumulations. Over 220 km of Chirp profiles were digitally acquired with a Datasonics CAP-6000W Chirp sonar during the RIAV99, RIAV02 and RIAV02A cruises. The signal bandwidth was 1,5-10KHz, the output power was 1KW and the chirp length 10ms (approximate vertical resolution of 10-15cm). During the RIAV03 cruise, 47km of additional Boomer profiles (EG&G Uniboom) were also acquired. The output energy used was 100-watt s^{-1} and the receiver array consisted of a single-channel streamer with 24 hydrophones. The signal frequency spectrum ranged from 250 to 1400Hz (estimated vertical resolution <2m). Seismic processing was carried out with the SPW software package (Seismic Processing Workshop, from Parallel Geoscience Corporation).

The processing of the boomer records included frequency band-pass filtering and time-variant amplitude gain correction. Deconvolution was also applied on some of the boomer records. The estimated depths of the seismic reflections were calculated using velocities of 1,500 m/s for the seawater and 1,700 m/s as an average for the soft sediments. From these 4 surveys, 11.5 km and 59 km of Boomer and Chirp profiles, respectively, were selected to obtain a

dense grid of seismic profiles that covers the navigable part of the channels in the study area, with a separation between profiles that ranges from 10 to 75m (Fig. IV-2). The ship speed was about 4-5 knots. Dynamic positioning of the profiles was done with differential GPS in the 2002 and 2003 cruises, and with conventional single-frequency GPS (affected by Selective Availability) in the RIAV-99 cruise (the 6 km of profiles in the study area from this cruise were mainly used for interpretation, but not for mapping, given the large associated positioning errors).

A constant time shift was applied to each profile to account for tidal fluctuations and the depth of the towed equipment (fish and streamer). Residual misties, in general, did not exceed 1 ms. The vertical datum of the surveys was corrected to match the Hydrographic Zero Datum used by the Portuguese Hydrographic Survey, by matching the estimated horizon depths with the true depths for the same horizons derived from geotechnical soundings that cut through the Mesozoic bedrock (based on unpublished reports from the Harbor Authority kindly made available for this study). SEG-Y seismic data management and interpretation was carried out using the Kingdom Suite (Seismic Micro-technology Inc.) and the Openworks and Seisworks-2D (Landmark Graphics Corporation) seismic interpretation software packages. All the available borehole, seismic and geographical data was inserted into a GIS database (ArcGis, ESRI; see Fig. IV-2 for location of seismic lines and borehole data), which was used throughout this work for spatial computations.

4.4. Results

4.4.1. Acoustic evidence of gas accumulation and seepage

The changes in acoustic character that characterize gas evidence (as described for marine environments by Hovland and Judd, 1988; or, for coastal environments, by Garcia-Gil *et al.*, 2002) are not always easily perceptible due to specific characteristics of the seismic acquisition conditions in a shallow lagoon environment.

Figure IV-2: Boomer and Chirp seismic coverage in the study area. Thick solid lines show the location of the seismic profiles shown in this paper. The inset shows the location of the available seismic lines and boreholes in the vicinity of the study area. Although there are no boreholes within the study area, the extent of the seismic coverage allowed the use of the particularly dense borehole data in the southern edge of the inset to calibrate the main seismic units, in particular the reflection corresponding to the top of the Cretaceous limestones and marls, and to adjust the vertical datum of the seismic surveys.

In these shallow systems, the survey coverage variability, the frequent changes in profile direction, the strong and variable bottom multiple interference caused by shallow water depth and the tidal altitude changes (about 2 meters), and the scarcity of reflections, due to sediment homogeneity or the lack of signal penetration in the presence of sandy sediments, all limit the identification of gas evidence. Taking into account all these limitations, all diagnostic seismic features that could potentially be related to gas in the Ria de Aveiro were identified on each seismic line, compared with the neighboring lines to check for the lateral consistency, and mapped.

The seismic evidence of the presence of gas identified on the seismic data falls into two main groups:

1. Sub-bottom/bottom seismic features: acoustic turbidity in the sediment layers, enhanced reflections, acoustic blanking, domes;
2. Water-column seismic features: acoustic plumes (flares), bottom acoustic turbidity and cloudy acoustic turbidity in the upper water layer (cloudy turbidity; Garcia-Gil *et al.*, 2002).

Sub-bottom/bottom seismic features

Acoustic Turbidity

Acoustic turbidity (AT) is recognized as a variable degree of disturbance on the seismic record (AT in Fig. IV-3), which sometimes allows coherent reflections to be followed through, with reduced amplitude (Hovland and Judd, 1988; Garcia-Gil *et al.*, 2002). Acoustic turbidity can be caused by gas bubbles or vesicles in typically impermeable sediments, although it can also be caused by other point scatterers like e.g. coarser grains in poorly sorted sediments. Small percentages of gas volume (1%) are enough to generate acoustic turbidity (Fannin, 1980).

Enhanced reflections

Enhanced reflections (ER) are characterized by a marked lateral increase in the amplitude of coherent reflections (ER in Fig. IV- 3). They can be caused by the accumulation of gas bubbles below an impermeable interface, generally at the top of a sediment bed or at an angular truncation, or by the presence of methane-derived authigenic carbonates. Lateral facies variations non-related to gas can

also cause enhanced reflections. The frequency content of gas-related enhanced reflections will in general be lower than the original reflections and phase reversal generally occurs (Hovland and Judd, 1988).

Acoustic blanking

Acoustic blanking (AB) is characterized by a transparent or signal-starved domain in the seismic section, topped either by an enhanced reflection, broken or coherent, or by acoustic turbidity (AB in Figs. IV-3, IV-4 and IV-5). The signal starvation is interpreted as the result of the attenuation of the acoustic signal caused by gas in the sediments. Depending on the amount of gas, reflections that cross or lie below the area with gas often exhibit a pull-down effect caused by the lower sound propagation velocity in the gassy sediments. In areas such as the Ria de Aveiro, where old shipwrecks are abundant, it should also be noted that wooden debris can also cause localized acoustic blanking because the acoustic response of dry wood in wet sediments is similar to that of gas (Quinn *et al.*, 1997).

Domes

The domes (DM) observed in the study area (DM in Figs. IV-3 and IV-5) are small elongated elevations, 2 meters high and 30 to 50 meters long, found at the bottom of the lagoon, usually capped by a strong reflection at the water-sediment interface, and are associated with acoustic evidence of gas accumulations (Fig. IV-3). Although the nature of these features is not yet fully understood due to the lack of sampling, they may result from mud extrusion caused by gas overpressure of clayey sediments, from accumulation of organic debris, or they may correspond to small (methane related?) carbonate build-ups.

Seismic features in the water column

Acoustic plumes (flares), acoustic turbidity near the channel bottom, and cloudy turbidity in the upper water layer (upper 10 ms) are extensively observed on the Chirp records from the study area (Figs. IV-3 and IV-6). These features may result from a variety of factors, including gas bubbles in the water column,

suspended matter, gas in fish swimming bladders, acquisition system artifacts, or ship noise.

Acoustic plumes

The Chirp records reveal several localized areas with well defined plumes (PL in Fig. IV-3) of acoustic turbidity in the water layer (flares), usually elongated, either vertical or strongly dipping, often starting near the water-bottom and extending towards the surface (Fig. IV-6). The amplitude of the acoustic reflections in these plumes is often stronger in their upper part. These features are similar to those described in other locations (e.g. the Ria de Vigo, Spain, Garcia-Gil *et al.*, 2002) as resulting from sound reflecting off gas bubbles that are escaping from the sediments to the water column. Occasionally, some of these plume-like features do not start at the water-bottom. Although in some cases they may correspond to fish shoals, several of them are interpreted here as gas bubbles escaping obliquely to the seismic profile, particularly when they are found over sediments with other evidence of gas accumulation.

Bottom acoustic turbidity

Bottom acoustic turbidity is also locally observed on Chirp sections in the Ria de Aveiro, close to the lagoon bottom, usually above enhanced reflections or acoustic blanking (Fig. IV-3). These features can be caused by gas escape, where the gas is being quickly dissolved as it rises through the water column, or by a high density of benthic/pelagic organisms, possibly benefiting from a gas-enriched feeding environment.

Cloudy acoustic turbidity in the upper water layer

Cloudy turbidity, similar to that described by Garcia-Gil (2002) in the Ria de Vigo, is also frequently observed in the upper water layer, on the Chirp seismic sections (upper 5-10 ms; Fig. IV-7). It can be caused by point scatterers in the water column, like gas bubbles, matter in suspension or gas in the swimming bladders of fish. The fact that this shallow turbidity in the study area generally occurs at a typical water depth, suggests the existence of some sort of control on

the occurrence of these point scatterers or the existence of a water depth detection threshold for these features, possibly due to signal energy loss in the water column. The observed frequency of point reflections is also clearly related with the tidal altitude. Point reflections counted on a total of ca. 20000 traces, are 10 times more frequent at lower tidal altitudes (37 point reflections per 1000 traces during low tide, ebb and flood) than at high tidal altitudes (4 point reflections per 1000 traces during high tide).

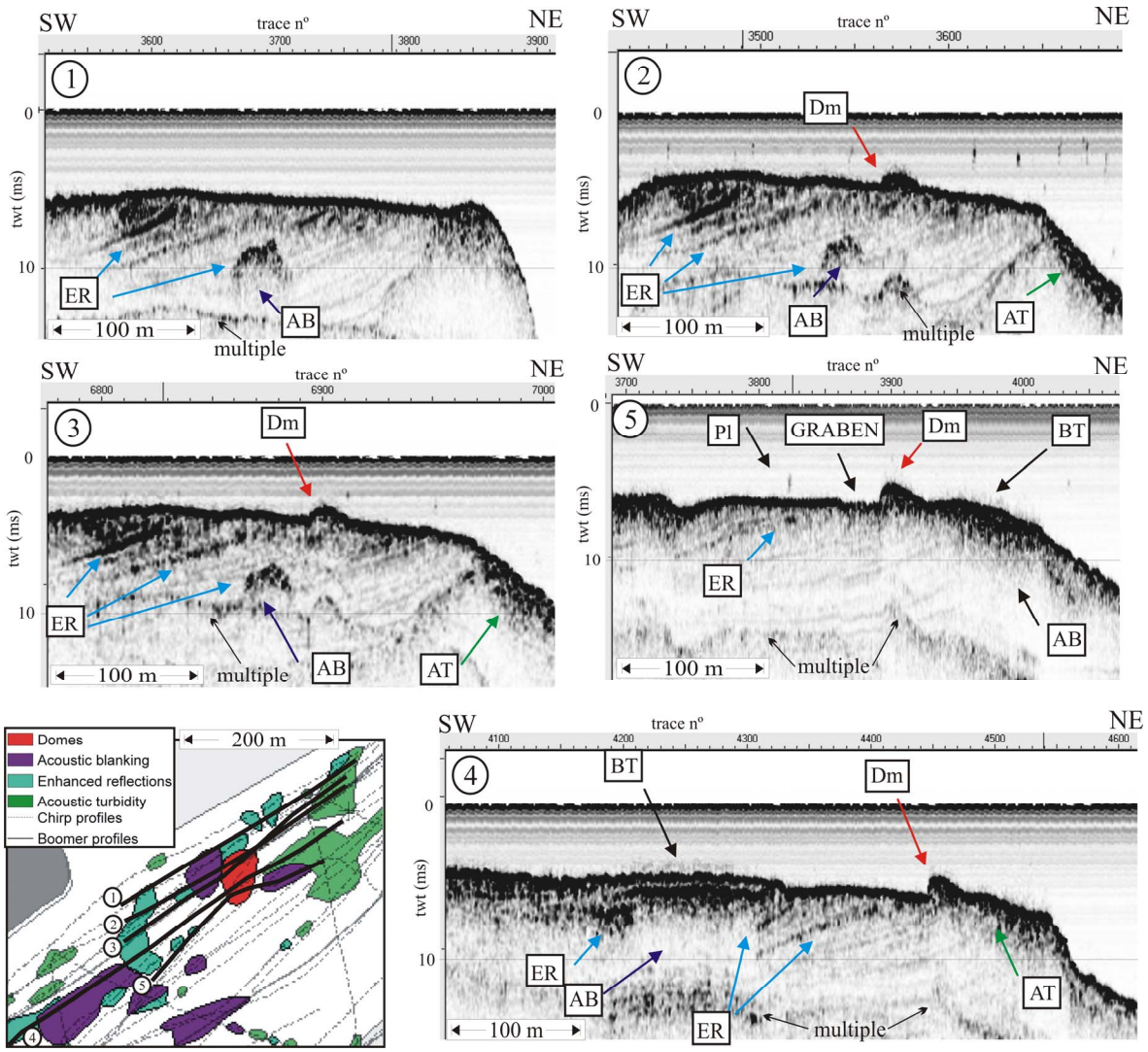

Figure IV-3: Acoustic evidence of gas accumulation and seepage from the NW gas field (GF1) observed on Chirp profiles. Note the association of the observed dome structure (40x20 m and 2 m high) with evidence of gas accumulation in the sediments observed on these 5 Chirp profiles in the Espinheiro Channel. Also notice the marked difference in the strength and extent of the gas evidence on the profiles 2 and 3, acquired at low tide (stronger and more extensive), with the evidence on the profile 5, acquired at high tide (weaker). Location of the profiles is represented in the lower left map of gas evidence, (see Fig. IV-2 for the location of this inset in the study area). Dm: Dome; AB: Acoustic Blanking; ER: Enhanced Reflection; AT: Acoustic Turbidity; BT: Bottom Acoustic Turbidity; Pl: Acoustic Plume.

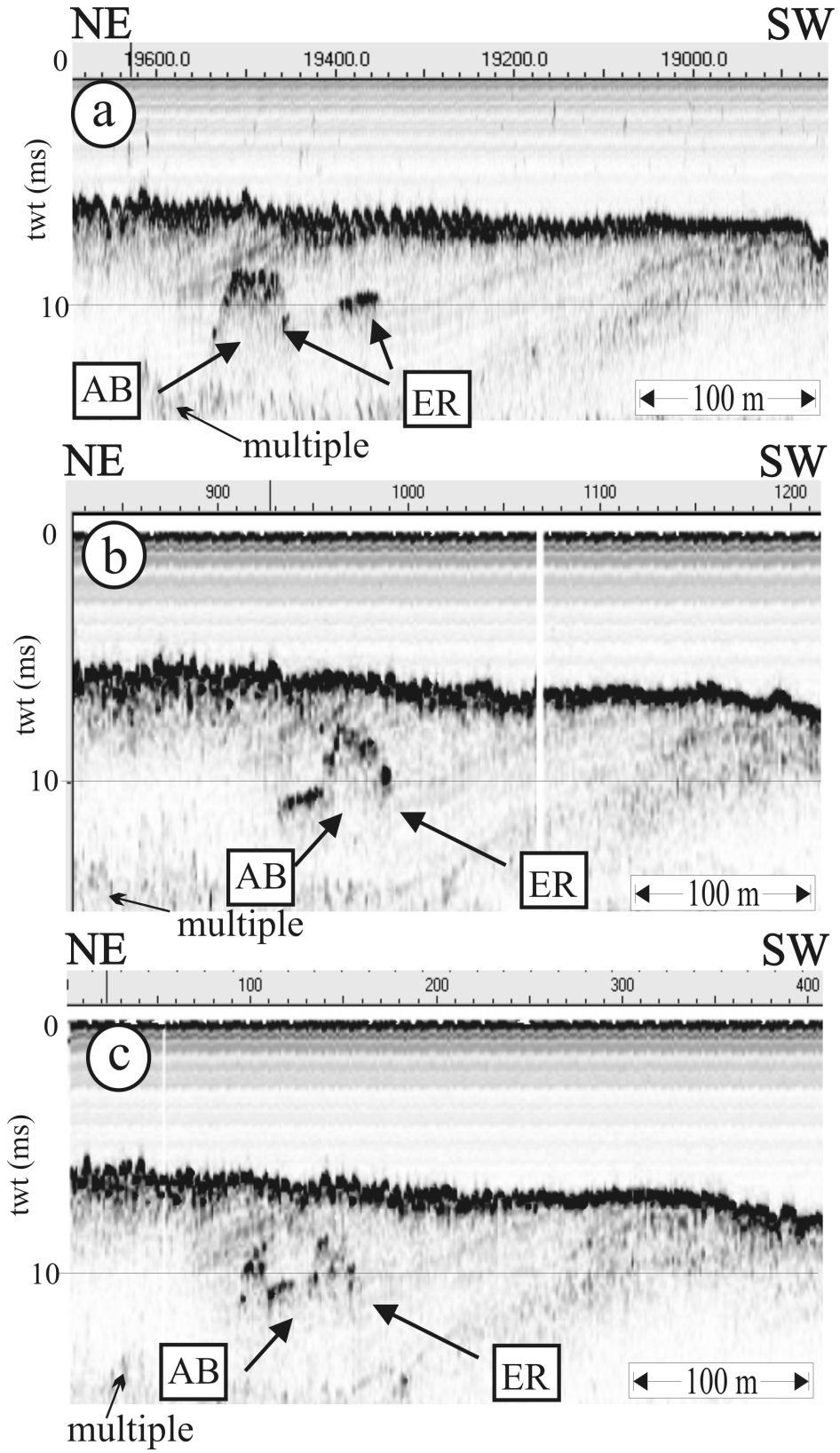

Figure IV-4: Acoustic blanking observed in three Chirp profiles from the SW gas field (GF2) (a – profile 16, RIAV02A cruise; b – profile 1, RIAV02 cruise; c – profile 3 RIAV02 cruise). AB: Acoustic Blanking; ER: Enhanced Reflection. See location in Fig. IV-2.

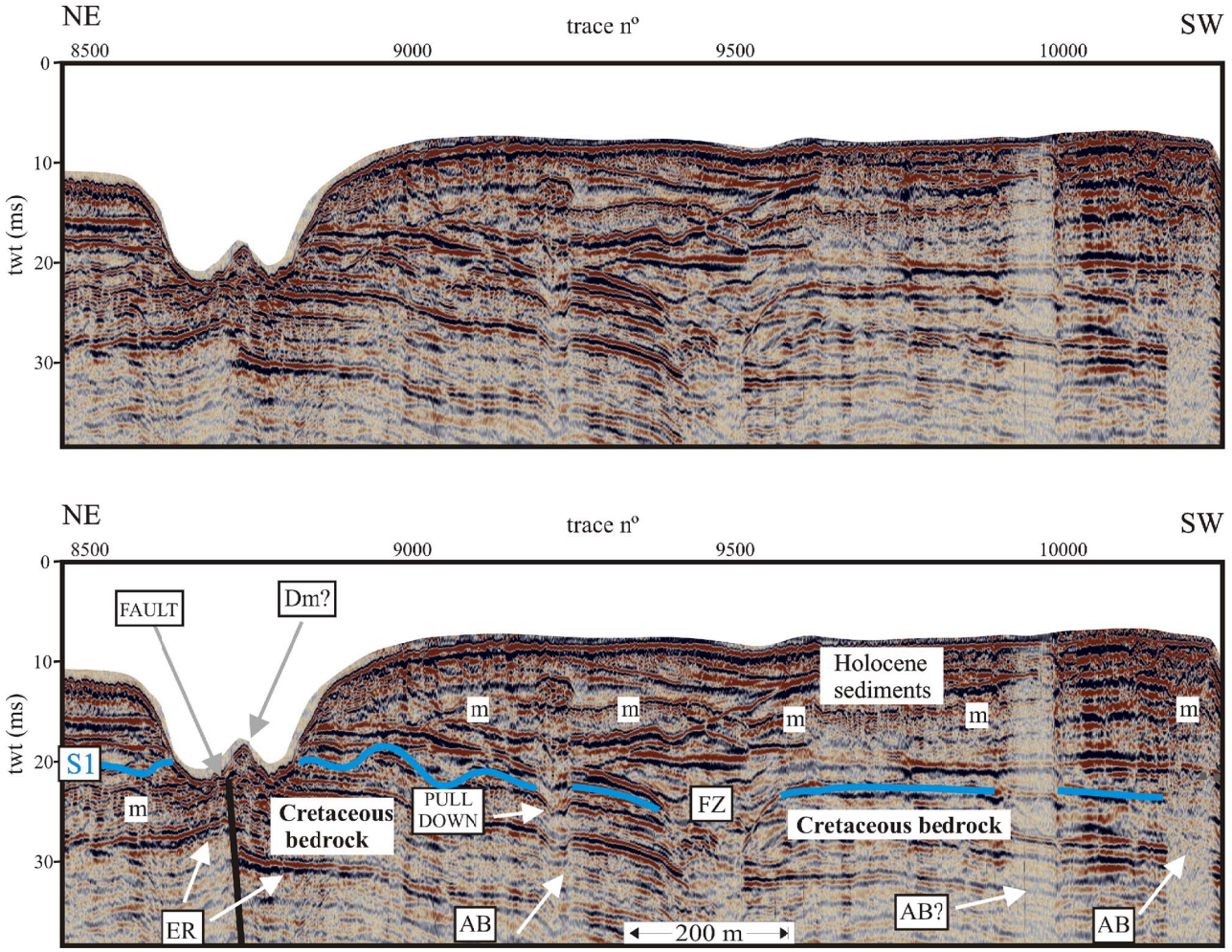

Figure IV-5: Acoustic evidence of gas on the Boomer profile P02 from the RIAV03 cruise (see location in Fig. IV-2). Examples of acoustic blanking and possible fault-controlled dome, with associated enhanced reflections at depth. The fact that this dome is only crossed by this seismic line does not allow an unambiguous interpretation of this feature. Dm: Dome; AB: Acoustic Blanking; ER: Enhanced Reflection; FZ: fault zone; S1 – erosive top of the Cretaceous bedrock; m –water bottom multiple.

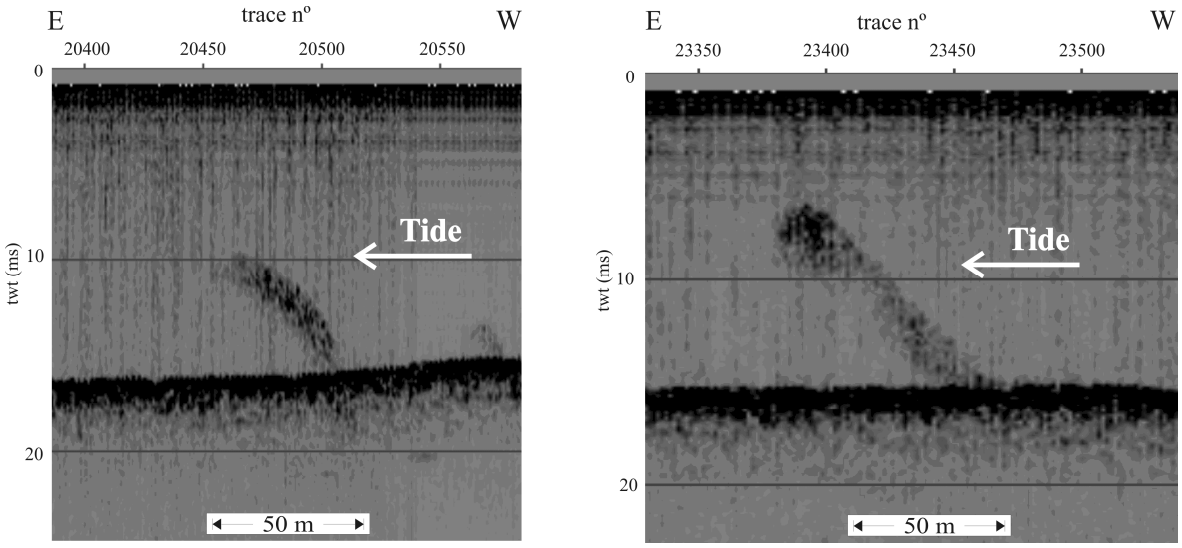

Figure IV-6: Acoustic plumes observed on different segments of the Chirp profile RIAV99 P06, in the Vila Channel (see location in Fig. IV-2). These features may correspond to gas bubbles or fish shoals. Notice that the inclination of acoustic plumes is consistent with the tidal current sense (white arrow).

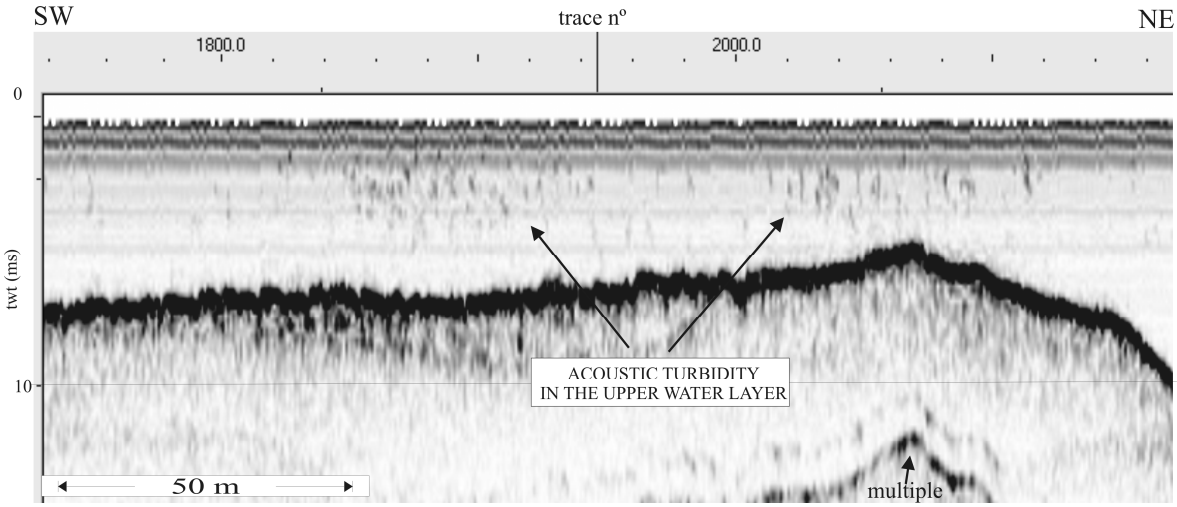

Figure IV-7: Cloudy acoustic turbidity in the upper water layer observed on the Chirp profile RIAV02A-P10 (see location in Fig. IV-2). These features can be caused by point scatterers in the water column, such as gas bubbles, matter in suspension or gas in the swimming bladders of fish. See discussion in the text.

4.4.2. Distribution and extent of gas accumulation and seepage

Acoustic evidence of gas accumulation in the sediments is abundant in the study area (ca. 14% of the total area) and it is concentrated in two main gas fields in the northeast and in the southwest sectors (GF-1 and GF-2; Fig. IV-8), where

the water is shallower, usually less than 4 meters. Both gas fields exhibit several of the characteristic acoustic evidence of gas accumulations.

On the Chirp sections, acoustic evidence of gas accumulations is generally observed in the first few meters of the sediments and rarely reaches the water-bottom interface. Where a dense seismic coverage is available and the interpretation well constrained, the gas accumulations generally consist of roughly circular or elongated patches, 30 to 150 m long. This shows why it is necessary in these systems to acquire a dense seismic coverage, with separations between lines of less than 15m, in order to adequately map these accumulations without spatial aliasing. As such, in this study, interpolation and extrapolation of gas anomalies for mapping was only carried out when the separation between adjacent profiles was less than 20 meters, and therefore the mapped evidence of gas accumulation may underestimate the total area of gas accumulation.

Areas with acoustic blanking are frequent and are often associated with adjacent enhanced reflections. These reflections are interpreted as resulting from gas migration from the zones of acoustic blanking, to the neighboring sedimentary layers. Acoustic blanking is also frequently adjacent to and in apparent continuity with acoustic turbidity on neighboring profiles. Often, this adjacent acoustic turbidity is very similar to the top of the acoustic blanking zones but it is not mapped as such, given the difficulty in sometimes unambiguously determining the occurrence of blanking below the turbidity (either due to multiple interference, absence of reflections due to an homogeneous sedimentary section or poor signal penetration in sandy sediments). It has also been observed that gas-prone areas with strong evidence of acoustic blanking on profiles acquired at low tide, often appear as areas of acoustic turbidity (sometimes very tenuous and of reduced extent) on almost coincident profiles acquired at high tide (see Fig. IV-3 and compare the overall strength and extent of gas evidence on profiles 2 and 3, acquired at low tide, with the gas evidence on profile 5, acquired at high tide).

In the study area, the acoustic evidence of gas accumulation is generally observed in the upper seismic unit that corresponds to Holocene tidal channel-fill sediments (probably ca. 800-200 years BP, Duarte *et al.*, 2005). The typical dimensions of the areas with spatially coherent acoustic evidence of gas

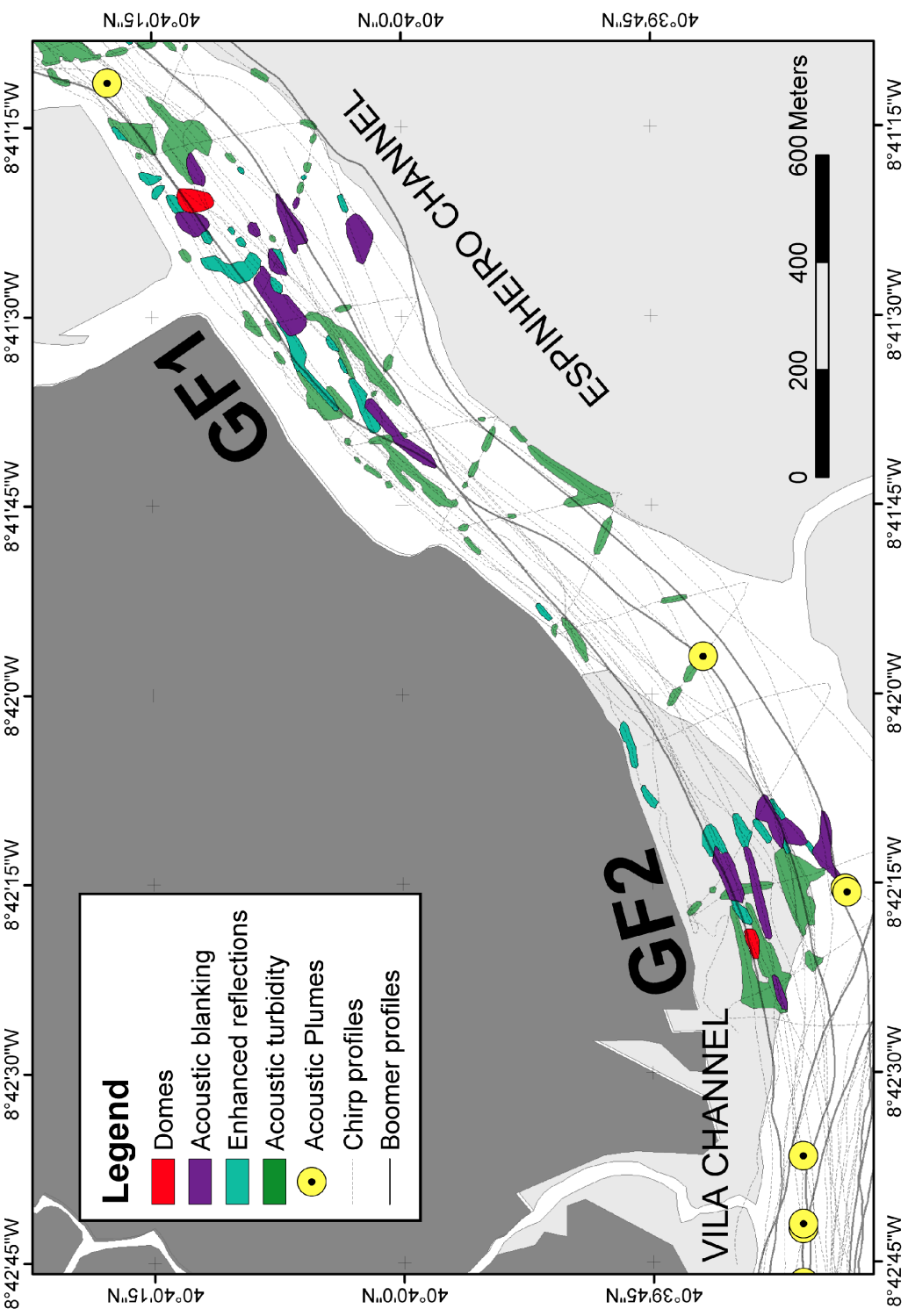

Figure IV-8: Map of the acoustic evidence of gas accumulation and seepage in the study area (see also Fig. IV-1 for a more general geographical context). GF1 and GF2 are the two gas fields described in the text.

accumulation (typically 30 to 150 meters long) probably reflect the size of the host sedimentary bodies.Considering that the tidal channels in the "Ria de Aveiro" are usually 20 to 300 meters wide, it should be expected that their sediment infill bodies, where gas may be generated or trapped, have a similar range of dimensions.

The two roughly elliptical, 40 meters long domes observed in the study area are strongly spatially associated with clear evidence of gas accumulation in the sediments. This relationship is particularly obvious in the northwestern dome on GF1 (Fig. IV-3), where the dome clearly mimics the shape of an acoustic blanking zone located down-dip, a few meters to the west (Fig. IV-3). On the Chirp profile that crosses the southern edge of this dome, there is no evidence of acoustic blanking; instead, a 20 meter-wide graben is observed, with a small offset affecting the sediment layers and the water-bottom, suggesting that the degassing of the deeper sediments might be causing the subsidence and deformation of the upper sedimentary layers (Fig. IV-3).

Unlike the other gas evidence, the eight acoustic plumes observed in the study area occur in deeper waters (more than 6 meters), where currents are stronger, the bottom sediments are coarser and where, sometimes, the Mesozoic clays and limestones outcrop. No clear evidence of a nearby source of gas accumulation was found for the acoustic plumes. Nevertheless, six of the eight observed plumes occur above a 1.5 km-wide graben with an offset of approximately 40 meters, that affects the Mesozoic bedrock (Fig. IV-9). A spatial relationship of gas evidence with the Mesozoic bedrock fracture pattern is also observed in other places, such as near the GF1 where a possible dome rests above the faulted Mesozoic bedrock (Fig. IV-5).

4.5. Discussion and Conclusions

Middelburg (2002) estimates that estuaries emit between 1.8 and 3.0 Tg CH_4 yr^{-1}. This estimate represents <9% of the total oceanic emission (Bange *et al.*, 1998), which in turn is a very small component of the global methane emission.

While the well mixed assumption is most probably valid for the larger, open systems, evidence presented here for the tidal channels of these smaller but very organic rich environments, points to the existence of focused fluid escape structures and a very heterogeneous spatial and time control of distribution and extent of gas accumulation.

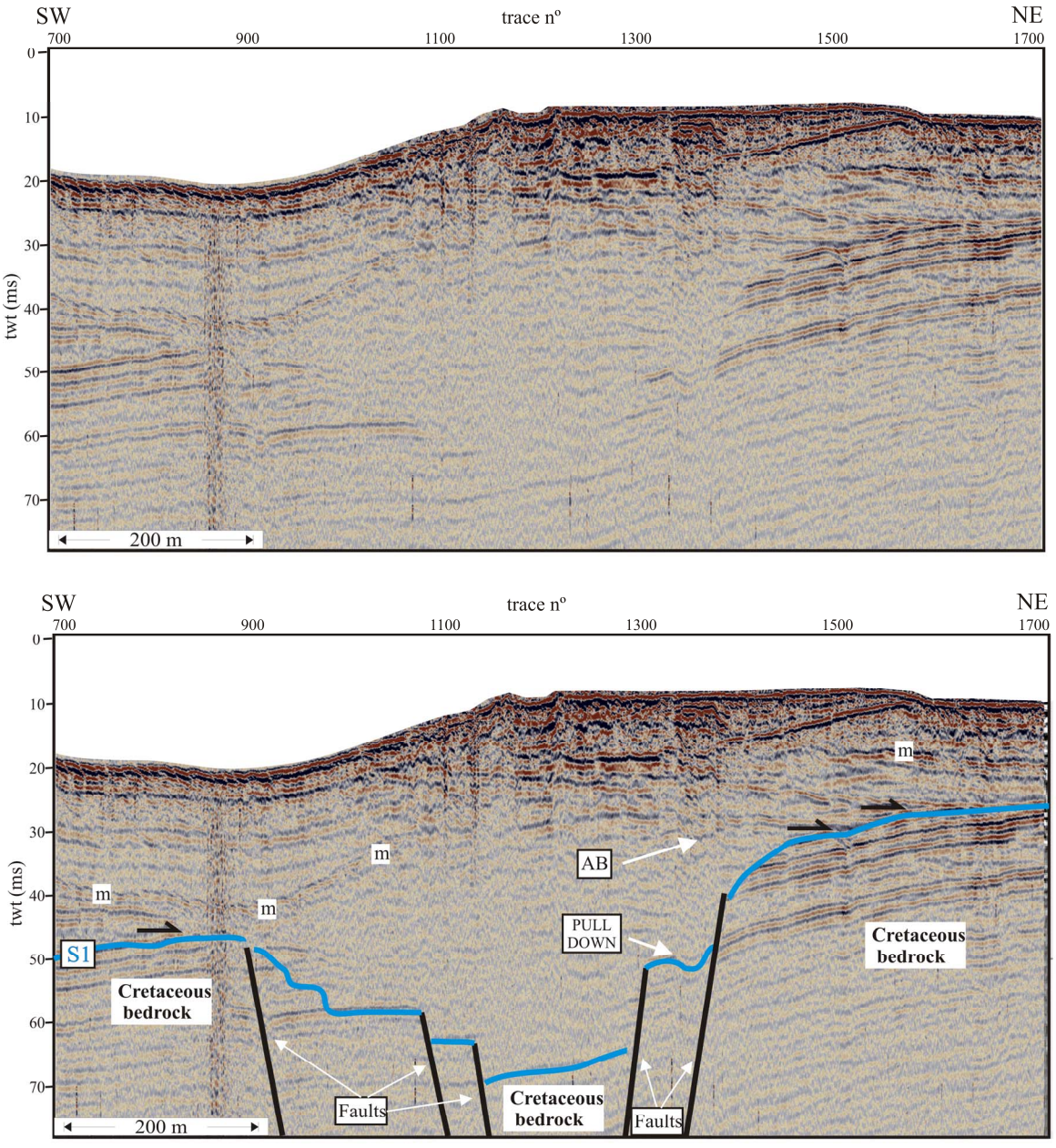

Figure IV-9: NW-SE oriented graben affecting the Mesozoic bedrock, observed on the Boomer profile RIAV03-P01 (see location in Fig. IV-2). The acoustic plumes observed on Chirp profiles in the study area occur mostly above this graben structure. AB: Acoustic Blanking; S1 – erosive top of the Cretaceous bedrock; m –water-bottom multiple.

This focusing of gas escape and space and time heterogeneities suggests that the premise of good water mixture might not hold true in this specific type of coastal lagoon systems and that the kind estimation presented by Middelburg (2002) may significantly underestimate gas emissions from small coastal lagoons.

The variability in space (distribution and extent) and time (with the tidal cycle) of the acoustic evidence of gas in the studied area is in accordance with and illustrates in detail the fact that methane concentrations in rivers, estuaries and other coastal environments are highly variable at various spatial and temporal scales (Sansone *et al.*, 1999). Unlike other very high resolution seismic-reflection gas studies of coastal environments, such as Chesapeake Bay (Hagen and Vogt, 1999) or the Ria de Vigo (Garcia-Gil *et al.*, 2002), that recognized and mapped large gas accumulations with a typical seismic profile separation of 200-250 meters, the seismic investigation of gas accumulation and seepage in the sediments of the "Ria de Aveiro" required specific surveying and mapping strategies. This is because of the high spatial and temporal variability of barrier lagoon environments like the "Ria de Aveiro". Aspects like the strong and variable bottom multiple interference caused by shallow water depth and tidal altitude changes (about 2 meters), and the scarcity of high-amplitude laterally continuous reflections, due to sediment homogeneity or the lack of signal penetration in the presence of sandy sediments, all limit the ability to detect gas evidence, in particular the characteristic blanking effect or lateral changes of amplitude of the reflections. Also, the typical acoustic evidence for gas in the Ria de Aveiro consists of patches, 30 to 150 meters long, probably due to the characteristic size of the tidal channel infill sediment bodies that host the majority of the gas accumulations. Thus, the sizes of the gas-related objects to be studied required a profile separation of the order of 10 meters, or less, to adequately to map the gas evidence.

Comparison of approximately coincident seismic sections acquired at different tidal altitudes, revealed that the acoustic detection of gas in the sediments and in the water layer of the Ria de Aveiro is particularly influenced by tides, with amplitudes and size of the evidences being stronger and larger in profiles acquired during low tide than on profiles acquired during high tide. The same influence is

also apparent on the observation of the cloudy turbidity in the water layer of the Chirp seismic lines, which could be gas-related, and that probably corresponds to the cloudy turbidity also observed in the Ria de Vigo (Garcia-Gil *et al.*, 2002). Again, the frequency of these turbidity events varies with the tidal cycle, being roughly 10 times more frequent at low tide than at high tide. The simplest explanation for the observed tidal altitude control on the frequency of the occurrence of cloudy turbidity is a possible tide-related control on the behavior of some specific fish assemblages, more easily detectable by the acoustic systems used in this study. Nevertheless, it should be noted that ichthyofauna studies in the Ria de Aveiro (e.g. Garnerot *et al.*, 2004; Pombo *et al.*, 2005), showed that a decrease in marine influence results in a decrease in total density and biomass of fish assemblages; this is in disagreement with the pattern observed here: if the point reflections result from fish, then a higher density of reflections in the water column would be expected during high tide, which is just the opposite of what is observed. An alternative explanation is that there is a tidal control on the abundance of gas bubbles of optimal resonance-size for the acoustic frequencies used in this investigation (250 Hz to 1.4 KHz of the Boomer system and 1.5 to 10 KHz of the Chirp system) caused by changes in pressure and or salinity resulting in ebullition and/or bubble size variation. This is consistent with a preferential detection of gas bubbles at low tide, when lower hydrostatic pressure and salinity could trigger ebullition and/or bubble size variations. An increase in bubble size towards the surface could explain why most point reflections are observed in the upper part of the water column (need for the bubbles to reach an optimal resonance size for detection with the frequencies used).

The described relationships between tidal altitude and the gas evidence in the Ria de Aveiro can probably be explained by tidal fall triggered methane ebullition (e.g. Jackson *et al.*, 1998) and/or by tidal induced changes in the number of optimal resonance size bubbles for the used frequencies (Best *et al.*, 2004). Therefore, one needs to be careful when using acoustic methods to map gas accumulations, because areas with a similar amount of methane content in the sediments may produce a different acoustic response, such as seen in the Ria de Aveiro, depending on the stage of the tidal cycle during which they where

surveyed. Further data acquisition and modeling of the methane solubility and the variations in bubble size with the tidal cycle in the Ria de Aveiro is required to understand the relative importance of methane ebullition and the relationship of bubble resonance with the frequency range of the seismic reflection system in the detection acoustic evidence of gas.

The fact that, where the acoustic plumes are observed, the sediments are generally relatively coarse and permeable (fine to coarse sands, Duarte *et al.*, 2003), could indicate a more diffuse fluid escape through these sediments. On the other hand, the lack of associated evidence of gas accumulation in the Holocene sediments, and the observed spatial relationships between the acoustic plumes and the fracture pattern of the Mesozoic bedrock, support the hypothesis of focused gas escape through the fractures in the Mesozoic bedrock. It should be noted, however, that a clear association between the acoustic plumes and some sort of gas source in the Mesozoic bedrock was not unambiguously found in the study area, nor gas analyses are yet available, and therefore the gas source of these acoustic plumes still remains unknown.

The results obtained with this high resolution seismic study have shown that the Ria of Aveiro is an interesting natural laboratory to study the generation, migration and escape of shallow gas on a typical barrier lagoon system. The dense grid of seismic data allowed the detailed mapping of the different types of seismic evidence of gas accumulation and seepage. Moreover, seismic data acquired in different years showed that these gas accumulations are found consistently in the same area for long time periods, although minor changes in the character of the reflections can be observed. The interpreted evidence of gas accumulation and seepage ranges from acoustic blanking and turbidity, enhanced reflections in the sediments, to the presence of flares in the water column and, also possibly, the occurrence of small domes at the bottom of the lagoon, closely associated with gas accumulations at depth. Boomer records, in particular, suggest that the faults observed in the Mesozoic bedrock may also constitute pathways for the escape of deeper gas of yet unknown source and composition.

Chapter 5.

Structural and tidal controls on shallow gas occurrences in the Ria of Aveiro barrier lagoon (Portugal): new results from a pseudo 3D high-resolution seismic survey

Duarte, H & Pinheiro, L.M (to be submitted)

This chapter is presented in a paper format to be submitted to a peer reviewed SCI journal.

Abstract

This work presents results from a Chirp high-resolution pseudo 3D seismic survey carried out in 2002 to investigate the occurrence of shallow gas in major tidal channels of the Ria of Aveiro barrier lagoon (Portugal). Evidence of gas includes: acoustic turbidity, enhanced reflections, acoustic blanking, pockmarks and buried trough pockmarks, disrupted horizons and acoustic plumes in the water column (flares). The impact of the tidal altitude variations on the detection of gas with seismic methods is analysed and a quantitative analysis of the changes of the amplitude strength of reflections with tidal altitudes is presented. Reflection amplitudes in gas-prone areas are clearly stronger during low tide with maxima during ebb, decreasing with flood with minima during high tide; this pattern confirms that ebullition and gas escape is triggered mainly by the decrease of pressure (hydraulic load) that occurs during the falling tide. Detailed mapping showed evidence of gas accumulations both in the Holocene sediments and in the Mesozoic bedrock of marls and clays. The location and geometry of fluid the escape features follows the fracture pattern that affects the Mesozoic bedrock, indicating that these fractures are preferential pathways for fluid migration and exert a structural control on the gas occurrences in the Ria of Aveiro.

5.1. Introduction

The study of gas occurrence and seepage, mainly methane, is of significant interest for its role as a greenhouse gas and potential contribution to climate changes (Hovland *et al.*, 1993; Houghton *et al.*, 2001; Etiope, 2004; Judd, 2004), as an important energy source and as a cause of natural hazards (Best et al., 2006). According to Best (2006), understanding these roles of methane gas requires the development of models of methane gas generation and gas flux, as well as the acquisition of reliable model input data, such as sediment accumulation rates, organic matter concentrations, amount of gas present, sediment shear strength, etc. Considering that the organic rich muddy sediments of estuaries and coastal lagoons are prime sources of methane gas (Kelley *et al.*, 1995; Van der Nat and Middelburg, 2000), modern day estuaries and coastal lagoons are preferential objects for these studies on methane gas generation and gas flux (Garcia-Gil, 2003; Duarte *et al.*, 2007).

The present work presents new data from a Chirp high-resolution pseudo-3D seismic survey, carried out to investigate shallow gas occurrences in a main tidal channel of the Ria of Aveiro barrier lagoon, located in North-West Portugal (Pinheiro and Duarte, 2003b). This study aims at understanding the geological controls of the distribution and extent of acoustic evidence of gas accumulations and seepage, continuing previous work carried out in other areas of the Ria (Duarte et al., 2007). The dense pseudo-3D seismic coverage was chosen to characterize the 3D geometry of the Holocene lagoon sediments architecture and of the structure of the Mesozoic bedrock, allowing the identification of the structural controls on the fluid migration pathways and gas accumulation zones.

The abundance of seismic data, both in time and space allowed a quantitative investigation of the hypothesis that the tidal cycle affects the extent and distribution of seismic evidence of gas, which was proposed in previous work in the Espinheiro Channel sector (see chapter IV; Duarte *et al.*, 2007). The amplitudes of the bottom reflection of the Chirp data were investigated at the same locations at different tides in order to determine if there was a significant change in

amplitude strength as the tidal cycle evolved and the main results are presented here.

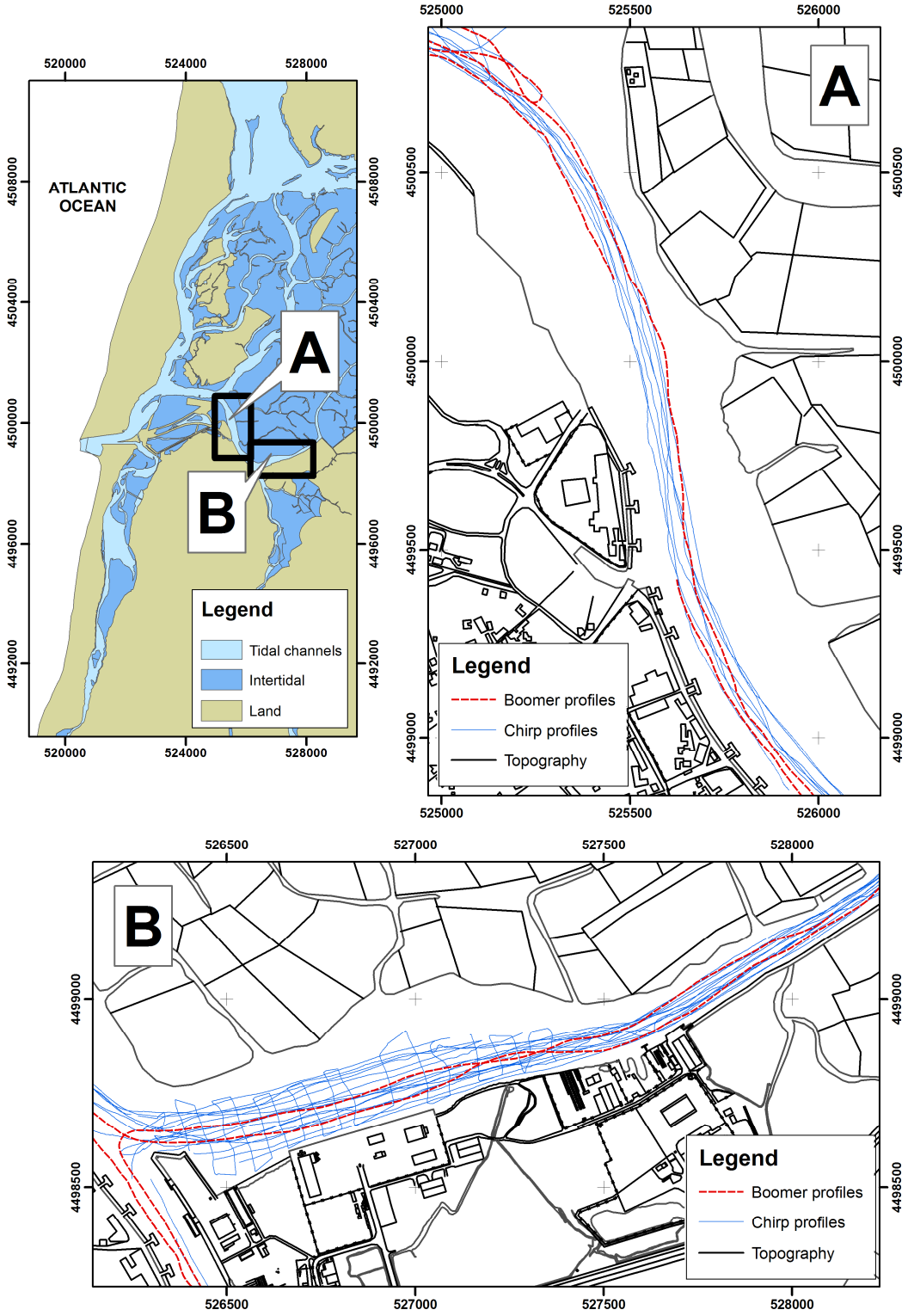

Figure V-1: Location of the study areas and seismic profile coverage of the tidal channel domains in the Ria of Aveiro barrier lagoon, Northwestern Portugal. A) The Cidade channel area; B) The Terminal Sul harbor docking area. The coordinates of this and all subsequent maps are UTM, Zone 29N in Datum WGS84.

5.2. Setting: the Ria de Aveiro

The Ria de Aveiro is a recent barrier-lagoon system, located along the northwest Portuguese coast, composed of a complex network of tidal channels, tidal flats, salt marshes and supra-tidal sand isles. It encompasses an area of approx. 530 km^2, making it the largest coastal lagoon system in Portugal (Fig. V-1). It is located at the mouth of a drainage basin of 3,635km^2, fed mostly by the Vouga River and its tributaries. Water depths are usually quite shallow, 1-2m, locally reaching more than 20m in the navigable channels, with maxima greater than 29m at the artificial inlet that establishes communication with the sea.

The semi-diurnal tidal cycle is the strongest forcing mechanism in the dynamics of the Ria of Aveiro. The small water volume at low spring tides is $65x10^2$ m^3, and barely covers the main tidal channels. The tidal prism at spring tides is about $80x10^2$ m^3, and more than doubles the water mass in the lagoon, covering the extensive tidal flats and salt marshes the constitute the majority of the lagoon area. The estimated time of residence of the water in the lagoon is of 3 days (Teixeira, 1994). Tidal amplitudes at the inlet average 1.90 m, ranging between 1.22 and 2.57 during neap and spring tides, respectively (Teixeira, 1994). The tidal amplitude decreases with distance from the inlet but it is measurable in the entire lagoon. The phase lag, variable at high and low water, increases upstream up to 5h, with low and high tides sometimes occurring simultaneously in different parts of the lagoon (Dias et al., 2000).

The coastal and lagoon sediments are essentially unconsolidated dune, beach, barrier and lagoonal sands and clays, deposited during the Pleisto-Holocene transgression and highstand. Elevated sand and gravel beach deposits from prior Quaternary cycles are described towards inland (Teixeira and Zbyszewski, 1976). The Quaternary sedimentary sequence lays unconformably over the Mesozoic sedimentary succession of clays and limestones of the Lusitanian basin, deposited during the opening of the Atlantic. Borehole log data reaching down to 200m in depth and seismic reflection profiles (Chirp and Boomer) show that the Quaternary sediments are less than 10m thick to the eastern end of the lagoon, and over 100m thick closer to the inlet; the deeper

sediments in this area are of unknown age, possibly Neogene (Marques da Silva, 1992; Teixeira and Pinheiro, 1998).

The consolidated lagoon bedrock of Mesozoic age is cut by a marine ravinement surface that dips gently westwards (less than 1º) and by an older fluvial erosion surface probably dating from the last glacial maximum, 18Ky BP (Duarte et al., 2007). The Mesozoic units dip approximately 3-6º to the west. The major structural feature cutting the Cretaceous rocks is a 2km wide, 40-60m deep, NNW-SSE trending graben of unknown age mapped in the Espinheiro sector (Teixeira and Pinheiro, 1998; Duarte *et al.*, 2007) and that probably extends through much of the lagoons' bedrock (see Figs V-2 and V-3).

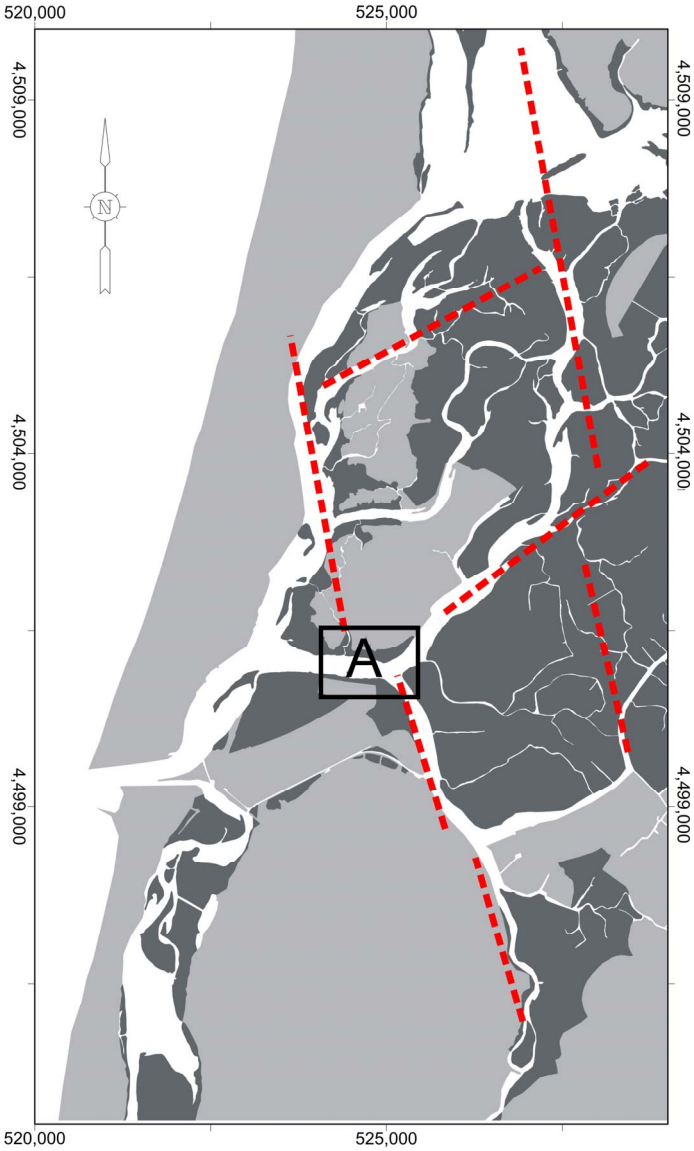

Figure V-2: The main sub-cropping fault trends in the Ria of Aveiro as inferred from available seismic data adapted from Teixeira and Pinheiro (1998). Inset A is shown in Fig. 3.

Early descriptions of possibly methane gas related phenomena in the lagoon area date back to the 1755 great Lisbon earthquake. The answers from local parishes to the Marquês de Pombal enquiries on the 1755 earthquake report that the Vouga river waters “boiled as if they were on fire” and that the waters from the Mira lagoon (at the south end of the Ria) “appeared to boil so hard that they would break at the lagoon shore as if they were sea waves” (Coelho, 2005; Oliveira, 2005); these tales may be explained by gas releases from seismically destabilized sediments.

The first unequivocal direct observations of escape of biogenic methane from several drill holes in Quaternary sediments from the area surrounding the Ria of Aveiro were reported by the Portuguese Geological Survey in 1967 (Faria et al., 1967). Since then, similar evidence has been observed in other land wells for water exploration. During previous work, Duarte *et al.* (2003) identified several high-backscatter patches on sidescan sonar images acquired in other parts of the Ria de Aveiro by the Portuguese Hydrographic Institute in 1998, which they interpreted as related to gas escape; some of these features may correspond to pockmarks. More recent investigations with chirp and boomer high resolution seismics in the Espinheiro tidal channel of the Ria de Aveiro (Pinheiro and Duarte, 2003a; Pinheiro and Duarte, 2003b; Pinheiro *et al.*, 2003; Duarte *et al.*, 2007) have shown extensive acoustic evidence of gas accumulation and seepage, including acoustic turbidity, enhanced reflections, acoustic blanking, domes and acoustic plumes in the water column (flares). Recently, in September of 2006, gas samples were collected from extensive bubble trains observed during falling tide in a docking pier (“Doca Pesca”) in the Ria of Aveiro. The analysis of the gas samples composition by chromatography revealed that the gas was mostly methane (L.M. Pinheiro, personal communication)

The study area investigated in this work (Fig. V-1) consists of two tidal channel domains in the Ria de Aveiro, including the Cidade channel and the Terminal Sul harbor docks area, each surveyed over an area of roughly 0.5km^2. These tidal channels are part of the main navigation channel of the Aveiro harbor and are frequently dredged for ship navigation purposes down to a minimum water depth of approximately 6,5 m below the hydrographic zero.

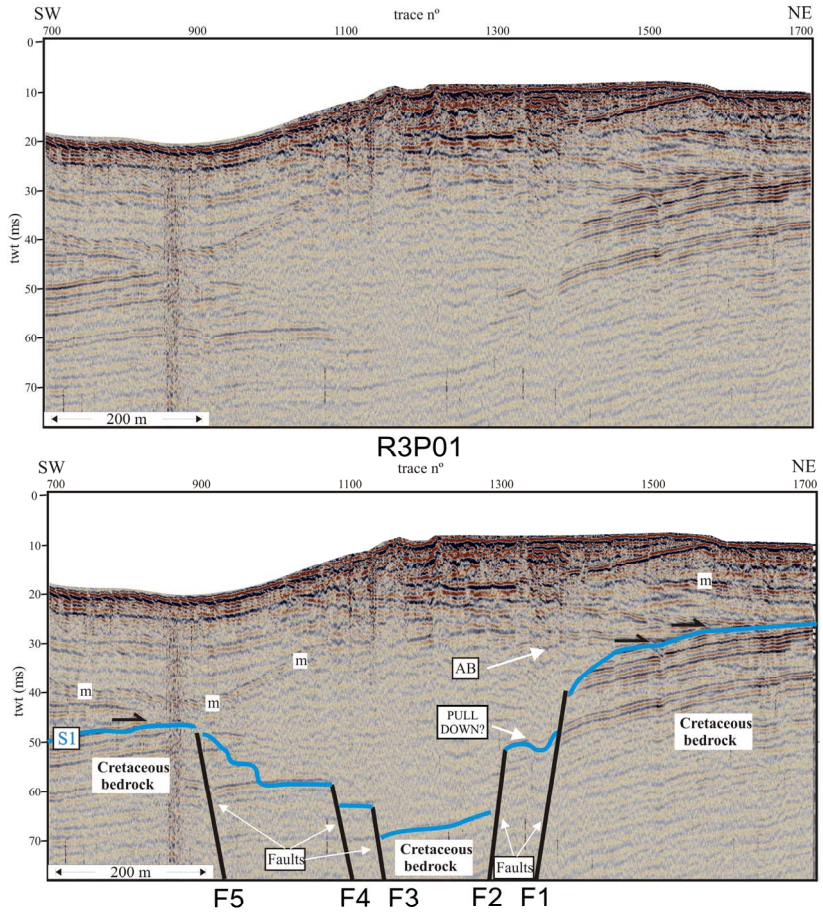

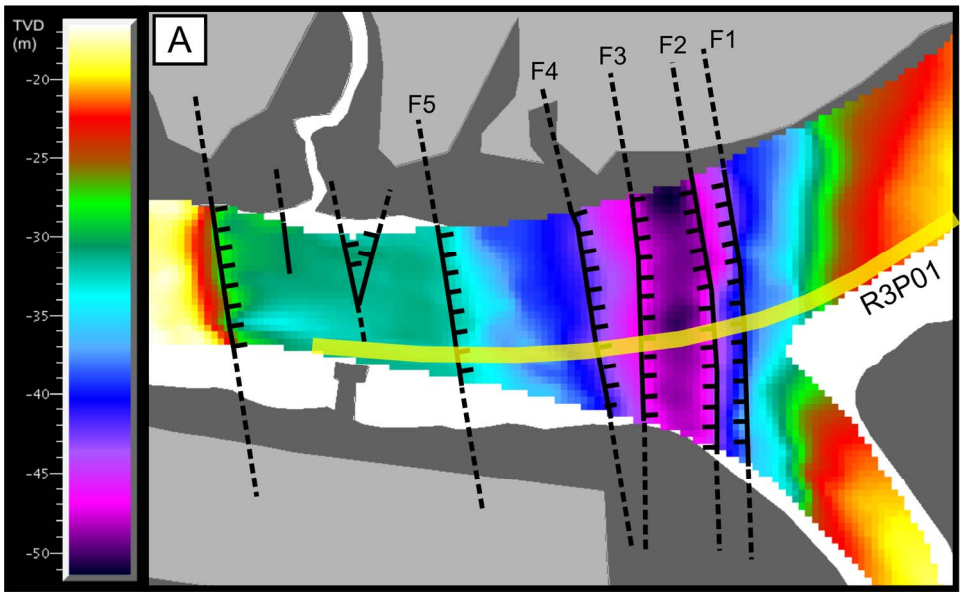

Figure V-3: Graben observed in the Boomer profile RP01 acquired in the Espinheiro sector of the Ria of Aveiro during cruise RIAV03 (Pinheiro *et al.*, 2003). Top: non-interpreted and interpreted profile P01, adapted from chapter IV. AB – acoustic blanking. Bottom: Isobath map of the top of the Mesozoic bedrock, and faults affecting the bedrock, derived from the interpretation of the boomer profiles (see location in Fig. V-2); depths in vertical depth (TVD) estimated with a constant speed of sound of 1500 m/s.

5.3. Database and methods

A major pseudo 3D chirp high resolution seismic survey, RIAV02A, was carried out in 2002 in the Terminal Sul harbor area of the Ria de Aveiro (Pinheiro and Duarte, 2003b). This pseudo 3D data set was complemented with a second chirp survey and a boomer survey, RIAV02 and RIAV03 (Pinheiro and Duarte, 2003a; Pinheiro *et al.*, 2003). All surveys were carried out onboard the launch Ria Azul of the Aveiro Harbor Authority. More than 220 km of chirp profiles were digitally acquired with a Datasonics CAP-6000W Chirp sonar from the Marine Geology unit of LNEG (DGM-LNEG) during the RIAV02 and RIAV02A cruises. The signal bandwidth was 1.5-10 kHz, the output power 1 kW, and the chirp length 10 ms (approx. vertical resolution of 10-15 cm). During the RIAV03 cruise, 47 km of additional boomer profiles (EG&G Uniboom, also from DGM-LNEG) were also acquired. The output energy used was 100 W s^{-1}, and the receiver array consisted of a single-channel streamer with 24 hydrophones. The signal frequency spectrum ranged from 250 to 1,400 Hz (estimated vertical resolution <2 m).

Seismic processing was carried out with SPW software package (Seismic Processing Workshop, from Parallel Geoscience Corporation), and with Radex Pro (from Deco Geophysical). The processing of the boomer records included frequency band-pass filtering and time-variant amplitude gain correction. Deconvolution and Stolt-FK migration (single sound velocity model of 1500 m s^{-1}) were also applied on some of the boomer records. The estimated depths of the seismic reflections were calculated using velocities of 1,500 m s^{-1} for seawater, and 1,700 m s^{-1} as an average for soft sediments. The pseudo 3-D data set consists of 18km of profiles, covering an area of 1000x150m, with inlines 10 m apart and crosslines 40 m apart. The remainder boomer and chirp profiles have a more heterogeneous layout, with a separation of roughly 50 m, and extend the seismic coverage northwestards onto the Cidade channel (see Fig. V-1). The ship speed was about 4 knots. Dynamic positioning of the seismic profiles was done with a Real Time Kynematic GPS. A constant time shift was applied to each profile to account for tidal fluctuations and the depth of the towed equipment (fish and streamer). Residual misties for the pseudo 3-D data set do not exceed 0.5 ms

(approximately 38cm, for a sound velocity of 1500m/s), whereas for the remainder of the profiles this value is slightly greater, of approximately 1ms (approximately 76cm, for a sound velocity of 1500m/s).

The vertical datum of the surveys was corrected to match the Hydrographic Zero Datum used by the Portuguese Hydrographic Survey, by matching the estimated horizon depths with the true depths for the same horizons derived from geotechnical soudings cutting through the Mesozoic bedrock (based on unplublished reports from the harbor; see Fig. V-4 for a example of the location of the geotechnical soundings near the chirp and boomer profiles, and the correlation of the two types of data). SEG-Y seismic data management and interpretation was carried out using the Kingdom Suite (Seismic Micro-technology Inc.) and the Openworks and Seisworks-2D (Landmark Graphics Corporation) seismic interpretation software packages.

Hydrological and geotechnical probing of Ria of Aveiro is relatively extensive due to the intensive human occupation of the area. Cores drilled for hydrological purposes frequently aim at the confined aquifer lying below the “Argilas de Aveiro” formation of the Maestrichtian Sedimentary Complex (Teixeira and Zbyszewski, 1976), including descriptions of rocks down to the Middle Cretaceous (Marques da Silva, 1992). The geotechnical log data of Standard Penetration Tests (SPTs) are usually shorter than the hydrogeological ones, normally reaching the top of the Mesozoic consolidated sediments, usually the “Argilas de Aveiro” formation. Only a couple of hydrological core logs are available close to the seismic profiles in the structurally more complex area of the lagoon (see core locations in Fig V-4). Still, these logs are close enough to the seismic profiles to allow for a calibration of the main geological units. The geotechnical logs are located near harbor infrastructures and the Terminal Sul area has been densely surveyed (see core locations in Fig. V-4). Over 120 geotechnical logs were used for the calibration of the vertical datum of the seismic data and for the geological interpretation.

All available borehole, seismic and geographical data were collated into a GIS database (ArcGis ESRI), which was used throughout this work for spatial computations.

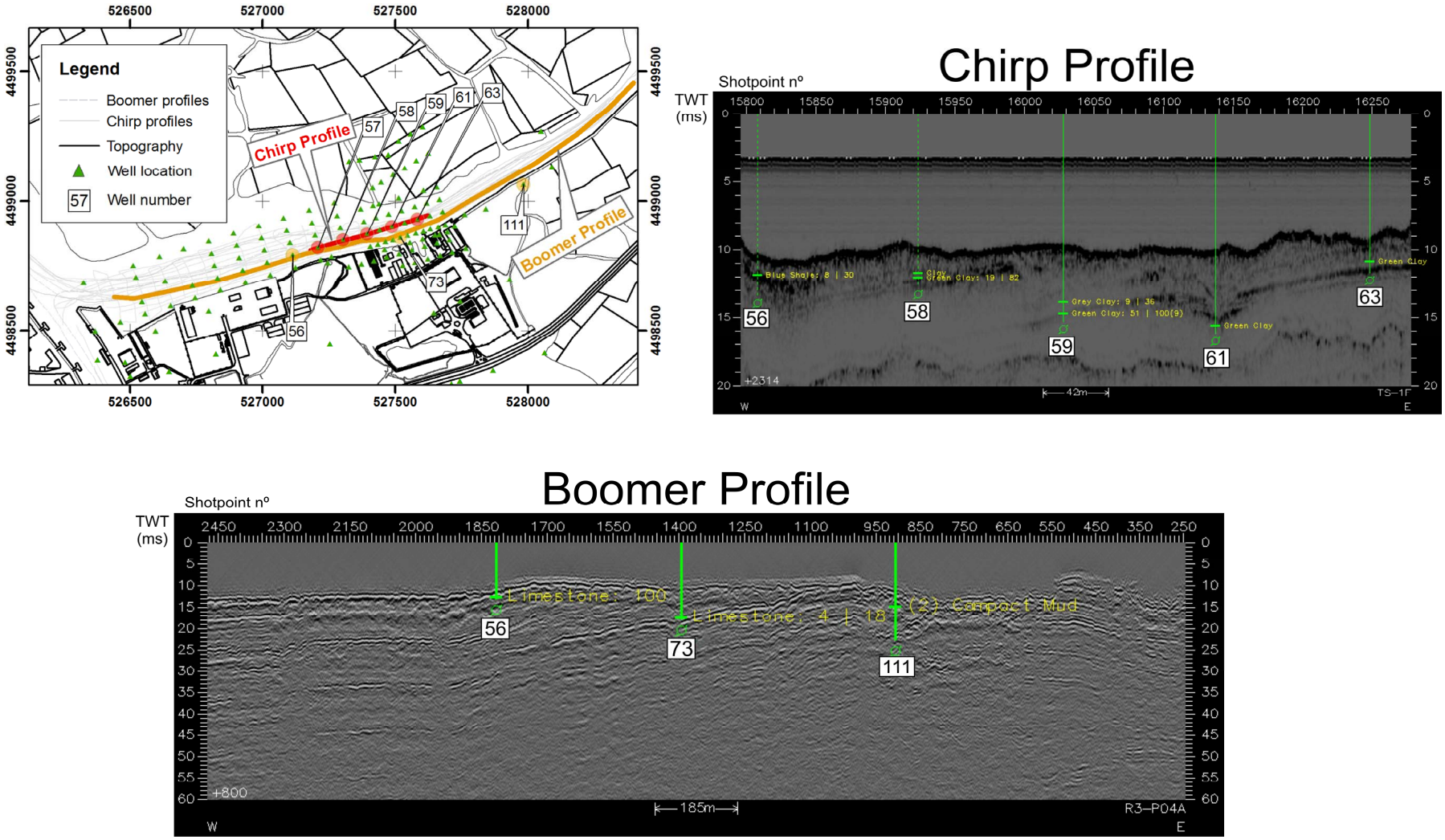

Figure V-4: Example of geotechnical logs plotted on top of the chirp and boomer profiles used to correct the vertical datum of the profiles. The Green Clay and Limestone events indicate to the top of the Mesozoic, and strongly correlate with the strong and coherent western dipping reflections observed both in boomer and chirp profiles in the Terminal Sul Area. The green triangles represent the available geotechnical well logs compiled for this work.

5.4. Results

The acoustic evidence of gas accumulation and seepage in the studied area consists of acoustic turbidity, enhanced reflections, acoustic blanking, pockmarks and buried trough pockmarks, disrupted horizons, cloudy turbidity and acoustic plumes (flares) in the water column (see also Duarte *et al.*, 2007). With the exception of the pockmarks, buried trough pockmarks and the disrupted horizons, all other types of evidence of gas were previously found and described in the Espinheiro channel of the Ria of Aveiro (Duarte et al., 2007), and the terms used here respect the meanings described in that work. Pockmarks are a type of gas related features not found in previous work in the Espinheiro area. These are circular to elliptical depressions with a common v-shaped cross-section, formed by fluid escape through the sediments that promote localized erosion and generate circular to elliptical depressions in the water bottom. When this fluid escape is focused through fractures, sometimes trough-like alignments of pockmarks occur on the water bottom along the fracture line. Buried pockmarks are past fluid escape structures such as those just described that were filled by sediments (Hovland and Judd, 1988). The disrupted horizons observed in the seismic profiles (e.g. Figs. V-7 and V-11) are probable/possible fluid escape structures that consist of near vertical ruptures of consolidated layers that exhibit uncommon localized deformation, indicating that hydraulic fracture processes may have contributed to their deformation.

All the interpretation problems related to the specific seismic acquisition conditions in a shallow lagoon environment that Duarte *et al.* (2007) described in the study of the Espinheiro channel, also occurred here, e.g. the survey coverage variability, the frequent changes in profile direction, the strong and variable bottom multiple interference caused by shallow water depths and tidal altitude changes (about 2 m in the present case), and the scarcity of reflections due to lack of sediment heterogeneity or the lack of signal penetration in sandy sediments, limiting the identification of gas evidence. Taking into account these constraints, all gas related features identified in each profile were mapped for the Cidade channel and the Terminal Sul (see Figs. V-5 and V-6). The main structures affecting

Figure V-5: Map of the acoustic evidence of gas accumulation and seepage in the Terminal Sul area.

Mesozoic guide horizons were also mapped and overlaid on isobath maps of the those horizons.

5.4.1. Distribution and extent of gas in the Terminal Sul sector

The Terminal Sul area has been covered by a very dense, pseudo-3D chirp profile coverage, with inlines approximately every 10m and crosslines approximately every 50m, which allows a confident determination of the distribution and extent of the areas of gas accumulation and mapping of the various seepage-related features. The evidence for gas in the Terminal Sul consists of: (1) two gas accumulations, named here as Terminal Sul Western Gas Field (TS-WGF) and Terminal Sul Eastern Gas Field (TS-EGF), (2) pockmarks and buried pockmarks, and (3) possible generalized gas accumulations within the outcropping/sub-cropping Mesozoic Marls and clays (Fig. V-5).

The TS-WGF gas field is characterized by acoustic blanking and acoustic turbidity covering an area of 60,440m^2 (22% of the seismic coverage area of Terminal Sul). These accumulations occur approximately 1m below the channel floor, and appear to be trapped underneath soft Holocene tidal channel deposits (black muds: Pinheiro and Duarte, 2002). An acoustic plume was observed ascending from this gas pocket (see profiles over TS-WGF in Figs. V-7, V-8 and V-9).

The Mesozoic clays and marls outcrop or subcrop (less than 1 m below the channel bottom) over a significant part of the Terminal Sul area. The majority of these Mesozoic horizons have enhanced reflections that may result from either gas bubbles in the sediments, or sharp differences in the physical properties between the soft Holocene sediments and the consolidated Mesozoic marls and clays. The sharp changes in the patterns of enhanced reflections with tidal altitude suggest that these enhancements are more likely related to gas bubbles in the sediments (see Fig. V-10). Pending confirmation of the presence of gas, the Mesozoic enhanced reflections observed may correspond to an important gas accumulation zone with an area of 74,300m^2 (27% of the seismic coverage area of Terminal Sul).

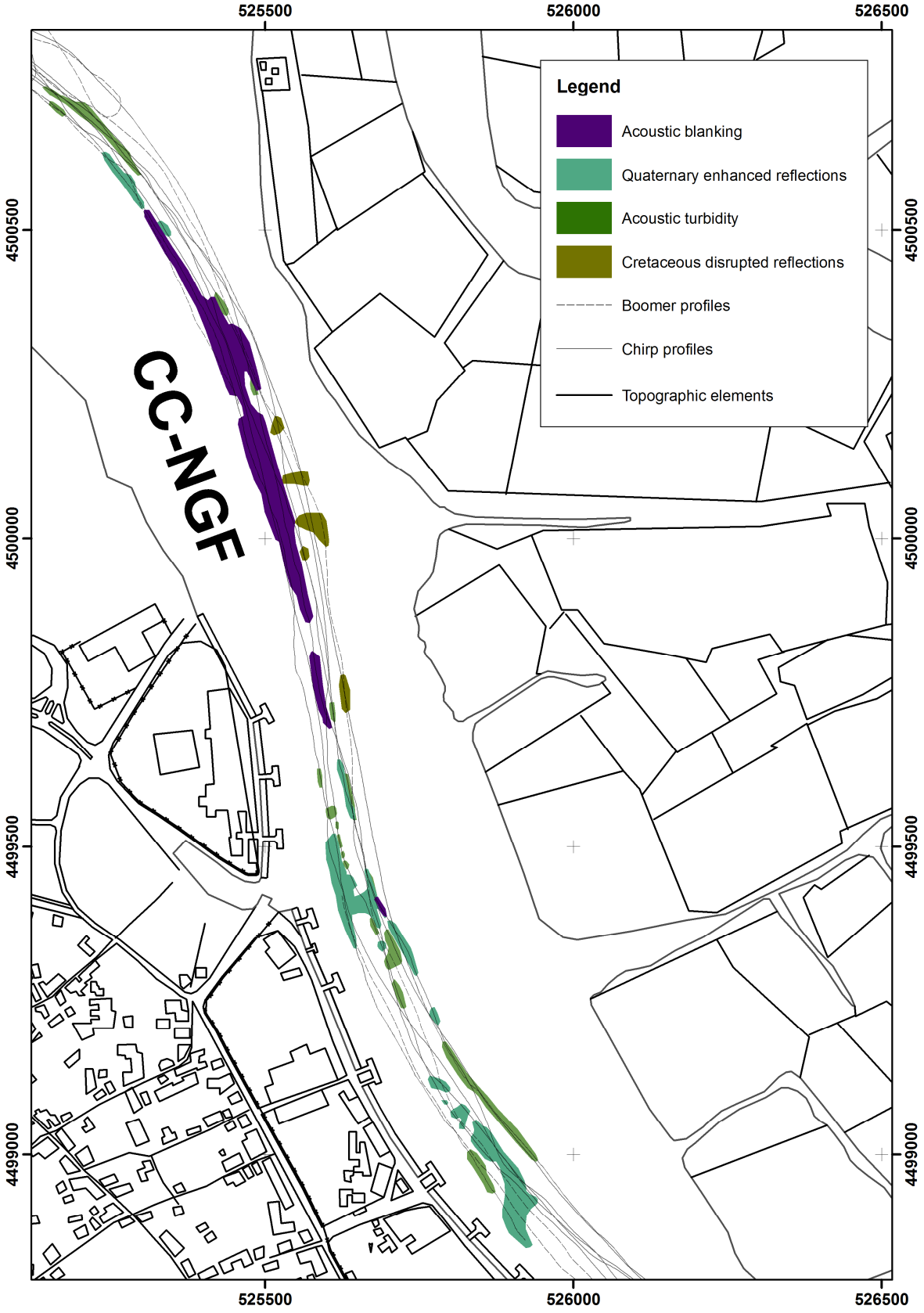

Figure V-6: Map of the acoustic evidence of gas accumulation and seepage in the Cidade channel.

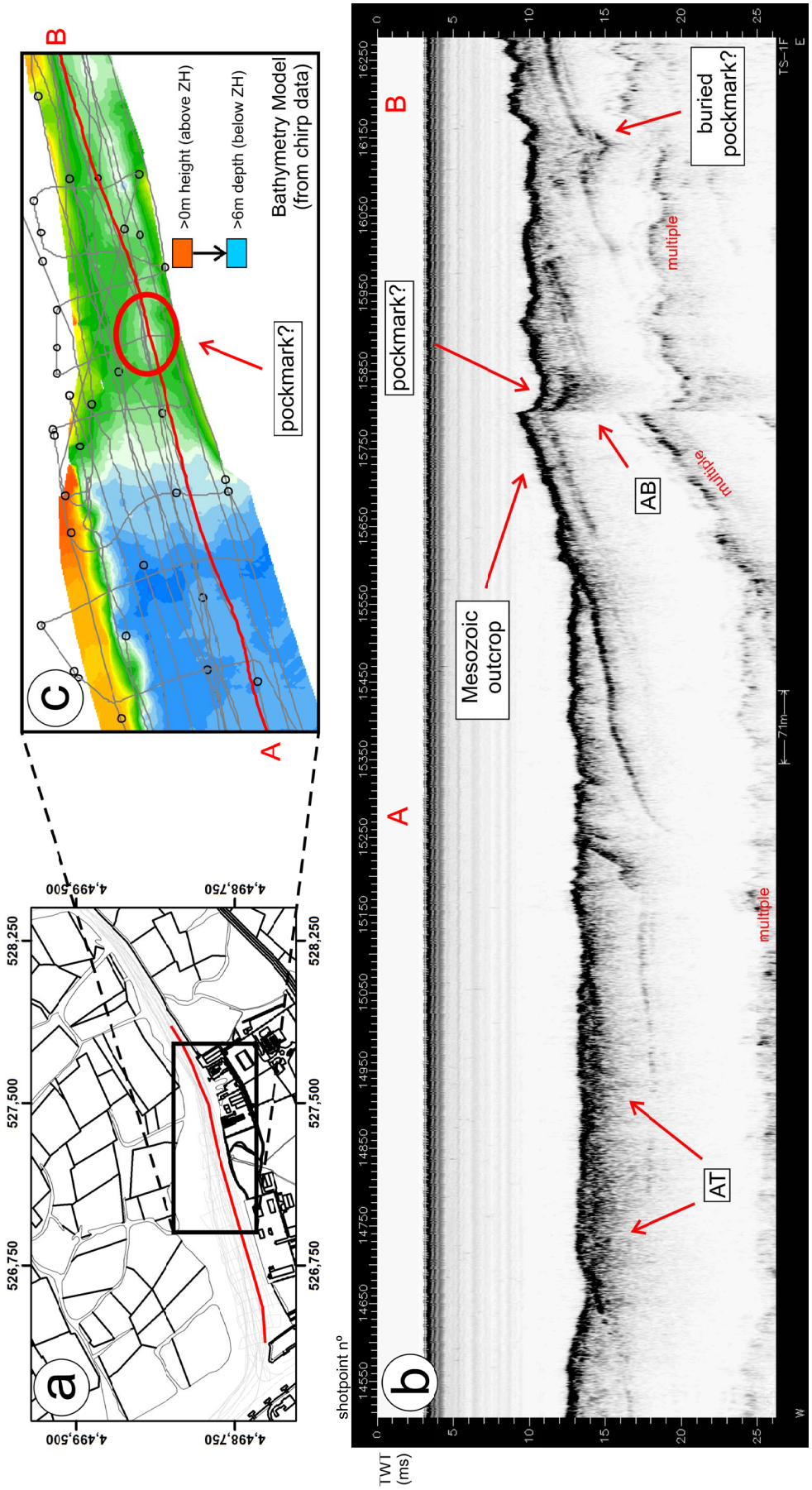

Figure V-7: West dipping Mesozoic basement outcropping in the channel bottom in the Terminal Sul, observed on Chirp profile TS1F, cruise RIAV02a. Evidence of gas was also observed: acoustic turbidity (AT), acoustic blanking (AB) and pockmarks on the channel bottom and buried by sediments. An elliptical depression on the channel bottom 70m long, 40m wide and 2m deep corresponding to a possible active/recently active pockmark is also observed on the detailed bathymetric model derived from the chirp data. **(a)** – red line indicates profile location; **(b)** – profile TS-1F; **(C)** – bathymetry.

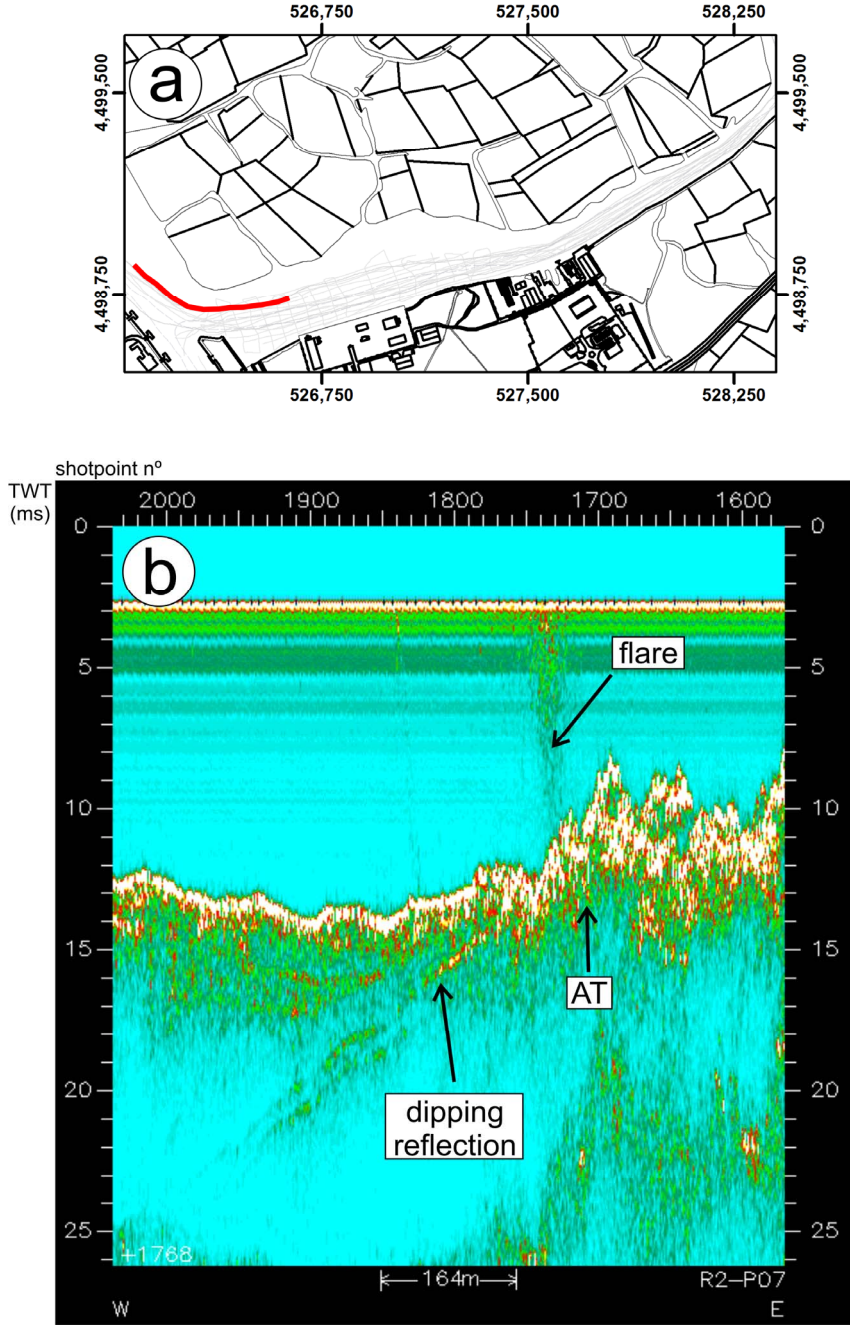

Figure V-8: Acoustic flare observed over acoustic turbidity zone (AT), on profile P07, cruise RIAV02, in the Terminal Sul. The flare possibly results from fluid seepage channeled through the dipping sediments layers. **(a)** – red line indicates profile location; **(b)** – profile R2-P07.

The outcropping Mesozoic marls and clays are affected by an elliptical depression 70m long, 40m wide and 2m deep found in the central part of the channel bottom in the Terminal Sul area. This depression is underlined by coincident near bottom acoustic blanking and is interpreted as a possible active or recently active pockmark (see Figs V-7 and V-13).

Further to the east, two buried trough pockmarks, 10-20m wide and 1-2m deep, extending beyond the limits of the mapped area (at least 100m long), are observed cutting the Mesozoic horizons in the chirp and boomer profiles (see Figs. V-11, V-12 and V-13). Gas evidence in the form of acoustic turbidity and enhanced reflections are common in the sediments that cover these pockmarks, raising the possibility that gas may still be rising through the pockmark structures. The trough pockmarks are aligned NNW-SSE (24ºW and 15ºW, quadrant notation), with the eastern pockmarks slightly closer to the North-South direction. These directions are common to many tidal channels in the lagoon, and the eastern buried pockmark is aligned in the continuation of a modern tidal channel. At low tide, the chirp profiles show an overall strong acoustic turbidity in the water column (cloudy turbidity), similar to what was previously observed in the Espinheiro Channel (Duarte *et al.*, 2007), above the area of the buried pockmarks (see Fig 14).

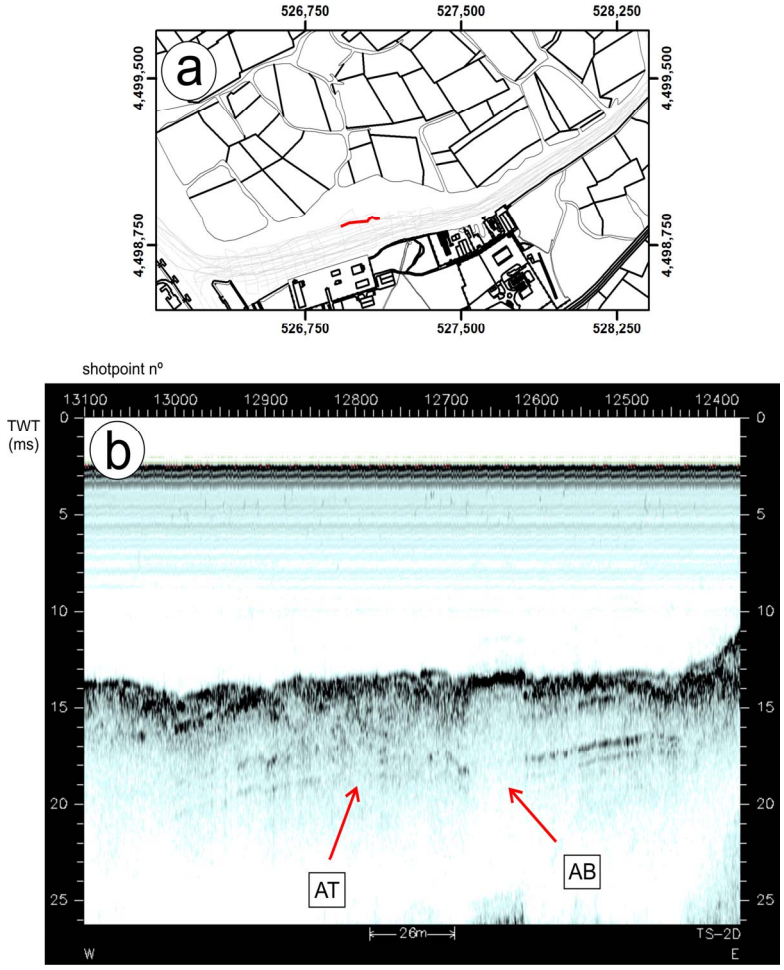

Figure V-9: Acoustic turbidity (AT) and acoustic blanking (AB) observed on chirp profile TS02D, cruise RIAV02a, in the Terminal Sul. **(a)** – red line indicates profile location; **(b)** – profile TS02D.

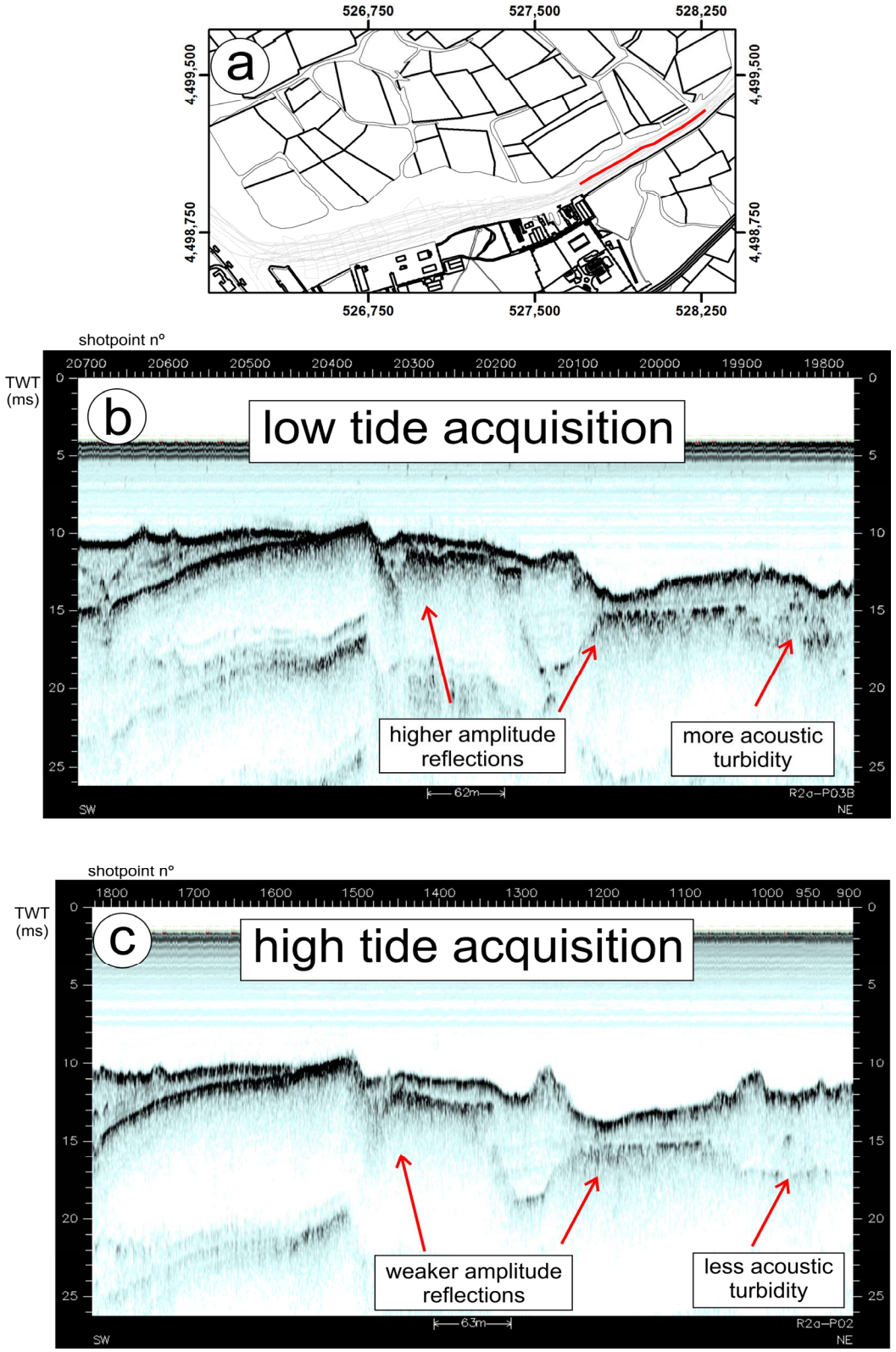

Figure V-10: Comparison of approximately coincident chirp profiles P02 and P03B acquired in the Terminal Sul during cruise RIAV02A, respectively during high tide and low tide. Evidence for gas is stronger in the profile acquired during low tide, when compared with the profile acquired during high tide. The amplitude of the reflections is stronger and acoustic turbidity is more abundant during low tide. **(a)** – red line indicates profiles location; **(b)** – profile P02; **(c)** – profile P03B.

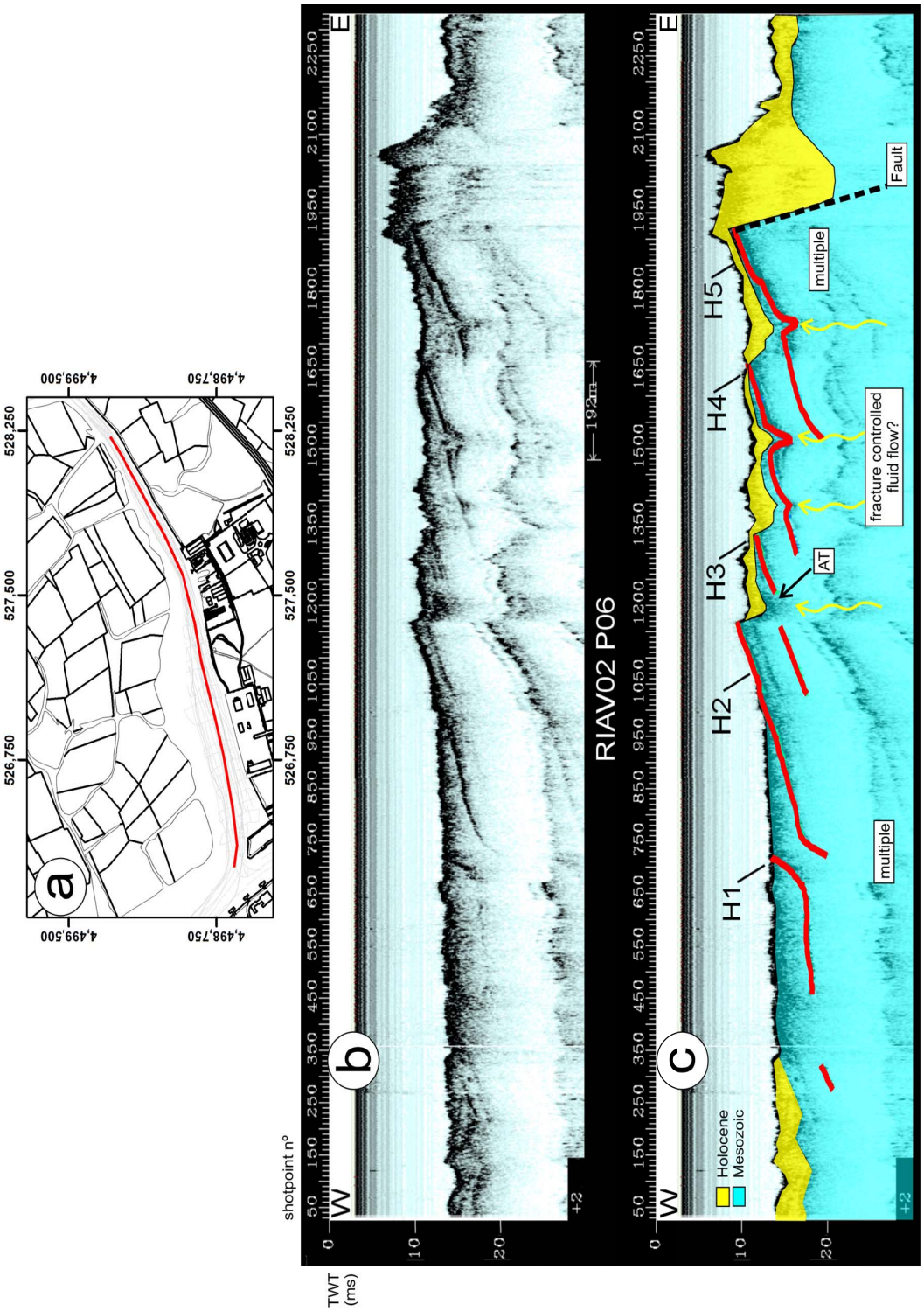

Figure V-11: Non-interpreted (above) and interpreted (below) chirp profile P06, cruise RIAV02, in the Terminal Sul area. The interpretation shows the Mesozoic horizons H1 through H5, with the possible pockmark related acoustic turbidity (AT) cutting Horizon H3, and with the buried pockmarks observed on H4 and H5 (indicated by fluid flow arrows). **(a)** – red line indicates profile location; **(b)** – profile P06; **(c)** – interpretation of P06.

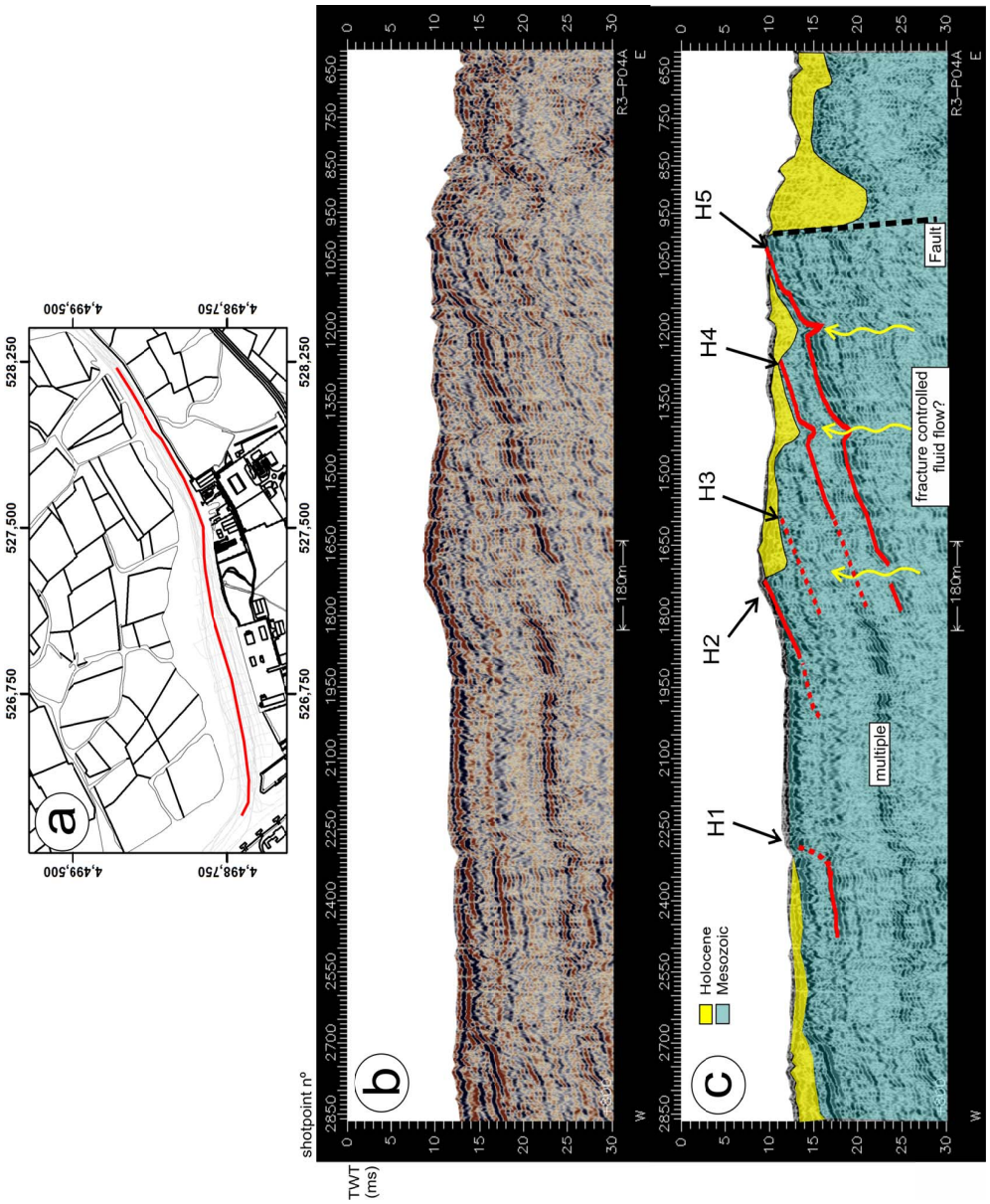

Figure V-12: Non-interpreted **(b)** and interpreted **(c)** boomer profile P04A, cruise RIAV03, in the Terminal Sul area. This profile closely coincides with the chirp profile P06, in figure V-11 and the same features are observed here. The interpretation shows the Mesozoic horizons H1 through H5. The evidence for the pockmark features are v-shaped depressions, most clearly seen in horizon H5, and acoustic transparency columns (indicated by fluid flow arrows) that affect most of the vertical section shown. There is good evidence for a fault (dashed line) which supports the hypothesis that the pockmark features were caused by fluid flow through fractured Mesozoic marls and limestones. **(a)** – red line indicates profile location.

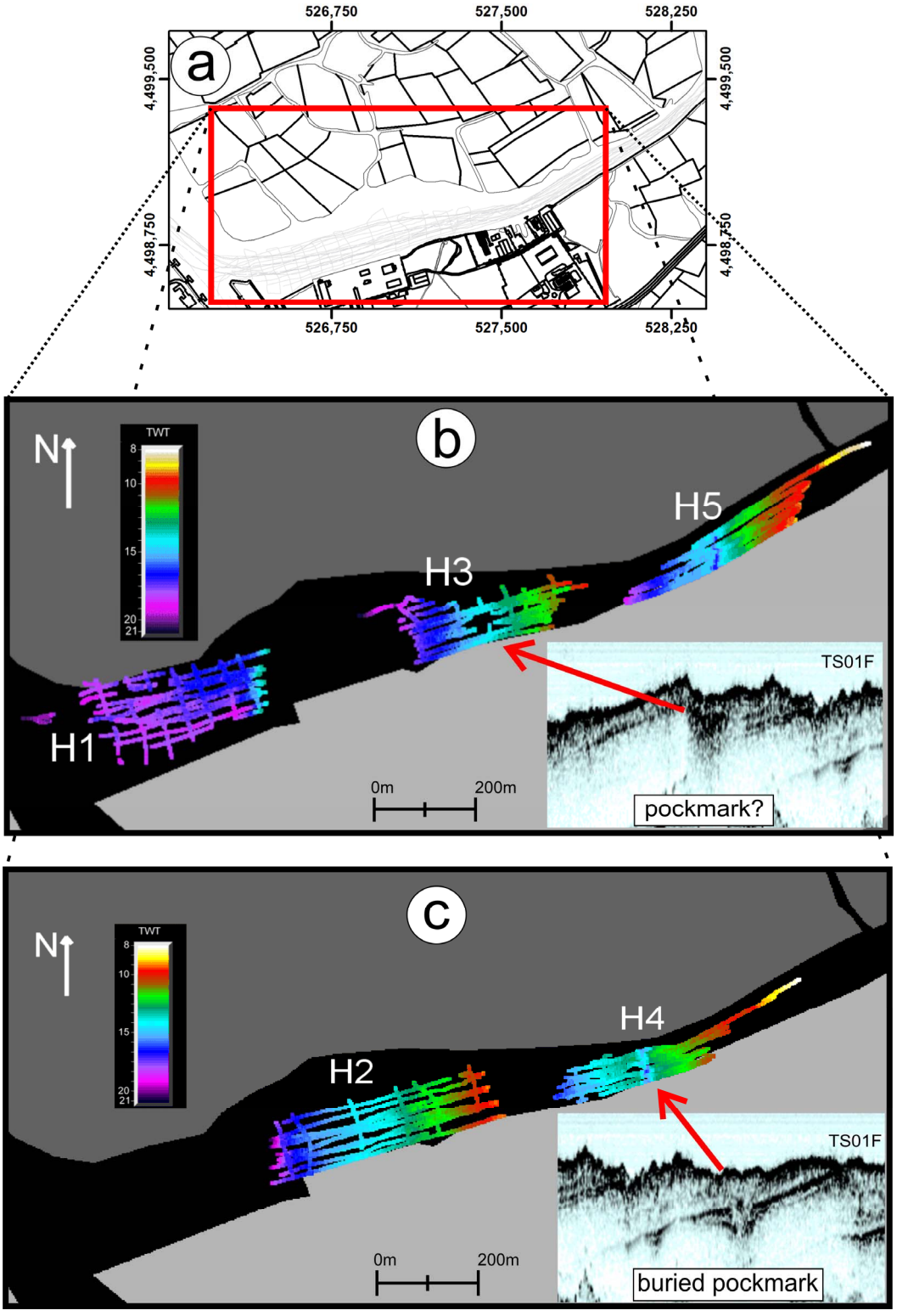

Figure V-13: Isobaths of Mesozoic horizons H1, H3, H5 (**b**) and H2 and H4 (**c**), interpreted in the boomer and chirp profiles in the Terminal Sul area (see interpretation in Fig. V-11 and V-12). Horizon H1 is mostly horizontal and the other horizons dip gently to the west. Horizon H3 has central area, 70m long by 40m wide, where interpretation is not possible due to strong acoustic turbidity, suggesting the existence of an active pockmark in this location (corroborating evidence presented in Fig. V-7). Horizons H4 and H5 show a NNW-SSE trough, 10-20m wide, with pockmark-like depressions. 1-2m deep. (**a**) – red box locates maps **b** and **c**.

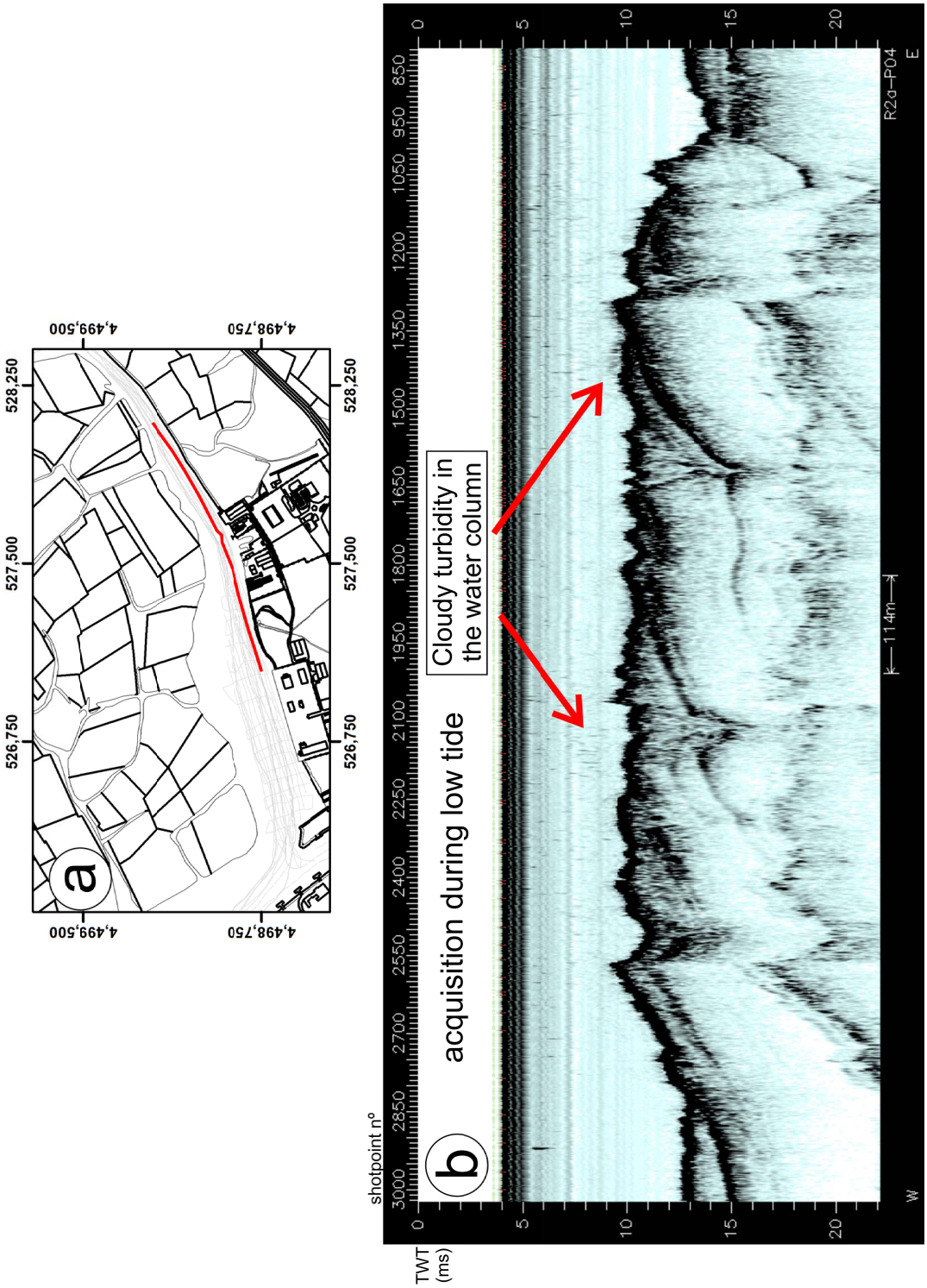

Figure V-14: Cloudy turbidity in the water column observed during low tide in the chirp profile P04, cruise RIAV02A. **(a)** – red line indicates profile location; **(b)** – profile P04.

The TS-EGF, in the easternmost part of the Terminal sul area, is characterized by enhanced reflections and acoustic turbidity that vary significantly with tidal height; stronger amplitudes and more abundant acoustic turbidity are observed during low tide when compared with high tide (see Fig. V-10). The TS-EGF occurs near the top of the Mesozoic bedrock, 1 to 3m below the channel bottom. Here, the Mesozoic sediments are faulted and the eastern blocks are downthrown to the East as confirmed by the geotechnical cores logs, more than 15m down and do not intercept the Cretaceous "Argilas de Aveiro" formation. The potential gas accumulation area is of 14,240m^2, 5% of the total seismic coverage area of the Terminal Sul (see Fig. V-5).

5.4.2. Distribution and extent of gas in the Cidade Channel sector

The seismic profiles in the Cidade channel area cover the central 100m wide portion of the main navigation channel. Profile separation is locally irregular ranging from a few meters to approximately 25m (see Fig. V-1), which means that some smaller areas of gas accumulation areas were probably not imaged. The Cidade channel has a gas field in its northern half (CC-NGF), and a few smaller patches of less unequivocal evidence of gas towards the south (Fig. V-6).

The CC-NGF has an area of 31,460m^2 (17% of the seismic coverage area of the Cidade Channel) and is mainly characterized by acoustic blanking. The acoustic blanking occurs below an enhanced reflection, approximately 1-2m below the channel bottom, which clearly blocks the acoustic signal from the normally strong Mesozoic reflectors below (see Fig. V-15). One relatively weak flare was observed at the northern edge of this gas field, where the top of the acoustic blanking reaches the channel bottom (see Fig. V-15).

The CC-NGF occurs above folded and faulted Mesozoic horizons. The structural pattern of strongly dipping faults with apparent reverse kinematics, with limited spatial extension of the strain accommodation, is interpreted as a series of strike-slip shear zones (see Fig. 16). Towards the eastern margin of the channel,

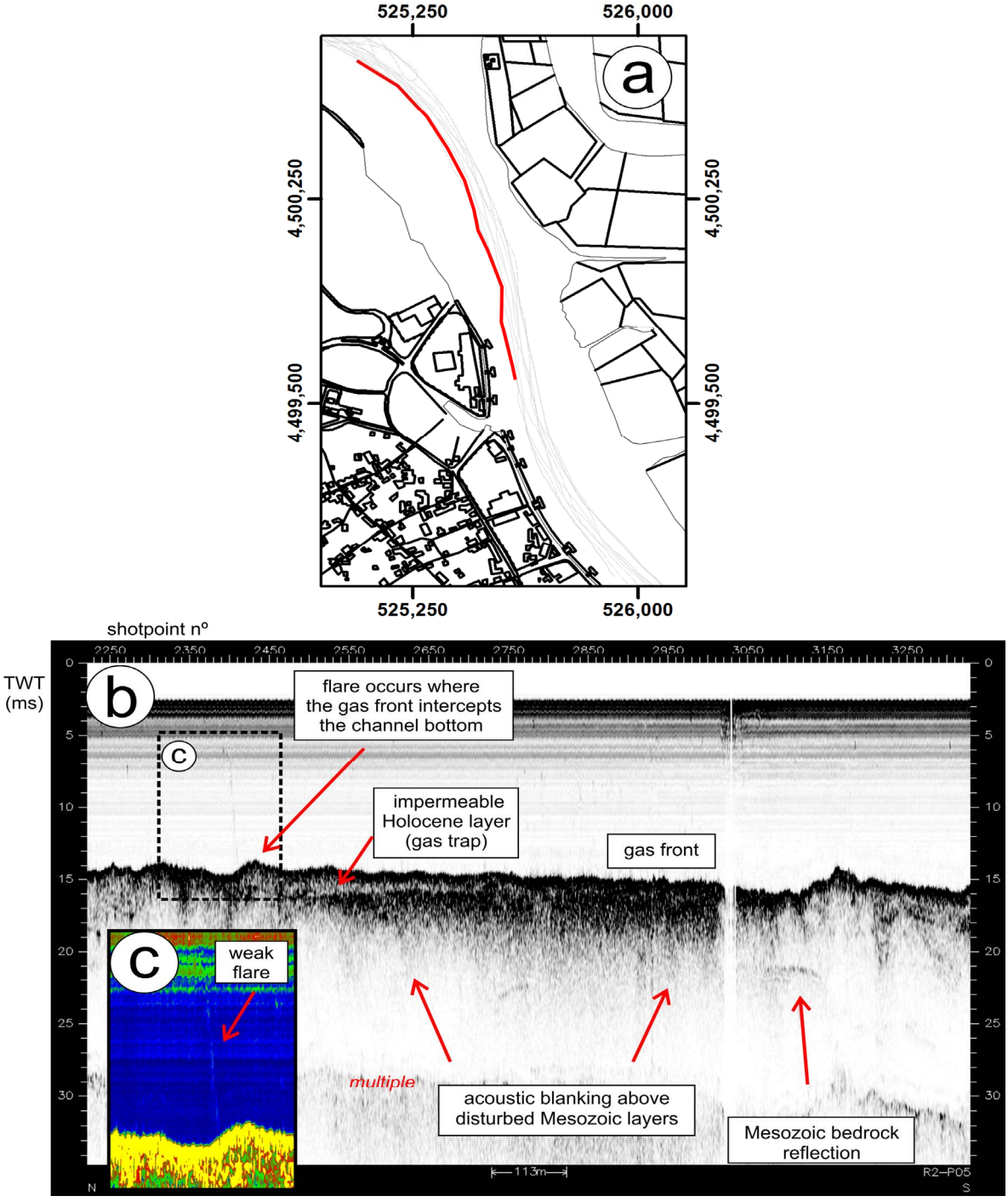

Figure V-15: Acoustic blanking of deeper Mesozoic bedrock reflections observed in the chirp profile P05 (**b**), acquired in the Cidade channel during cruise RIAV02 (**a** – red line indicates profile location). A weak flare is observed where the enhanced reflection of the Holocene layer traps the gas front intercepts the channel bottom (**c** – flare shown with a spectrum color amplitude display).

the disrupted Mesozoic horizons are clearly observed in both chirp and boomer profiles (Figs. V-16 and V-17. These horizons are partially or totally blanked below the gas accumulations closer to the western margin of the channel. It is emphasized that the disrupted Mesozoic strata is only well imaged below the

Holocene sediment cover where the gas trapping horizon is absent. Also, the gas accumulation occurs specifically in the area above the disrupted Mesozoic clays and marls and is absent to the north and to the south of this disrupted zone (see Fig V-17). The association between the shear zones that affect the Mesozoic bedrock and the overlying gas accumulation raises the possibility that the shear zones serve as fluid pathways and, also, that part of the intense strain accommodated by the Mesozoic bedrock were possibly caused by hydraulic fracturing processes.

Evidence for gas in the southern half of the Cidade channel area is also common, although less unequivocal. Acoustic turbidity is the most frequently type of evidence, and is observed in the first couple of meters of the Holocene sedimentary cover. Absence of reflections possible due to a homogenous sedimentary section and lack of signal penetration did not allow the identification of significant acoustic blanking, and no other strong type of evidence of gas was observed associated with the acoustic turbidity (Fig. V-18). The potential gas accumulations occur in a couple of patches with total area of 26,120m^2 (covering 14% of the total seismic coverage area of the Cidade channel).

5.4.3. Structural control of fluid escape structures

The Cidade channel and the Terminal Sul areas both show evidence of structurally controlled fluid migration pathways in the Mesozoic bedrock (see Figs V-11, V12, V-16 and V-17). The general structural pattern in the Terminal Sul area follows the trend of the Ria of Aveiro of gently dipping Mesozoic marls and clays (10-20ºW,4-6ºESE) covered by soft Holocene lagoon sediments. However, the Mesozoic bedrock in the Terminal Sul area appears to constitute a structural high, bordered by NNW-SSE to NNE-SSW normal faults (Figs. V-19, V-20 and V-21). The west dipping NNW-SSE normal fault is inferred at depth from a drape fold of the outcropping Cretaceous bedrock, and from the possible intra-Cretaceous unconformity on the hanging wall (Fig. V-20). The east dipping NNE-SSW normal faults affect the Mesozoic horizons and an unconformity of unknown age (intra-

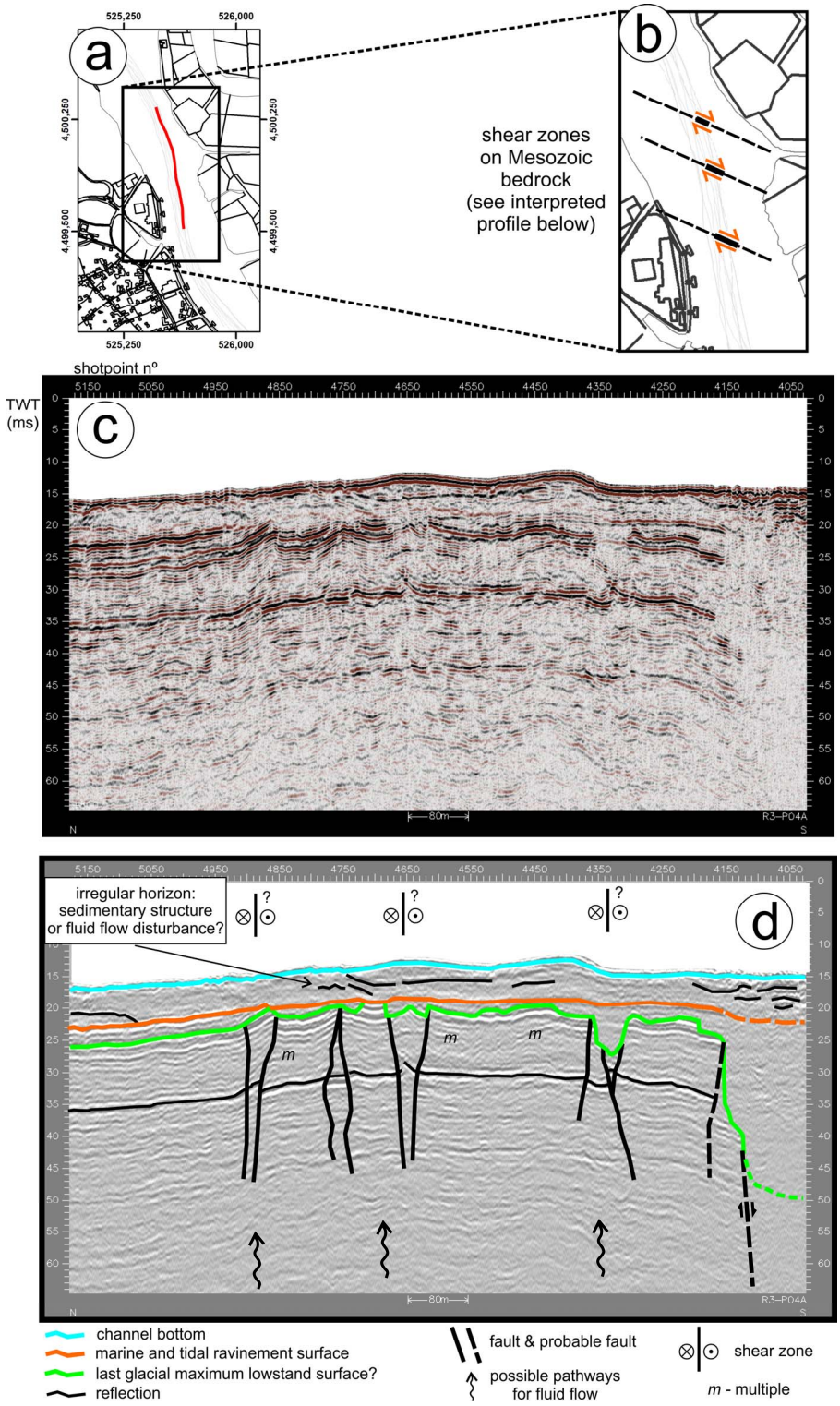

Figure V-16: Structural pattern of the Mesozoic bedrock with disturbed layers, observed on the boomer profile P04A, acquired in the Cidade channel during cruise RIAV03 (**a** – profile location in red, **c** and **d** – profile without and with interpretation). The disturbed layers are cut by predominantly sub-vertical faults with local evidence of shortening, suggesting that these are shear zones (possibly right lateral strike-slips – map view in inset **b**). The limited expression of the intense strain may result from hydraulic fracture processes caused by fluid flow through the higher permeability shear zones. The irregular Holocene reflectors observed above some shear zones may be a result of escaping fluids.

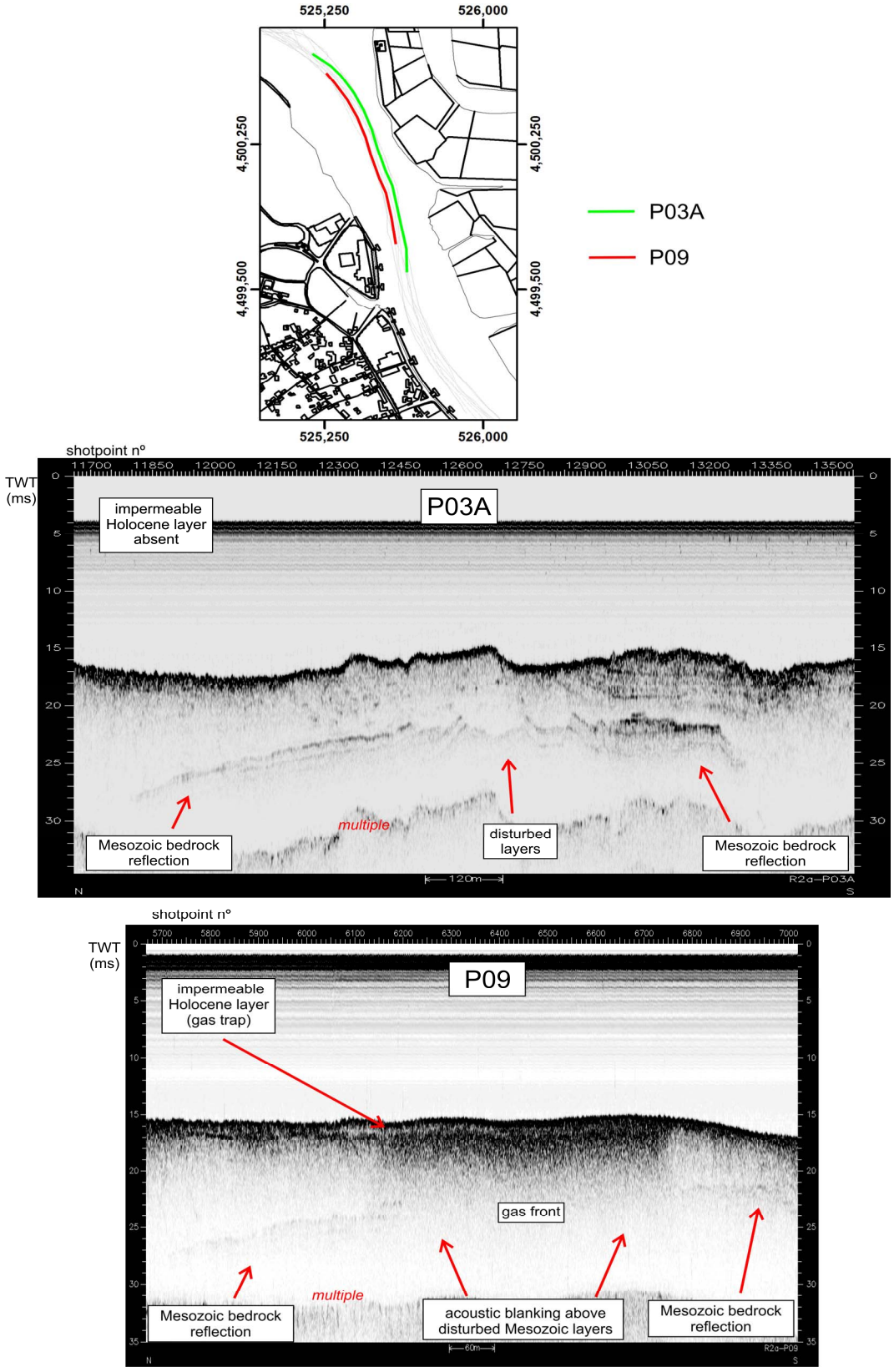

Figure V-17: Comparison of two neighbor chirp profiles, profiles P03A and P09 (cruise RIAV02A), that show the disturbed Mesozoic bedrock reflections. The top of the Mesozoic bedrock is clearly imaged in profile P03A whereas the zone of disturbed layers is blanked below an acoustic turbidity zone in profile P09.

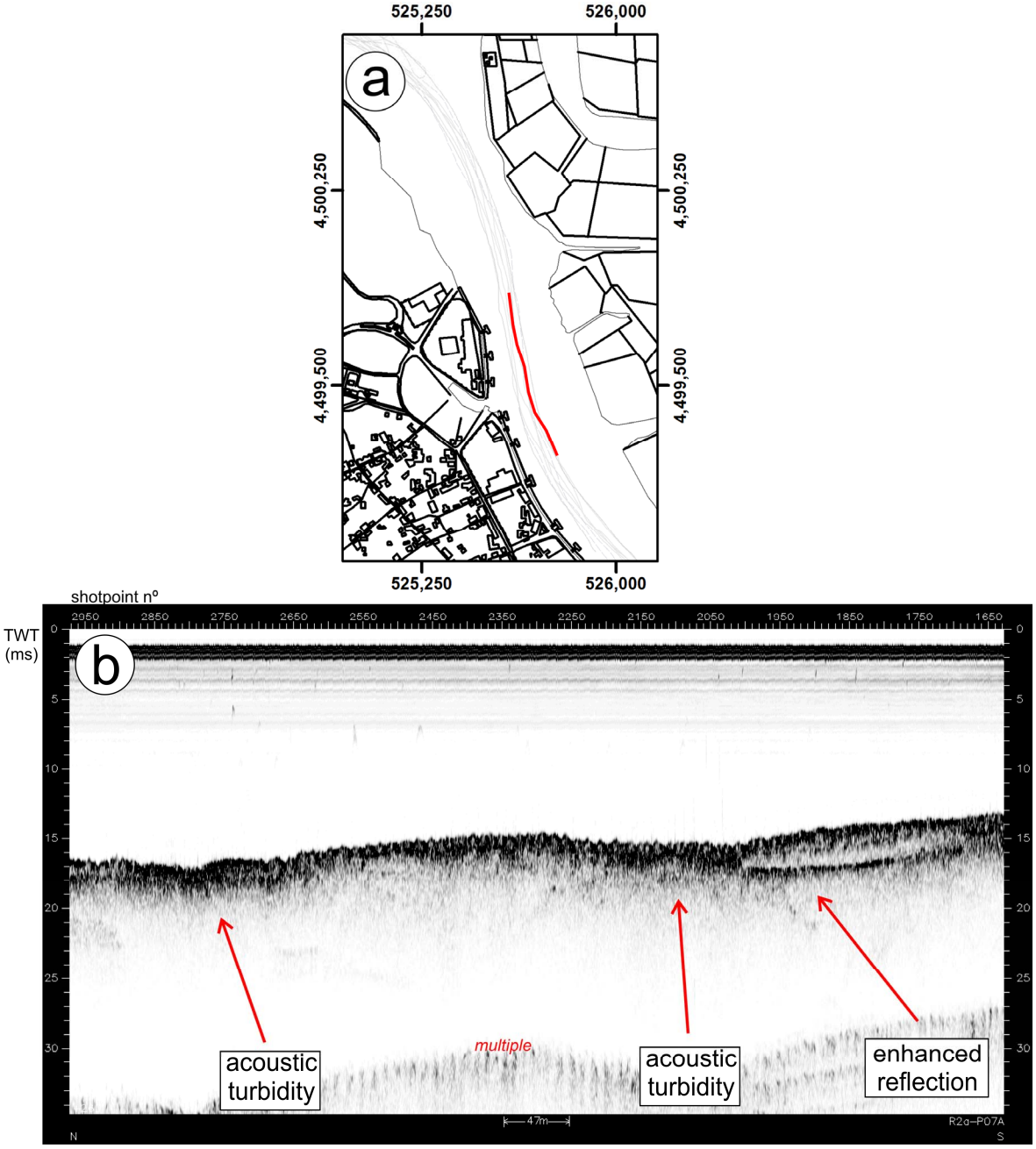

Figure V-18: Acoustic turbidity and enhanced reflection observed in the chirp profile P07A, acquired in the southern part of the Cidade channel during cruise RIAV02A. **(a)** – red line indicates profile location; **(b)** – profile P07A.

Cretaceous or Miocene?) is clearly observed on the hanging wall of the westernmost fault (Fig. V-20), which probably dates a significant part of the deformation. The TS-WGF and the TS-EGF gas fields occur above the hanging walls of these faults (Fig. V-22). A set of 10-24ºW sub-vertical, probably strike-slip, faults with sub-meter apparent vertical displacement, and with localized strain, are observed in the boomer profiles affecting the Cretaceous bedrock and are below

the active/recent pockmark as well as the buried pockmarks (Figs. V-11, V-12, V-20 and V-21). A small wavelength, gentle fold appears to affect the drape fold suggesting that it is a ductile bead (a zone of ductile deformation near fault tips; for a discussion see Hossack, 1983) of a right lateral strike-slip WNW-ESE shear zone (fold axis is gently undulating along the 98º azimuth) that post-dates the NNE-SSW normal faulting (see Figs V-21).

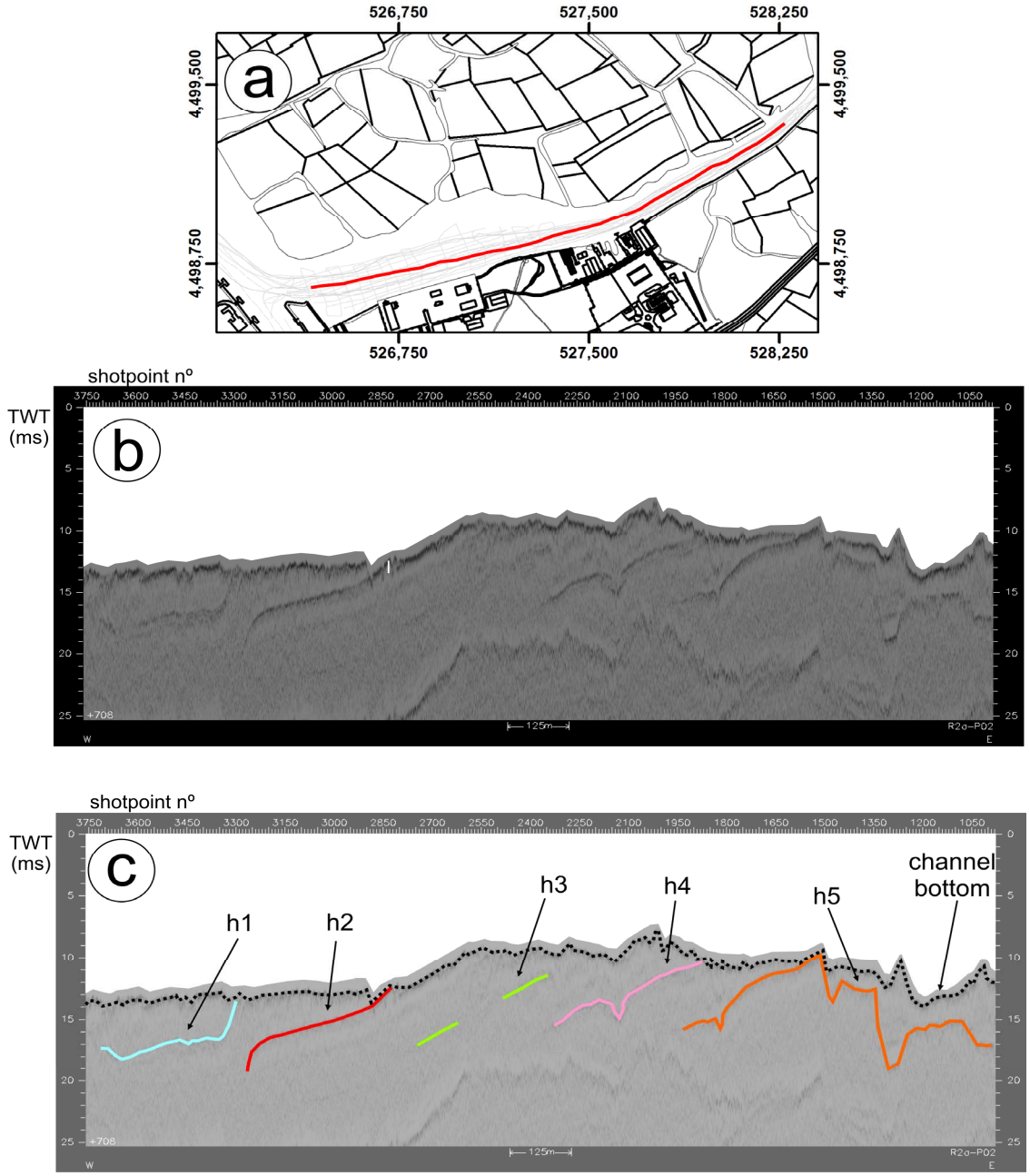

Figure V-19: Mesozoic bedrock horizons used as geometrical markers for the structural map of the Mesozoic bedrock in the Terminal Sul area, interpreted on the chirp profile P02, cruise RIAV02A. The chirp profile has Automatic Gain Control applied to enhance reflection continuity. (**a**) – red line indicates profile location; (**b**) – profile without interpretation; (**c**) – interpreted profile.

There is a clear spatial association between the gas fields in the Terminal Sul (TS-WGF and TS-EGF) and the hanging walls of the main normal faults; also the pockmark evidence is also spatially associated with vertical fault zones in the Mesozoic bedrock (see Figs. V-20 and V-22). These clear spatial relations between fluid evidence and fault structures strongly suggest that the faults in the Mesozoic bedrock constitute preferential fluid migration pathways.

The disrupted horizons of the Mesozoic bedrock in the Cidade channel underlie gas accumulations in trapped in the Holocene sediments. The Mesozoic structure in this area follows the westerly gently dipping monocline regional trend (apparent folding observed in the profiles appears to be a result of the intersection of an arcuate trackline with the west dipping monocline). The localized strain shown by the disrupted horizons materialize shear zones of flower structure patterns with general WNW-ESE trends (68ºW) suggestive of transpressive deformation (both shortening and strike-slip). Considering the hypothesis that the gas accumulated in the Holocene sediments has escaped through the disrupted Mesozoic horizons, then fluid escape in the Cidade channel is controlled by these WNW-ESE fractures of the Mesozoic (see Fig. V-22). The gas composition found until now in the Ria of Aveiro consists mainly of methane and, therefore appears to be of biogenic origin. The interpretation proposed here raises the possibility of also a potential deeper source for the gas.

Stratigraphic and geometrical evidence of the relative chronology and kynematics of the structures observed in the study areas is incomplete and, until further evidence is found, an explanatory hypothesis for the deformation history has to be based on the proposed Meso-Cenozoic regional geodynamical evolution of the Western Iberian Margin. In this sense, the observed deformation can be explained by the roughly E-W extension related to the late Cretaceous Atlantic rifting, and by the NW-SE convergence of the Eurasia and Africa plates during the Miocene (for an overview of post-Jurassic tectonics in Iberia see Wilson *et al.*, 1989; Ribeiro *et al.*, 1990; Srivastava *et al.*, 1990; Rasmussen *et al.*, 1998; Andeweg, 2001; Alves *et al.*, 2003).

The strain accommodated by the NNW-SSE and NNE-SSW normal faults probably occurred during the late Cretaceous extension. During the Miocene

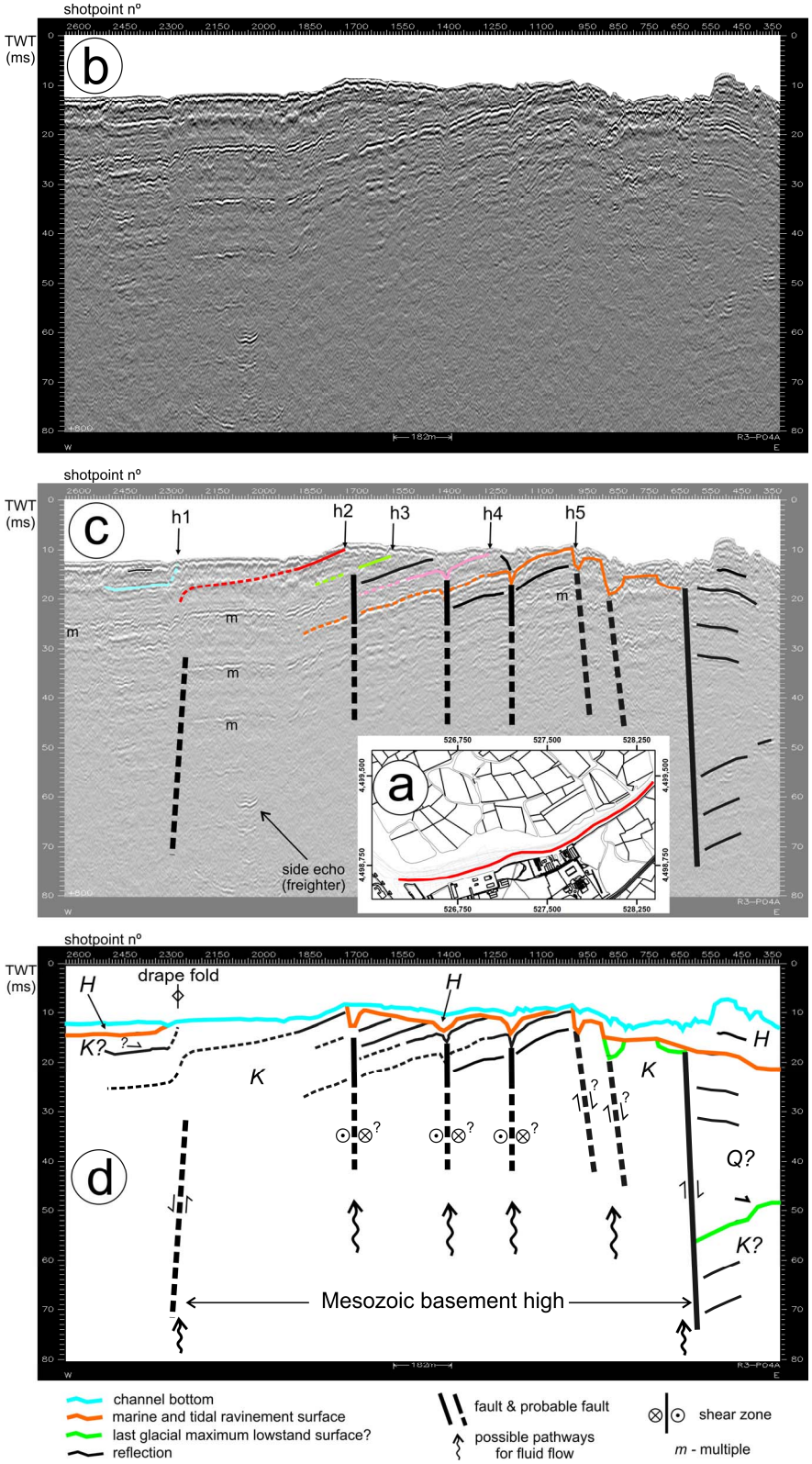

Figure V-20: Structural interpretation of the Boomer profile P04A, acquired in the Terminal Sul area during cruise RIAV03. (**a**) – red line shows profile location; (**b**) – profile without interpretation; (**c**) – interpretation of the Mesozoic bedrock horizons used as geometrical markers and of the main structures (without kinematic interpretation); (**d**) – Sedimentary surfaces and geometrical and kinematic interpretation of the main structures. H – Holocene, Q – Quaternary, K - Cretaceous. See text for further explanation.

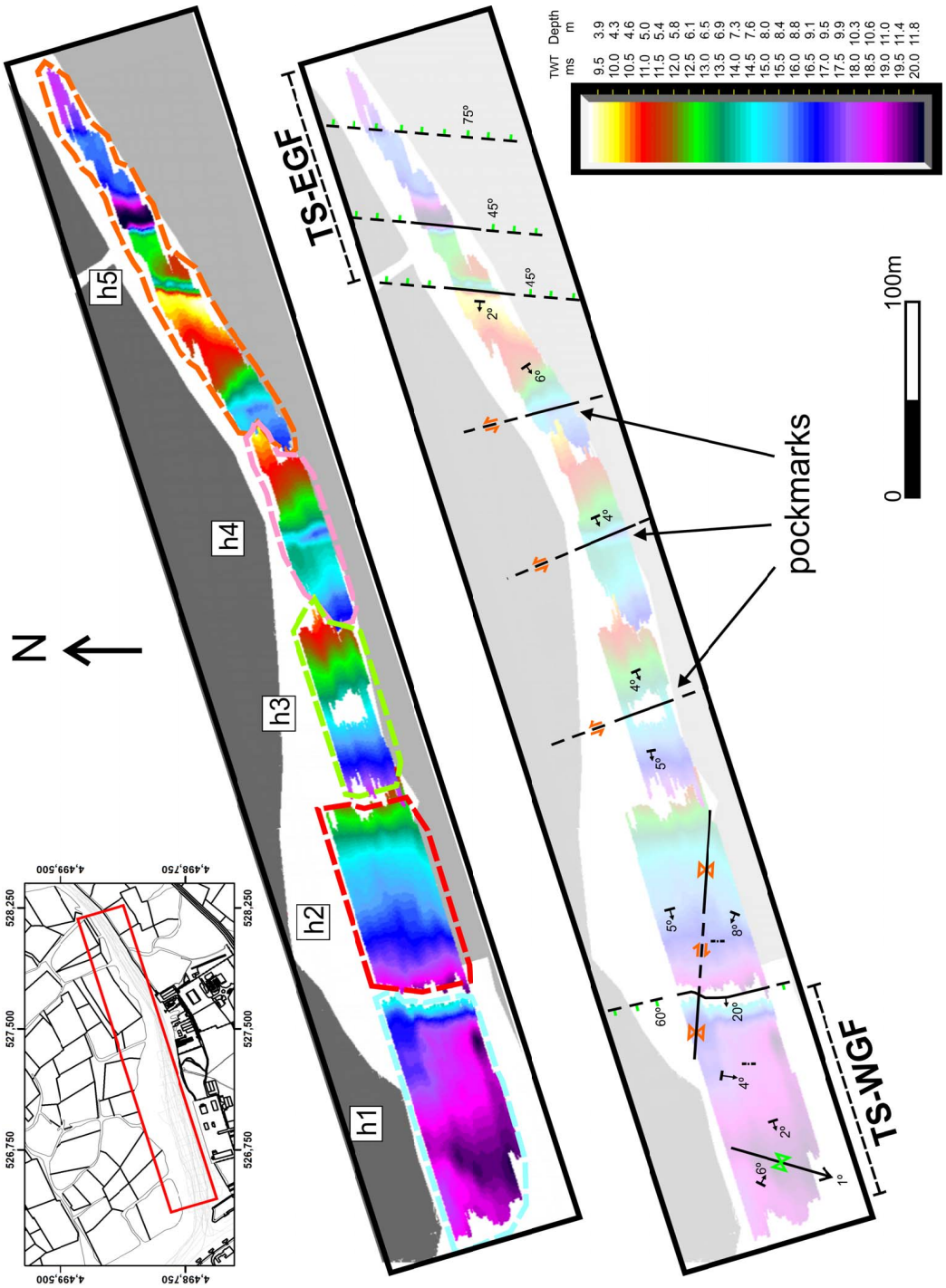

Figure V-21: Top - Isobaths of Mesozoic bedrock horizons used as geometrical markers for the structural map of the Mesozoic bedrock in the Terminal Sul area (red box on track line map locates mapped area). Dashed lines circumscribe each horizon. The vertical color scale is the same for every horizon. Bottom – Faded isobath map with the main deformation structures interpreted from the Mesozoic horizons and from the chirp and boomer profiles. The general location of pockmarks and gas fields (TS-WGF and TS-EGF) are indicated for comparison.

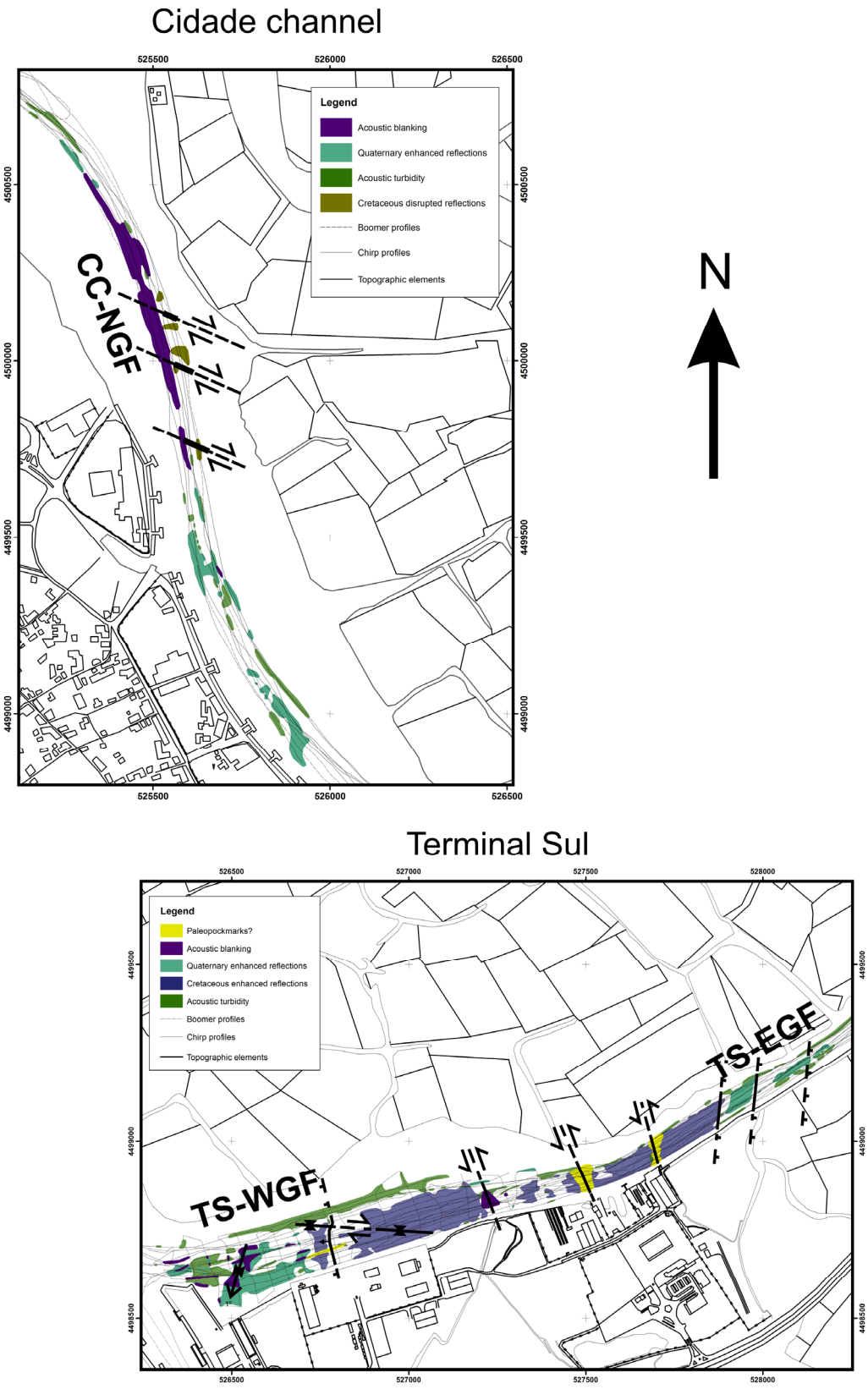

Figure V-22: Map of the main structural features and of the seismic evidence of gas, observed on the Chirp and Boomer profiles acquired in the Cidade and Terminal Sul areas of the Ria of Aveiro. The interpreted faults were mapped in the Cretaceous basement.

inversion, these faults were probably reactivated with oblique movements with predominance for left lateral strike-slip component. The 68-82ºW and 15-24ºW vertical faults may constitute conjugate fault family pairs with a tight angle of 44-67º and a corresponding compression direction roughly on 45ºW, compatible with the Miocene NW-SE convergence. In this setting, the 68-82ºW fault set would have had right lateral strike-slip movement and the 15-24ºW fault family left lateral strike-slip movement.

5.4.4. Tidal altitude and the amplitude of the bottom reflection

One of the initial purposes of the pseudo-3D Chirp coverage was to study and map amplitude variations of reference horizons. The map of raw amplitudes (unprocessed data) extracted from the bottom reflection of the Chirp profiles revealed a systematic pattern of higher amplitudes in the profiles acquired at lower tides (mainly E-W profiles) when compared with the amplitudes from profiles acquired at higher tides (mainly N-S lines, see Fig. V-23).

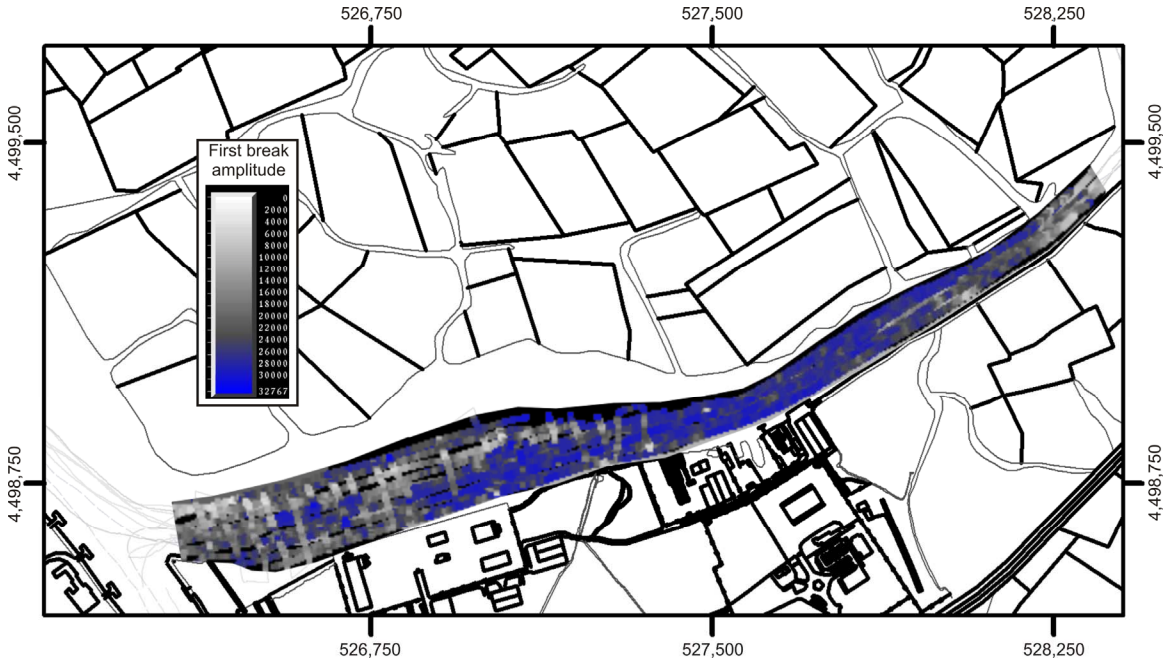

Figure V-23: Map of raw amplitudes extracted from first-break picks (water bottom) of the chirp profiles in the Terminal Sul area. The net like amplitude pattern did not allow a meaningful geological interpretation of maps of reflection amplitudes. Possible explanations for this pattern were sound energy loss and attenuation related to differences in two way time to first break and/or the abundance/size of gas bubbles in the sediments.

Attempts to balance amplitudes between the various profiles were unsuccessful and the evidence of a possible effect of tidal height on the gas evidence (see Fig. V-10) led to the test of the hypothesis that the changes in bottom amplitudes were in part related to gas bubbling during falling tides. The data used for this specific purpose was the bottom amplitudes measured in the Chirp profiles in the Terminal Sul and the Cidade Channel areas.

The analysis of the first break two-way times (TWT) versus amplitudes scatter plots shows that the Terminal Sul data is strongly clustered towards low TWT and high amplitude values, whereas the Cidade Channel data has no obvious clustering (see Fig. V-24). The least squares linear regression lines for the first break amplitude as the dependent variable, show trends consistent with an expected decrease in amplitude with increasing TWT due to sound energy reductions caused by spherical divergence of the sound wave and attenuation effects in the water column.

Each amplitude value extracted from the picks of the bottom reflection was classified according to the tidal altitude at the time of the trace acquisition: class 1 ***high tide*** – corresponds to the upper quarter of the tidal altitude range (e.g. from 2.5m increasing to 3m and decreasing to 2.5m altitude in the northern end of the Cidade channel); Class 2 ***ebb*** – corresponds to the descending quarter of tidal altitudes (e.g. from 2.5m decreasing to 1.5m altitude in the northern end of the cidade channel); Class 3 ***low*** tide – corresponds to the lowest quarter of tidal altitudes (e.g. from 1.5 m decreasing to 1m and increasing to 1.5m altitude in the northern end of the cidade channel) and; Class 4 ***flood*** – corresponds to the increasing quarter of tidal altitudes (e.g. from 1.5m increasing to 2.5m altitude in the northern end of the cidade channel).

The box plots of the first break TWT at each tidal stage (Fig. V-25) show that the TWT coverage for the various tidal stages in the Terminal Sul is heterogenous with smaller TWT ranges during low tide and flood (75% of the samples between 5 and 7ms) when compared with the TWT ranges during high tide and ebb (75% of the data between 5 and 14ms). First break times in the Cidade channel have a more homogeneous range for all tidal stages (75% of the data is roughly between 12 and 18ms). The TWT range heterogeneties of the

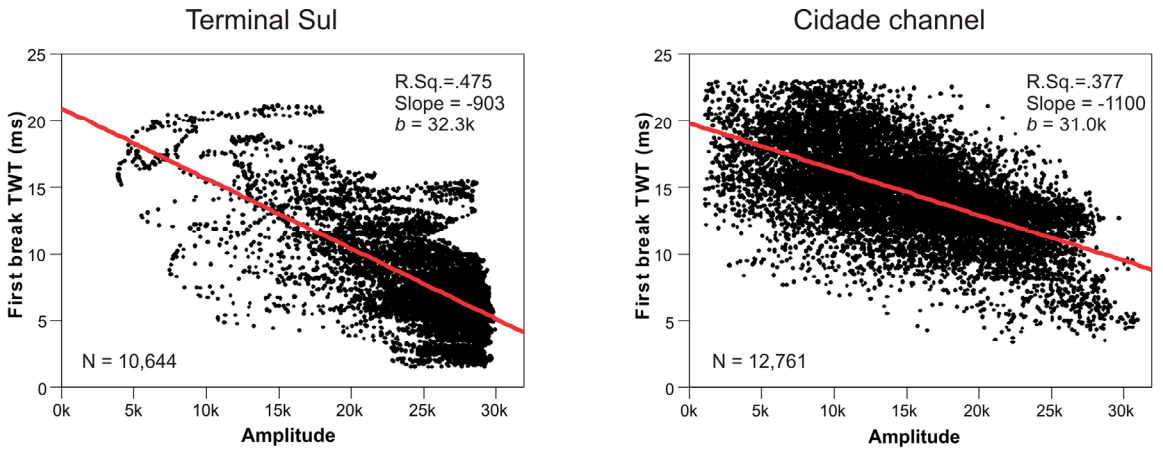

Figure V-24: Scatter plots with respective least squares linear regression lines of pairs of first break times (TWT) and amplitudes (16 bits half range – between 0 and 32767), sampled in the Chirp profiles acquired in the Terminal Sul and Cidade channel areas during cruises RIAV02 and RIAV02A. The Terminal Sul data is strongly clustered towards low TWT and high amplitude values; the Cidade Channel data has no obvious clustering. Least squares linear regression parameters: **Terminal Sul** – ***R square*** = .0475, ***slope*** = -903, ***b*** = 32302; **Cidade channel** – ***R square*** = .377, ***slope*** = -1100, ***b*** = 31077

Terminal Sul area are greater than the tidal range (approximately 2m-3ms) indicating that the sampling in Terminal Sul area during each tidal stage Sul had an irregular distribution in space: i.e. certain parts of the Terminal Sul area were probably undersampled, particularly during low tide and flood.

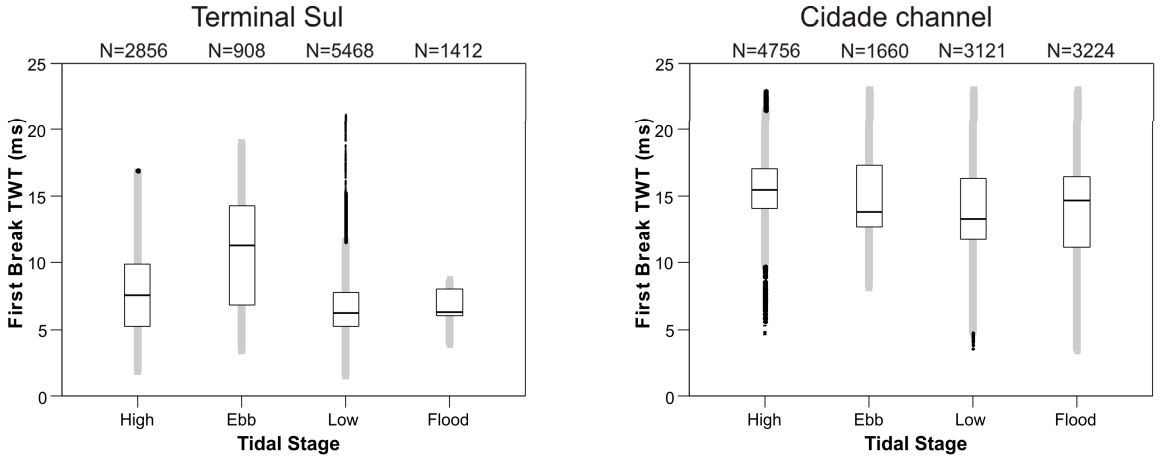

Figure V-25: Box plots of the first break times (TWT) at each tidal stage of the Chirp profiles acquired during cruises RIAV02 and RIAV02A, in the Terminal Sul and Cidade channel areas. First break time coverage for the various tidal stages in the Terminal Sul area is heterogeneous with smaller TWT ranges during low tide and flood (75% of the samples between 5 and 7 ms) when compared with the TWT ranges during high tide and ebb (75% of the data between 5 and 14 ms). First break times in the Cidade channel have a more homogenous range for all tidal stages (75% of the data is roughly between 12ms and 18ms). The TWT range heterogeneities of the Terminal Sul are greater than the tidal range (approximately 2m – 3ms) indicating that different zones of the Terminal Sul were sampled during the various tidal stages.

The residual first break amplitudes were determined from the least squares linear regression lines determined previously. The histogram of the residual amplitudes of the Terminal Sul is skewed with marginally positive amplitudes more frequent and a long tail of negative amplitudes (Fig. V-26). This indicates that the linear regression is a poor model for the observed time and amplitude samples and is in sharp contrast with the bell curve shaped histogram of the Cidade channel (Fig. V-26).

The box plots of first break amplitudes at each tidal stage provide further evidence of the relative sampling conditions of study area (Fig. V-27). Overall amplitudes values in the Terminal Sul area are marginally smaller during high-tide with minima during ebb. Nevertheless, amplitudes for the Terminal Sul area are concentrated towards the upper end of the systems recording range (positive half of the 16 bits integer – 32767) indicating that many samples may have been clipped due to excessive amplitude gain settings during seismic acquisition. This data clip prevents a comparative analysis of the amplitudes in the Terminal Sul. Amplitudes for the Cidade Channel are broadly spread over the recording range, with higher values during ebb and low tide, and lower values during flood with minima during high tide (Fig. V-27).

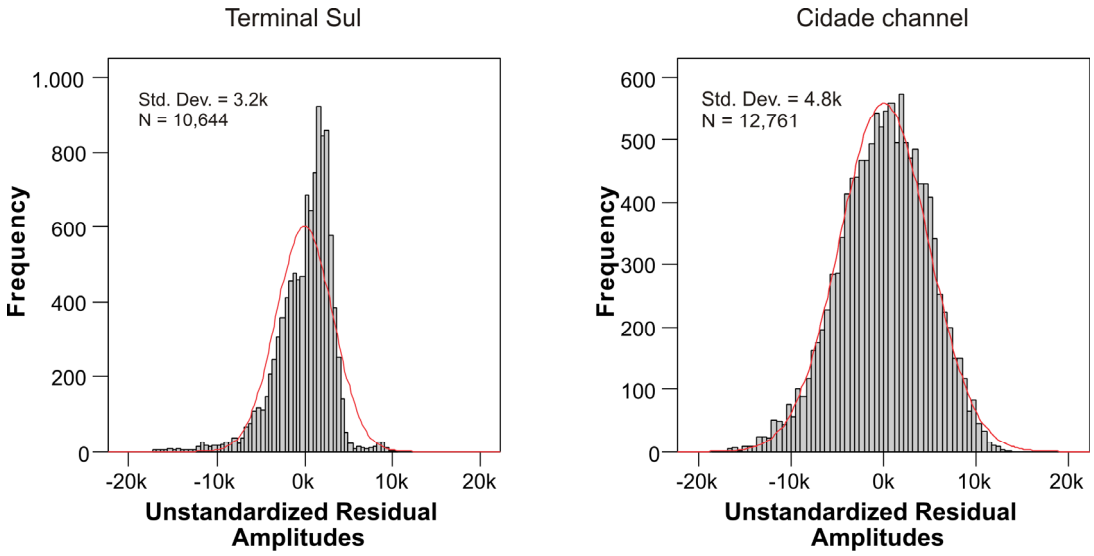

Figure V-26: Histograms of unstandardized residual first break amplitudes of the Chirp profiles acquired during cruises RIAV02 and RIAV02A, in the Terminal Sul and Cidade channel areas. Residual values were determined from the least square linear regression lines previously determined (see text for explanation). The Terminal Sul histogram is skewed towards a higher frequency of negative residuals, i.e. first break amplitudes lower than predicted are more frequent. This indicates that the linear regression may be a poor model for the observed time and amplitude samples, and is in contrast to the bell shaped histogram of the Cidade Channel.

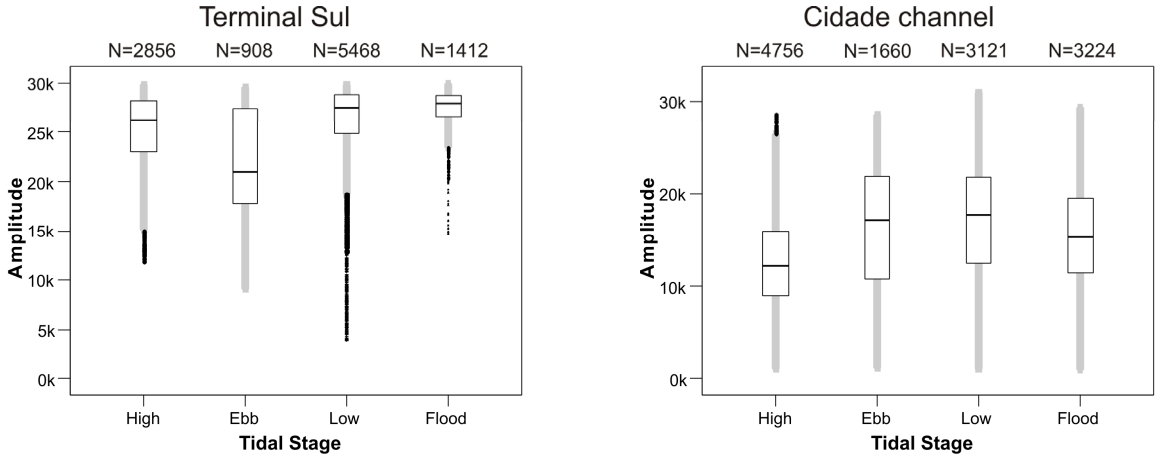

Figure V-27: Box plots of first break amplitudes at each tidal stage of the Chirp profiles acquired during cruises RIAV02 and RIAV02A, in the Terminal Sul and Cidade channel areas. Amplitudes for the Terminal Sul are concentrated towards the upper end of the systems recording range (positive half of the 16 bits integer – 32767) indicating that many may have been clipped due to excessive gain during acquisition. Overall, amplitude values in the Terminal Sul are smaller during high tide with minima during ebb. Amplitudes for the Cidade channel are broadly spread over the recording range, with higher values during ebb and low tide, and lower values during flood with minima during high tide.

The relationship between the residual amplitudes determined from the least squares regression line and each tidal stage was analyzed to see if changes in tidal stage could explain part of the dispersion of the amplitude versus TWT scatter plots (Fig. V-28). The residual amplitudes for the Terminal Sul are mostly within -2000 and +2000 (75% of the data). Interpretation of this plot is probably meaningless due to the suspected sampling problems described before (poor spatial coverage for each tidal stage, poor linear regression model and amplitude clipping during acquisition) but is shown for reference. The Cidade Channel residual amplitudes have different biases for each tidal stage, with greater than predicted amplitudes during low tide with maxima during ebb; residual amplitudes during flood are evenly distributed around 0; the lowest residual amplitudes occur mostly during high tide.

The analysis of the first break amplitudes of the Chirp data shows that the Terminal Sul area data has sampling problems that prevent a comparative analysis of the amplitude data. Nevertheless, the Cidade Channel data shows an inverse linear relationship between amplitude and two way time which can be explained by sound energy reduction processes related to sound wave spherical divergence and energy attenuation in the water column. The residual amplitudes determined from the linear regression show different biases for each tidal stage.

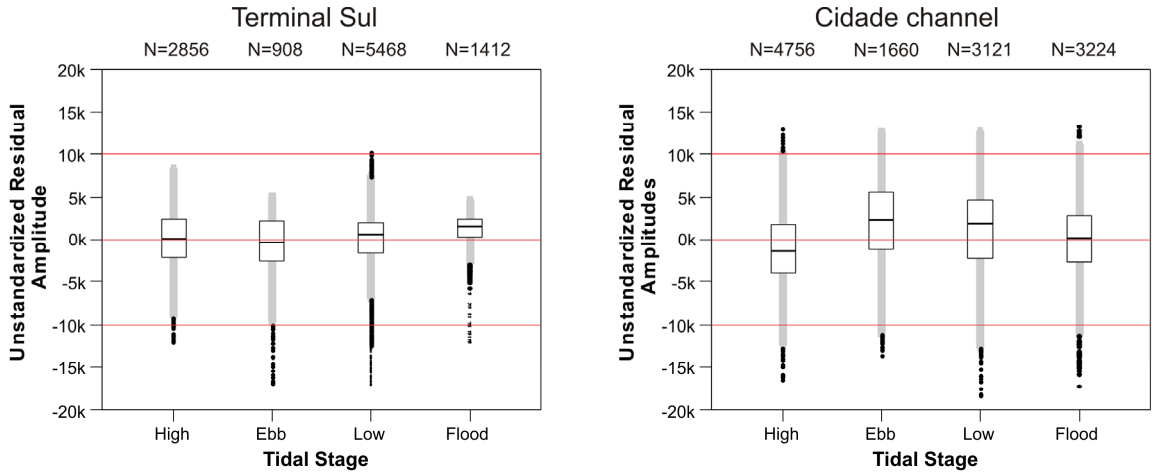

Figure V-28: Box plots of unstandardized residual first break amplitudes at each tidal stage of the Chirp profiles acquired during cruises RIAV02 and RIAV02A, in the Terminal Sul and Cidade channel areas. Residual amplitudes for the Terminal Sul are mostly within -2000 and +2000 (75% of the observations). Interpretation of this plot difficult due to the suspected sampling problems of the various tidal stages in the Terminal Sul, and because of the linear regression was found to be a poor model of the sampled data. Residual amplitudes for the Cidade channel vary have different biases according to the tidal stage, with greater than predicted amplitudes during low tide with maxima during ebb; residual amplitudes during flood are evenly distributed around 0; the lowest residual amplitudes occur mostly during high tide.

This means that a tide related phenomenon is affecting the recorded amplitudes independently of the distance of the seismic source to the reflector. Considering the widespread evidence of gas in the Ria of Aveiro, the stronger than expected amplitudes during low tide with maxima during ebb may be explained by gas ebullition and/or gas bubble size changes triggered by falling pressure with falling tide (Best et al., 2004).

The methane gas bubbles observed escaping the sediments in the “Doca Pesca” pier of the Ria de Aveiro, outside the study areas, showed a similar pattern with tidal altitude to the one between amplitude strengths and tidal altitude. The gas bubbling started with falling tide and petered down as the tide turned and rose. This independent observation supports the hypothesis that bubbling and gas escape in the Ria de Aveiro is triggered mainly by falling tide and that its effect is detected pervasively by the chirp system.

5.5. Discussion and conclusions

Evidence of gas in the Terminal Sul and Cidade Channel covers respectively, 28% and 31% of the total seismic coverage area, a value that, for the Terminal Sul, may reach 55% if the possible evidence for gas in the Mesozoic bedrock is added. The evidence occurs at a wide range of depths below the water surface, from 3m downw to 15m. The distribution and extent of seismic evidence of gas in the Terminal Sul and Cidade Channel sectors, as well as, the increase in relative extent and depth range of gas accumulations when compared to the 14% area and 4m depth of the gas accumulations in the Espinheiro Channel sector, have methodological and natural explanations.

The analysis of the data from the Espinheiro Channel (Chapter IV, Duarte *et al.*, 2007) showed that the use of seismic evidence to map gas accumulations tends to underestimate the areas of accumulations because the absence of seismic evidence of gas does not necessarily imply its absence. This is particularly important when comparing the gas accumulation areas of the shallower Espinheiro Channel sector with the deeper Cidade Channel and Terminal Sul sectors. The closer proximity of the water bottom multiple in the shallower Espinheiro Channel shortens the window of observation of the seismic profiles and limits the ability to identify diagnostic reflection patterns, thereby underestimating the extent of the mapped areas of gas accumulation. Furthermore, the distance between profiles in the Espinheiro Channel sector reaches 75m which is three times more than the maximum distance between profiles in the Terminal Sul and Cidade Channel sectors. This means that the extent of pockets of gas smaller than 75m is most probably underestimated in the Espinheiro Channel.

The problems of the depth of the survey area and the profile separation in mapping gas accumulations with seismic methods have implications for the assessment of uncertainty of measured gas accumulation areas; these should be addressed in subsequent surveys. Mapping gas accumulations in shallow waters will probably require a dense groundtruthing sampling for gas in order to clarify the expectedly ambiguous seismic evidence of gas in shallow waters. If this disambiguation through groundtruthing is not possible, then the use of seismic

data in shallow water will be limited to exploratory studies, i.e. to making new findings of gas accumulations where observation conditions are optimal. The issue of variable profile separation is a problem of observation scale already discussed in Chapter III. The gas accumulations in the Ria of Aveiro have a wide range of sizes and shapes probably reflecting the sizes and shapes of the potential gas traps, which in a coastal lagoon environment probably include a multitude of sediment bodies that fill small tidal channels. Furthermore, it is probably safe to assume that the size and extent of these gas traps have fractal properties; as discussed before (see Chapter III) this means that the interpretation and comparison of maps of seismic evidence of gas accumulations require the use of a constant scale of observation, in this case a constant profile separation. In the present work, the Terminal Sul sector has the most regular profile separation and, therefore, is the sector that provides the best conditions to study the size, distribution and controls of the gas accumulations.

The distribution of the evidence of gas accumulation in the Terminal Sul and Cidade Channel sectors has strong spatial correlation with the fracture pattern of the Mesozoic bedrock (see Fig V-22). Since the Mesozoic structure appears to exert a control on the distribution of gas, this implies the existence of a fluid source in the Mesozoic bedrock. The corresponding fluid my be either rich in methane gas or have chemical properties that promote methanogenesis in the Holocene sediments. The study of the Espinheiro Channel sector already raised the hypothesis of a deeper source of methane (see chapter IV), and the data from the Terminal Sul and Cidade Channel again raises this possibility. The Mesozoic bedrock in Terminal Sul and Cidade Channel sectors has a denser fracture pattern when compared with the Espinheiro sector, indicating the existence of higher permeability pathways for fluid migration. Furthermore, the Terminal Sul sector Mesozoic bedrock appears to constitute a structural high that may function as a trap for gas migrating from depth (Fig. V-20), which is in agreement with the occurrence of focused fluid escape structures such as the observed pockmarks (Figs. V-11, V-12 and V-13), as well as with the overall enhanced reflections in the Mesozoic bedrock.

The relationship between the deformation history and fluid flow history is

unclear. The intensity of the strain accommodated by the disrupted horizons in the Cidade Channel raises may be in part related to hydraulic fracturing processes. If the fluids overpressure conditions necessary for such processes were achieved through seismic pumping then fluids may have migrated through the WNW-ESE and NNW-SSE faults during the Miocene inversion tectonic episodes. Reports of extensive fluid escape in the Ria of Aveiro were recorded in the XVIII century during the 1755 Lisbon earthquake (Coelho, 2005; Oliveira, 2005). If these reports are true then, tele-seismic effects related to Quaternary tectonics may also be a driving mechanism for fluid migration in the Ria of Aveiro.

The association between the gas escape and accumulation features in Holocene lagoon sediments and the Mesozoic bedrock structure is indicative that, whether or not tectonic events were responsible for fluid flow, the present fractures are probably functioning as permeable pathways for fluid migration from depth to the Holocene sediments and out to the Ria of Aveiro and to the atmosphere. This means that deeper older accumulations of gas are probably a source of the gas accumulating and escaping from the Holocene sediments.

The existence of gas traps in the Holocene sediments also controls the distribution and extent of gas accumulation and escape in the Terminal Sul and Cidade Channels, as illustrated by acoustic turbidity in the sedimentary fills of the buried pockmarks in the Terminal Sul (Fig. V-13), and the extent of the CC-NGF and related gas escape evidence in the Cidade Channel (Fig. V-17). The importance of the Holocene sediment architecture in the distribution of gas accumulations was also evident in the Espinheiro Channel sector, for the main gas fields appear to have been trapped within layers of a prograding sediment wedge and within layers of a tidal channel sedimentary fill (see Chapter IV; Duarte *et al.*, 2007).

Local changes in gas related seismic features (see Fig. V-10) as well as the data on first break amplitudes from the Cidade Channel sector provide very strong evidence that tides have an effect on the acoustic response of gas rich sediments. This effect will impact the mapped distribution and extent of gas evidence and its use to quantify gas volumes. The relative increase in reflections amplitude during tidal fall probably reflects changes of methane solubility due to decreasing

pressure; either ebullition as observed in other parts of the lagoon or as observed in tidal marshes by other authors (e.g. Jackson *et al.*, 1998), or changes towards resonant bubble sizes (Best *et al.*, 2004) cause an increase in gas reflectors detected by the seismic systems and influence the interpretation of gas evidence. Either way, 4D surveying will be required to determine the impact of this semi-diurnal control on the extent and distribution of gas.

There are several other factors that may control the distribution and extent of the gas accumulation and escape in the study areas, for which the available data is insufficient to assess its importance. The organic rich Holocene sediments are probably a modern source of biogenic methane gas and bio-geochemical data is required to study the methane production. In fact, primary biological production, a pre-requisite for biogenic methane production, is very high in coastal environments like the Ria of Aveiro (Kelley *et al.*, 1995; Van der Nat and Middelburg, 2000) and primary biological production and geochemical conditions of the Holocene organic rich sediments influence methane gas production, accumulation and escape patterns; factors such as seasonal changes in primary production, water salinity, depth of oxygen reduction within the sediments, etc, all will affect the location and extent of methane gas production (Hagen and Vogt, 1999).

Anthropogenic activity may also affect the distribution and extent of gas. The Terminal Sul and Cidade Channel sectors in particular, are places of intense human activity with heavy construction, freight ship traffic, fishing and dredging. These activities change the water and sediment chemistry, the morphology of the channels, as well as strongly influence the hydrodynamics of the lagoon.

In summary, the seismic evidence of gas covers approximately one third of surveyed tidal channels of the Ria of Aveiro. Evidence of gas includes: acoustic turbidity, enhanced reflections, acoustic blanking, pockmarks and buried trough pockmarks, disrupted horizons and acoustic plumes in the water column (flares). The tidal altitude variations impact the detection of gas with seismic methods. Reflection amplitudes in gas-prone areas are clearly stronger during low tide with maxima during ebb, decreasing with flood with minima during high tide; this pattern confirms that ebullition and gas escape is triggered mainly by the decrease

of pressure (hydraulic load) that occurs during the falling tide. The location and geometry of fluid the escape features follows the fracture pattern that affects the Mesozoic bedrock, indicating that these fractures are preferential pathways for fluid migration and exert a structural control on the gas occurrences in the Ria of Aveiro. This structural control raises the hypothesis of the existence of a deep source of methane, possibly thermogenic, in or below the Mesozoic bedrock.

Chapter 6. Conclusions and future work

The subject of this thesis was the investigation of gas accumulation and seepage in the Ria of Aveiro barrier-lagoon using high resolution seismic reflection methods. The main problems addressed ranged from practical aspects of observation and data acquisition to questions related to the study of natural processes. The three main questions that were addressed were:

1. What are the best procedures to acquire and process seismic reflection data in a shallow barrier-lagoon environment?
2. What are the types of seismic evidence of gas accumulation and seepage in the tidal channels of the Ria of Aveiro and what is the appropriate way to map them?
3. What are the geological controls on gas accumulation and seepage in the tidal channels of the Ria of Aveiro?

This final chapter presents a summary of the results obtained when trying to answer these questions, discusses the main issues that arose from this investigation and proposes guidelines for future work in the study of gas generation and flow in the Ria of Aveiro, also applicable to other similar coastal environments.

6.1. Acquisition and processing of high resolution seismic reflection data in a shallow water environments

High resolution seismic reflection methods present significant advantages for the investigation of the sub-surface geology in shallow barrier-lagoon environments. The ability to survey the water column and sub-surface geology, both in time and space, over extensive areas of difficult access, provided the opportunity to make several new discoveries in the Ria of Aveiro, and illustrates the value of the use of seismic reflection in such an environment.

Nevertheless, seismic reflection systems have some limitations when applied in coastal environments. The ship traffic, tides, channel morphology and shallow bathymetry affects the deployment and operation of the seismic systems as well as restricts the extent of the profile coverage. The heterogeneity of the seismic coverage, signal quality, penetration and resolution all constrain the use of the data to mostly local but detailed interpretations and modeling of the geological objects.

Considering all these constraints, control of the acquisition geometry of the seismic systems and navigation systems and reliable information of tidal altitude variations during acquisition are of paramount importance. It was shown here that, when acquiring seismic data in an environment such as the Ria of Aveiro, changes in the system geometry parameters that may be safely disregarded in surveys of much larger scope (i.e. significantly greater profile separation) have to be well controlled. Changes of few meters in acquisition geometry such as the depth or the layback of the towed equipment, have significant impact on the accuracy and consistency of the interpretation of geological features (e.g. fault plane morphology, see chapter III). Also of significant importance for data positioning is the synchronization of the seismic acquisition and navigation systems. Trace positioning estimates depend strongly on matching the data timestamps of each system and, given acquisition speeds of 4-6 knots, a single second of synchronization error results in a 1-2m positioning error.

The processing flows for the navigation data and the seismic signal developed in the scope of this thesis improves and constrains the uncertainties in data positioning and interpretability of the seismic features. The case of the Ria of Aveiro shows that position estimates obtained through navigation data processing resulted in a mean horizon mistie value of 0.75ms, which allowed a confident correlation of the interpretation between profiles, without which mapping of the seismic evidence of gas would have been very difficult. Furthermore, the quality of the trace position estimates of the pseudo 3D Chirp survey in the Terminal Sul sector was clearly illustrated by the consistency and detail of the gas evidence, horizon isobats and structural maps. These maps allowed the identification of the spatial relationships between evidence of gas, sediment architecture and the

Mesozoic bedrock structure in the Terminal Sul, which was a major objective of this thesis.

The seismic signal processing improves not only signal to noise ratio, but also the geometric interpretability of the seismic/geological features. Of particular importance are the normal moveout correction and the Stolt F-K migration processes. The normal moveout correction of boomer data allows the correct correlation of the interpretation between chirp and boomer profiles in very shallow domains, such as those found in certain parts of the Espinheiro Channel sector. The Stolt F-K Migration has significant impact in collapsing diffraction from point diffractors in the Holocene sediments, improving profile interpretability and in improving the geometry of channels and deformation structures.

Concerning the issues of acquisition and processing of the seismic data, it should be emphasized here that best processing results are only accomplished after strong quality control procedures involving the analysis of the track line regularity, horizon misties and first-break surface models, which allows the revision and improvement of the processing parameters.

The main priority regarding future work in acquisition and processing of seismic data in shallow coastal environments is related to the most important limitation of seismic reflection methods. Models derived solely from geophysical methods, methods of indirect observation, require testing through groundtruthing. In this work, groundtruthing was mostly provided by available borehole log data, critical for the calibration of the seismic stratigraphy, but of no practical use in determining if specific reflections were caused by gas in the sediments. In the case of the Ria of Aveiro, direct observation of gas escape from the sediments, in other locations of the lagoon, provides support for the interpretation of the seismic evidence of gas. Nevertheless, future work must take into account that it is important that the reflector(s) responsible for the reflection events interpreted as gas are identified through groundtruthing at the surveyed locations. Furthermore, groundtruthing should be done, if possible, at the time of the seismic surveying in order to prevent errors in testing due to the temporal variations in gas generation, accumulation and flow.

As concerns the practical aspects of seismic acquisition and data processing, the following improvements will increase the range of usability and reliability of seismic surveying in shallow coastal environments such as the Ria of Aveiro:

1. Maintain a constant acquisition speed. Considering that this requirement is extremely difficult to respect in environments such as the Ria of Aveiro, then binning and stacking of the trace data should also be considered in order to obtain a constant trace separation;

2. Follow survey plans with regularly spaced, orthogonal profiles, both to improve interpretability and to maintain a constant observation scale, allowing for the comparison of Euclidian properties of the geological features to be mapped;

3. Improve real time synchronization of the clocks of the seismic acquisition and navigation systems, either through hardware or software; automate the positioning estimate procedure during acquisition in order to allow quality control of the data and cut post-processing times;

4. Acquire navigation data exactly above source and receivers, e.g. placing GPS antennas over the towed equipment. This will provide accurate geometry parameters for navigation and geometry related seismic signal processing;

5. Acquire 3D Kinematic GPS data to estimate source and receiver altitudes and infer tidal altitude for each trace, thus bypassing the need to measure tidal altitudes at control stations and having to resort to tide propagation models within the lagoon to estimate tidal altitudes for each trace location.

6. Test and implement predictive deconvolution processing to attenuate first break multiples, which are a major obstacle to interpretation in shallow

waters surveying. In the case of chirp data, this would require recording data in raw or pre-envelope processing formats;

6.2. Seismic evidence of gas accumulation and seepage

Seismic evidence of gas accumulations in the Holocene sediments and possibly, in the Mesozoic bedrock of the Ria of Aveiro are extensive, covering 14% to 55% of the surveyed tidal channels area. Types of seismic evidence for gas accumulations in the study area included acoustic turbidity, enhanced reflections and acoustic blanking. Gas escape through the water column was also detected as acoustic flares and, possibly, cloudy turbidity. Of particular interest for such a dynamic system as the Ria of Aveiro was the finding of mounds and pockmarks that indicated that gas generation and flow in the sediments of the lagoon may have played a role in shaping the morphology of the tidal channels. The relationships between the structure of the Mesozoic bedrock and the overlying lagoon sediments were also clarified by the new seismic data. Also, the high resolution and density of the seismic profiles allowed the geometrical characterization of a 2km wide, 50m deep graben and of families of fractures that appear to exert a structural control on the extent and distribution of gas. Furthermore, the high resolution of the Chirp and Boomer systems allowed the mapping of the typically small gas accumulations (30 to 150m long), whose size probably reflects that of the host sedimentary bodies.

Searching for seismic evidence of gas in tide-dominated environments such as the Ria of Aveiro had unexpected results. Comparison of seismic profiles acquired at different tidal altitudes and the statistical analysis of changes of first break amplitude strengths with changing tidal altitude, together revealed that the seismic records changed significantly during the tidal cycle.Independent observation of tidal fall triggered methane ebullition in other locations of the lagoon support the hypothesis that gas ebullition is being detected by the seismic systems and that, therefore one needs to be careful when using acoustic methods to map gas accumulations in tidal dominated environments, because areas with a similar amount of methane content in the sediments may produce a different acoustic

response, depending on the stage of the tidal cycle during which they where surveyed.

The impact of tidal fall triggered ebullition on the seismic records can be viewed as a constraint on future work, but also as an opportunity. In fact, future surveying can be planned to study the diurnal dynamics of gas generation and flow in a 4D perspective, through qualitative and quantitative analysis of the reflection data. Such data, coupled with bio-geochemical analysis of sediment, pore water, and water column samples, would provide the input data necessary to model short term generation and flow of methane gas in the Ria of Aveiro and similar environments.

6.3. Geological controls on gas accumulation and seepage

The geological controls on gas accumulation and seepage in the tidal channels of the Ria of Aveiro are shown in the diagrams for each sector shown in Fig. VI-1, and are summarized below.

1. The Holocene prograding wedge and the tidal channel fill deposits (Espinheiro sector) and Quaternary (Holocene?) sediments of unknown nature (Terminal Sul Sector) are probable producers of biogenic gas of the Ria of Aveiro.

2. Gas accumulations occur in the gas producing sediments and beneath what appear to be impermeable horizons, such as those occurring in the Holocene marine/lagoonal sediments of the Cidade channel and in the sediment fills of the buried pockmarks of the Terminal Sul.

3. Evidence of widespread gas accumulation in the Mesozoic bedrock, evidence of fluid escape structures (pockmarks) and gas accumulations on the hanging walls of the major extensional faults that bound the structural high of the Mesozoic bedrock in the Terminal Sul, all suggest that structural highs in the bedrock also constitute traps for gas migrating from depth.

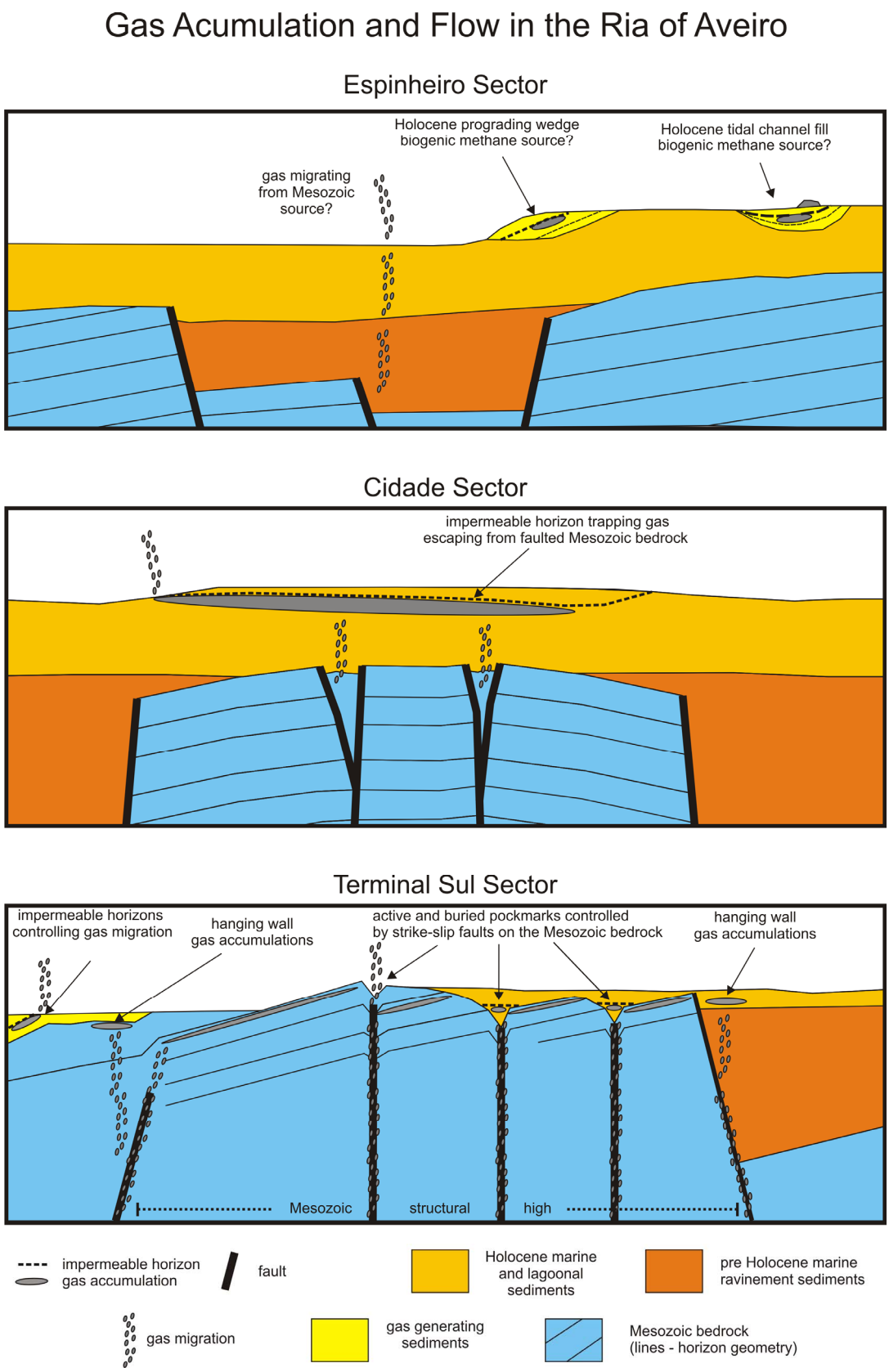

Figure VI-1: Proposed interpretation for the gas accumulation and seepage in the three studied tidal channel sectors of the Ria of Aveiro (not to scale). See text for further explanation.

4. The accumulation and seepage of gas in the sediments affects the morphology of the tidal channels in the form of pockmarks (70x40x2m, Terminal Sul sector) and gas domes (40x20x2m, Espinheiro sector).

5. The dynamics of gas flow and escape from the sediments is controlled by the tidal cycle, with falling tides causing ebullition. Focused fluid seepage occurs in the form of gas escaping from accumulations in the sediments, building bubble trains that rise through the water column (evident in every studied sector of the lagoon).

6.4. Future work

The present work provides strong evidence on the occurrence and controls on gas accumulation and seepage in the Ria of Aveiro. Given the exploratory nature of much of the research done, several key issues such as the seasonality of gas generation and seepage or the methane flow rates to the atmosphere could not be tackled and must be addressed in the future, in order to create a comprehensive model on gas generation and flow.

Considering that gas accumulations are extensive in the Ria of Aveiro, that gas escapes to the water column and the atmosphere, and that gas generation and flow affects morphology of the tidal channel floor, it is clear that the Ria of Aveiro is an excellent natural laboratory to study gas generation and flow in coastal sediments. Future work should emphasize two main questions, the first related to energy and climate issues, and the second related to geomorphology dynamics.

1. How much of the gas generated in the lagoon escapes to the water column and atmosphere? Conversely, how much of the gas generated in the lagoon remains trapped in the sediments?

The answer to this question will provide valuable information on the extrinsic and intrinsic factors that determine the capacity of a coastal system to

trap or lose the methane generated in the sediments. Such knowledge will provide energy exploration guidelines to find gas trapping coastal systems (modern and past), as well as inform climate models on the relative importance of coastal systems as a source of atmospheric methane.

2. Does fluid escape from the sediments exert a control on location and morphology of tidal channels? More specifically for the case of the Ria of Aveiro, is fluid escape the process through which the bedrock structure (faults and other permeable fluid migration pathways), buried beneath several meters of Holocene sediments, exerts a control on the location and morphology of the channels that mimic bedrock fault trends?

Modern drainage basins frequently show patterns that mimic deep seated structures without any apparent cause. The evidence of morphology shaping due to gas generation and flow in the Ria of Aveiro, a very dynamic system, provides an explanatory hypothesis for a mechanism of morphology control by deep structure: fluid escape from the sediments is capable of influencing erosion-transport-deposition patterns, thus shaping morphology.

References

Abecasis, C. K. (1954). The History of a Tidal Lagoon Inlet and Its Improvement (The Case of Aveiro, Portugal). Fifth Conference on Coastal Engineering, Grenoble, France.

Abecasis, F. M., I. M. Oliveira, et al. (1968). Estudo do restabelecimento artificial do transporte litoral da embocadura da Ria de Aveiro. H. Portuguesa. Lisboa**:** 138.

Alves, T. M., R. L. Gawthorpe, et al. (2003a). "Cenozoic tectono-sedimentary evolution of the western Iberian margin." Marine Geology **195**(1-4): 75-108.

Alves, T. M., R. L. Gawthorpe, et al. (2003b). "Post-Jurassic tectono-sedimentary evolution of the Northern Lusitanian Basin (Western Iberian margin)." Basin Research **15**(2): 227-249.

Andeweg, B. (2002). Cenozoic Tectonic Evolution of the Iberian Peninsula. Causes and effects of changing stress fields. Tectonics and Structural Geology Department. Amsterdam, Vrije Universiteit. **Ph.D.:** 178.

Andeweg, B. C., S. (2001). "Evidence for an active sinistral shear zone in the western Alboran region." Terra Nova **13**: 44-50.

Argus, F., R. G. Gordon, et al. (1989). "Closure of the Africa-Eurasia-North America plate motion circuit and tectonics of the Gloria fault." Journal of Geophysical Research **94**(B5): 5585-5602.

Bange, H. W., S. Dahlke, et al. (1998). "Seasonal study of methane and nitrous oxide in the coastal waters of the southern Baltic Sea." Estuarine Coastal and Shelf Science **47**(6): 807-817.

Baptista, P., L. C. Bastos, et al. (2002). A GPS based system for monitoring sand movements - The Aveiro Coastline case. Littoral 2002, The Changing Coast, Porto - Portugal.

Barahona Fernandes, J. A. (1971). Manual de Hidrografia. Lisboa, Ministério da Marinha, Instituto Hidrográfico.

Barbosa, B. (1981). Noticia Explicativa da Folha 16-C da Carta Geologica de Portugal, 1:50.000. Lisboa, Serviços Geologicos de Portugal.

Barton, C. C., P. R. LaPointe, et al., Eds. (1992). Fractals and their use in the Earth Sciences and in the petroleum industry. AAPG Short Course Manual. Houston, Texas, American Association of Petroleum Geologists.

Bernardes, C. (1987). "A sedimentologia da Formação Arenitos e Argilas de Aveiro - Cretácico Superior, Bacia Ocidental Portuguesa." Geociências, Rev.Univer.Aveiro **2 (1-2)**: 9:26.

Bernardes, C. (1992). A sedimentação durante o Jurássico Superior entre o Cabo Mondego e o Baleal (Bacia Lusitana): Modelos deposicionais e arquitectura sequencial. Geociências. Aveiro, Aveiro.

Bernardes, C. and F. Rocha (2007). "Temporal evolution of the sand-spit between Torreira and Furadouro (NW Portugal)." Journal of Coastal Research (Proccedings of the 9th International Coastal Symposium) **50**: 1092-1096.

Berthou, P. Y. (1973). "Le Cénomanien de l' Estramadure Portugaise." Mem. Serv. Geol. Portugal **23**.

Berthou, P. Y. and J. Lauverjat (1979). "Essai de synthèse paléogéographique et paléobiostratigraphique du bassin occidental Portugals au cours du Crétacé supérieur." Cienc. Terra **5**: 121-144.

Best, A. I., M. D. Richardson, et al. (2006). "Shallow seabed methane gas could pose a coastal hazard." EOS **87**(22): 213, 217.

Best, A. I., M. D. J. Tuffin, et al. (2004). "Tidal height and frequency dependence of acoustic velocity and attenuation in shallow gassy marine sediments." Journal of Geophysical Research-Solid Earth **109**(B8): -.

Boillot, G., J. L. Auxiètre, et al. (1979). The northwestern Iberian Margin: a Cretaceous passive margin deformed during Eocene. Deep Drilling Results in the Atlantic Ocean: Continental Margin and Paleoenvironment. M. Talwani, Hay, W., and Ryan, W.B.F, Am. Geophys. Union, Maurice Ewing Ser. **3:** 138-153.

Boillot, G. and J. Mallod (1988). "The north and northwest Spanish continental margin: a review." Rev. Soc. Geol. España **1**: 295-316.

Buforn, E., A. Udias, et al. (1988). "Seismicity, source mechanisms and tectonics of the Azores-Gibraltar plate boundary." Tectonophysics **152**: 89-118.

Cloetingh, S., E. Burov, et al. (2002). "Lithospheric Folding in Iberia." Tectonics **21**(5): 1041.

Coelho, A. G. (2005). Do "Inquérito do Marquês de Pombal" ao estudo de Pereira de Sousa sobre o Terramoto de 1 de Novembro de 1755. O grande terramoto de Lisboa. Lisbon, FLAD e Público. **1:** 143-188.

Condesso de Melo, M. T. (2002). Modelo matemático de fluxo e transporte de massa do sistema multiaquífero Cretácico da região de Aveiro (Portugal). Departamento de Geociências. Aveiro, Universidade de Aveiro. **Ph.D.:** 206 pp.

da Silva, J. F. and R. W. Duck (2001). "Historical changes of bottom topography and tidal amplitude in the Ria de Aveiro, Portugal - trends for future evolution." Climate Research **18**(1-2): 17-24.

Dashtgard, S. E., R. O. White, et al. (2007). "Effects of relative sea level change on the depositional character of an embayed beach, Bay of Fundy, Canada." Marine Geology **239**(3-4): 143-161.

Dias, J. M., J. F. Lopes, et al. (2000a). "Tidal Propagation in Ria de Aveiro Lagoon, Portugal." Physics and Chemistry of the Earth, Part B: Hydrology, Oceans and Atmosphere **25**(4): 369-374.

Dias, J. M. A., T. Boski, et al. (2000b). "Coast line evolution in Portugal since the Last Glacial Maximum until present - a synthesis." Marine Geology **170**(1-2): 177-186.

Dinis, J. L., J. Rey, et al. (2008). "Stratigraphy and allogenic controls of the western Portugal Cretaceous: an updated synthesis " Cretaceous Research **29**(5-6): 772-780.

Dinis, P. A. (2004). Evolução Pliocénica e Quaternária do Vale do Cértima. Departamento de Ciências da Terra, Universidade de Coimbra. **Ph.D.:** 351.

Duarte, H. (2006). PCable 3D navigation processing of the Mercator mud volcano site (cruise CD-178 onboard the RRS Charles Darwin, from 13th of February to the 3rd of April, 2006, at the Gulf of Cadiz). Relatório Técnico. Lisboa, Departamento de Geologia Marinha, INETI, I.P.**:** 15.

Duarte, H., B. Parsons, et al. (2003). Bottom features in the Ria of Aveiro (Portugal) revealed by side-scan sonar imaging. 4th Symposium on the Atlantic Iberian Continental Margin, Vigo, Thalassas.

Duarte, H., L. M. Pinheiro, et al. (2005). High-resolution seismic stratigraphy of the Ria of Aveiro (Portugal). Coastal Hope 2005, Lisbon, Portugal, University of Lisbon.

Duarte, H., L. M. Pinheiro, et al. (2007). "High-resolution seismic imaging of gas accumulations and seepage in the sediments of the Ria de Aveiro barrier lagoon (Portugal)." Geo-Marine Letters **27**(2-4): 115-126.

Etiope, G. (2004). "GEM - Geological Emissions of Methane, the missing source in the atmospheric methane budget." Atmospheric Environm. **38**(19): 3099-3100.

Fannin, N. G. T., Ed. (1980). The use of regional geological surveys in the North Sea and adjacent areas in recognition of offshore hazards. Offshore site investigation. . London, Graham & Trotman.

Faria, J. B., G. Zbyszewski, et al. (1967). "O aparecimento de gás na Gafanha da Boa Hora (Vagos)." Bol. Minas. Lisboa **4**(2): 125-130.

Faria, J. M. R. and M. J. Machado (1979). "Contribuição para o estudo hidroclimatológico da bacia hidrográfica do Rio Vouga." Rev. Inst. Nac. Meteor. Geof. **2**(1-2): 3-72.

Ferrin, A., R. Duran, et al. (2003). "Shallow gas features in the Galician Rias Baixas (NW Spain)." Geo-Marine Letters **23**(3-4): 207-214.

Fiúza, A. F., M. E. Macedo, et al. (1982). "Climatological space and time variation of the Portuguese coastal upwelling." Oceanologica Acta **5**(1): 31-40.

Galera, M., P. Jaen, et al. (1997). Recent Holocene stratigraphy in Mira tidal channel. Barrier Island complex of Aveiro, Portugal. Second Congress R.C.A.N.S., Salamanca (Spain).

Garcia-Gil, S. (2003). "A natural laboratory for shallow gas: the Rias Baixas (NW Spain)." Geo-Marine Letters **23**(3-4): 215-229.

Garcia-Gil, S., F. Vilas, et al. (2002). "Shallow gas features in incised-valley fills (Ria de Vigo, NW Spain): a case study." Continental Shelf Research **22**(16): 2303-2315.

Garcia Mondejar, J. (1988). "Plate reconstruction of the Bay of Biscay." Geology **24**: 635-638.

Garnerot, F., J. L. Bouchereau, et al. (2004). "Ichthyofauna in the biological organization of a paralic system: the Aveiro Lagoon (Portugal) in 1987-1988 and 1999-2000." Cybium **28**(1): 63-75.

Granja, H. M., I. C. Ribeiro, et al. (1999). "Some neotectonic indicators in quarternary formations of the northwest coastal zone of Portugal." Physics and Chemistry of the Earth, Part A: Solid Earth and Geodesy **24**(4): 323-336.

Gutowski, M., J. Bull, et al. (2002). "Chirp sub-bottom profiler source signature design and field testing." Marine Geophysical Researches **23**(5-6): 481-492.

Hagen, R. A. and P. R. Vogt (1999). "Seasonal variability of shallow biogenic gas in Chesapeake Bay." Marine Geology **158**(1-4): 75-88.

Hengl, T. (2006). "Finding the right pixel size." Computers & Geosciences **32**(9): 1283-1298.

Henkart, P. (2006). "Chirp sub-bottom profiler processing - A Review - Chirp signals may be recorded as correlates, analytic or envelope." Sea Technology **47**(10): 35-+.

Hirsch, R. L., R. Bezdek, et al. (2005). Peaking of world oil production: impacts, mitigation & risk management, Science Applications International Corporation (SAIC)**:** 91.

Hossack, J. R. (1983). "A cross-section through the Scandinavian Caledonides constructed with the aid of branch-line maps." Journal of Structural Geology **5**(2): 103-111.

Houghton, J. T., Y. Ding, et al. (2001). Climate change 2001: the scientific basis. Cambridge, U.K., Cambridge University Press.

Hovland, M. and A. Judd (1988). Seabed Pockmarks and Seepages. Impact on Geology, Biology and the Marine Environment. London, Graham and Trotman.

Hovland, M., A. G. Judd, et al. (1993). "The Global Flux of Methane from Shallow Submarine Sediments." Chemosphere **26**(1-4): 559-578.

I.P.C.C. (2001). Climate change 2001: The scientific basis. J. T. Houghton, Y. Ding, D. J. Griggset al. Cambridge, UK, Cambridge Univ. Press**:** 881.

Jackson, D. R., K. L. Williams, et al. (1998). "Sonar evidence for methane ebullition in Eckernforde Bay." Continental Shelf Research **18**(14/15): 1893-1915.

Janssen, M. E., M. Torne, et al. (1993). "Pliocene uplift of the eastern Iberian margin: Inferences from quantitative modelling of the Valencia Trough." Earth and planetary science letters **119**(4): 585-597.

Judd, A. G. (2004). "Natural seabed gas seeps as sources of atmospheric methane." Environmental Geology **46**(8): 988-996.

Kelley, C. A., C. S. Martens, et al. (1995). "Methane dynamics accross a tidally flooded riverbank margin." Limnology and Oceanography **40**(6): 1112-1129.

Klein, G. D. (1967). Comparison of recent and acient tidal flat and estuarine sediments. Estuaries. H. G. Lauff. Washington.

Loureiro, J. M., M. L. R. Machado, et al. (1986). Monografias Hidrológicas dos Principais Cursos de Água de Portugal Continental. Lisboa.

Mandelbrot, B. B. (1983). The fractal geometry of nature. New York, Wm. H. Freeman.

Marques da Silva, M. A. (1992). "Camadas-guia do Cretácico de Aveiro e sua importância hidrogeológica." Geociências, Rev.Univer.Aveiro **7 (1/2)**: 111:124.

Marsset, B., T. Missiaen, et al. (1998). "Very high resolution 3D marine seismic data processing for geotechnical applications." Geophysical Prospecting **46**(2): 105-120.

Matos, M. L. (1990). "Um estudo do balanço de sal num estuário de costa plana." Rec. Hídricos **10**: 13-21.

McClennen, C. E., A. J. Ammerman, et al. (1997). "Framework stratigraphy for the lagoon of Venice, Italy: Revealed in new seismic-reflection profiles and cores." Journal of Coastal Research **13**(3): 745-759.

Middelburg, J. J., J. Nieuwenhuize, et al. (2002). "Methane distribution in European tidal estuaries." Biogeochemistry **59**(1-2): 95-119.

Missiaen, T. (2005). "VHR marine 3D seismics for shallow water investigations: Some practical guidelines." Marine Geophysical Researches **26**(2-4): 145-155.

Monteiro, J. H. and L. M. Pinheiro (1986). Campanha Vouga-86 Technical Report (Unpublished), Dep. Geol. Marinha. Inst. Geol. Min.

Moreira, A. P. (1988). Relatório de Estágio no Núcleo de Geologia Marinha, Serviços Geológicos de Portugal (não publicado).

Mosher, D. C. and P. G. Simpkin (1999). "Environmental marine geoscience 1. Status and trends of marine high-resolution seismic reflection profiling: Data acquisition." Geoscience Canada **26**(4): 174-188.

Nobre, A. (1915). A Ria de Aveiro. Relatório oficial do regulamento da Ria. I. Nacional**:** 197.

Oliveira, C. S. (2005). Descrição do Terramoto de 1755, a sua extensão, causas e efeitos. O sismo. O tsunami. O incêndio. O grande terramoto de Lisboa. Lisboa, FLAD e PUBLICO. **1:** 23-86.

Oliveira, J. T., E. Pereira, et al. (1992). Carta Geológica de Portugal 1:500.000 Folha N, Instituto Geologico e Mineiro.

Pinheiro, L. M. and H. Duarte (2002). Amostragem por dragagem ao largo do Terminal Sul (Porto de Aveiro). Unpublished Report, Universidade de Aveiro**:** 4.

Pinheiro, L. M. and H. Duarte (2003a). Campanha RIAV02, Technical Report (unpublished), Dep. Geol. Mar., Inst. Geol. Min.

Pinheiro, L. M. and H. Duarte (2003b). Campanha RIAV02A, Technical Report (unpublished), Dep. Geol. Mar. Inst. Geol. Min.

Pinheiro, L. M. and H. Duarte (2006). Sampling of gas bubbles in the Doca-Pesca, Ria of Aveiro. Unpublished data, Acção Ciência Viva 2006 - Geologia sub-aquatica da Ria de Aveiro, http://www2.geo.ua.pt/Ciencia_Viva/2006/Geol_SubAq_06/index.html.

Pinheiro, L. M., H. Duarte, et al. (2003). Campanha RIAV03, Technical Report (unpublished), Dep. Geol. Mar., Inst. Geol. Min.

Pinheiro, L. M. and J. H. Monteiro (1999). Campanha RIAV-99. Technical Report (Unpublished), Dep. Geol. Marinha, Inst. Geol. Min.

Pinheiro, L. M., R. C. L. Wilson, et al. (1996). The western Iberia margin: a geophysical and geological overview. Proc. of the ODP, Scientific Results. R. B. Whitmarsh, D. S. Sawyer, A. Klaus and D. G. Masson. Washington. **149:** 3-23.

Pombo, L., M. Elliott, et al. (2005). "Environmental influences on fish assemblage distribution of an estuarine coastal lagoon, Ria de Aveiro (Portugal)." Scientia Marina **69**(1): 143-159.

Quinn, R., J. M. Bull, et al. (1997). "Imaging wooden artefacts using chirp sources." Archaeological Prospection **4**(1): 25-35.

Quinn, R., J. M. Bull, et al. (1998). "Optimal processing of marine high-resolution seismic reflection (Chirp) data." Marine Geophysical Researches **20**(1): 13-20.

Rasmussen, E. S., S. Lomholt, et al. (1998). "Aspects of the structural evolution of the Lusitanian Basin in Portugal and the shelf and slope area offshore Portugal." Tectonophysics **300**(1-4): 199-225.

Rebelo, J. E. (1992). "The ichthyofauna and abiotic hydrological environment of the Ria de Aveiro, Portugal " Estuaries and Coasts **15**(3): 401-413.

Ribeiro, A., M. T. Antunes, et al. (1979). Introduction à la Géologie generale du Portugal, Ed. Serv. Geol. Portugal.

Ribeiro, A., J. Cabral, et al. (1996). "Stress pattern in Portugal mainland and the adjacent Atlantic region, West Iberia." Tectonics **15**(3): 641-659.

Ribeiro, A., M. C. Kullberg, et al. (1990). "A Review of Alpine Tectonics in Portugal - Foreland Detachment in Basement and Cover Rocks." Tectonophysics **184**(3-4): 357-366.

Ribeiro, A. and A. Mateus (2002). Soft Plate and Impact Tectonics, Springer Verlag.

Rocha, F. T. (1993). Argilas aplicadas a estudos litoestratigráficos e paleoambientais na bacia sedimentar de Aveiro, University of Aveiro, Portugal. **Ph.D.**

Rocha, F. T. and C. S. F. Gomes (1989). "Geologia subsuperficial da região da "Ria de Aveiro" II - Alguns aspectos da mineralogia e da sedimentologia dos sedimentos atravessados pelos furos JK4 (Cacia) e AC6 (S. Bernardo)." Geociências, Rev.Univer.Aveiro **4 (1)**: 111:117.

Rosas, F. M., J. Duarte, et al. (2008). "Morphotectonic characterization of major bathymetric lineaments in NW Gulf of Cadiz (Africa-Iberia plate boundary): insights from analogue modelling experiments." Marine Geology **in press**.

Sansone, F. J., M. E. Holmes, et al. (1999). "Methane stable isotopic ratios and concentrations as indicators of methane dynamics in estuaries." Global Biogeochemical Cycles **13**(2): 463-473.

Sheriff, R. E. (1985). Aspects of Seismic Resolution. Seismic Stratigraphy II - An Integrated Approach: AAPG Memoir. O. R. Berg and D. G. Woolverton. **39:** 1:10.

Sheriff, R. E. and L. P. Geldart (1995). Exploration Seismology. Cambridge, Cambridge University Press.

Srivastava, S. P., W. R. Roest, et al. (1990). "Motion of Iberia since the Late Jurassic: results from detailed areomagnetic measurements in the Newfoundland Basin." Tectonophysics **184**: 229-260.

Stenbit, J. P. (2001). Global Positioning System standard positioning service performance standard. C. Assistant Secretary of Defense for Command, Communications, and Intelligence. Washington, Department of Defense, Government of the United States of America.

Stolt, R. H. (1978). "Migration by Fourier-Transform." Geophysics **43**(1): 23-48.

Teixeira, C. and G. Zbyszewski (1976). Notícia explicativa da Folha 16-A, Aveiro. Carta Geológica de Portugal na escala de 1/50.000. Lisboa, Serviços Geológicos de Portugal.

Teixeira, F. C. and L. M. Pinheiro (1998). Contribuição para o estudo da evolução geológica da Ria de Aveiro e da Plataforma Continental Adjacente. V Congresso Nacional de Geologia, Lisboa.

Teixeira, S. B. (1994). Dinâmica Morfosedimentar da Ria de Aveiro (Portugal). Departamento de Geologia. Lisboa, Universidade de Lisboa. **Ph.D.:** 396.

Uchupi, E. (1988). "The Mesozoic-Cenozoic geologic evolution of Iberia, a tectonic link between Africa and Europe." Rev. Soc. Geol. España **1**(3-4): 257-294.

Uphoff, T. L., D. P. Stemler, et al. (2002). "Lusitanian basin highlights important potential in Portugal." Oil & gas journal **100**(50): 32-38.

Van der Nat, F. J. and J. J. Middelburg (2000). "Methane emission from tidal freshwater marshes." Biogeochemistry **49(2)**: 103-121.

Vanney, J. R. and D. Mougenot (1981). "La plate-forme continental de Portugal et les provinces adjacentes: Analyse geomorphologique." Mem. Serv. Geol. Portugal **28**: 86.

Whitmarsh, R. B. and P. R. Miles (1995). "Models of the development of West Iberia rifted continental margin at 40º 30' N deduced from surface and deeptow magnetic anomalies." Journal of Geophysical Research **100**: 3789-3806.

Williams, D. W. and J. J. Frederick (2001). Microturbine operation with biogas from a covered dairy manure lagoon. 2001 ASAE Annual International Meeting, Sacramento, California, USA, ASAE.

Wilson, R. C. L., R. N. Hiscott, et al. (1989). "The Lusitanian basin of west-central Portugal: Mesozoic and Tertiary tectonic, stratigraphy and subsidence history." AAPG Memoir **46**: 341-361.

Woodroffe, C. D. (2003). Coasts. Form, process and evolution, Cambridge University Press.

Yilmaz, O. (1987). Seismic data processing. Tulsa, Society of Exploration Geophysicists.

Zechhin, M., L. Baradello, et al. (2008). "Sequence stratigraphy based on high-resolution seismic profiles in the late Pleistocene and Holocene deposits of the Venice area." Marine Geology **253**(3-4): 185-198.

Zitellini, N., E. Gràcia, et al. (2009). "The quest for the Africa–Eurasia plate boundary west of the Strait of Gibraltar." Earth and Planetary Science Letters **in press**.

APPENDIX

Other seismic evidence of gas

This appendix presents seismic evidence of gas that, for various reasons, was not presented in the main text of the thesis. It serves mainly to complement the figures of Chapter IV, which were limited in number because of the constraints of the chapters' publication in a scientific journal. It also serves to document evidence of gas in other surveyed sectors of the lagoon that were not investigated in detail due to the sparse seismic coverage.

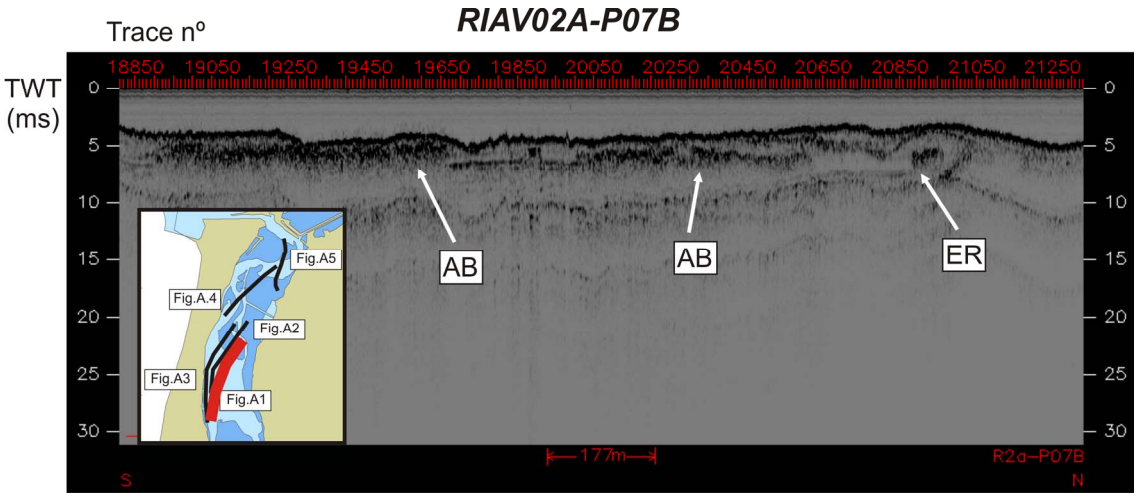

Figure A-1: Gas accumulations in the Mira channel, observed in the chirp profile P07B, cruise RIAV02A (Pinheiro and Duarte, 2003b). ***AB*** – acoustic blanking, ***ER*** – enhanced reflection; inset ***red line*** – trackline of the profile, see Fig.A-19 for location in the Ria of Aveiro.

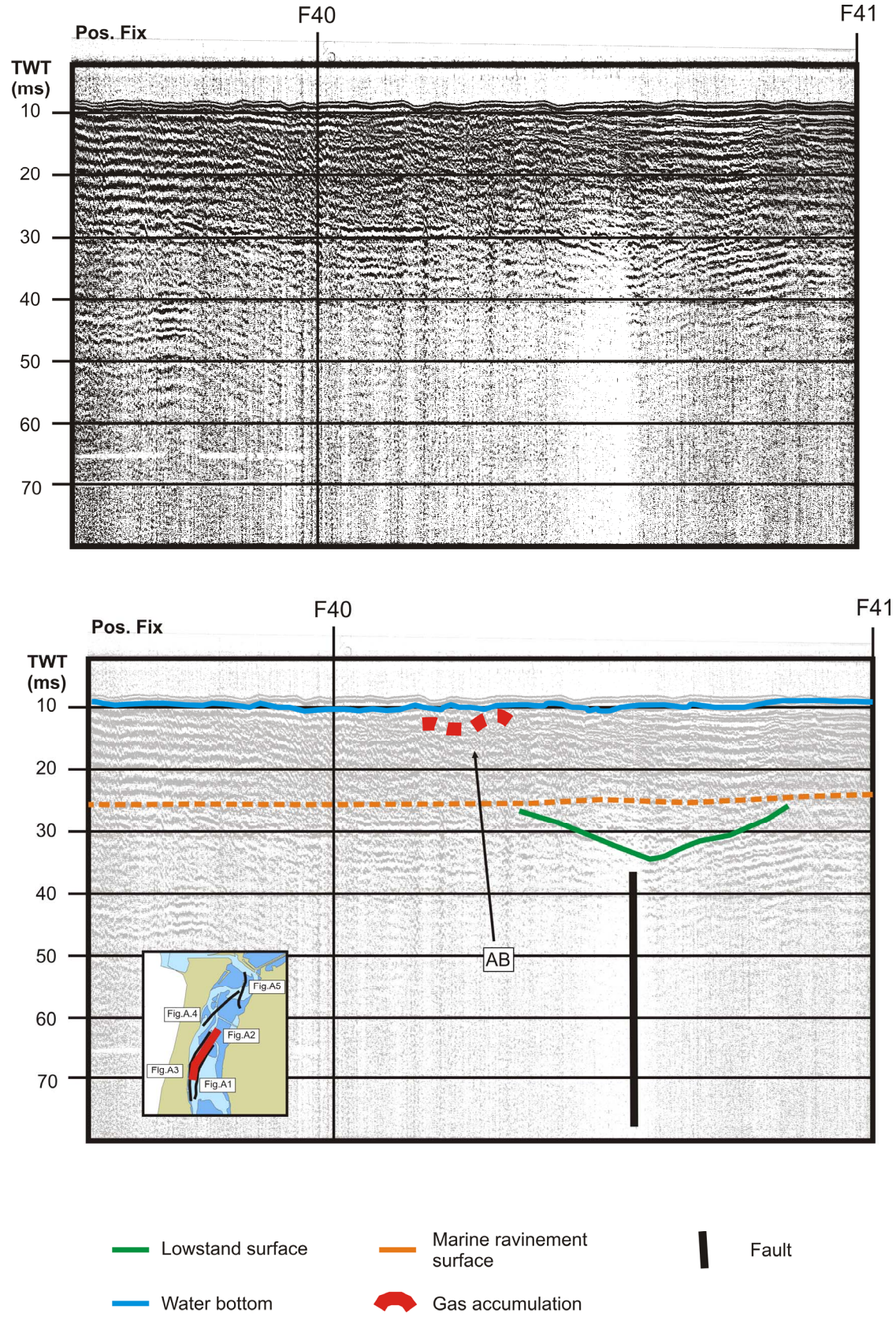

Figure A-2: Gas accumulations in the Mira channel, observed in the boomer profile F40-41, cruise VOUGA86 (Monteiro and Pinheiro, 1986). ***AB*** – acoustic blanking, inset ***red line*** – trackline of the profile, see Fig.A-19 for location in the Ria of Aveiro.

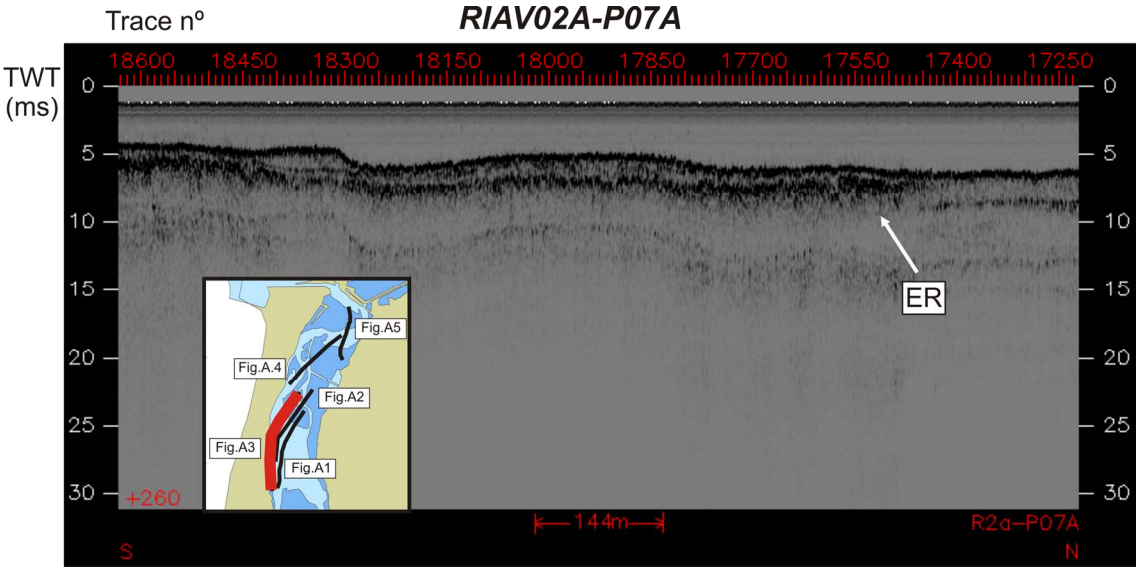

Figure A-3: Gas accumulations in the Mira channel, observed in the chirp profile P07A, cruise RIAV02A (Pinheiro and Duarte, 2003b). ***ER*** – enhanced reflection; inset ***red line*** – trackline of the profile, see Fig.A-19 for location in the Ria of Aveiro.

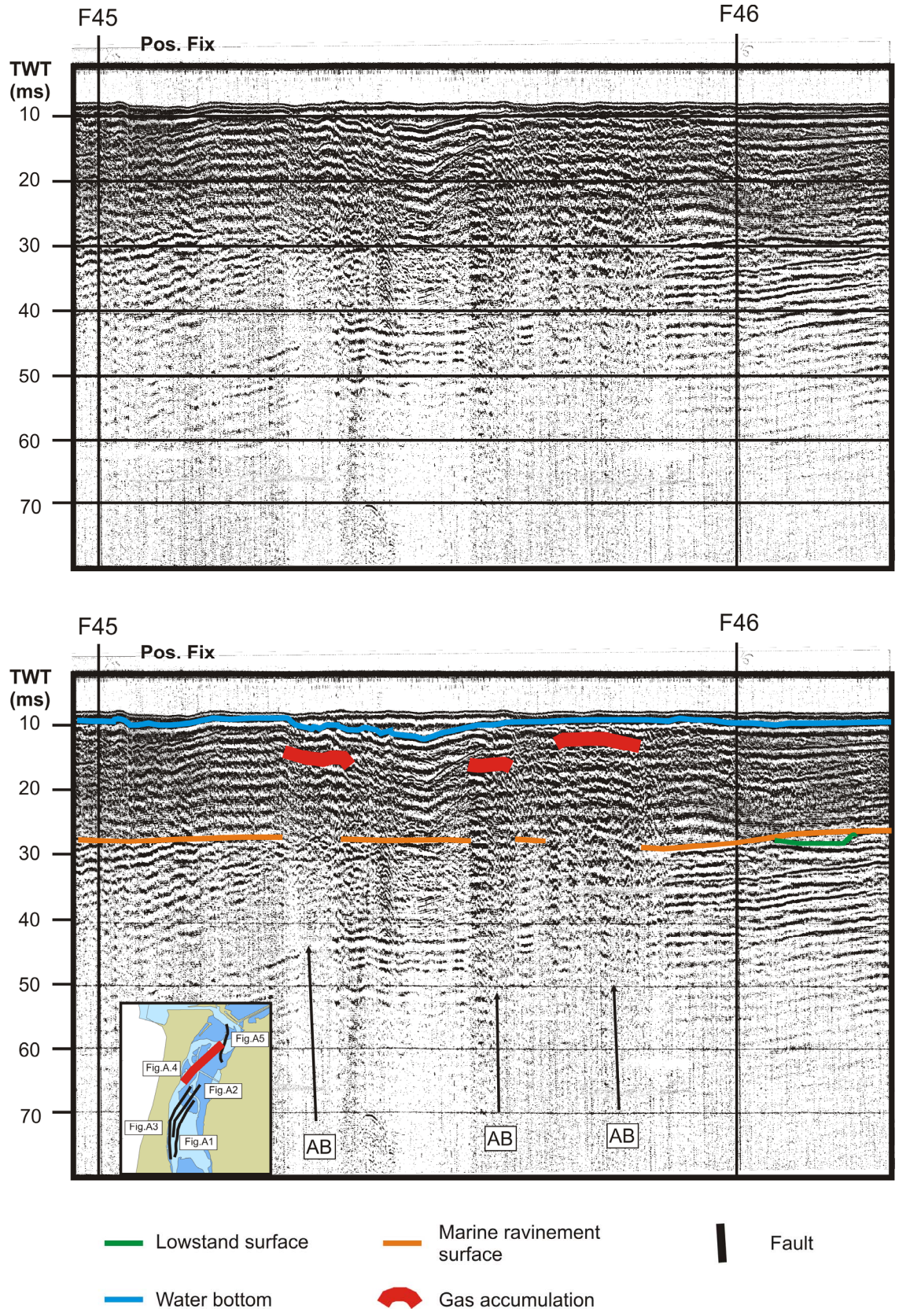

Figure A-4: Gas accumulations in the Mira channel, observed in the boomer profile F45-46, cruise VOUGA86 (Monteiro and Pinheiro, 1986). ***AB*** – acoustic blanking; inset ***red line*** – trackline of the profile, see Fig.A-19 for location in the Ria of Aveiro.

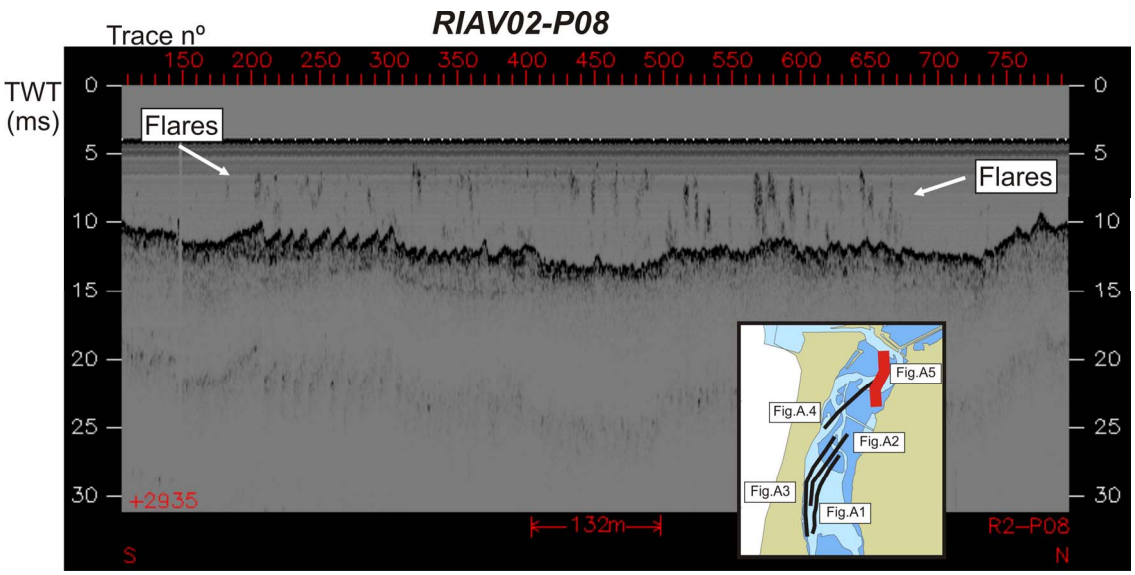

Figure A-5: Acoustic flares in the water column in the Mira channel, observed in the chirp profile P08, cruise RIAV02 (Pinheiro and Duarte, 2003a). Inset ***red line*** – trackline of the profile, see Fig.A-19 for location in the Ria of Aveiro.

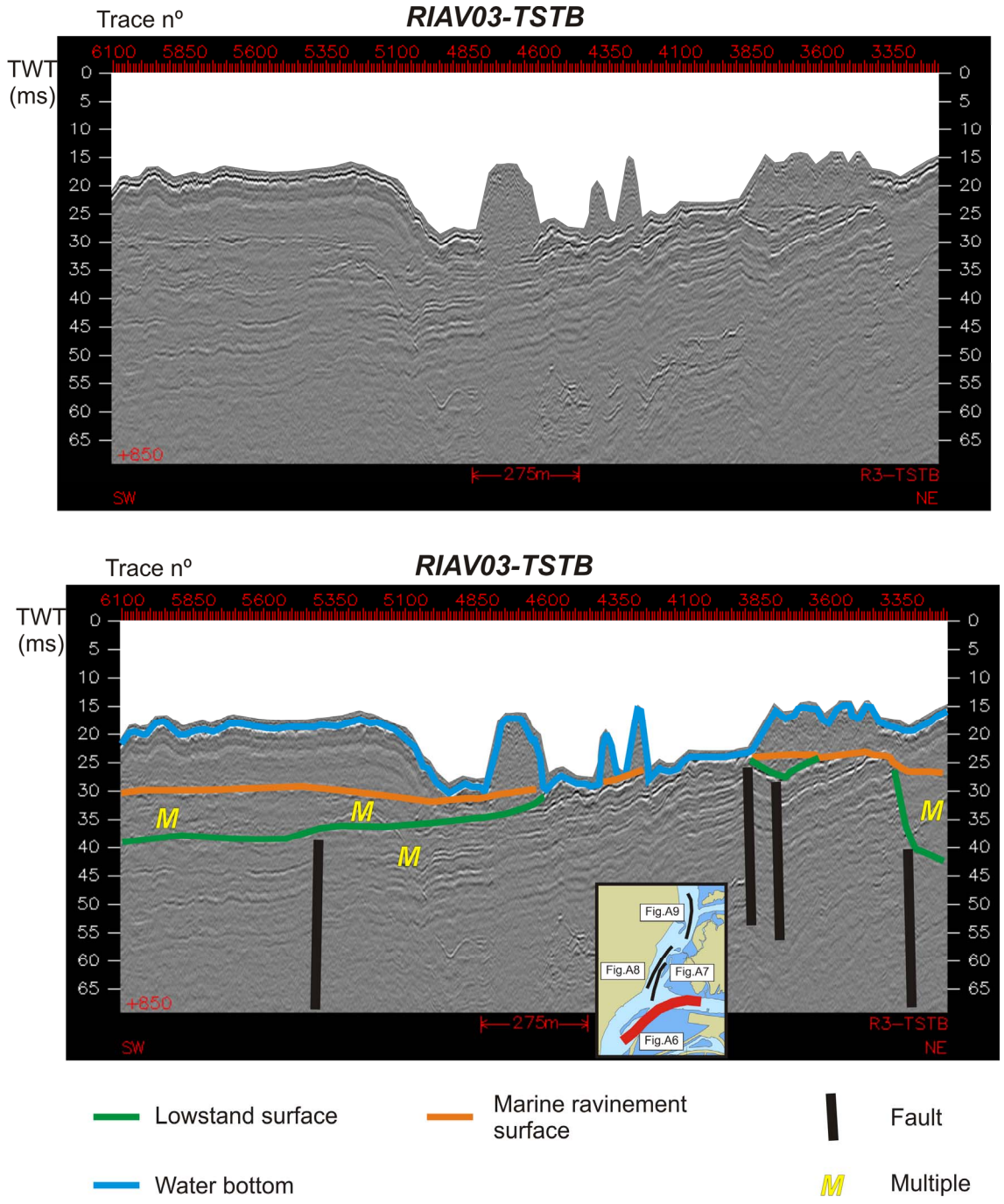

Figure A-6: Minor faults to the west of the Vila channel graben faults, observed in the processed boomer profile TSTB (Pinheiro *et al.*, 2003), cruise RIAV03. Inset ***red line*** – trackline of the profile, see Fig.A-19 for location in the Ria of Aveiro.

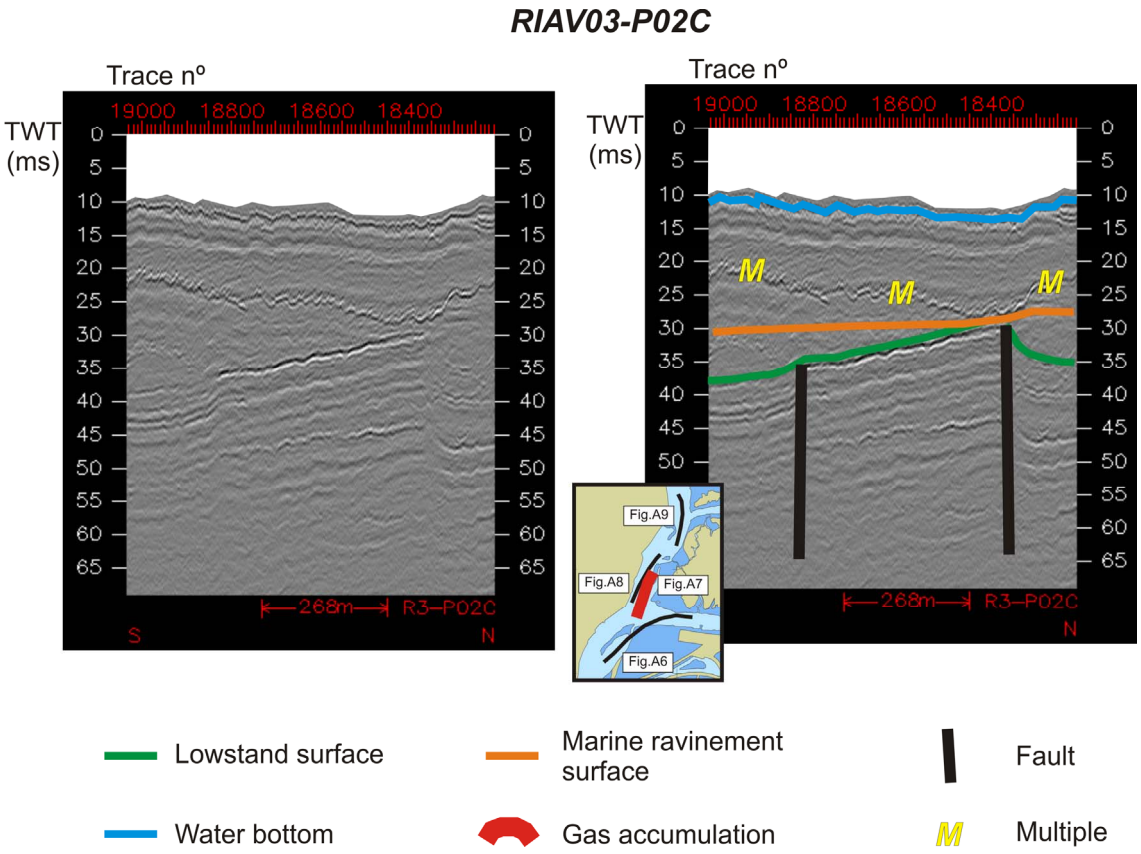

Figure A-7: Minor faults in the S. Jacinto channel, related to the Vila channel graben faults, observed in the processed boomer profile P02C, cruise RIAV03 (Pinheiro *et al.*, 2003). Inset ***red line*** – trackline of the profile, see Fig.A-19 for location in the Ria of Aveiro.

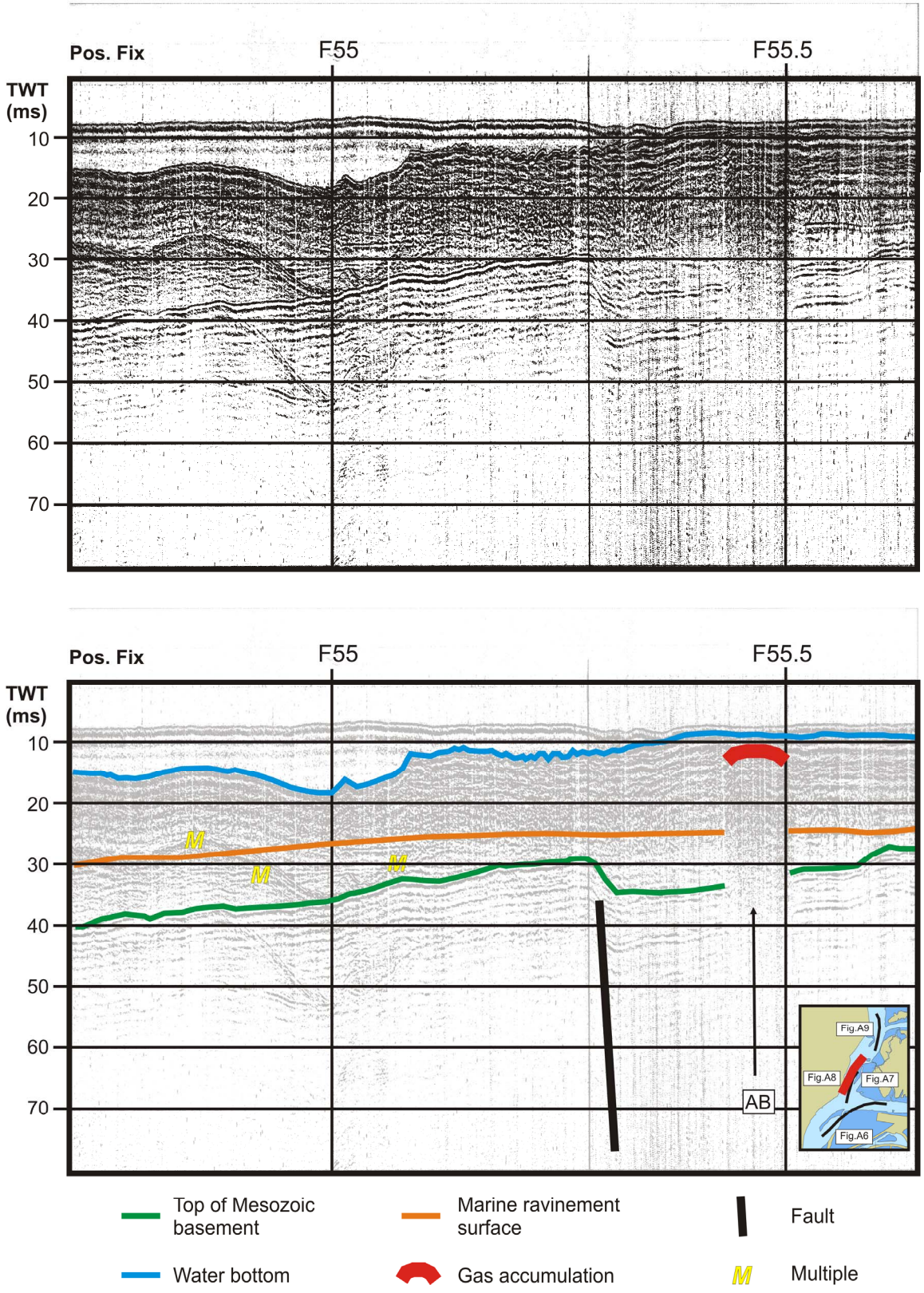

Figure A-8: Gas accumulation and minor fault in the S. Jacinto channel related to the Vila channel graben faults, observed in the boomer profile F55, cruise VOUGA86 (Monteiro and Pinheiro, 1986). ***AB*** – acoustic blanking; inset ***red line*** – trackline of the profile, see Fig.A-19 for location in the Ria of Aveiro.

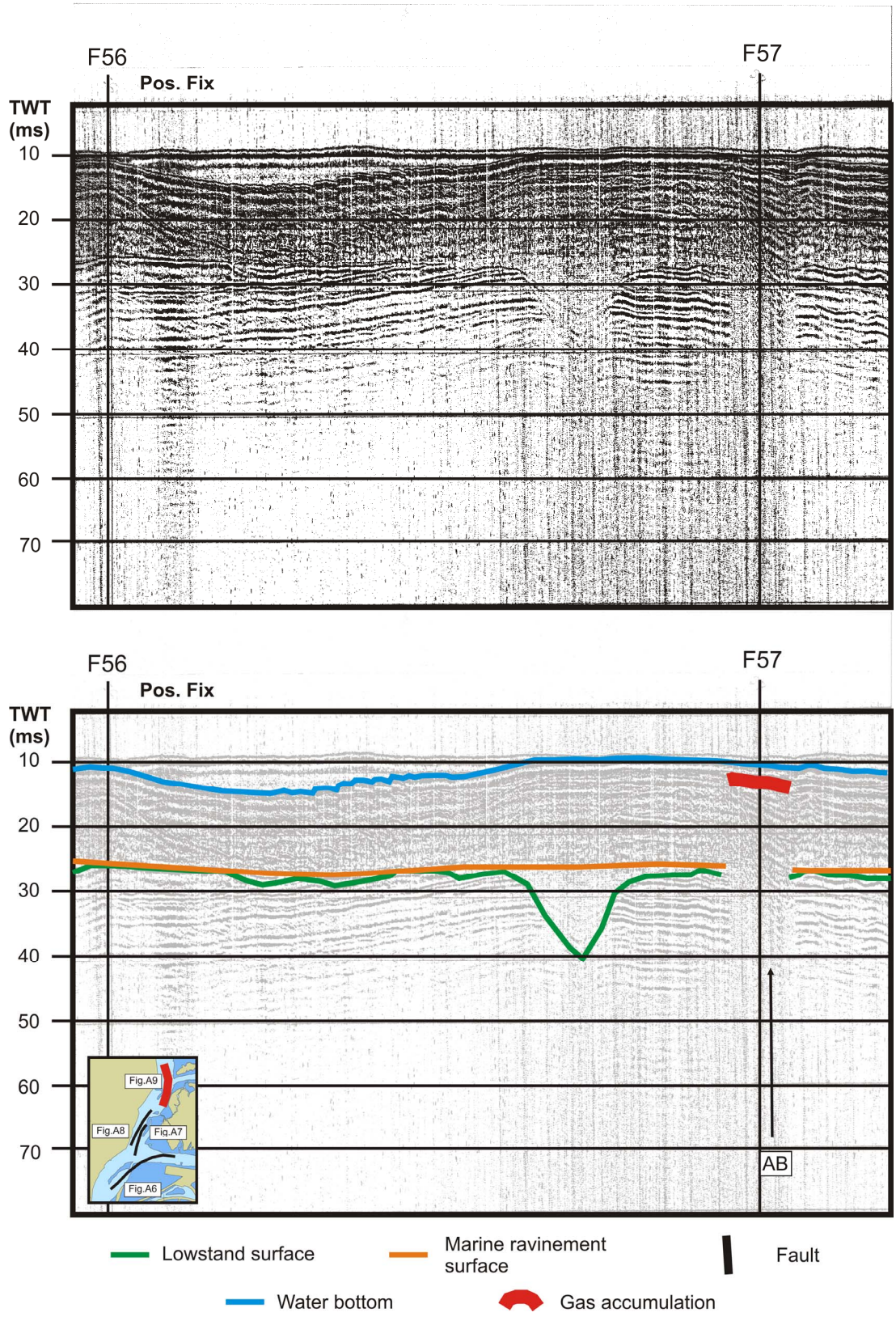

Figure A-9: Gas accumulation in the S. Jacinto channel observed in the boomer profile F56-57, cruise VOUGA86 (Monteiro and Pinheiro, 1986). ***AB*** – acoustic blanking; inset ***red line*** – trackline of the profile, see Fig.A-19 for location in the Ria of Aveiro.

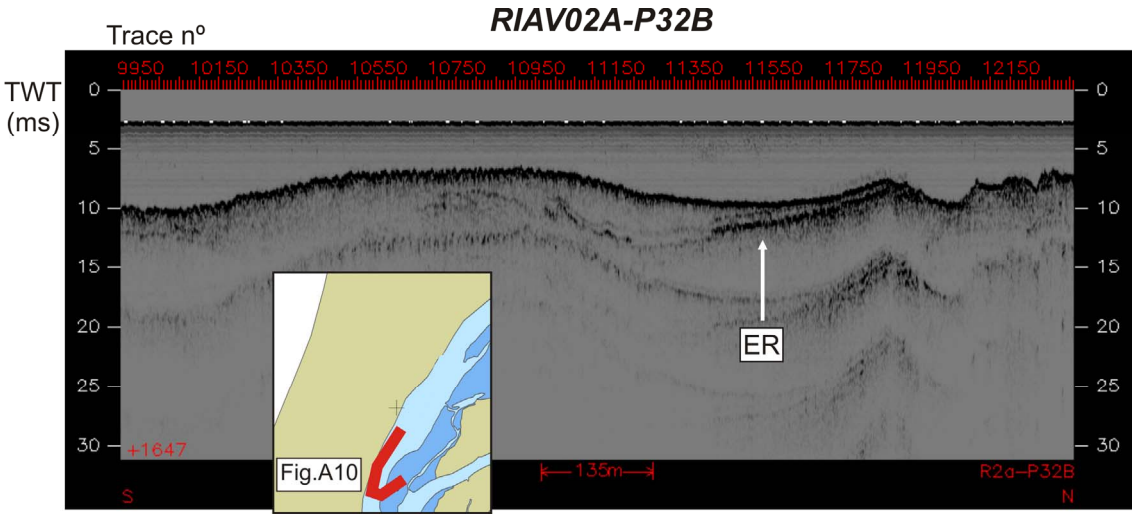

Figure A-10: Gas accumulations in the Ovar channel, observed in the chirp profile P032B, cruise RIAV02A (Pinheiro and Duarte, 2003b). ***ER*** – enhanced reflection; inset ***red line*** – trackline of the profile, see Fig.A-19 for location in the Ria of Aveiro.

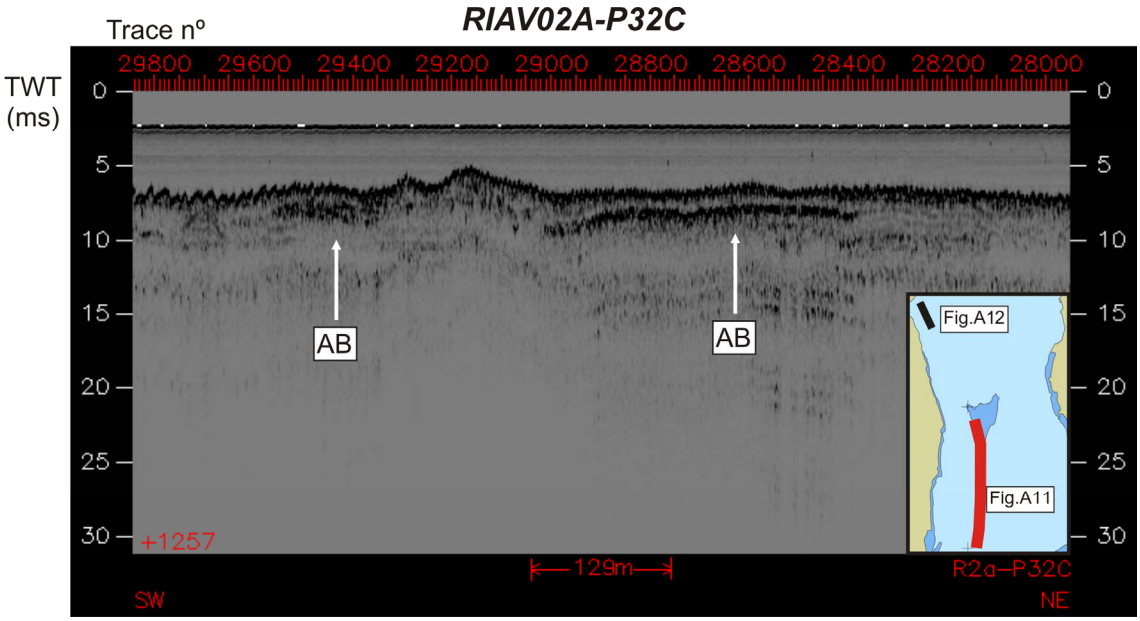

Figure A-11: Gas accumulations in the Ovar channel, observed in the chirp profile P32C, cruise RIAV02A (Pinheiro and Duarte, 2003b). ***AB*** – acoustic blanking, inset ***red line*** – trackline of the profile, see Fig.A-19 for location in the Ria of Aveiro.

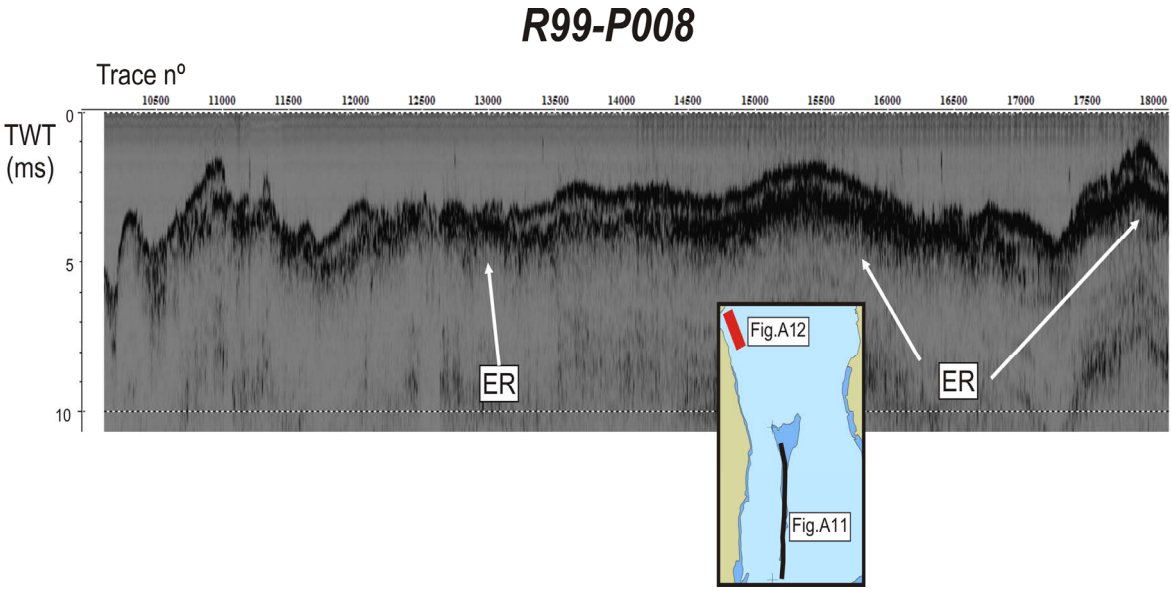

Figure A-12: Gas accumulations in the Ovar channel, observed in the chirp profile P008, cruise RIAV99 (Pinheiro and Monteiro, 1998). ***ER*** – enhanced reflection, inset ***red line*** – trackline of the profile, see Fig.A-19 for location in the Ria of Aveiro.

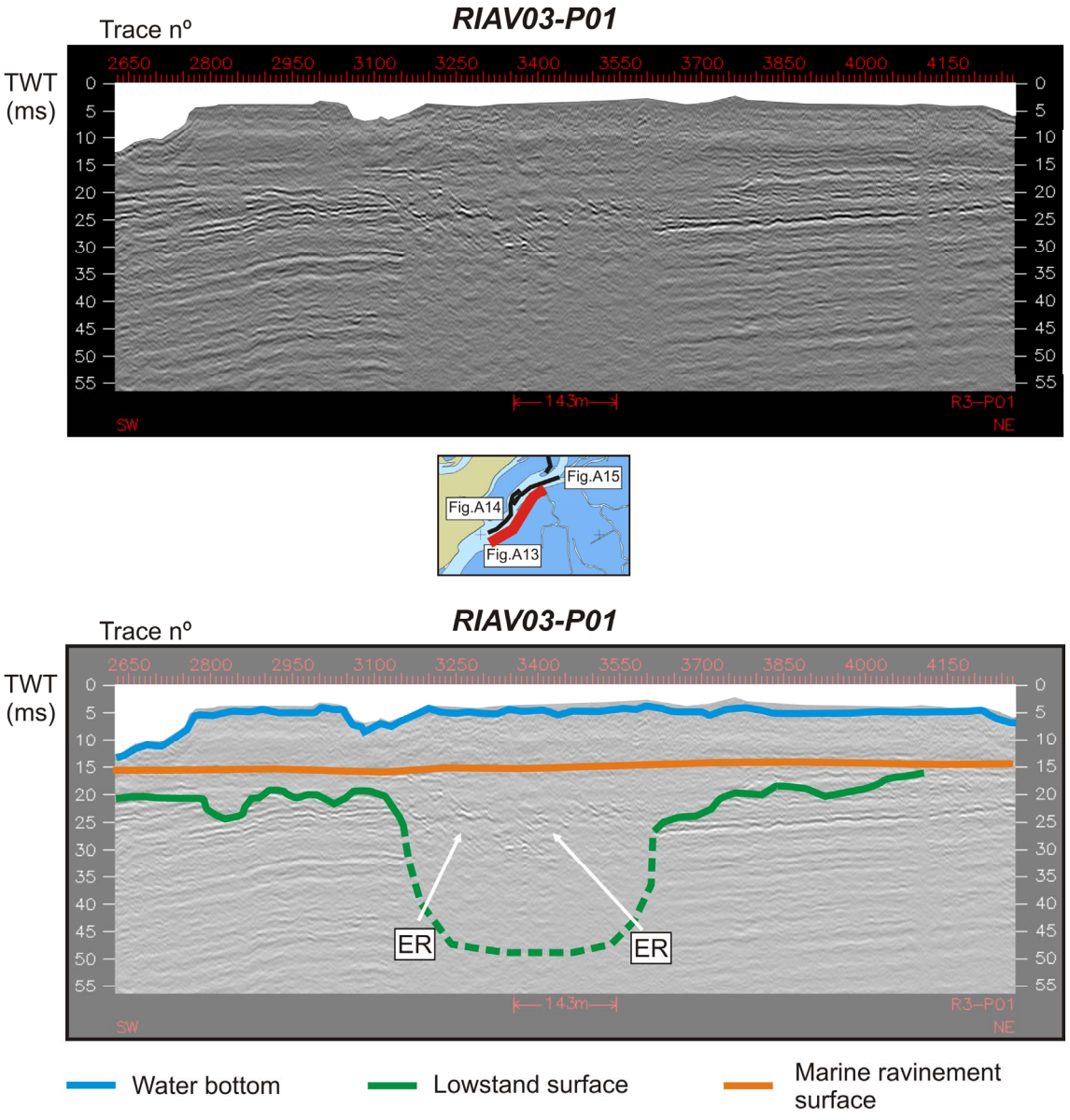

Figure A-13: Possible gas accumulations in a paleochannel in the Espinheiro channel, observed in the processed boomer profile P01, cruise RIAV03 (Pinheiro *et al.*, 2003). ***ER*** – enhanced reflection; inset ***red line*** – trackline of the profile, see Fig.A-19 for location in the Ria of Aveiro.

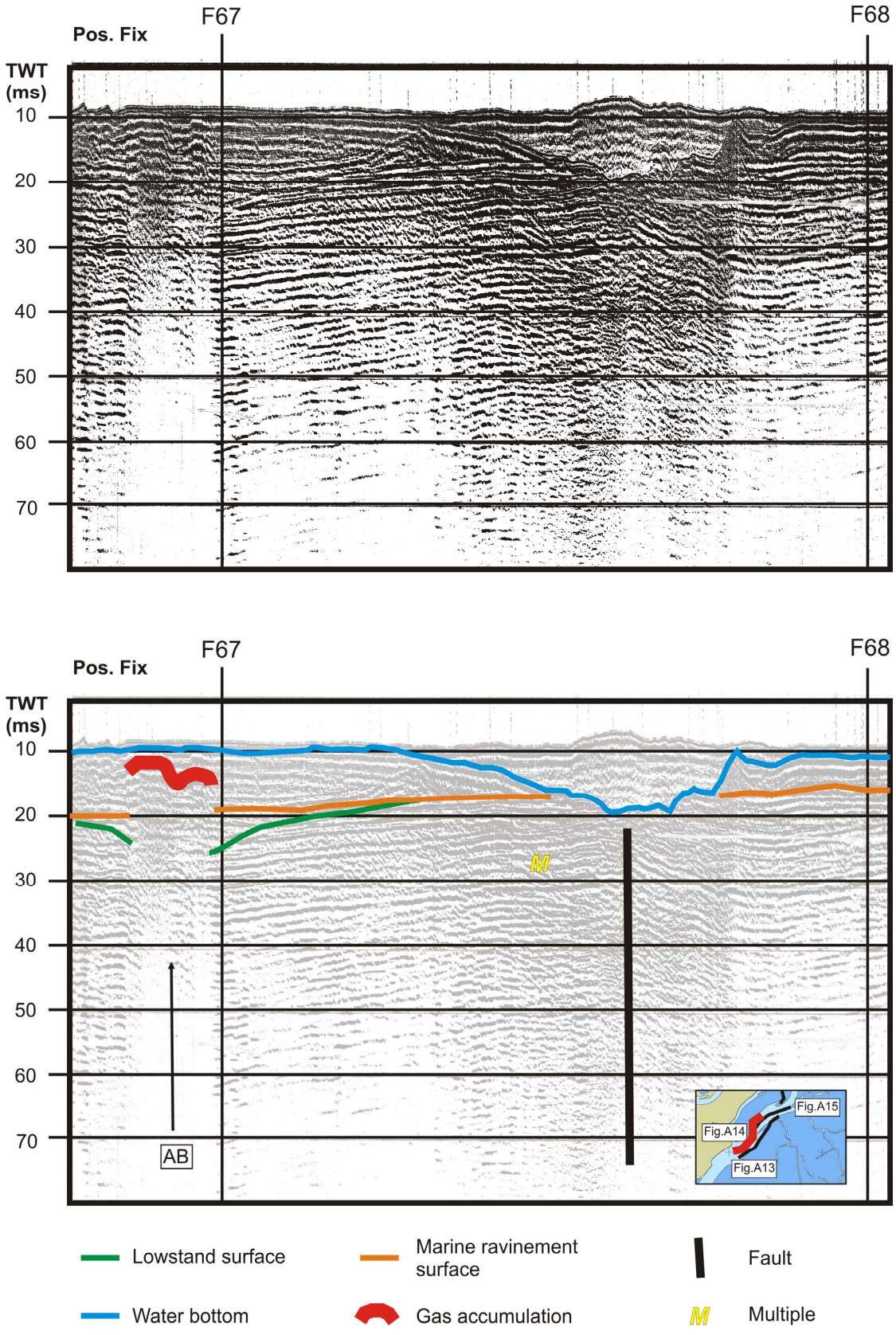

Figure A-14: Gas accumulation in the Espinheiro channel, observed in the boomer profile F67-68, cruise VOUGA86 (Monteiro and Pinheiro, 1986). ***AB*** – acoustic blanking, inset ***red line*** – trackline of the profile, see Fig.A-19 for location in the Ria of Aveiro.

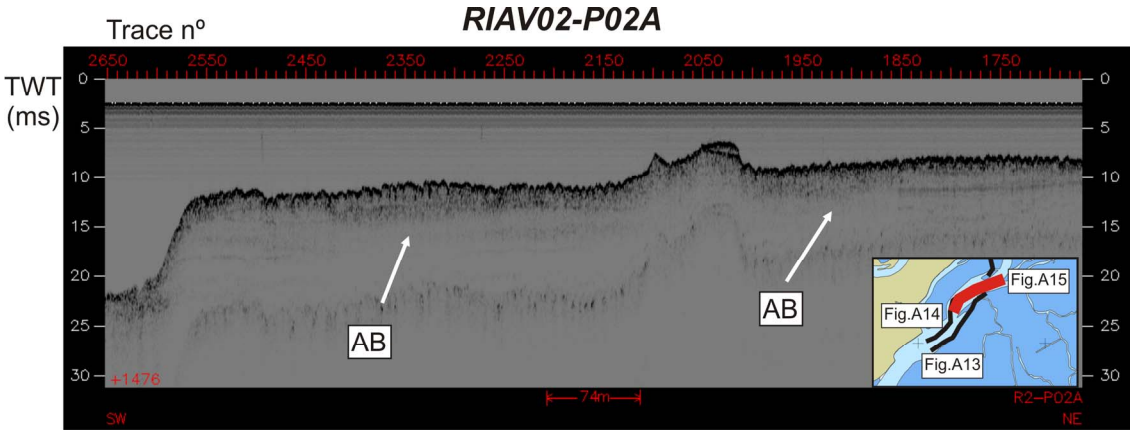

Figure A-15: Gas accumulations in the Espinheiro channel, observed in the chirp profile P02A, cruise RIAV02 (Pinheiro and Duarte, 2003a). ***AB*** – acoustic blanking, inset ***red line*** – trackline of the profile, see Fig.A-19 for location in the Ria of Aveiro.

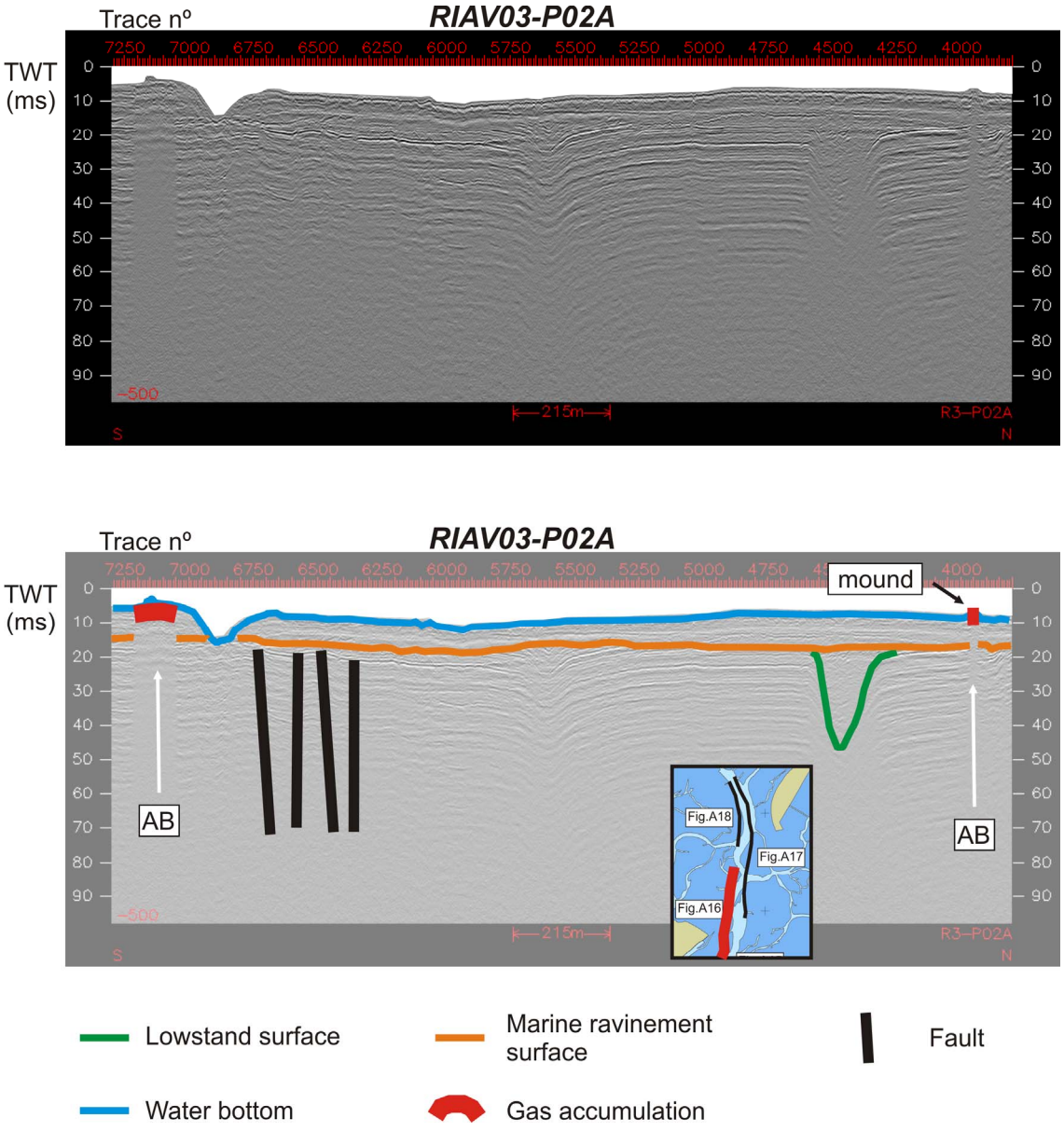

Figure A-16: Gas accumulation and mound in the Espinheiro channel, observed in the processed boomer profile P02A, cruise RIAV03 (Pinheiro *et al.*, 2003). ***AB*** – acoustic blanking, inset ***red line*** – trackline of the profile, see Fig.A-19 for location in the Ria of Aveiro.

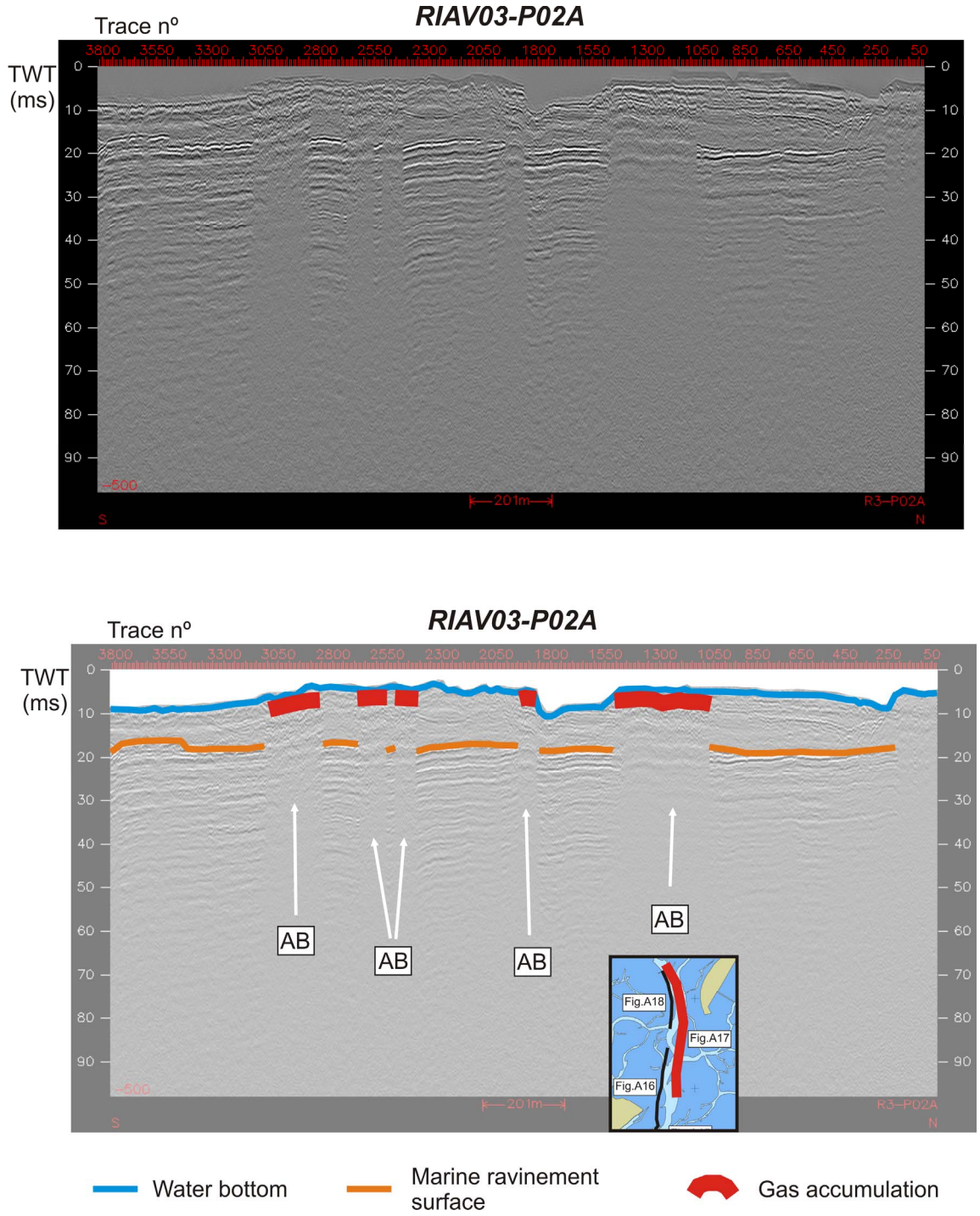

Figure A-17: Gas accumulations in the Espinheiro channel, observed in the processed boomer profile P02A, cruise RIAV03 (Pinheiro *et al.*, 2003). ***AB*** – acoustic blanking, inset ***red line*** – trackline of the profile, see Fig.A-19 for location in the Ria of Aveiro.

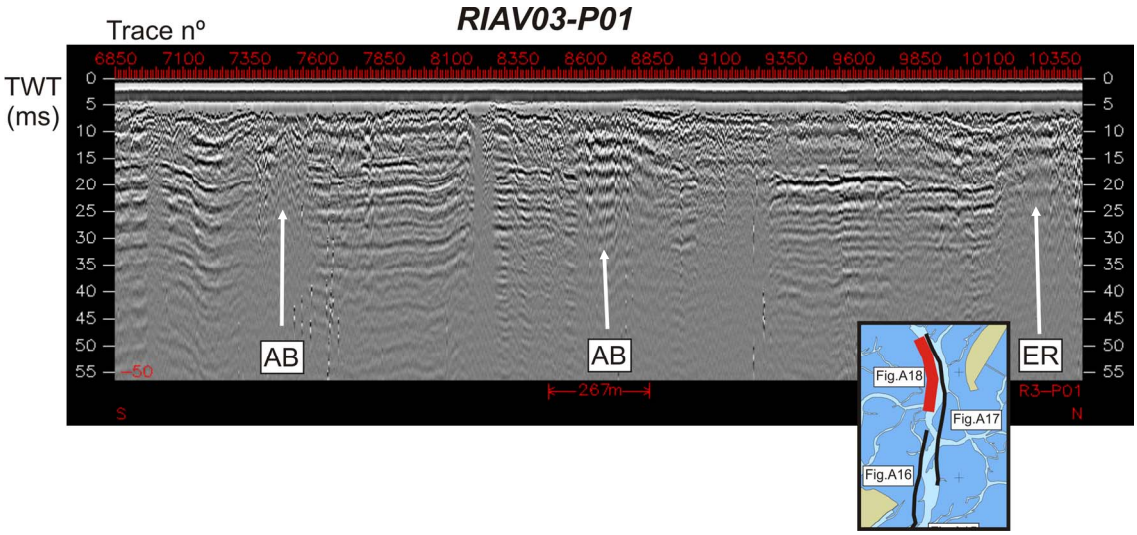

Figure A-18: Gas accumulations in the Espinheiro channel, observed in the unprocessed boomer profile P02A, cruise RIAV03 (Pinheiro *et al.*, 2003). ***AB*** – acoustic blanking, ***ER*** – enhanced reflection; inset ***red line*** – trackline of the profile, see Fig.A-19 for location in the Ria of Aveiro.

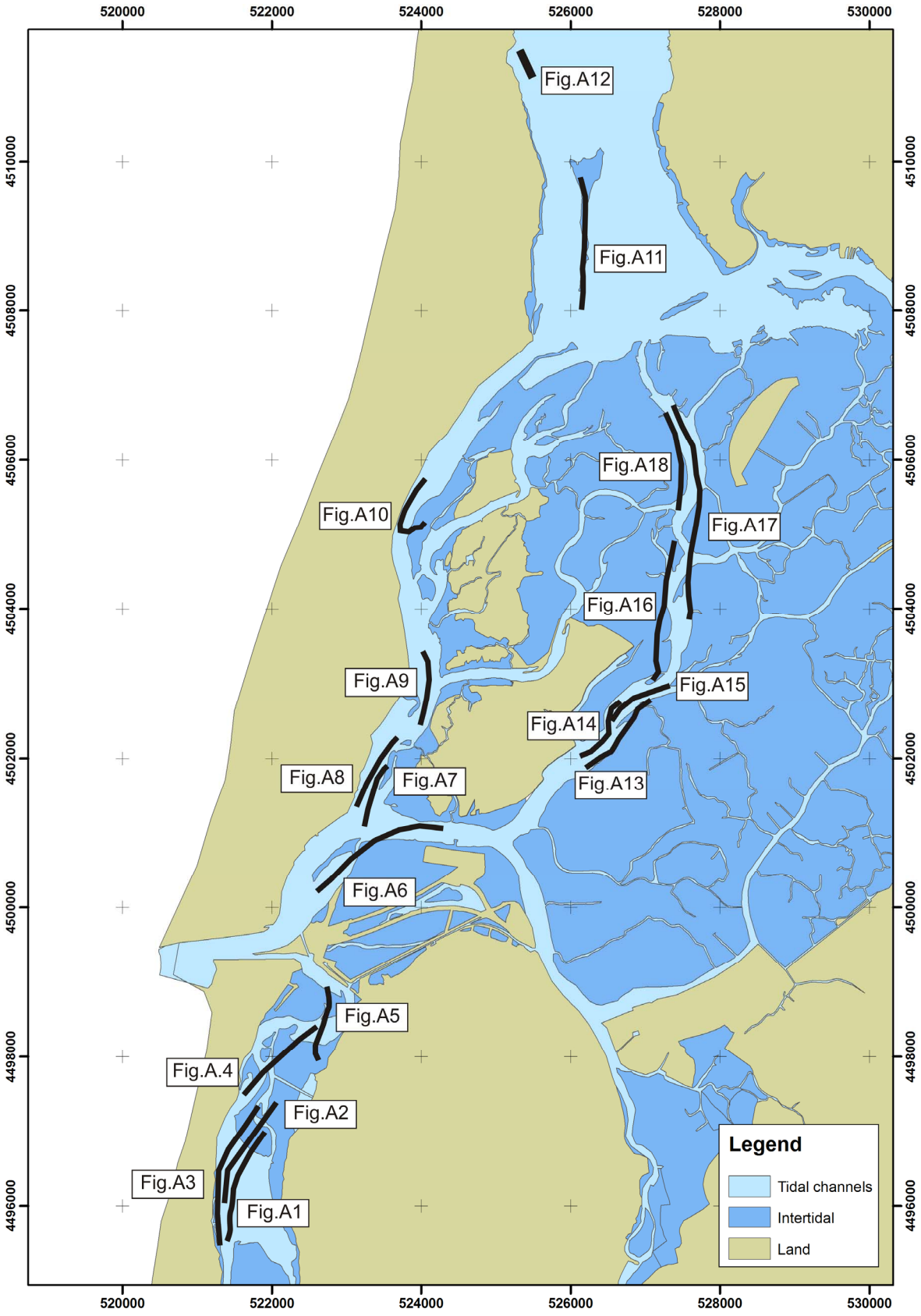

Figure A-19: Location of the profiles shown in this Appendix.